U.S. DEPARTMENT OF COMMERCE
National Technical Information Service

PB-272 063

Evaluation of Analytical and Experimental Methodologies for the Characterization of Wheel/Rail Loads

Battelle Columbus Labs, Ohio

Prepared for

Transportation Systems Center, Cambridge, Mass

Nov 76

PB 272 063

REPORT NO. FRA-OR&D-76-276

EVALUATION OF ANALYTICAL AND EXPERIMENTAL METHODOLOGIES FOR THE CHARACTERIZATION OF WHEEL/RAIL LOADS

Donald R. Ahlbeck
Harold D. Harrison
Robert H. Prause

Battelle-Columbus Laboratories
505 King Avenue
Columbus OH 43201

Milton R. Johnson

IIT Research Institute
10 West 35th Street
Chicago IL 60616

NOVEMBER 1976

INTERIM REPORT

Prepared for

U.S. DEPARTMENT OF TRANSPORTATION
FEDERAL RAILROAD ADMINISTRATION
Office of Research and Development
Washington DC 20590

NOTICE

This document is disseminated under the sponsorship of the Department of Transportation in the interest of information exchange. The United States Government assumes no liability for its contents or use thereof.

NOTICE

The United States Government does not endorse products or manufacturers. Trade or manufacturers' names appear herein solely because they are considered essential to the object of this report.

Technical Report Documentation Page

1. Report No	2. Government Accession No	3. Recipient's Catalog No
FRA-OR&D-76-276		

4. Title and Subtitle
EVALUATION OF ANALYTICAL AND EXPERIMENTAL METHODOLOGIES FOR THE CHARACTERIZATION OF WHEEL/RAIL LOADS

5. Report Date
November 1976

6. Performing Organization Code

7. Author(s) Donald R. Ahlbeck,* Harold D. Harrison,* Robert A. Prause,* and Milton R. Johnson**

8. Performing Organization Report No
DOT-TSC-FRA-76-10

9. Performing Organization Name and Address
*Battelle-Columbus Laboratories
505 King Avenue
Columbus OH 43201

**IIT Research Institute
10 West 35th Street
Chicago IL 60616
(Subcontractor)

10. Work Unit No. (TRAIS)
RR 619/R 6365T

11. Contract or Grant No
DOT-TSC-1051

12. Sponsoring Agency Name and Address
U. S. Department of Transportation
Federal Railroad Administration
Office of Research and Development
Washington DC 20590

13. Type of Report and Period Covered
Interim Report
July 1975 - February 1976

14. Sponsoring Agency Code

15. Supplementary Notes
*Under Contract to: U.S. Department of Transportation
Transportation Systems Center
Kendall Square
Cambridge MA 02142

16. Abstract

This report has been prepared as part of the Improved Track Structures Research Program sponsored by the Office of Rail Safety Research of the Federal Railroad Administration. The major modes of track degradation have been reviewed to identify the significant wheel/rail loading mechanisms. Analytical models for vehicle/track interaction have been selected for predicting the loads in appropriate formats for each of the major modes of track degradation. This report also evaluates the data required to validate the analytical procedures, and both track and vehicle-borne instrumentation are reviewed for fulfilling these requirements. Available data on wheel/rail loads have been used to assemble a preliminary statistical characterization for interim use.

17. Key Words	18. Distribution Statement		
Track loading, Track degradation, Wheel/rail loads, Load measurement instrumentation	DOCUMENT IS AVAILABLE TO THE U.S. PUBLIC THROUGH THE NATIONAL TECHNICAL INFORMATION SERVICE, SPRINGFIELD, VIRGINIA 22161		
19. Security Classif. (of this report)	**20. Security Classif. (of this page)**	**21. No. of Pages**	**22. Price**
UNCLASSIFIED	UNCLASSIFIED	278	A13-A01

Form DOT F 1700.7 (8-72) Reproduction of completed page authorized

PREFACE

This report was prepared by Battelle's Columbus Laboratories (BCL) under Contract DOT-TSC-1051 as part of the Improved Track Structures Research Program managed by the Transportation Systems Center (TSC). This program is sponsored by the Office of Rail Safety Research, Improved Track Structures Research Division, of the Federal Railroad Administration, Washington, D.C.

The overall objective of this contract is to apply existing data, analyses and instrumentation to develop a statistical characterization of wheel/rail loads for U.S. railroads and to evaluate strategies for the reduction of these loads. This interim report is the first report for this contract.

Dr. Leonard Kurzweil and Mr. Donald McConnell at the Transportation Systems Center were the technical monitor and alternate technical monitor, respectively, for the work reported herein. Their cooperation and suggestions are gratefully acknowledged. Dr. Thomas Johns of BCL also deserves recognition for his contribution to formulating the load requirements related to rail failure mechanisms.

METRIC CONVERSION FACTORS

Approximate Conversions to Metric Measures

Symbol	When You Know	Multiply by	To Find	Symbol
	LENGTH			
in	inches	2.5	centimeters	cm
ft	feet	30	centimeters	cm
yd	yards	0.9	meters	m
mi	miles	1.6	kilometers	km
	AREA			
in^2	square inches	6.5	square centimeters	cm^2
ft^2	square feet	0.09	square meters	m^2
yd^2	square yards	0.8	square meters	m^2
mi^2	square miles	2.6	square kilometers	km^2
	acres	0.4	hectares	ha
	MASS (weight)			
oz	ounces	28	grams	g
lb	pounds	0.45	kilograms	kg
	short tons (2000 lb)	0.9	tonnes	t
	VOLUME			
tsp	teaspoons	5	milliliters	ml
tbsp	tablespoons	15	milliliters	ml
fl oz	fluid ounces	30	milliliters	ml
c	cups	0.24	liters	l
pt	pints	0.47	liters	l
qt	quarts	0.95	liters	l
gal	gallons	3.8	liters	l
ft^3	cubic feet	0.03	cubic meters	m^3
yd^3	cubic yards	0.76	cubic meters	m^3
	TEMPERATURE (exact)			
°F	Fahrenheit temperature	5/9 (after subtracting 32)	Celsius temperature	°C

Approximate Conversions from Metric Measures

Symbol	When You Know	Multiply by	To Find	Symbol
	LENGTH			
mm	millimeters	0.04	inches	in
cm	centimeters	0.4	inches	in
m	meters	3.3	feet	ft
m	meters	1.1	yards	yd
km	kilometers	0.6	miles	mi
	AREA			
cm^2	square centimeters	0.16	square inches	in^2
m^2	square meters	1.2	square yards	yd^2
km^2	square kilometers	0.4	square miles	mi^2
ha	hectares (10,000 m^2)	2.5	acres	
	MASS (weight)			
g	grams	0.035	ounces	oz
kg	kilograms	2.2	pounds	lb
t	tonnes (1000 kg)	1.1	short tons	
	VOLUME			
ml	milliliters	0.03	fluid ounces	fl oz
l	liters	2.1	pints	pt
l	liters	1.06	quarts	qt
l	liters	0.26	gallons	gal
m^3	cubic meters	35	cubic feet	ft^3
m^3	cubic meters	1.3	cubic yards	yd^3
	TEMPERATURE (exact)			
°C	Celsius temperature	9/5 (then add 32)	Fahrenheit temperature	°F

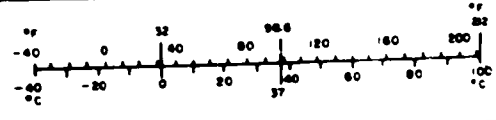

CONTENTS

CONTENTS (Continued)

CONTENTS (Continued)

CONTENTS (Continued)

CONTENTS (Continued)

ILLUSTRATIONS

ILLUSTRATIONS (Continued)

ILLUSTRATIONS (Continued)

ILLUSTRATIONS (Continued)

ILLUSTRATIONS (Continued)

ILLUSTRATIONS (Continued)

TABLES

COMMON ABBREVIATIONS

AAR	Association of American Railroads
AREA	American Railway Engineering Association
B&LE	Bessemer & Lake Erie Railroad
BJR	Bolted joint rail
CPSD	Cross-Power spectral density
CPU	Central processor unit
CSMP	Continuous system modeling program
CU/ASU	Clemson University/Arizona State University
CWR	Continuous welded rail
DOT	U. S. Department of Transportation
FRA	Federal Railroad Administration
Hz	Hertz (cycles per second)
L/V	Ratio of lateral to vertical load
MGT	Million gross tons (traffic)
MU	Multiple unit
NEC	Northeast Corridor (Washington-Boston)
PC	Penn Central Railroad
PSD	Power spectral density - narrow-band mean square value normalized to unity bandwidth
RPI	Railway Progress Institute
SF/BA	Side frame/bearing adapter interface
SP	Southern Pacific Railroad
TDA	Transportation Development Agency (Canada)
TSC	Transportation Systems Center
TTD	Track Train Dynamics Program
UP	Union Pacific Railroad
W/R	Wheel/rail.

1. INTRODUCTION

The Federal Railroad Administration of the U.S. Department of Transportation (DOT/FRA) has sponsored a Track Performance Improvement Program under the technical direction of the Transportation Systems Center. The overall objective of this program is to develop the engineering data and analysis techniques that are needed to design and maintain railroad track with improved safety and serviceability.

The development of a systematic technique for predicting the reliability of rail and other track components is an important part of the track improvement program. Research efforts which are being conducted concurrently within this program are:

- Characterization of rail loads for the range of vehicles, operating and track conditions representing North American railroad service.
- Analysis and design requirements for improved cross-tie railroad track.
- Development of analytical procedures for predicting rail stresses due to the service load environment.
- Development of a rail material failure model to predict the growth characteristics of flaws in rail steels.

The characterization of the rail loading environment is a key factor for all aspects of track performance. The quantitative description of rail loads will be used as inputs to the other concurrent programs on cross-tie track imporvement, rail stress analysis, and rail failure prediction, as well as for other research and testing of rail and track structural components.

The development of a validated predictive technique for wheel/rail (W/R) loads will be used to extend the data base obtained from the measurement phases of this program and to evaluate strategies for reducing those W/R loads which cause significant track damage.

The specific objectives of this wheel/rail load characterization program are:

(1) To provide a description of W/R loads to which North American Track is subjected.

(2) To provide a measurement methodology for the characterization of W/R loads.

(3) To provide a prediction methodology capable of extrapolating W/R load data to alternate track, vehicle, and operating conditions.

(4) To identify alternate stategies for reducing the rate of track degradation through the reduction of W/R loads.

The emphasis of this program is on the use of existing data, analysis models, instrumentation, and data reduction and analysis techniques, wherever these are adequate. A secondary objective of this program is to provide a better evaluation of the operating limits for some of the track and vehicle-borne instrumentation that has been used previously for measuring W/R loads.

This Interim Report includes the results from work on the following Task Items of Contract DOT-TSC-1051:

Item 1: Definition and Organization of Existing Data and Predictive Tools.

Item 4: Evaluation and Selection of Instrumentation.

The major conclusions and recommendations resulting from this work are summarized in Section 2 of this report. A preliminary characterization of the wheel/rail load environment is provided in Section 3, based on currently-available data. This section includes a discussion of track degradation and failure modes as related to loading mechanisms, vehicle and track parameters, and track performance indices. Load-predictive methodologies are addressed in Section 4 with a review of modeling techniques and the available vehicle/track models and load-predictive algorithms. Section 5 provides a review of wheel/rail load measurement requirements, as well as requirements for secondary measurements (displacements, etc.) needed to characterize the vehicle and track. Load measurement instrumentation, data reduction and analysis techniques are reviewed in this section for both trackside and vehicle-borne measurement systems.

Finally, in Section 6, two sample cases are used to illustrate the analytical techniques currently available for predicting wheel/rail loads. These include a digital computer-mechanized simulation of a 100-ton freight car in response to random track geometry variations, and a mathematical model for predicting peak impact forces at a dipped joint. The unsprung masses of a freight car, locomotive, and MU passenger car are used in this model over a typical range of track parameters.

Although this Interim Report is addressed specifically to a technical audience of researchers in the Track Performance Improvement Program, the information contained in the various sections can prove valuable to a much wider audience of readers. The preliminary wheel/rail load environment outlined in Section 3 can, for example, provide information to the track component designer on realistic load levels for mechanical design, as well as for the design of laboratory performance and fatigue experiments. The review of load data formatting in Section 3, and the instrumentation and data reduction techniques in Section 5 can provide the test engineer guidelines for the design of field experiments for the measurement of vehicle or track dynamic response. Indeed, the conclusions and recommendations of this report will provide a basis for the detailed Test Plan for field measurements to be conducted in the later tasks of this contract.

It is the authors' hope that background information contained in this report from a wide range of track load-related subjects will be of benefit to the railroad community as a whole.

2. SUMMARY OF CONCLUSIONS AND RECOMMENDATIONS

The scope of this report includes the following four major technical areas:

(1) The characterization of wheel/rail loads from currently-available field and laboratory measurements.

(2) The prediction of W/R loads using analytical models of vehicle/track interactive dynamics.

(3) The evaluation and selection of instrumentation and data analysis procedures for trackside measurements of W/R loads.

(4) The evaluation and selection of instrumentation and data analysis procedures for vehicle-borne measurements of W/R loads.

Conclusions and recommendations for each of these technical areas and the field measurement pilot program are summarized in this section of the report.

2.1 CHARACTERIZATION OF WHEEL/RAIL LOAD ENVIRONMENT

Wheel/rail load data from a number of available sources from both trackside and vehicle-borne measurements were evaluated to provide an interim characterization of the W/R load environment. Information from many sources was reviewed to identify the important track degradation modes and associated W/R loading mechanisms; to identify the key vehicle, track, operating, and climatic factors affecting W/R loads; and to evaluate the several formats used to present W/R load data.

Track degradation and failure modes provide the key to the W/R load characterization requirements in terms of the desired measurements, data reduction and analysis techniques, and application of results. These modes may be categorized broadly as wear, fatigue, or failure, whereby the track fails to maintain the desired running surface or guidance geometry or fails to maintain

structural integrity. The W/R load characterization must, therefore, provide sufficient information to evaluate the track structural resistance to degradation or failure in any of these several modes.

The results of an evaluation of W/R load mechanisms are summarized in Table 2-1. This review of the major track degradation/failure modes (in the left-hand column of the table) was made to determine the data requirements and applicable vehicle/track models (at the right of the table) best suited as a load-predictive methodology. Intermediate columns summarize the types or sites of occurrence of these particular degradation/failure modes, the important loading mechanisms, and the critical track, vehicle, operating or climatic factors affecting these modes. Specific data requirements and formats best suited for model validation, parameter variation studies, or load- and failure-prediction studies are also given. Track performance indices cited in the table are based on economic performance indicators or safety standards currently in use by the railroads or presently under development by industry or government-sponsored research programs.

The measurement of W/R loads from either trackside or vehicle presents one dimension in a two-dimensional matrix. This is illustrated in Figure 2-1. Wheel/rail loads at each track site are basically a series of pulses for each passing car, and these loads encompass a full spectrum of rail vehicles and vehicle condition. Wheel/rail loads on a specific vehicle are continuous, fluctuating forces covering the broad spectrum of track conditions. Data from many combinations of track sites and vehicles would be needed to completely fill the matrix using measured data. However, available analytical procedures provide a more efficient method for characterizing a wide range of conditions once the analytical procedures have been validated by measurements.

Formats in which the W/R load characterization data are presented depend to a great extent on the specific use of the data. Some projected uses of the load characterization are:

- Validation of W/R load-predictive models
- Validation of track stress and failure-predictive models
- Studies of rail materials and rail reliability

TABLE 2-1. DEFINITION AND ORGANIZATION OF EXISTING WHEEL/RAIL LOAD DATA AND PREDICTIVE TOOLS

	FAILURE OR DEGRADATION MODE	TYPE OR SITE OF TYPICAL OCCURRENCE	LOADING MECHANISM	CRITICAL TRACK AND VEHICLE PARAMETERS
1.	Vertical settlement (random) -ballast flow or failure -subgrade flow or failure	Rail surface geometry (track surface, cross level error) CWR or BJR (mid-rail)	Static wheel loads Vertical dynamic wheel loads	Vehicle static weight Vehicle and suspension design (parameter mean and range) Unsprung mass (vehicle, track) Track stiffness and damping Track geometry Speed Traffic density and consist Ambient factors (temperature, moisture, etc.)
2.	Vertical settlement (discrete) -service-bent rail -tie failure -ballast flow or failure -subgrade flow or failure	Rail surface geometry (track surface, cross level error) Rail joint Grade crossing Special trackwork (turnout, crossing, etc.)	Static wheel loads Vertical dynamic wheel loads Impact loads (joint, frog or crossing impact, flat wheel, etc.)	Vehicle static weight Vehicle and suspension design (parameter mean and range) Unsprung mass (vehicle, track) Track stiffness and damping Rail/joint effective stiffness Track geometry Speed Traffic density and consist Ambient factors (temperature, moisture, etc.)
3.	Alignment deterioration (random) -fastener/tie fatigue or failure -tie shift in ballast -ballast/subgrade flow or failure	Rail alignment geometry (track alignment, gage error) CWR or BJR (mid-rail) Tangent or curved track	Lateral dynamic wheel loads High L/V ratios (per wheel or per truck) Curving forces Lateral components of longitudinal (train-action) forces Thermal (buckling) loads	Vehicle static weight (vertical loads, L/V ratios) Vehicle and suspension design (parameter mean and range) Unsprung mass (vehicle, track) Track lateral stiffness Track geometry Wheel/rail profile geometry Speed Traffic density and consist Ambient factors (temperature, moisture, etc.)
4.	Alignment deterioration (discrete) -fastener/tie fatigue or failure -tie shift in ballst -ballast/subgrade flow or failure -service-bent rail or special trackwork	Rail alignment geometry (track alignment, gage error) Rail joint Spiral (transition curve) Special trackwork (turnout, crossing, etc.) Rail rollover	Lateral dynamic wheel loads Impact loads (flange impact, suspension stops) High L/V ratios (per wheel or per truck) Curving forces Lateral components of longitudinal (train-action) forces Thermal (buckling) loads	Vehicle static weight (vertical loads, L/V ratios) Vehicle and suspension design (parameter mean and range) Unsprung mass (vehicle, track) Track stiffness characteristics Track geometry Wheel/rail profile geometry Speed Traffic density and consist Ambient factors (temperature, moisture, etc.)

TRACK PERFORMANCE INDICES	DATA REQUIREMENTS AND FORMAT	APPLICABLE VEHICLE/TRACK MODEL	FREQUENCY RANGE
Rate of differential settlement vs. wavelength (geometry PSD) Rate of change in track profile "index" (cumulative slope, differential area, etc.) vs. traffic (MGT/yr) Peak and rms W/R loads, component stresses and deflections Track speed limit (TSS)	W/R load PSD vs. frequency (speed/wavelength) W/R load spectral peak value and phase vs. wavelength W/R load rms values (1/3 octave, octave, and wide band) W/R load probability density and distribution vs. range and "mix" of speeds, traffic and track conditions	Linear, frequency-domain vehicle model (Model I)	0.5 - 50 Hz
Priority geometry defect (maximum MCO for surface or cross level per Track Safety Standards) Rate of change of track geometry error vs. traffic (MGT/yr) Peak W/R loads, component stresses, deflections Track speed limit (TSS)	W/R load time-history at given point in track W/R load time-history along track (beneath wheel) W/R peak load probability density and distribution vs. range and "mix" of speeds, traffic, and track condition W/R peak load mean, variance, and skew	Nonlinear, time-domain vehicle model (Model III)	0 - 150 Hz
Rate of change vs. wavelength (geometry PSD) Rate of change in track alignment or gage "index" (mean and variance, differential area, etc.) vs. traffic Peak and rms W/R loads, component stresses and deflections Track speed limit (TSS)	W/R load PSD vs. frequency (speed/wavelength) W/R load spectral peak value and phase vs. wavelength W/R load rms values (1/3 octave, and wide band) W/R load probability density and distribution vs. range and "mix" of speeds, traffic and track conditions	Linear frequency-domain vehicle model (Model I) Quasi-linear, frequency-domain vehicle model (Model II) Quasi-linear, frequency-domain truck hunting model (Model IV)	0.5 - 50 Hz 0.5 - 50 Hz 1 - 50 Hz
Priority geometry defect (maximum MCO for line or gage per TSS) Rate of change of track geometry error vs. traffic (MGT/yr) Peak W/R loads, component stresses, deflections Critical load stability Track speed limit (TSS)	W/R load time-history at given point in track W/R load time-history along track (beneath wheel) W/R peak load probability density and distribution vs. speed, traffic and track) Peak L/V ratio probability density, distribution vs. speed, traffic and track) W/R peak load, peak L/V ratio mean, variance and skew L/V vs. V joint probability	Nonlinear time-domain vehicle model (Model III) Nonlinear time-domain truck hunting model (Model V) Quasi-static, steady-state curving model (Model IX)	0 - 150 Hz 0 - 150 Hz SS

TABLE 2-1. Continued

	FAILURE OR DEGRADATION MODE	TYPE OR SITE OF TYPICAL OCCURRENCE	LOADING MECHANISM	CRITICAL TRACK AND VEHICLE PARAMETERS
5.	Rail running surface geometry deterioration (continuous rail)	Service-bent rail Corrugation Shelling Rail head wear Surface plastic flow Wheel burn	Static and dynamic wheel loads Curving forces Traction/braking forces	Vehicle static weight Rail effective mass Unsprung mass (vehicle, track) Track stiffness and damping Track geometry Wheel/rail profile geometry Speed Traffic density and consist Traction and braking dynamics (adhesion, etc.) Track curvature
6.	Rail running surface geometry deterioration (rail discontinuity)	Rail end batter (joint) Switch point or frog batter or wear Service-bent rail Weld wear (differential)	Static and dynamic wheel loads Impact loads at discontinuity Impact loads (flat wheel)	Vehicle static weight Unsprung mass (vehicle, track) Rail effective mass Track stiffness and damping Rail/joint effective stiffness Wheel/rail profile geometry Track geometry Speed Traffic density and consist
7.	Track component fatigue or failure (continuous rail)	Rail fracture (transverse fissure, split head, head/web separation, etc.) Fastener failure (yield or fracture) Tie failure (plate cutting, fastener shear or pullout, fracture)	Static and dynamic wheel loads Impact loads (flat wheel, hard flange impact, etc.) Traction/braking loads	Vehicle static weight Unsprung mass (vehicle, track) Rail effective mass Track stiffness and damping Wheel/rail profile geometry Track geometry Speed Traffic density and consist Vehicle and suspension design
8.	Track component fatigue or failure (rail discontinuity)	Rail fracture (rail end fracture, bolt hole star crack, etc.) Special trackwork (frog fracture, switch point wear and fracture, etc.) Joint failure (joint bar wear and fracture, loose bolts, blowing or pumping joint, tie cutting, etc.)	Static and dynamic wheel loads Impact loads at discontinuity Impact loads (flat wheel, etc.)	Vehicle static weight Unsprung mass (vehicle, track) Rail effective mass Wheel/rail profile geometry Track discontinuity geometry Speed Track stiffness and damping Traffic density and consist

TRACK PERFORMANCE INDICES	DATA REQUIREMENTS AND FORMAT	APPLICABLE VEHICLE/TRACK MODEL	FREQUENCY RANGE
Rate of change of surface geometry vs. wavelength (PSD) vs. traffic Peak and rms W/R loads Maximum component stress and deflection levels Fatigue-related component stress and deflection levels Track speed limit (TSS)	W/R load PSD vs. frequency (speed/wavelength) W/R load spectral peak value and phase vs. wavelength W/R load rms values (1/3 octave, octave, and wide band)	Linear, frequency-domain truck model (Model VI)	5 - 150 Hz
Maximum component degradation per TSS Rate of degradation vs. traffic (MGT/yr) Peak W/R loads Maximum component stress and deflection levels Fatigue-related component stresses, deflections Track speed limit (TSS)	W/R load time-history at given point in track W/R load time-history along track (beneath wheel) W/R peak load probability density and distribution (vs. speed, traffic and track)	Analytical wheel/rail impact mode (Model VII) Nonlinear, time-domain wheel/rail impact model (Model VIII)	 15 - 2,000 Hz
Component failure criteria per TSS Maximum component stress and deflection levels Fatigue-related component stresses, deflections Rate of degradation vs traffic (MGT/yr) Track speed limit (TSS)	W/R load time-history at given point in track W/R load time-history along track (beneath wheel) W/R peak impact load vs. geometry and speed W/R peak load probability density and distribution vs. speed, traffic and track L/V vs. V joint probability	Nonlinear, time-domain vehicle model (Model III) Nonlinear, time-domain truck hunting model (Model V) Nonlinear, time-domain wheel/rail impact model (Model VIII)	0 - 150 Hz 0 - 150 Hz 15 - 2,000 Hz
Component failure criteria per TSS Maximum component stress and deflection levels Fatigue-related component stresses, deflections Track speed limit (TSS)	W/R load time-history at given point in track W/R load time-history along track (beneath wheel) W/R peak impact load vs. geometry and speed W/R peak load probability density and distribution vs. speed, traffic and track L/V vs. V joint probability	Nonlinear, time-domain vehicle model (Model III) Nonlinear, time-domain truck hunting model (Model V) Nonlinear, time-domain wheel/rail impact model (Model VIII)	0 - 150 Hz 0 - 150 Hz 15 - 2,000 Hz

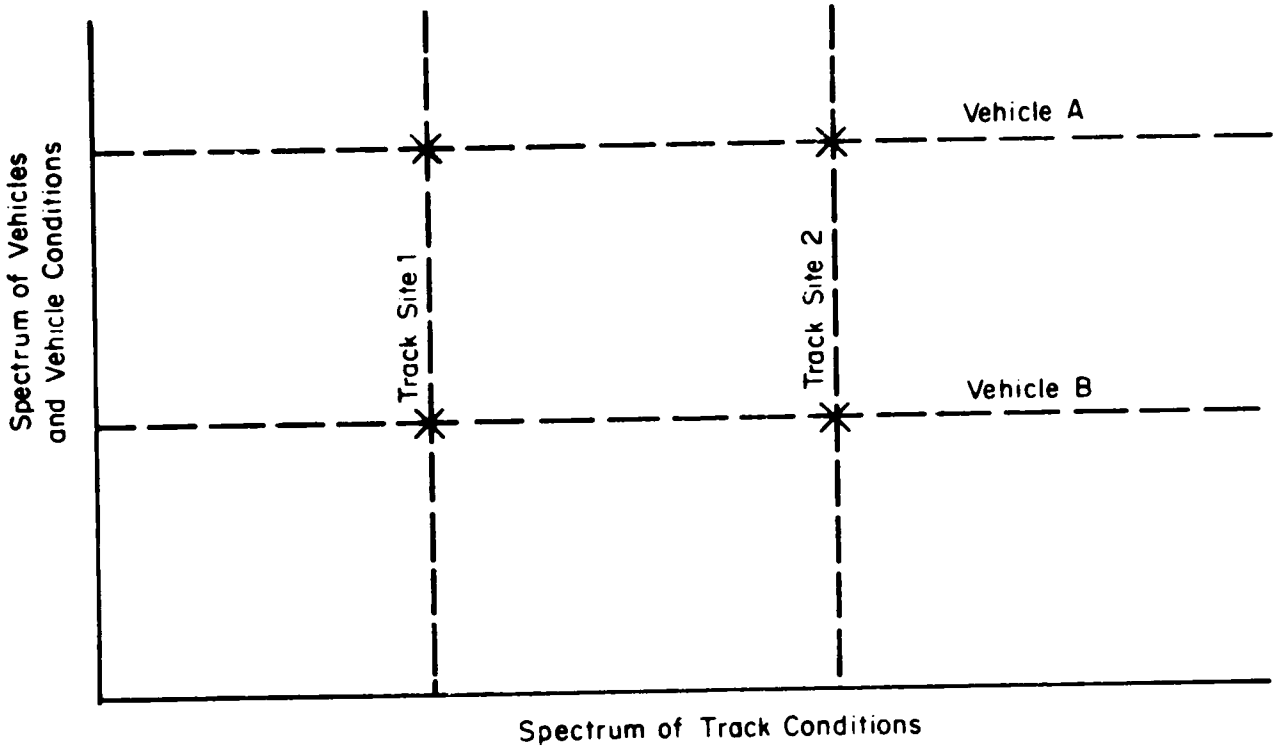

FIGURE 2-1. THE WHEEL/RAIL LOAD MATRIX OF TRACKSIDE AND VEHICLE-BORNE MEASUREMENTS

- Design of track components and structure
- Laboratory fatigue and proof tests of track components
- Design of field experiments for study of vehicle and track fatigue life
- Prediction of load environment with new vehicle or track configurations
- Prediction of track maintenance cycles and costs.

Data formats appropriate for the presentation of W/R loads and associated response measurements (tie plate loads, deflections, accelerations, etc.) are summarized in Table 2-2 under the three generic data categories: the time-domain (time history), frequency-domain (PSD or amplitude spectra), and amplitude statistical descriptions. Some specific uses for data in these particular formats are given. Typical examples of these three basic formats are shown in Figure 2-2 for trackside measurements. Statistical descriptions shown in this figure include the probability density and the cumulative probability distribution functions, which may be plotted for different categories of vehicles, track conditions or operating conditions (speed, for example) to analyze trends due to changes in these variables. Note that statistical data from vehicle-borne measurements show variations in track, while statistical data from wayside measurements show variations in the vehicle population.

Other data reduction methods and data formats have been considered: for example, the several statistical counting methods such as the peak, level crossing, or range pair count. These methods, specific to strain measurements and stress calculations, are inappropriate for relating W/R load to component stress where a linear relationship is not maintained.

While the results of many load measurement programs have been published, these results often lack sufficient detail on the measurement conditions or they use a format that cannot be used directly to validate a load-predictive model, or for analysis of track strength or fatigue life. Most load data consist of a few representative time-histories, a few tabulated peak values, and some qualitative conclusions. Few frequency or

TABLE 2-2. FORMATS FOR PRESENTATION OF WHEEL/RAIL LOAD CHARACTERIZATION DATA

Category	Data Format	Uses of Data in Format
Time Domain Description	Load Time History (Vehicle-Borne Measurements)	Validation of vehicle model in response to track geometry and operating conditions Prediction of W/R load variations along track in response to track geometry Evaluation of dynamic transient response to track geometry anomalies
	Load Time History (Wayside Measurements)	Validation of track model in response to vehicle passage Prediction of track component loads, stresses and deflections due to vehicle passage Evaluation of track dynamic response to track or wheel geometry anomalies
Frequency Domain Description	Power Spectral Density vs. Frequency (speed/wavelength)	Validation of vehicle-track model by comparison with vehicle-borne measurements Evaluation of important vehicle/track resonances and system response to track geometry
	Load Spectral Peak vs. Wavelength and Speed	Prediction of discrete differential settlement in response to random or periodic excitation for specific vehicle and speed (operating condition)
	Static plus One-Sigma (or 3-Sigma) Load vs. Speed	Validation of W/R load-predictive model by comparison with vehicle-borne measurements Description of fatigue-related W/R load environment for predicting track degradation and failure
Amplitude Statistics	Load Probability Density and Cumulative Distribution	Statistical description of W/R load experienced by vehicle over range of track conditions Statistical description of W/R loads experienced by track under range of vehicles and operating conditions Description of W/R loads for cumulative damage calculations and laboratory fatigue tests
	Load Mean and Variance	Statistical indices for description of W/R load environment Description of loads for cumulative damage calculations and laboratory fatigue tests Estimates of track degradation and failure for track, vehicle, and operating parameters
	Load Joint Probability Density	Statistical description of joint occurrence of loads (L/V vs. V, Transverse moment vs. V, etc.) Definition of biaxial load environment for track component and design laboratory test

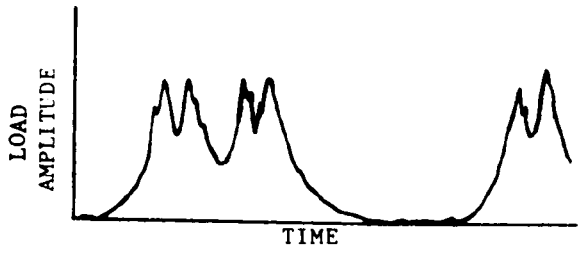

a. Time History Format

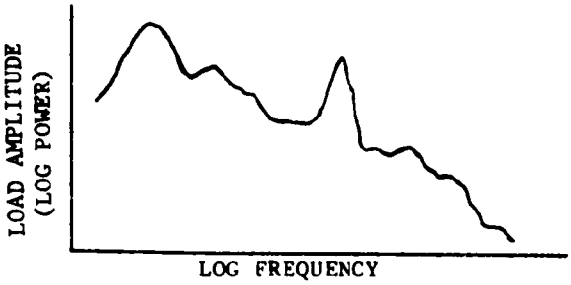

b. Power Spectral Density Format

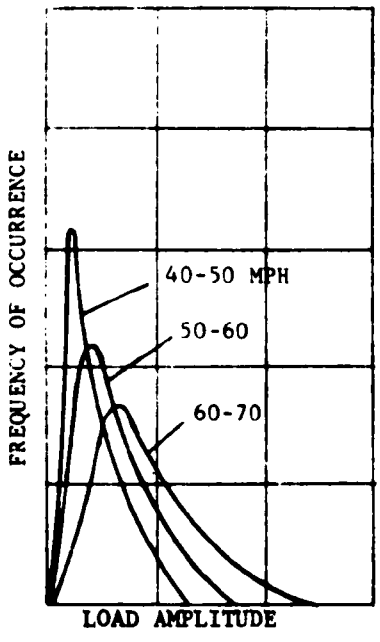

c. Probability Density Format

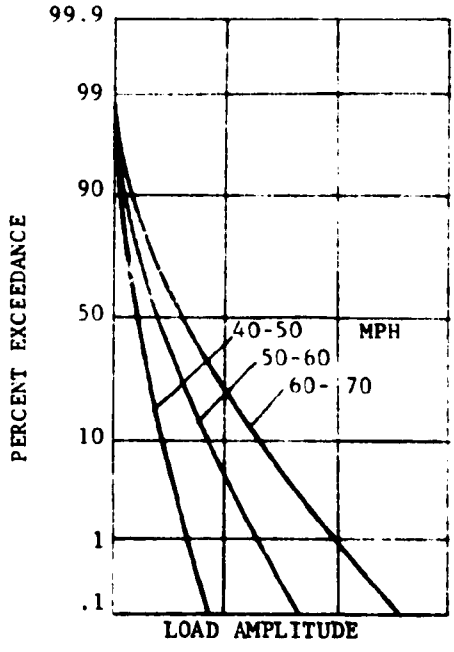

d. Cumulative Probability Distribution Format

FIGURE 2-2. EXAMPLES OF LOAD DATA FORMATS BASED ON TIE PLATE VERTICAL LOAD (WAYSIDE MEASUREMENTS)

amplitude statistical analyses are available, particularly for North American track and operating conditions. Recent vehicle-oriented load measurement programs (see Reference 3-35, for example) have developed load data formats that are directly useful for fatigue studies on vehicle components. These concepts must now be extended to the railroad track, so that a consistent set of data in the basic formats of Table 2-2 can be generated. The field measurement phase recommended for this pilot program is intended to fill in some of the noticeable gaps in the present W/R load characterization in order to validate load-predictive models and to provide a more comprehensive description of the load environment.

2.2 WHEEL/RAIL LOAD PREDICTIVE METHODOLOGY

An extensive review of existing vehicle/track models and analytical load-predictive methodologies was conducted during the early stages of this program. Several of the most promising models and analytical methods were evaluated, and the models or algorithms appropriate to the specific track degradation/failure modes were selected. These are listed generically in Table 2-1, and described more fully in Table 4-1 and Section 4.2.

One important factor in the choice of predictive models or methods is the need by DOT/FRA for immediate results from validated programs. It is apparent from Table 2-1 that the required models can range from linear, frequency-domain to highly-complex, nonlinear, time-domain models, depending on the particular track degradation or failure mode of interest. Several frequency-domain models are immediately available, and one of these has been used to demonstrate the prediction of W/R loads for the 100-ton hopper car as a sample case in Section 6.1. Other more complex models, particularly truck hunting models predicting wheel flange impact forces, and curving models for both transient and steady-state curving force analysis, are currently in the final stages of development and will be available before the end of 1976. Still other models (such as the hybrid, full-vehicle model) are in need of further development and validation.

Most models are "validated" by comparison of one or more model output variables with measured variables from the prototype in response to

specific inputs. Because of the inherent uncertainty in the definition of the prototype vehicle parameters, track parameters and track geometry, the accuracy of validation is frequently questionable. The capability of the model for evaluating parameter changes depends on simulating all the effects for a specific objective.

Applications of the predictive methodologies vary according to the type of model or algorithm and the specific track degradation or failure mode of interest. The linear, frequency-domain models are particularly useful for estimating vehicle/track response and W/R forces due to low-amplitude stochastic track geometry errors (good track), where the linear range of response is not exceeded. These models may be used to evaluate the effects of parameter variations (changes in track stiffness or geometry, train speed, vehicle suspension characteristics, for example) on W/R forces. Transient response to large-amplitude geometry errors that might occur at grade crossings, turnouts or low joints requires the use of a nonlinear, time-domain model for accurate W/R load predictions. Since several track degradation/failure modes result from high-amplitude impact forces, accurate load and failure prediction will depend on the eventual development and validation of these more complex vehicle/track models.

As noted above, the DOT/FRA is vitally interested in predictive methods that can give timely results. On this basis, we recommend that a linear, frequency-domain model be used for the W/R load predictions and track degradation/failure studies until more accurate, nonlinear models are operational and fully validated. Transient and quasi-static curving programs under development at Clemson University should be operational within the time-frame of this pilot study and can serve to predict loads on curved track for comparison with the recommended vehicle tests. In addition, the analytical methods developed by British Rail for predicing W/R impact forces (see Reference 3-4) can be used in the interim period until a detailed, nonlinear wheelset/track model can be obtained or developed.

2.3 INSTRUMENTATION AND DATA ANALYSIS PROCEDURES

2.3.1 Trackside Measurement System

The primary objectives of the trackside measurements in this pilot study are as follows:

(1) To define the statistical characteristics of W/R loads and track dynamic response under revenue traffic

(2) To provide W/R load and track dynamic response time-histories for validating W/R load prediction models

(3) To determine typical track vertical and lateral dynamic characteristics under load

(4) To demonstrate the performance of track and vehicle-borne measurement systems.

Based on the evaluation of current trackside measurement techniques discussed in Section 5.1 and the W/R load data requirements summarized in Section 2.1, a trackside measurement system has been recommended for this pilot study. Specific measurements include W/R loads using strain gages on the rail web, tie loads using instrumented tie plates, rail displacements using displacement transducers, and rail and tie accelerations.

Rail strain gage patterns provide an excellent means for monitoring both vertical and lateral loads on the rail. Because of the very short "influence zone" of these strain gage patterns, the resulting measurement is essentially a sample of load as the wheel passes the measurement point. Some European measurement programs have used long strain gages or have summed the outputs of a number of individual gages to provide a wider measurement zone. However, these methods entail problems with reduced sensitivity and indeterminant load paths. A method for combining the signals from strain gage patterns and tie plate load cells to provide a longer vertical W/R load measurement zone is described in Section 5. It is desirable to have a continuous measurement of vertical W/R load over at least one-half an average wheel revolution so that the probability density of high-impact loads (flat

wheels) for the total wheel population can be determined. Continuous measurement over a relatively long zone will aid in the determination of the special characteristics of the W/R load, which cannot be obtained from the narrow pulse of a single strain gage measurement zone. (It is also important to measure W/R loads over a short section, say 6 to 10 inches in length, to determine the statistical character of the W/R load, which cannot be obtained from the narrow pulse of a single strain gage measurement zone.

The dynamic loading of uniform tangent track can be assumed to be randomly distributed along the track, with equal probability of peak loads occurring at any given point. If a significant track geometry disturbance is present in the immediate vicinity, however, the spatial location of the peak loads is then deterministic rather than random, and the location then depends on the vehicle/track response to the geometry error. In this case, measurements made at a single point in the track are not sufficient to characterize the load environment, and several measurement points must be chosen based on vehicle/track response wavelengths and desired spatial resolution.

A statistical characterization of any trackside measurement (tie plate load, for example) will combine the statistical variations due to several distinct causes. These include:

- The vehicle population (statistical characteristics of the train consists, which may vary by the day of the week or seasonally)
- Variations in vehicle parameters within one class of vehicle (manufacturing tolerances, maintenance level)
- Variations in operating techniques (train speed, train handling)
- Variations in ambient conditions (wet rail vs. dry rail, for example).

Spatial variations can also influence the measurements, resulting in some uncertainty in the statistical characterization of results from a

single location. These include:

- Constructional variations within an otherwise uniform section of track
- Track dynamic impedance variations from one location to another or from one season to another (ambient changes)
- Track geometry deterministic or random variations.

The choice of the number of measurement locations for achieving a desired statistical confidence level can be influenced by several of these factors -- tie plate loads, for example, may be strongly influenced by constructional variations within a given test zone. Based on the discussion in Section 5, an adequate measurement of mean tie plate load can be established with 4 to 6 adjacent measurement locations. Similar statistical criteria can be used to determine the number of data points needed for amplitude statistics based on the required resolution (range of data and range subdivision or "bin" size) for probability density and the estimated size of the population in the smallest subcategory (vehicle type, speed range, track condition, train handling, et cetera).

The site selection criteria for this pilot study indicate that the following types of sites are recommended for wayside measurements:

(1) High-speed tangent CWR track of good geometry (Class 5 or 6), uniform tie and ballast conditions, general freight traffic, 20-30 MGT/yr traffic density.

(2) Curved track of good geometry (Class 5 or 6) with 3^{o} to 6^{o} curves of long duration, uniform tie and ballast conditions, general freight traffic, 20-30 MGT/yr traffic density.

On uniform track of good geometry, the response of revenue traffic will be random in nature and greater confidence can be placed in the statistical analysis. Measurements will include vertical and lateral W/R loads; rail-to-tie vertical, lateral and rotational displacements; tie-to-"ground" vertical and

lateral displacements; tie plate vertical load and transverse moment; and rail and tie vertical accelerations. Although tie plate lateral load measurements are desirable to define the lateral load distribution in the "influence zone", it is judged that the available lateral load-measuring tie plates significantly affect the rail/tie load bearing characteristics of wood tie track. The development and construction of an improved lateral load-measuring tie plate is recommended for future programs of this type.

2.3.2 Vehicle-Borne Measurement System

The primary objectives for the vehicle-borne measurements are to provide sufficient data for validation of the load-predictive methodologies recommended in Section 2.2 and to measure typical W/R loads over a variety of track conditions. Vehicle-borne measurements can provide a more direct comparison with predicted values in defining vehicle/track dynamic response to track geometry than can the wayside measurements.

An evaluation of current vehicle-borne W/R load measurement techniques was conducted, and a vehicle-borne system was chosen to meet the requirements for both validation of models and W/R load characterization. The recommended instrumentation system consists of a 100-ton freight car truck on which suitable transducers have been applied for the measurement of vertical and lateral W/R forces. One vehicle is recommended for the pilot study: a 100-ton, 50-foot car of the type used in the B&LE studies (see Reference 3-36) or the recent DOT/TSC wheel thermal strain measurements on the Union Pacific Railroad. Most measurements will be made with the car loaded to capacity, although a few runs should be made with the empty car to provide a validation of the analytical model at another load level.

Vertical and lateral W/R loads occur over a wide range of frequencies, from the static and quasi-static (curving) forces, to car body-induced oscillations in the 0.5 to 7 Hz range, to higher-frequency truck and axle-induced oscillations ranging well above 100 Hz. It is recommended that vertical forces from static weight, curve negotiating and low-frequency

(rigid body) oscillations be measured by strain-gaged side frames, which will provide the average vertical load on front and rear wheels of one side of the truck over a bandwidth from 0 to roughly 10 Hz. For measuring higher-frequency vertical loads (with a bandwidth up to perhaps 100 Hz, depending on the effective wheel rim mass), a single wheelset will be instrumented with strain gages spaced at 15^{o} intervals on the wheel plates. A single wheelset is used on the premise that there is no statistical difference in the magnitude of the higher-frequency loads at the leading or trailing wheels, and this assumption will be checked by running the wheelset in both directions. Lateral loads will be measured from bending strains in the axles using strain gages spaced at 60^{o} intervals. This will provide a low-frequency force measurement system, but since the loaded car is expected to run stably within the normal speed range, higher-frequency W/R loads from flange impact will occur infrequently. Higher-frequency vertical and lateral load information will be derived from the track measurements.

The instrumented vehicle will be run at several different speeds over sections of track (including the wayside measurement sites) having more-or-less uniform characteristics with sufficient length for good data averaging. Track sections should include tangent track, curved track, CWR and bolted-joint track, as well as discrete features such as turnouts and crossings. Track geometry measurements will be required to define the inputs to the load-predictive computer model, so that a direct comparison between measured and computed response may be made. An event mark will be provided on the analog recordings on-board when passing the wayside site (an optical or magnetic location detector) to correlate the two sets of data. Analog time-histories of wayside and vehicle-borne loads can then be compared directly.

3. PRELIMINARY CHARACTERIZATION OF WHEEL/RAIL LOADS

This section of the report provides a preliminary characterization of wheel/rail loads for North American track and traffic conditions, to be used as an interim specification until more extensive and more refined measurements are completed. To provide a background to the wheel/rail load characterization, track degradation and failure modes are reviewed in the context of loading mechanisms, frequency content and load range, and critical track and vehicle parameters. Track performance indices based on the common degradation and failure modes are also discussed in this section. Finally, the wheel/rail load characterization based on available data is reviewed in two basic categories: data from track-side measurements, and data from vehicle-oriented measurements, with representative load data formats illustrated for each category.

3.1 TRACK DEGRADATION AND FAILURE

3.1.1 Loading Mechanisms

Rail loads include the vertical, lateral, and longitudinal wheel forces from rail vehicles, plus the slowly-changing forces from the thermal environment. These rail loads are reacted by forces and torques at the rail fasteners, rail anchors, and tie plates or pads, and they are transmitted through the complex load paths of this indeterminant structure to the ties, ballast, and subgrade. The forces transmitted through the wheel/rail interface are:

(1) Vertical forces due to the vehicle static weight, and dynamic forces from wheel irregularities and the response of vehicle and track to track geometry irregularities,

(2) Lateral forces from the vehicle response to track geometry irregularities, components of longitudinal train-action forces, external disturbances such as wind forces, self-excited hunting motions, and the creep and flange forces necessary to guide the vehicle through curves,

(3) Longitudinal forces due to traction, braking, and wheel/rail creep.

It is important to realize that railroad track is a complex structure, and that the tie reactions (fastener and tie plate forces and moments), rail deflections, and rail bending moments are dependent not only on the overall track stiffness in the different loading directions, but also on localized variations in support stiffness. With a specified wheel load applied to rail having uniform tie supports, the portion of the load transmitted to individual ties is determined by the rail bending stiffness and the effective stiffness of the track at each tie. A single tie directly under the load carries typically from 30 to 60 percent of the vertical W/R load and from 60 to 80 percent of the lateral W/R load, with almost all the vertical load supported by this tie and the four immediately-adjacent ties. The track overall (or "driving point") dynamic impedance affects the magnitude of W/R forces caused by the dynamic interaction of vehicle and track. Variations in support conditions from one tie to the next cause considerable variation in support reactions and rail bending stresses, and (if support is very poor) may produce variations in W/R load due to geometry changes under load. Consequently, the rail loading environment is a function both of track conditions and the variety of vehicle types and operating conditions representing normal railroad traffic.

3.1.1.1 Vertical Rail Loads

Vertical loads at the wheel/rail interface are characterized by an average value representing the car static weight, with fluctuations about this level due to the dynamic interaction between car and track. Maximum static wheel loads range typically from 6400 lb (small, empty freight cars) to 40,000 lb (125-ton-capacity freight cars on 4 axles) in North American operations, with locomotive static wheel loads typically 25,000 to 33,000 lb. Standard practice for track design is to use the maximum expected static wheel load, then increase this value by a speed-dependent impact factor (typically 50 to 100 percent) to arrive at an equivalent design wheel load that includes dynamic effects. Axle spacing and distance between truck

centers for the adjacent ends of two coupled cars are also needed to determine the superimposed loads on the track. Axle spacings on freight cars range typically from 54 to 72 inches, while truck centers on two adjacent cars may range from 145 to 355 inches apart. These values are needed to predict the overall bending moments and deflections of the rail for vertical loads.

In most cases the car body (sprung-mass) dynamics of a well-designed rail vehicle operating on good track will result in minor variations in vertical W/R load. On poor track with large geometry errors, however, the motion limits of even a good suspension system may be exceeded, and high load variations will then be transmitted to the track. One of the best-publicized problems [3-1] in freight car body dynamics has been the 100-ton hopper car rocking phenomenon. This is a car resonance problem where the in-phase roll excitation of cars having 39-foot truck centers operating on staggered low joints of 39-foot bolted rail lengths produces a harmonic rocking sufficient to lift wheels and derail cars. Severe car rocking can cause centerplate separation and spring groups to go solid, so that peak vertical W/R loads well in excess of twice the static load can be generated. Peak vertical wheel loads in the 70,000 to 80,000 lb range have been measured [3-2] and predicted by computer simulation [3-3].

In addition to this well-documented case, other examples of car body dynamics may be cited. Severe vertical bounce sufficient to completely unload the spring groups, in the 50-60 mph speed range on staggered-joint track, has been observed with 50-ton loaded hopper cars. Heavily-loaded cars (coil steel cars, for example) may bounce sufficiently hard, particularly at grade crossing with poor surface geometry, to "bottom-out" on the springs. Occasionally, car body-bending dynamics are sufficiently severe to also cause high W/R loads. For example, a 70-ton pulpwood car was observed to respond at the car center with a 2-Hz, 1 G peak oscillation at its critical speed, which would result in a dynamic W/R load factor approaching two.

The dynamic response of the wheelset (unsprung mass) on the track mass and stiffness is critical in the generation of W/R impact forces. Rail surface anomalies such as joints, frog and crossing flangeways, and surface or wear patterns such as corrugations cause high W/R vertical forces and rail contact stresses. Analytical work by British Rail [3-4] has described

joint impact forces in terms of the "P1" short-duration impact about one-half millisecond at the joint, followed by the longer-duration "P2" force (5 to 10 milliseconds) with a peak in the vicinity of the running-on tie. Depending upon train speed and rail geometry, these impact forces may range typically up to 5 times the static wheel load.

Wheel flats are another important source of vertical impact loads. Measurements by the Japanese [3-5] on the New Tokaido Line have shown an increase in rail vertical bending stress of nearly 3 over the static stress, with rail vertical accelerations as high as 600 G. Estimated wheel impact loads up to 90,000 lb (for a 25,000 lb static load and a 4-1/2 inch flat) were projected from rail strain measurements conducted by the AAR [3-6]. An example of flat wheel impact loads recorded at tie plate load cells is shown in Figure 3-1, while in Figure 3-2 the wheel flat loads recorded on a vehicle are illustrated. In both examples the peak W/R contact force has been attenuated by the mass between the contact patch and the measurement point; in Figure 3-1 by the rail effective mass, and in Figure 3-2 by the wheelset mass.

Quasi-static vertical wheel loads may increase significantly when operating at unbalance speeds on curved track, particularly on the low rail at speeds well under the curve balance (equilibrium) speed. For example, the vertical wheel load of a 125-ton capacity car running at low speed on a curve with a 6-inch superelevation would increase from 40,000 to 53,500 lb static.

3.1.1.2 Lateral Rail Loads

While the wheelset (unsprung mass) is strongly coupled to the rail vertically through the wheel/rail contact stiffness, it is only weakly coupled to the rail laterally (up to the point of flange contact) through creep forces and gravitational stiffness. Creep forces are generated by the relative motions of wheel and rail which occur between pure rolling and pure sliding, while gravitational stiffness forces are dictated by wheel set and rail contact geometry and relative displacement. The combination of these lateral forces may be outwardly or inwardly-directed on the rail, and are generally less than a few thousand pounds per wheel.

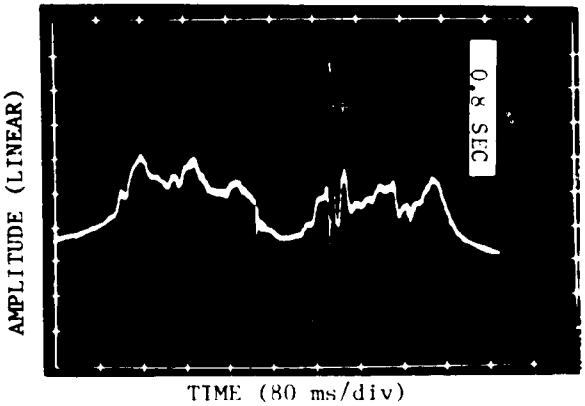

TIME (80 ms/div)

a. Tie Plate Load Transient Under Flat Wheel on Locomotive

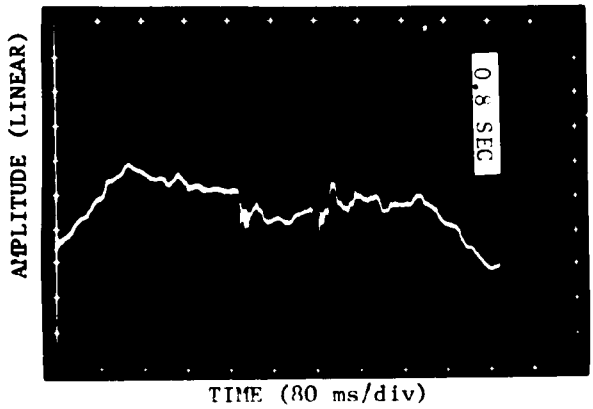

TIME (80 ms/div)

b. Rail Vertical Displacement Transient Under Flat Wheel on Locomotive

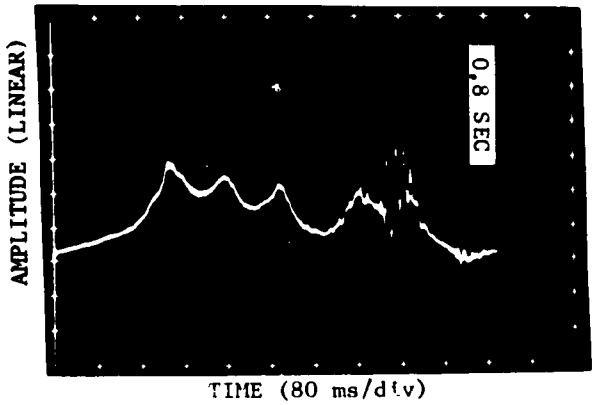

TIME (80 ms/div)

c. Tie Plate Load Transient Under Heavy Car (Adjacent to Locomotive)

FIGURE 3-1. EXAMPLES OF TRACK DYNAMIC RESPONSE TO IMPACT LOADS FROM FLAT WHEELS ON LOCOMOTIVE AND FREIGHT CAR

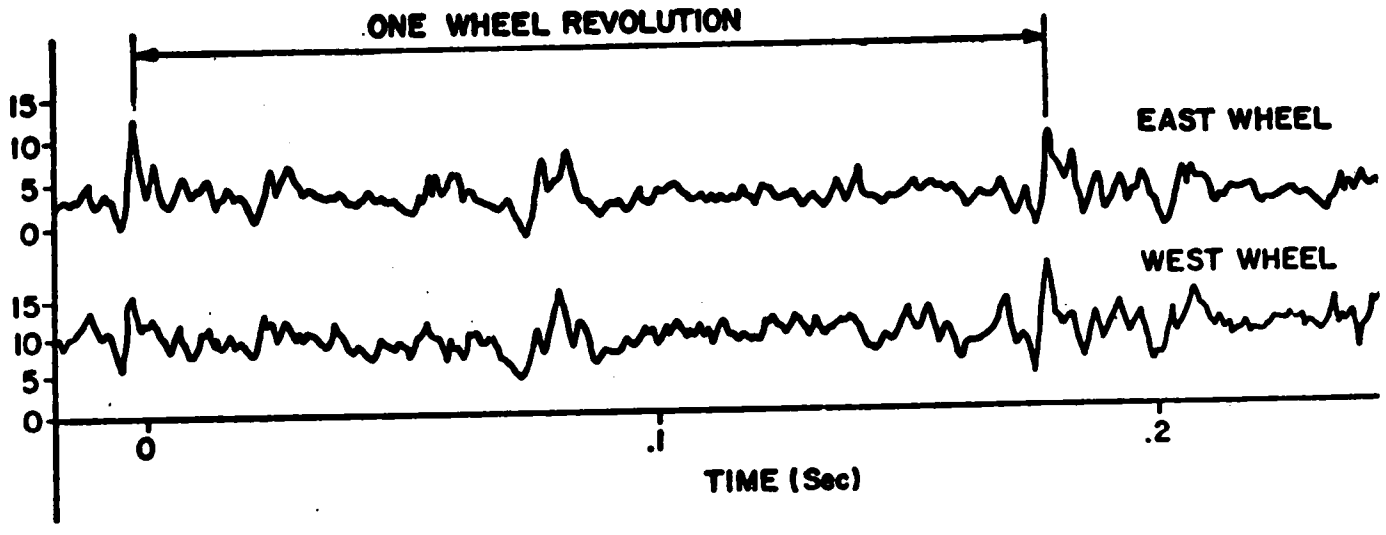

FIGURE 3-2. VERTICAL LOADS AT SIDE FRAME/BEARING ADAPTER LOAD CELLS FOR WHEELS WITH 2-INCH FLAT SPOTS [Ref. 3-35]

Rails can be subjected to large lateral loads by vehicle hunting on tangent track. Wheelsets are prone to a dynamic instability called secondary, or "truck", hunting when a "critical speed" is exceeded. At speeds above a critical speed wheelset oscillations will increase in amplitude to a stable, nonlinear limit cycle with flange-to-flange impacts. The critical speed for truck hunting is dependent upon a number of truck suspension and wheel/rail geometry parameters, and is particularly sensitive to the effective wheel taper or conicity. Freight cars, particularly empty or lightly-loaded cars on roller-bearing-equipped trucks, can hunt violently at speeds as low as 35 miles per hour if wheels are badly worn. Measurements of dynamic gage increase from hard flange contact from hunting trucks has indicated (from measured track lateral stiffness) that these impact forces, with time-durations as high as 250 milliseconds, may range up to 20,000 lb lateral [3-7]. Recent lateral force measurements on Northeast Corridor track have recorded single-axle forces under hunting freight cars as high as 23,000 lb, with an estimated L/V ratio greater than 1.0, and a pulse time-duration of 50 milliseconds.

Defects in track alignment can also induce severe lateral impact loads, particularly with rail vehicles having design or maintenance deficiencies. Measurements at track alignment disturbances on the Northeast Corridor track have recorded peak lateral loads up to 55,000 lb on a single axle, with an L/V ratio greater than one, and a pulse time-duration typically 50 to 100 milliseconds, under electric locomotives. Total truck lateral forces in excess of 75,000 lb (a truck L/V ratio as high as 0.8) were also recorded. Severe impact loads can occur at switch points and frogs or guard rails in high-speed operation, and high lateral loads can be induced in a turnout or crossover.

Operating on curved track usually produces the highest quasi-static lateral loading on the rail. This includes both the creep and slippage forces at the wheel/rail contact zone and the lateral forces from flange contact. Lateral forces on curves include a component known as the "base curving" forces, to which additional forces due to centrifugal acceleration, coupler angularity, and track geometry irregularities are superimposed. The base curving forces occur even when the vehicle is operating at the balance speed for a specified curvature and superelevation. They represent the

creep forces between the wheel and rail that are caused by the deviation of the axles from a pure rolling position due to the restraint from the truck primary suspension. Lateral forces imposed during curving are different for each of the wheels of a truck. This is illustrated in Figure 3-3, which shows the typical W/R forces on a 4-wheel freight car truck during curving. Variations in the lateral quasi-static rail force depends on track curvature and operating speed in terms of net unbalance. Dynamic loads are superimposed on these load levels, as shown in Figure 3-4, where the loads from the lead axle of a truck going through a reverse curve from 4° 54' to 6° 20' are recorded.

Lateral components of longitudinal train-action loads can cause high rail loads on curved track. Tests conducted by the Southern Pacific Railroad to measure lateral and vertical W/R loads under heavy grade and curved-track operating conditions recorded lateral loads in excess of 40,000 lb and L/V ratios greater than 1.0 [3-8]. Buff loads from the high adhesion on sanded rail typical of dynamic braking operations can often produce lateral wheel loads over 30,000 lb. In addition to these dynamic forces, rail in curves is subject to lateral components of the thermal compressive load which may combine with dynamic loads under extreme conditions to cause track buckling.

3.1.1.3 Longitudinal Rail Loads

Rail forces from thermal loads are the principal longitudinal loads that have been included in conventional track design procedures. However, the longitudinal forces from locomotive traction, and the braking forces of both locomotives and cars do contribute to the rail load environment and consequent wear and damage. Longitudinal shear forces are particularly important in curves because they have been identified as a contributor to rail shelling. The coefficient of adhesion is sensitive to rail surface condition, track curvature, rail profile, speed, and weight transfer. Under sanded, dry-rail conditions, the coefficient of adhesion can approach 0.4 [3-9], and a longitudinal W/R force component approaching 13,000 lb may be generated. Gross wheel slip upon loss of adhesion, unless quickly corrected, can result in damage to the rail surface through thermal effects

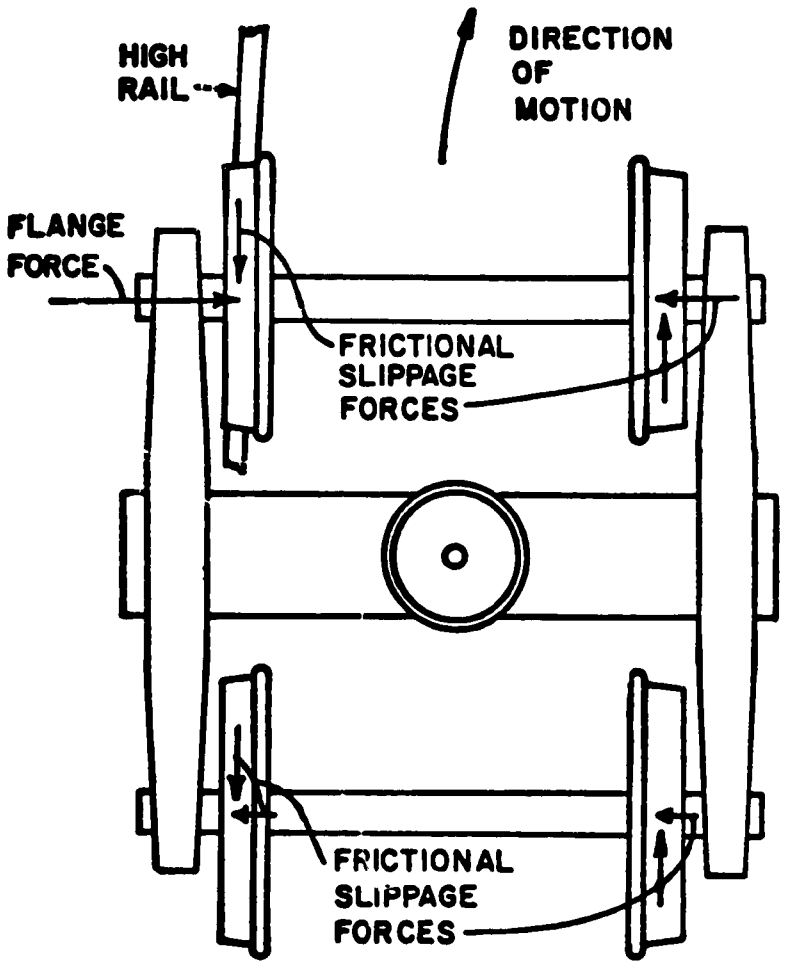

FIGURE 3-3. CURVED TRACK FREIGHT CAR TRUCK FORCES AT WHEEL/RAIL INTERFACE

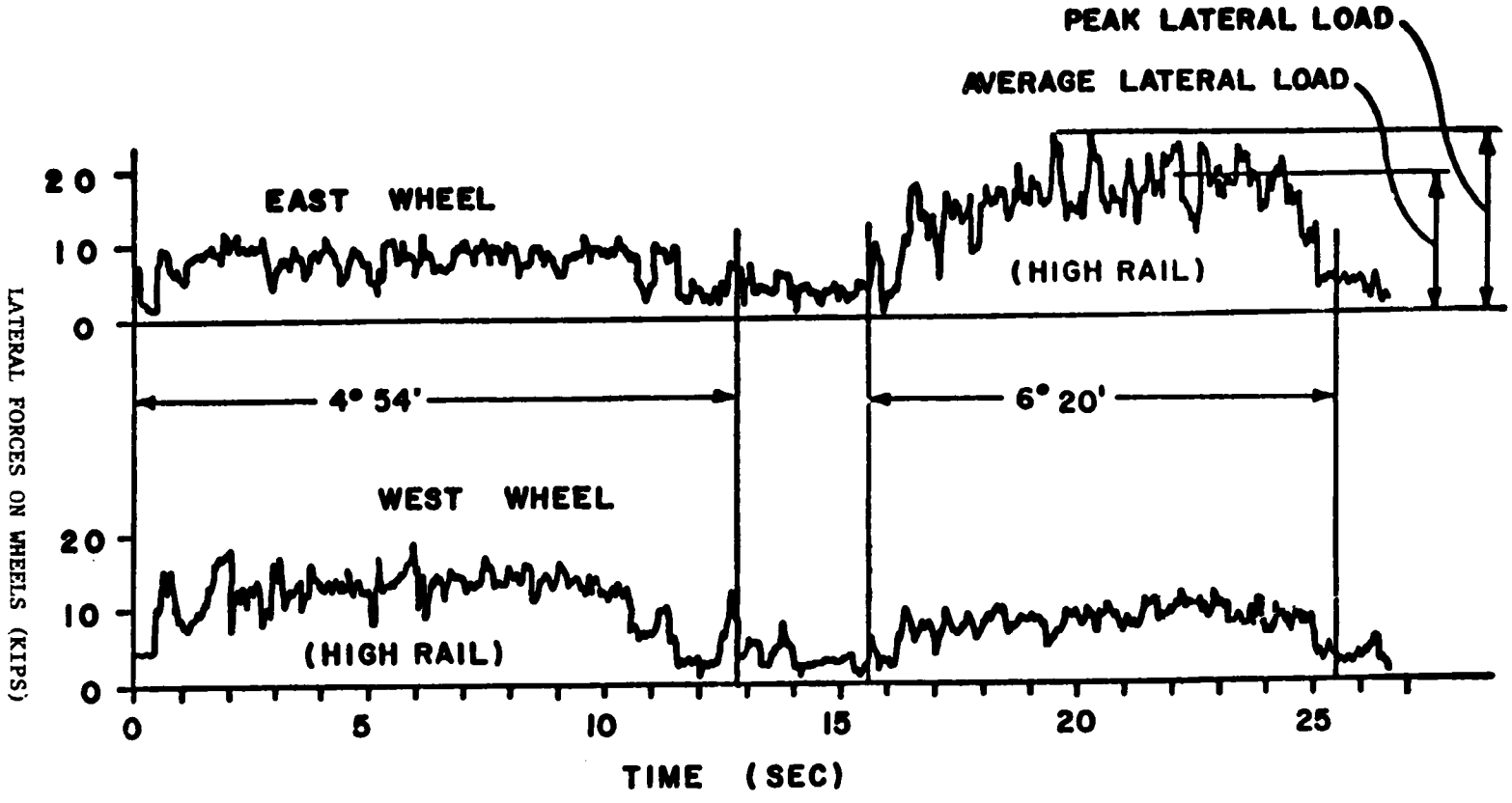

FIGURE 3-4. EXAMPLE OF LATERAL WHEEL LOADS ON LEAD AXLE OF FREIGHT CAR TRUCK TRAVERSING CURVES (35 MPH) [Ref. 3-35]

(wheel burn). This involves the dynamic response of the wheelset, traction motors, gears, and wheel slip control system.

Few longitudinal force measurements have been cited in the literature. The AREA has reported forces up to 16,200 lb ahead of a 5,000-ton train under a full service application of brakes, while maximum longitudinal tensile forces due to tractive effort (under pusher units) were 35,100 lb [3-10]. Battelle has measured rail anchor loads under traction as high as 4300 lb; but due to the complex load path in securing the rail, the actual rail load cannot be determined accurately.

3.1.2 Degradation/Failure Modes

The overall track structure and individual track components are subjected to a wide spectrum of loading conditions and may deteriorate or fail in a variety of modes. As a first step in the development of predictive techniques for W/R loads, the most important generic categories of track and component degradation and failure modes were reviewed, and are listed in Table 3-1. In each of the eight categories are listed specific subcategories of degradation or failure for illustrative purposes.

New track construction will display both random and periodic variations in track geometry due to construction techniques and tolerances. As traffic passes over the track, both random and periodic differential settlement may occur that affects track surface and cross level geometry, due to variations in ballast or subgrade, ties or rail stiffness (at a joint, for example). Geometry spectral components can be accentuated by the dynamic interactions between vehicle and track, and excitation near a vehicle natural frequency can produce a rapid deterioration of both vehicle and track. An example of the track geometry which causes "rock and roll" of 100-ton freight cars (staggered-joint track having deteriorated rail joints) as shown by the track profile measured under load in Figure 3-5.

Random and periodic track geometry may be described by a "geometry power spectrum", shown for example in Figure 3-6, which provides a measure of the frequency content of the mean-square displacement error [3-11]. Periodic phenomena such as rail joints at 39-foot intervals show up as spectral peaks in the curve, even on CWR track laid on old ballast (the "ballast

TABLE 3-1. TRACK DEGRADATION AND FAILURE MODES

1. Vertical Differential Settlement (Random or Periodic)
   - Track surface geometry, BJR
   - Track surface geometry, CWR
   - Track cross level geometry, BJR
   - Track cross level geometry, CWR

2. Vertical Differential Settlement (Discrete)
   - Rail joint, BJR
   - Rail joint, CWR
   - Grade crossing
   - Bridge or structure
   - Special trackwork (turnout, crossing, etc.)

3. Alignment Deterioration (Random or Periodic)
   - Track alignment geometry, BJR
   - Track alignment geometry, CWR
   - Track gage deterioration, BJR
   - Track gage deterioration, BWR
   - Track gage deterioration, curved track

4. Alignment Deterioration (Discrete)
   - Rail joint, BJR
   - Rail joint, CWR
   - Spiral or curve geometry
   - Special trackwork (turnout, crossing, etc.)

5. Rail Running Surface Geometry Deterioration (Continuous Rail)
   - Service-bent rail
   - Corrugation
   - Shelling
   - Rail head wear
   - Rail surface plastic flow
   - Wheel burn

6. Rail Running Surface Geometry Deterioration (Rail Discontinuity)
   - Rail end batter
   - Switch point or frog batter or wear
   - Service-bent rail
   - Weld differential wear
   - Special track work (crossing, etc.)

7. Track Component Fatigue or Failure (Continuous Rail)
   - Rail rollover
   - Rail fracture (transverse fissure, etc.)
   - Fastener failure (yield or fracture)
   - Tie failure (plate cutting, fastener shear or pullout, splitting or fracture, etc.)

8. Track Component Fatigue or Failure (Rail Discontinuity)
   - Rail rollover
   - Rail fracture (rail end fracture, bolt hole star crack, etc.)
   - Special trackwork (frog or switch point fracture, etc.)
   - Joint failure (joint bar fracture, loose bolts, etc.)
   - Weld fracture

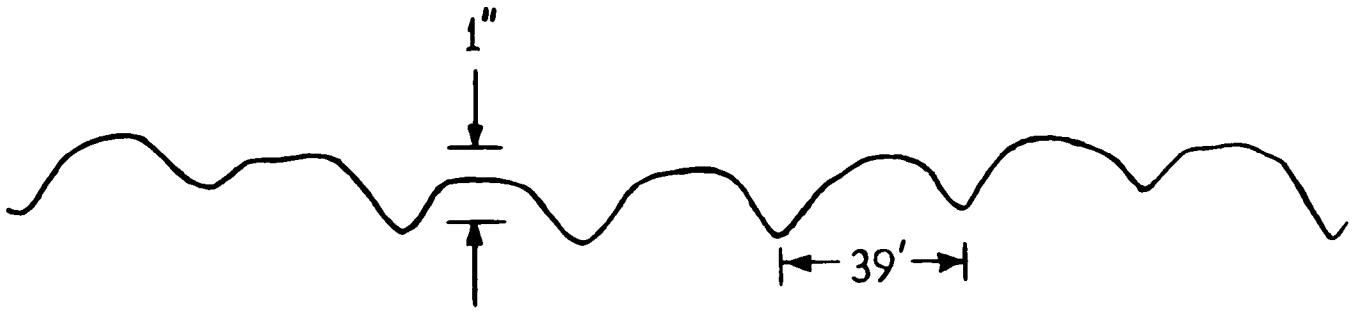

FIGURE 3-5. MEASURED RAIL SURFACE PROFILE, BOLTED-JOINT TRACK IN POOR CONDITION

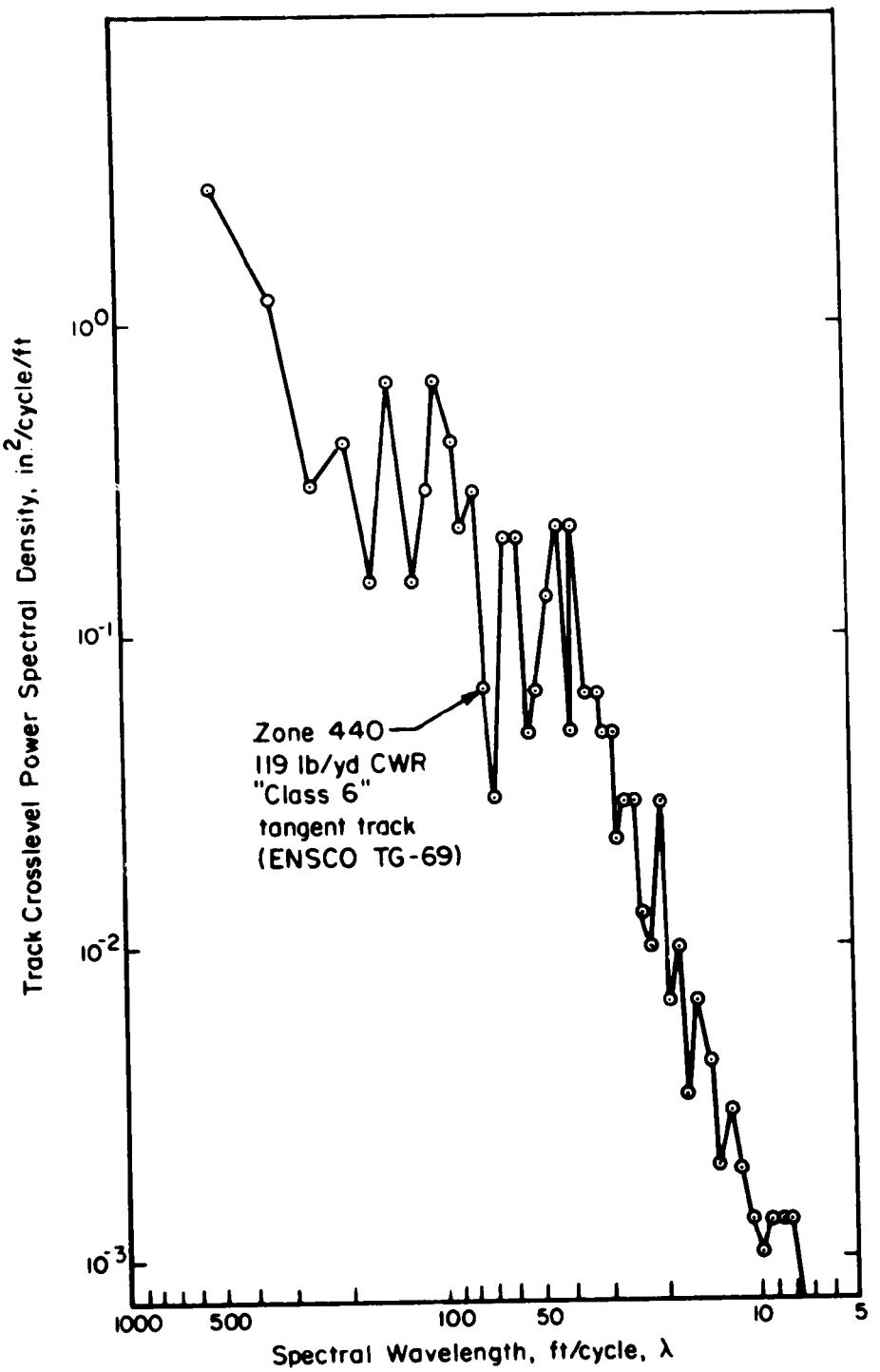

FIGURE 3-6. TRACK CROSS LEVEL GEOMETRY POWER SPECTRUM DERIVED FROM TRACK SURVEY DEVICE ON "CLASS 6" CWR TANGENT TRACK

memory " effect). It is interesting to note that while the geometry spectrum is accentuated at some wavelengths due to periodic loading by specific vehicles and differential settlement of the track, it may be statistically "smoother" at the nodal wavelengths of these vehicles [3-12], which may account for the "valleys" in the PSD plots. Comparison of geometry PSD plots taken from the same track over a period of several years may verify this hypothesis.

Alignment and gage of the track may also deteriorate in both random and periodic variations due to constructional techniques and the interaction between vehicle and track. High lateral loads on the track may cause deterioration of ties or fasteners, or may shift the track in the ballast. For example, Battelle has observed occasional sinusoidal alignment patterns of approximately 100-foot wavelength during recent measurements of track forces on Northeast Corridor track. These can probably be attributed to excitation of the yaw natural frequency of the older electric locomotives used in passenger service on this line. Freight car truck hunting with randomly-occurring, high lateral impact forces, has been found to contribute to the generation of wide gage on tangent, high-speed track [3-13].

Discrete vertical settlement is often noted at the approaches to bridges and other structures, where sudden changes in track overall stiffness occur, or at grade crossings, switches or crossings, where drainage problems can produce differences in subgrade and ballast moisture content and stiffness. The degradation of bolted rail joints is recognized universally as a major track problem. The standard bolted rail joint is more flexible structurally than the continuous rail, even when the joint is new and the bolts are tight. In service the joint loosens, reducing the effective stiffness at this point in the rail. Impacts at the joint can produce degradation typified by rail end batter, service-bent rail, tie plate cutting, and pumping or blowing of fines.

Degradation of the rail running surface geometry may also occur in a random or periodic fashion. Long wavelength corrugations (typically 8 to 30 inches in length) have in recent years become a serious problem for railroads involved in unit train operations with 100-ton freight cars. Although the causes of corrugation are still unresolved, recent publications [3-14, 3-15] have advanced several theories in track-train dynamics, wheel/rail

geometry and metallurgy to explain the formation of these rail surface waves.

Finally, track failure may occur through fatigue and fracture of components, particularly the rail itself. An excellent review of these failures is contained in the book by Srinivasan [3-16]. In recent years the phenomenon of rail rollover has become an important track failure mode, particularly with the increasing use of heavy locomotives with three-axle trucks. Current research by the Association of American Railroads (AAR) is investigating rail rollover from simultaneous lateral and longitudinal loads to determine if rail buckling is a significant factor for rail rollover.

To establish which degradation/failure modes (and therefore which predictive methods or models) should receive greatest emphasis, an approximate priority ranking of the modes in Table 3-2 was undertaken. To provide a basis for evaluation, two separate categories were chosen for ranking the modes: (1) economic - a comparison of the estimated cost impact of the modes, and (2) safety - a ranking of modes by importance to catastrophic failure and possible loss-of-life due to track-related accidents. Sources of relative cost and accident frequency included trade magazines [3-17, 3-18], the NEC High-Speed Rail Passenger Improvement Project [2-19], and AREA sources [3-20]. The results of this approximate priority ranking are tabulated in Tables 3-2 and 3-3 in order of descending priority. The emphasis from the economic and safety viewpoints may, indeed, be decidedly different.

3.1.3 Frequency Content and Ranges

The development of techniques for prediction of W/R loads requires different types of vehicle/track analytical models for the different frequency ranges that are characteristic of the different loading mechanisms affecting track damage. The specific frequencies of interest for the causal mechanisms and degradation modes are discussed in this section of the report.

There are three major frequency bands of interest for the generation of W/R loads through vehicle/track interaction. The first of these, from 0 to 15 Hz, includes static loads and the sprung-mass dynamics of the vehicle such as car body bounce, pitch, roll or yaw, and the lower-frequency body bending modes, and truck frame resonances. A second frequency band, from about 15 to 150 Hz, includes the resonances of the vehicle unsprung

TABLE 3-2. APPROXIMATE RANKING OF TRACK DETERIORATION/FAILURE MODES BY ECONOMIC FACTORS

Rank in Order of Priority
1. Vertical Differential Settlement (Random or Periodic)
2. Alignment Deterioration (Discrete)
3. Vertical Differential Settlement (Discrete)
4. Alignment Deterioration (Random of Periodic)
5. Rail Running Surface Geometry Deterioration (Rail Discontinuity)
6. Track Component Fatigue or Failure (Rail Discontinuity)
7. Track Component Fatigue or Failure (Continuous Rail)
8. Rail Running Surface Geometry Deterioration (Continuous Rail)

TABLE 3-3. APPROXIMATE RANKING OF TRACK DETERIORATION/FAILURE MODES BY SAFETY FACTORS

Rank in Order of Priority
1. Track Component Fatigue or Failure (Rail Discontinuity)
2. Track Component Fatigue or Failure (Continuous Rail)
3. Rail Running Surface Geometry Deterioration (Rail Discontinuity)
4. Vertical Differential Settlement (Discrete)
5. Alignment Deterioration (Discrete)
6. Alignment Deterioration (Random or Periodic)
7. Vertical Differential Settlement (Random or Periodic)
8. Rail Running Surface Geometry Deterioration (Continuous Rail)

(wheelset) masses on the track overall stiffness, typically 20 to 30 Hz, plus some resonant frequencies inherent in the track structure. Finally, a third frequency band of interest, from 150 to 2000 Hz, covers the frequencies of the track and wheelset that are excited by transient impacts. These are characterized by the rail effective mass oscillating on the wheel/rail contact stiffness.

Because of ride quality considerations, rail passenger vehicles have sprung-mass resonant frequencies in the 0.7 to 1.5 Hz range. Typical freight car natural frequencies as measured by the Canadian Pacific Railway [3-21] are somewhat higher. Some of these values are listed in Table 3-4 for several common freight car configurations.

Experimental work by the C&O/B&O [3-22] on the vibration environment of a 70-ton boxcar showed low-frequency resonances to vary from 2.0 to 4.3 Hz, depending upon load and spring group friction damping values. Because of the friction snubbers, the freight car "sprung mass" resonant frequency is quite amplitude-dependent. For example, using typical 100-ton freight car suspension and track vertical stiffness values, the frequencies may vary as follows:

	Locked (low amplitude)	Sliding (high amplitude)
Bounce	9 to 18 Hz	1.9 to 2.4 Hz
Pitch	12 to 25 Hz	2.6 to 3.3 Hz

Measurements of track dynamic response to traffic, particularly through tie plate vertical loads, rail vertical and lateral displacements, and subgrade pressures, have defined the more pronounced resonant frequencies due to track and unsprung mass dynamics. Important observed frequencies from measurements on the Northeast Corridor track [3-23, 3-24] of 140 lb/yd CWR included 25-30 Hz, 45-70 Hz, 100-130 Hz, and 150-170 Hz. Noticeable oscillations in subgrade pressure were recorded in the 45-50 Hz range.

Recent measurements on Union Pacific track of 133 lb/yd CWR [3-13] were examined by means of a real-time frequency analyzer, and important spectral peaks in vertical tie plate load were found in the 15-19 Hz and

TABLE 3-4. NATURAL FREQUENCIES OF SOME HEAVY FREIGHT CARS (REFERENCE 3-21)

Car Type	Gross Weight, lb.	Natural Frequency, Hz			
		Bounce	Pitch	Roll	Twist
LPG Tank Car	86,320	4.4	5.8	0.8	-
	217,540	3.2	4.2	0.9	-
100T Covered Hopper Car	59,000	5.8	7.4	1.0	-
	262,500	3.3	5.7	0.7	-
	256,060	2.8	4.3	1.1	-
80T Open-Top Hopper Car	51,980	5.2	5.2	1.7	4.8
	204,700	3.0	3.9	1.3	4.0
89 Container Car	62,540	8.0	12.5	2.2	9.5
100T "Bathtub" Coal Cars	54,700	5.7	5.7	0.9	4.0
	272,640	2.8	4.9	0.9	-
-With C-PEP-	271,580	3.1	4.9	1.3	-

47-53 Hz ranges. Spectra for a typical transient event and the average for the complete train are shown in Figure 3-7. Similar spectra from data recorded during wintertime (frozen ballast) conditions showed the higher-frequency peak to fall more typically in the 60-68 Hz range. A track lateral resonance was found in the measurement of dynamic gage (the relative lateral motion of the rail heads) falling between 18 and 20 Hz under locomotives and heavy cars, and as low as 16 Hz (and sometimes a strong 50 Hz) under the caboose. This spectral peak was particularly pronounced, as shown in Figure 3-8, when the rail temperature was high and the track in compression. At these train speeds the "axle pass" pulse repetition frequency may typically range from 10 to 20 pulses per second, which tends to excite both vertical and lateral resonances in the track.

Recent experimental work on field measurement of track dynamic impedance [3-25] has shown the track vertical resonance under preloads ranging up to 15,000 lb (but without the additional unsprung mass of a wheelset) to fall between 30 and 45 Hz on typical branchline track with light (85 lb/yd) rail.

Higher-frequency resonances have been measured at the rail by use of both accelerometers and strain gages. A particularly strong frequency component in the 700-800 Hz range has been recorded for rail response to joint impact and wheel flats on 132 lb/yd BJR track [3-23]. Other measurement programs have also observed this rail resonance [3-26], which may be due to the effective rail mass on the wheel/rail contact (Hertzian) stiffness. British investigators [3-4] have recorded the "P1" impact force at rail joints with a typical pulse duration time of less than one millisecond. Other frequencies due to localized structural resonances of rail, fasteners, or even the vehicle wheel plate have been observed [3-27].

Low frequency W/R force components due to vehicle sprung mass dynamics are important in the generation of longer wavelength track geometry errors due to differential settlement or track shift. Mid-range frequency components (including the joint-impact "P2" force peak) are detrimental to track components, producing fastener and tie fatigue and failure, service-bent rail, and ballast degradation (particularly at joints), as well as (possibly) generating corrugations in the rail. High-frequency components of W/R force (including the "P1" impact component) produce both surface and

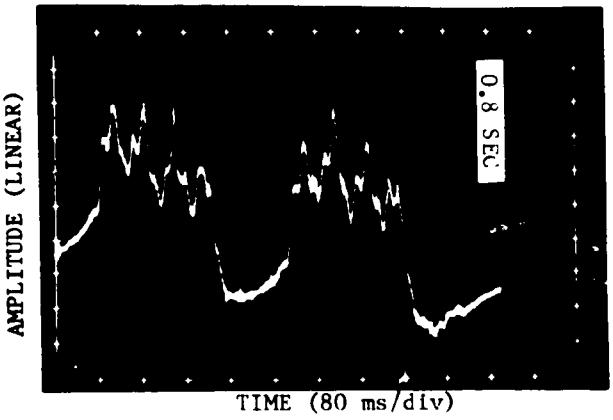

a. Tie Plate Load Transient (Adjacent 4-Axle Trucks)

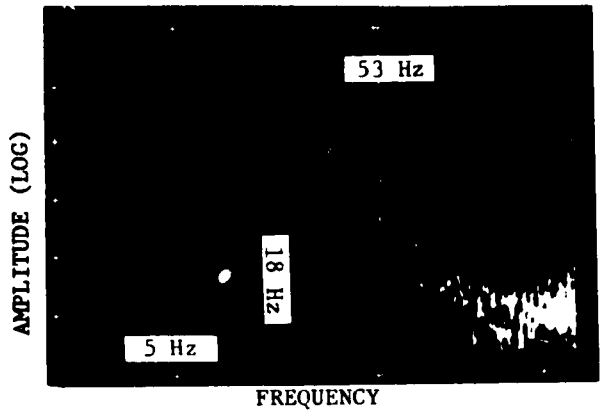

b. Amplitude Spectrum of Transient (Under Locomotive Trucks)

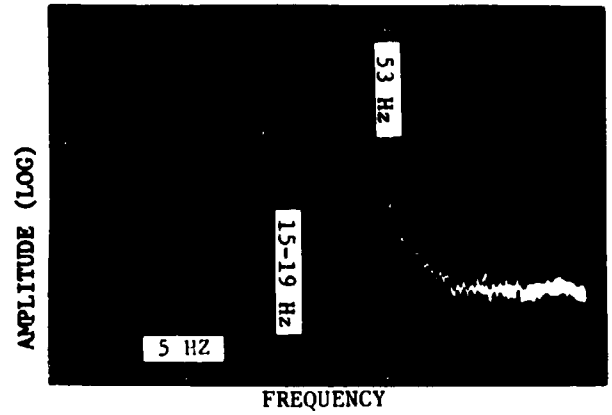

c. Average of Tie Plate Load Spectra (Complete Train, Run 44A)

FIGURE 3-7. SPECTRAL ANALYSIS OF TRACK DYNAMIC RESPONSE, RAIL TEMPERATURE 53° F, TRAIN SPEED 63 MPH, 133 LB/YD CWR TRACK

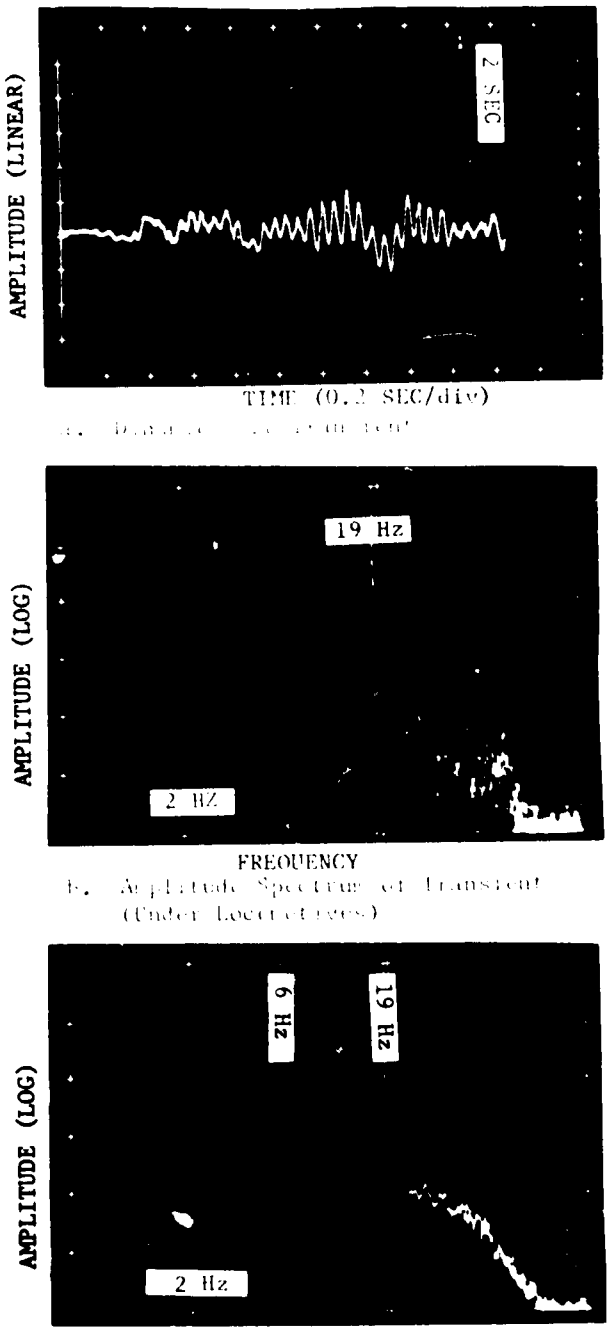

FIGURE 3-8. SPECTRAL ANALYSIS OF TRACK DYNAMIC RESPONSE, RAIL TEMPERATURE 114° F, TRAIN SPEED 73 MPH, 133 LB/YD CWR TRACK

interior rail flaw growth, and may be of importance in both fastener and tie fatigue and failure.

3.1.4 Critical Track and Vehicle Parameters

The identification of those track and vehicle parameters which have the greatest influence on each damage mode is an important step in selecting analytical models for predicting wheel/rail loads, and in developing cost-effective strategies for improved design, maintenance or operating practices. From the standpoint of W/R loads, the most important single parameter is track geometry. On a perfectly smooth and straight, uniformly supported track, the dynamic W/R loads (except for instabilities such as truck hunting and, of course, wheel flats) would be minimal. At the primary level of analysis, the track and the vehicle may each be viewed as a "black box" interacting one to the other through the track geometry. The track may be characterized at this level by a driving-point impedance representing the dynamic response of the track to a W/R load applied at the rail head. On a second level of analysis where the forces, stresses or displacements of the vehicle or track are important for a detailed study of system response, a more detailed analytical model and more complete representation of internal parameters becomes necessary.

The loading at rail joints represents a complex type of track loading because there is a combination of low and high frequency response which contributes to different modes of joint degradation. The standard bolted rail joint is more flexible structurally than continuous rail even when the joint is new and the bolts are tight. As the joint degrades, the resulting dip presents a severe irregularity in the vertical rail profile that produces high dynamic impact forces as the wheel crosses the joint to impact on the running-on rail. These impact loads excite response in two frequency ranges, from 15 to 80 Hz, and from 500 to 2000 Hz. The dynamic system which is responsible for these forces is determined primarily by the effective mass of the rail in the local impact zone (about one foot), the unsprung mass of the vehicle, the nonlinear contact stiffness at the wheel/rail interface, and the track overall stiffness and damping.

British Rail has done considerable work on developing an analytical model for predicting rail joint forces [3-4]. This event presents a good example for defining some of the critical track and vehicle parameters in W/R load generation. Time-histories of typical rail forces and bolt-hole strains due to joint impact loads are shown in Figure 3-9. When the car wheel crosses a dipped joint, a very short duration impact force P1 occurs first, followed by a second peak force P2, which occurs at a relatively long time-period later. The P1 force typically occurs about 1/4 to 1/2 millisecond after the wheel passes the rail end. The dynamic force may actually drop below the static momentarily if a substantial gap or batter zone exists. The P2 force peak typically occurs 6 to 8 milliseconds later, near the running-on tie. Track and vehicle parameters which have a major influence on the magnitude of P1 and P2 forces, based on the data reported by British Rail, are summarized in Table 3-5 Reducing vehicle speeds and reducing the joint dip angle by improving its structural rigidity are two obvious ways to reduce joint loads, but both have severe practical limitations based on economics.

Track forces developed by vehicle/track response to long wavelength geometry errors are dependent more on the sprung mass dynamics of the vehicle. The static axle load is, of course, a critical parameter. Aside from this, the vehicle geometry, masses and inertias, suspension parameters, and even the cargo dynamics can be important in the generation of W/R loads. One of the more important suspension parameters is the limit of suspension travel before contacting hard stops. High W/R forces can result if vehicle response to track geometry exceeds these limits.

Since for W/R load prediction the track may be characterized as a dynamic "driving point" impedance, the critical track parameters are stiffness, damping, and effective mass at a given excitation frequency. Track vertical stiffness presents a nonlinear, "hardening" force/deflection curve as a result of inherent slack (constructional irregularities) between rail and tie, and in the ballast itself. Track "modulus", the stiffness of the supporting structure beneath the rail in force per length squared, has traditionally been derived from the secant force/deflection characteristic of a track from unloaded (or lightly loaded) to fully loaded:

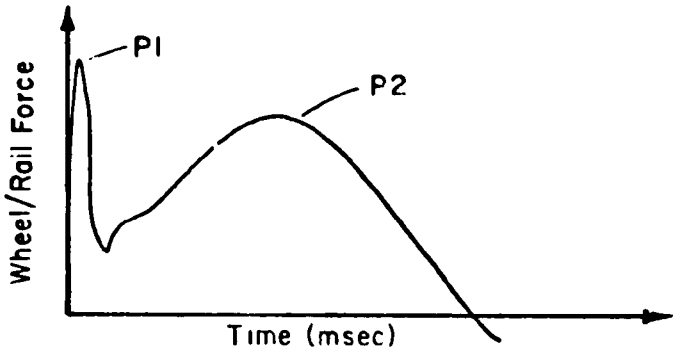

a. Rail Force at Joint Impact

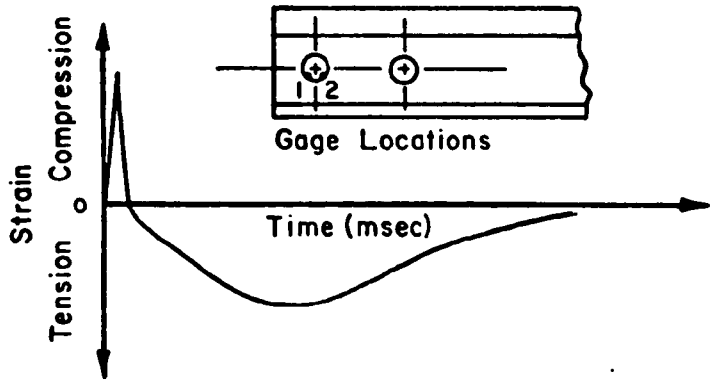

b. Strain Measured at No. 1 Gage

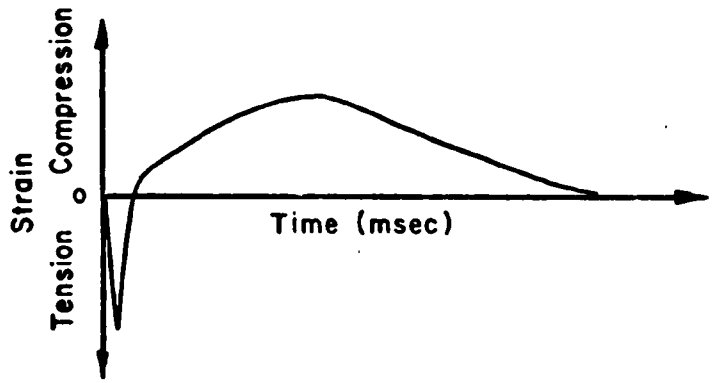

c. Strain Measured at No. 2 Gage

FIGURE 3-9. TIME HISTORIES OF RAIL FORCE AND BOLT HOLE STRAIN MEASUREMENTS FROM JOINT IMPACT

TABLE 3-5. PARAMETERS WHICH HAVE A MAJOR EFFECT ON RAIL JOINT LOADS

Parameter	Joint Loads	
	P_1	P_2
Vehicle Unsprung Mass	No*	Yes
Track Stiffness	No	Yes
Track Damping	No	Yes
Track Effective Mass	No	Yes
Rail Effective Mass	Yes	No
Primary Suspension	No	No**
Vehicle Speed	Yes	Yes
Joint Dip Angle/Joint Deflection	Yes	Yes
W/R Contact Stiffness	Yes	No
Static Wheel Load	Yes	Yes

* Except for very low mass.
** Only if very stiff.

$$U = \sqrt[3]{(P/y)^4/64EI} \quad \text{, track modulus (per rail),} \tag{3-1}$$

where P = point load (or difference between light and heavy loads)
y = rail vertical defection (or difference in deflections)
E = Young's modulus of rail material
I = rail area moment of inertia .

Track modulus values range typically from 1000 (poor track) to 5000 lb/in/in for wood tie track in good condition, and values as high as 13,000 lb/in/in have been noted for concrete-tie track [3-28]. This latter value would correspond to a secant stiffness of 775,000 lb/in per rail to a point load. Track deflection under a point load can be calculated ideally from the equations for a beam on an elastic foundation, as shown in Figure 3-10:

$$Y = \frac{P\,\beta}{2\,U}\left[e^{-\beta X}(\cos\beta X + \sin\beta X)\right] \quad \text{, vertical deflection} \tag{3-2}$$

where $\beta = (U/4EI)^{0.25}$
X = distance along rail from point load, P .

Load and deflection measurements under traffic have shown the non-linear behavior of track "stiffness" and deflection. Typical test data are compared in Figure 3-11 with the ideal deflection curves for adjacent axle loads of empty or loaded freight cars.

Tangent stiffness has been estimated at several track locations based on load and deflection data. On Northeast Corridor track (140 lb/yd CWR), tangent point-load stiffness ranged from 340,000 to 580,000 lb/in, depending on several factors. Typical data ranged as follows:

	Percent Vertical Load on Tie Plate	Tangent Stiffness, lb/in
Moderate Load (14,000 lb)	22 to 26	340,000 to 390,000
Heavy Load (31,000 lb)	29 to 33	460,000 to 580,000
Unsettled Tie (tamped)	41 to 46	350,000 to 490,000

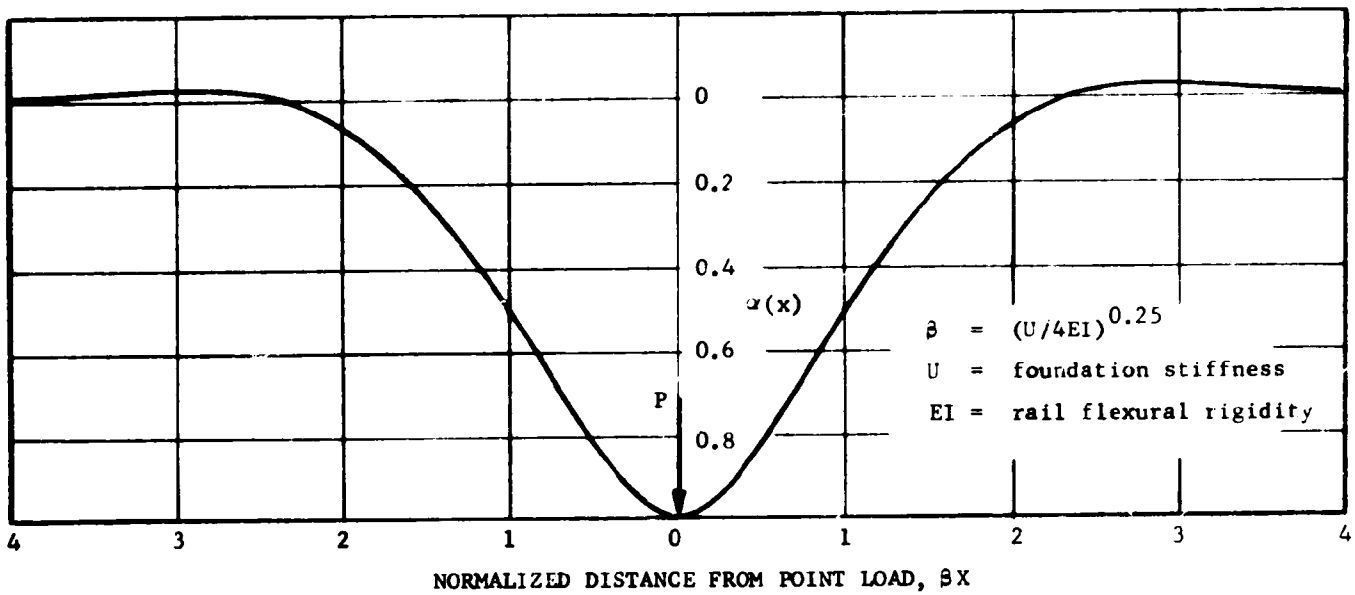

FIGURE 3-10. IDEAL RAIL DEFLECTION SHAPE DUE TO POINT LOAD, P, AS A FUNCTION OF NORMALIZED DISTANCE, βX

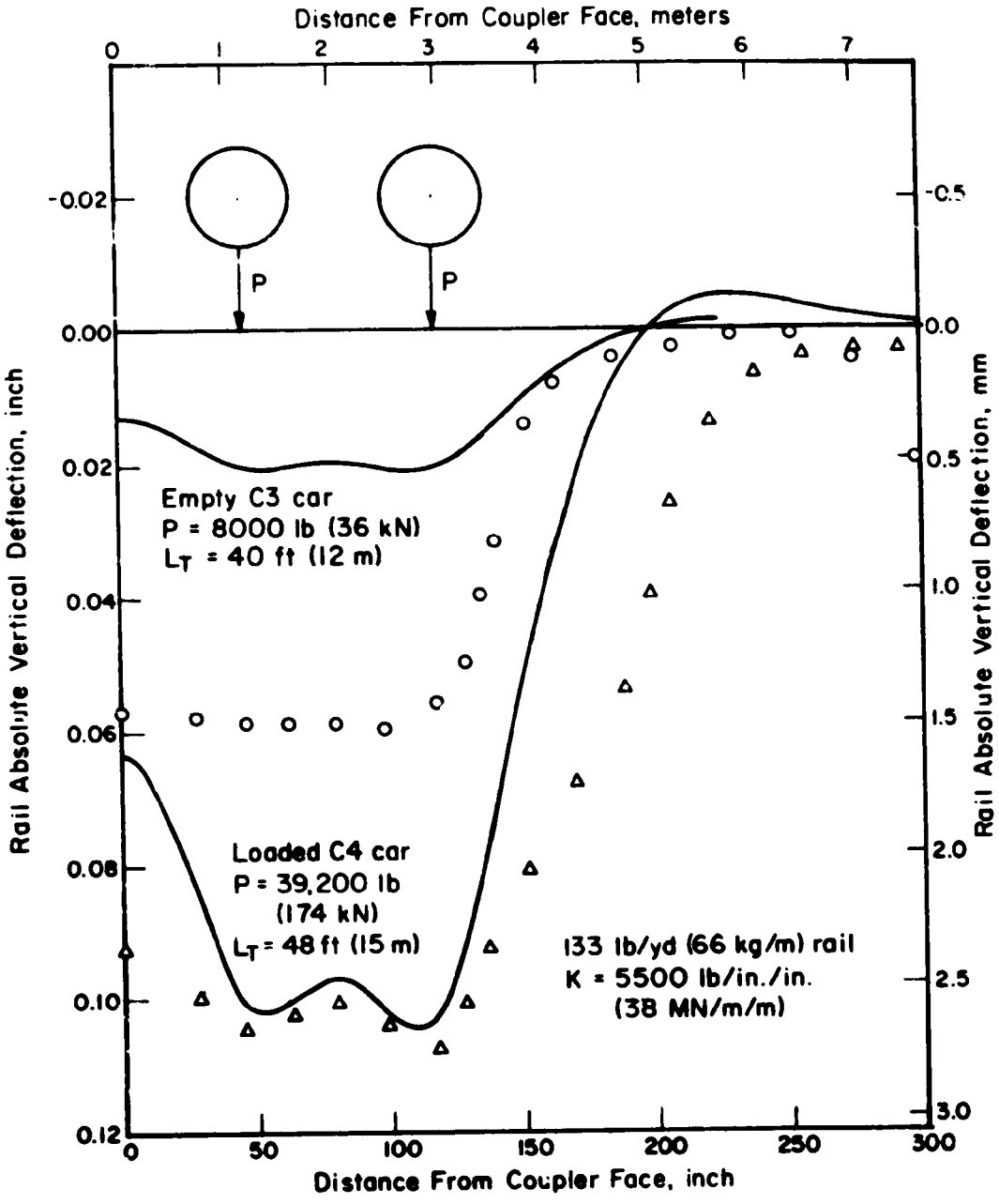

FIGURE 3-11. COMPARISON OF IDEALIZED (LINEAR BEAM ON ELASTIC FOUNDATION) AND MEASURED RAIL DEFLECTION SHAPES UNDER WHEEL LOADS OF COUPLED CARS

On Union Pacific track in Idaho, measurements were made during summertime and wintertime (frozen ballast) conditions. The following range of data was estimated from deflections under heavy wheel loads:

	Summer	Winter
Secant stiffness (heavy wheel load)	290,000	425,000 lb/in
Tangent stiffness (heavy wheel load)	520,000-660,000	650,000-920,000 lb/in

The rail joint, depending on condition, presents a less stiff structure. The idealized ratio of joint stiffness to continuous rail stiffness is shown in Figure 3-12 for two assumed joint conditions. Measurements at a "typical" joint on Northeast Corridor track showed a stiffness of 13,500 to 19,000 lb/in until roughly 0.2 inch of slack was taken up, and a stiffness between 120,000 and 160,000 lb/in for further deflections.

Track damping consists of a combination of hysteretic loss and energy dissipation into a half-space. Both theoretical studies [3-29] and field measurements [3-25] have indicated that track damping is typically between 15 and 50 percent of critical, based on the effective track mass and stiffness. Response of track to flat wheel impacts recorded in Idaho [3-13] would indicate damping toward the higher end of this range. The effective track mass calculated during dynamic impedance measurements [3-25] is also higher than previously estimated, ranging from 2500 to 5500 lb/rail on the particular branchline track evaluated. Although tangent stiffness was found to increase with higher preload (wheel load), the effective mass also increased, so that track natural frequency did not increase significantly.

Track lateral dynamic characteristics are considerably more complex than the vertical. Up to the point of flange contact, the wheel is rather weakly coupled laterally to the rail through the creep forces and gravitational stiffness. Critical parameters are the wheel/rail contact geometry, vertical load and vehicle forward speed. After contact with the flange, the track consists of a nonlinear (or at best, piecewise linear) spring in the lateral direction, in series with a Coulomb friction element (the ties in the ballast). Both the stiffness and friction damping "element" are highly dependent in value on the vertical wheel load.

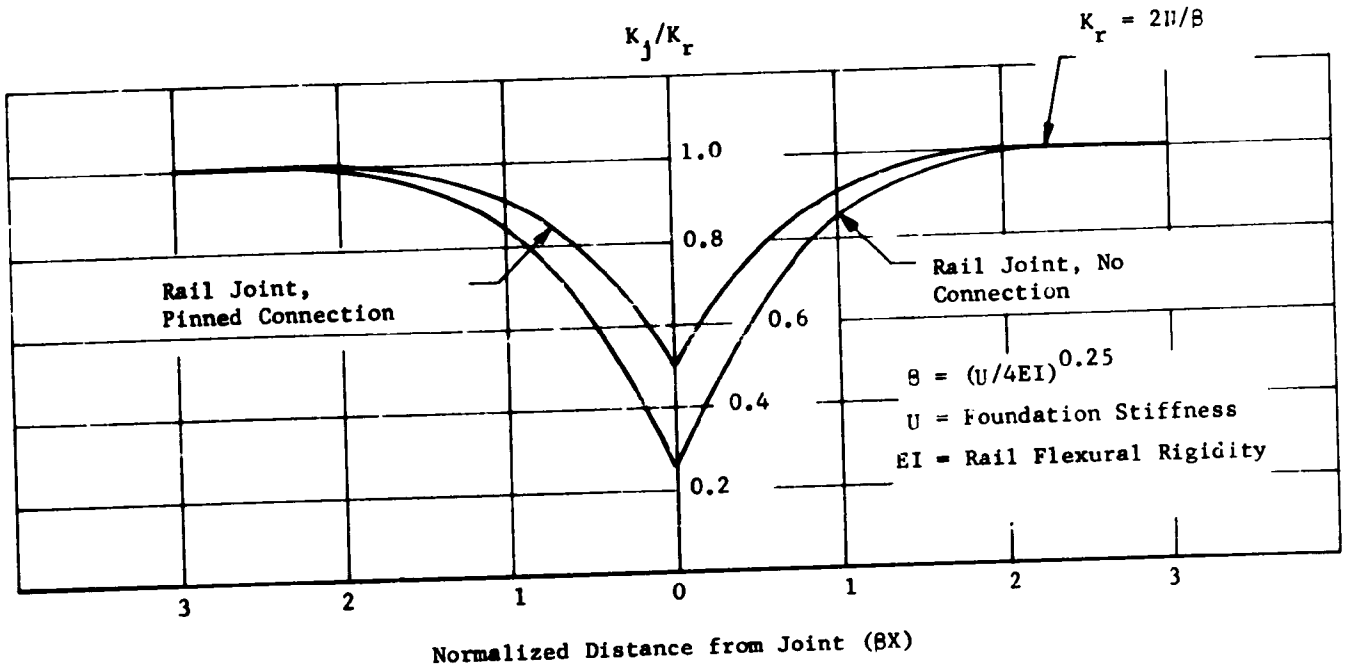

FIGURE 3-12. RATIO OF RAIL STIFFNESS NEAR A JOINT TO NOMINAL RAIL STIFFNESS NEAR MIDSPAN OF THE RAIL

Lateral force/deflection curves were developed for 136 lb/yd CWR track during a recent Track-Train Dynamics Program task. A lateral force was applied in increments between the rail heads, while simultaneous vertical load was applied by positioning a locomotive or freight car axle as close as possible to the measurement point. Teflon and molydisulphide grease was used at the wheel/rail contact patches to reduce lateral frictional components of force. Piece-wise linear approximations of the resulting force/deflection curves are shown in Figure 3-13. It can be seen that the rail lateral stiffness is quite dependent on the vertical load. For low lateral forces the rail is quite stiff, typically 100,000 to 500,000 lb/in. Once the total force vector falls outside the rail base, the rail begins to rotate, and the lateral stiffness drops typically to the 50,000 to 100,000 lb/in range. L/V ratios are shown in Figure 3-13 for reference.

Little is known about the effective damping of the track in the lateral direction, although from the oscillatory nature of the dynamic gage measurement (see Figure 3-8a), the damping may be quite low. The effective mass of the track may be assumed to be low, since the dominant spring (rail rotation) is in series between the wheel and the bulk of the track. Finally, the friction element represents the ability of the track to resist lateral shifting, and is dependent on vertical axle load and a variety of track conditions which are beyond the scope of this report. The absolute lateral stiffness of the rail to "ground" represents a complex overall stiffness which includes this friction element in a series parallel arrangement.

3.1.5 Track Performance Indices

Track performance indices are aimed toward the realization of two fundamental goals:

(1) To maintain track structural integrity and track geometry within given specifications as a function of traffic density (gross tons per year) or time;

(2) To maintain economically viable speed limits and shock/vibration environments for cargo, rolling stock, and track structure.

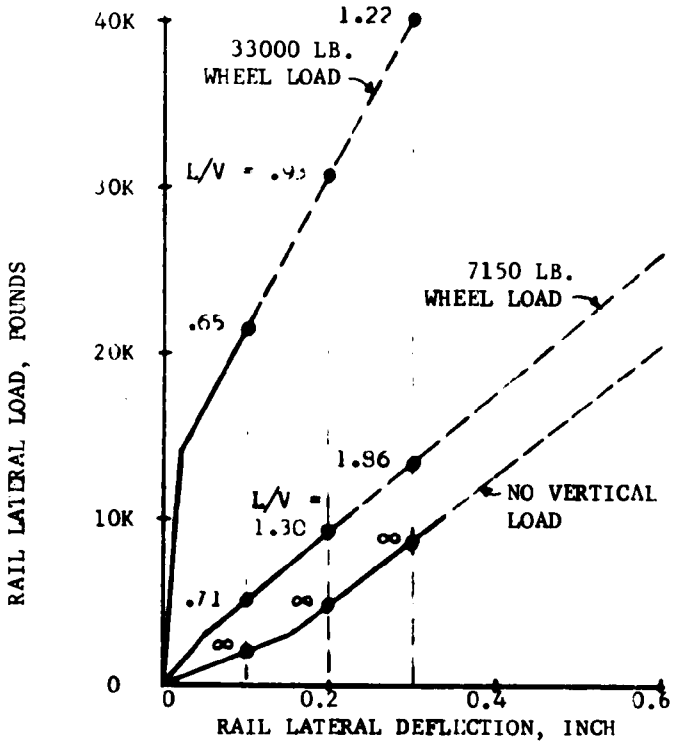

FIGURE 3-13. PIECEWISE LINEAR REPRESENTATION OF RAIL LATERAL FORCE/DEFLECTION CHARACTERISTICS

Much effort has been directed in recent years toward the characterization of track geometry in maintenance-of-way planning and budget allocations [3-30, 3-31]. Track performance indices, based in part on this work and directed specifically toward the track structure in the context of W/R loads, are summarized in Table 3-6.

3.2 WHEEL/RAIL LOADS - WAYSIDE MEASUREMENTS

Extensive data have been accumulated from a number of years of measuring track dynamic response using wayside instrumentation. Field experiments have been conducted by Battelle on the C&O/B&O, Penn Central, Union Pacific, and Southern Pacific railroads to measure rail and tie deflections and accelerations, tie plate and rail anchor loads, vertical and lateral wheel/rail loads, and subgrade pressures. From this available field data, and from the published data from other research efforts, a preliminary characterization of the wheel/rail load environment has been made.

3.2.1 Wayside Instrumentation

Wheel/rail load-measuring instrumentation and recording systems are discussed in detail in Section 5.0. It is sufficient here to briefly discuss some of the measurement techniques and to provide examples of the type of data acquired. Instrumenting the rail web with strain gages can provide a direct measurement of vertical and lateral W/R loads as each axle passes over a short section of instrumented rail. An example of this type of W/R load measurement is shown in Figure 3-14 for a diesel locomotive passing through a crossover on Northeast Corridor track. Three lateral force measurements about 5 feet apart were recorded near the switch point on the stock rail (Locations 132L-122L), and an additional 3 lateral locations (16L and 83L, north and south rails) were recorded approaching the switch frog and guard rail. Vertical W/R loads were recorded at one location, 83V. Each circuit was calibrated by use of an hydraulic jack between

TABLE 3-6. TRACK PERFORMANCE INDICES RELATED TO WHEEL/RAIL LOADS AND TRACK STRUCTURAL INTEGRITY

Performance Index	Degradation/Failure Mode (see Table 3.2)
1. Rate of differential settlement versus wavelength (track geometry PSD)	1, 3
2. Rate of change in track geometry "index" (cumulative slope, differential area, mean value, variance)	1, 3, 5
3. Priority geometry defect (per Track Safety Standards)	2, 4, 6
4. Rate of change of track geometry error versus traffic (MGT/year)	2, 4, 6
5. Peak and root-mean-square wheel/rail loads, component stresses and deflections	1, 2, 3, 4, 5, 6, 7, 8
6. Fatigue-related component stresses and deflections	5, 6, 7, 8
7. Component failure criteria per Track Safety Standards	7, 8
8. Track stability critical load level	4
9. Track speed limit per Track Safety Standards	1, 2, 3, 4, 5, 6, 7, 8

MGT = million gross tons of traffic

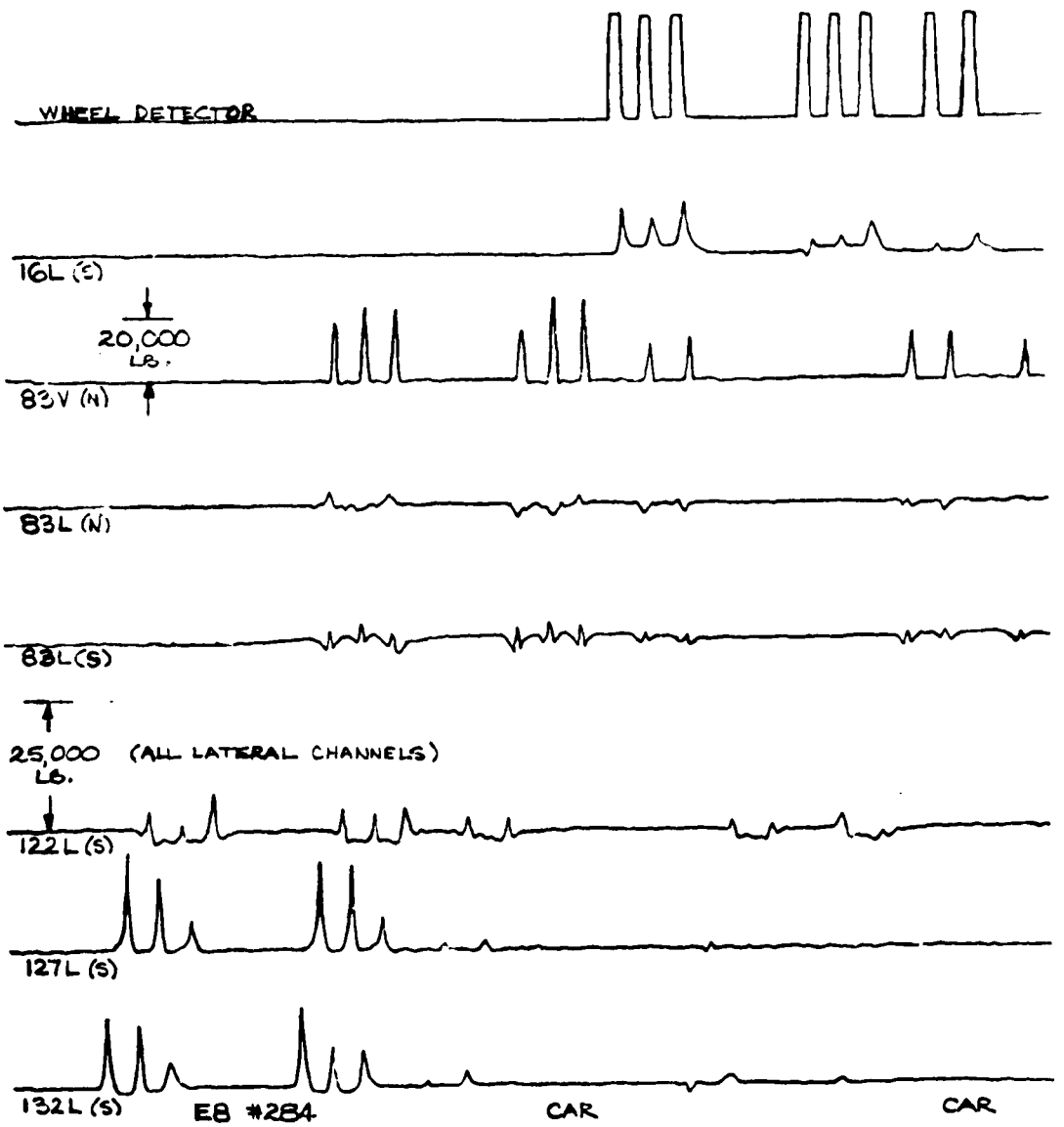

FIGURE 3-14. AN EXAMPLE OF VERTICAL AND LATERAL WHEEL/RAIL FORCE MEASUREMENTS FROM RAIL STRAIN GAGE CIRCUITS—DIESEL PASSENGER LOCOMOTIVE AND CARS THROUGH INTERLOCKING TEST SITE

the rail heads while loaded vertically with the locomotive wheel. Note that inwardly-directed creep forces are recorded, particularly at Site 83.

A second, but less-direct method for measuring W/R loads is by use of an instrumented tie plate. Several versions of instrumented tie plate have been developed in both Europe and North America to measure vertical and/or lateral loads on the tie. A recent version of Battelle's instrumented tie plate, designed for the AAR-FRA-RPI-TDA Track Train Dynamics Program [3-7] to measure vertical load and transverse moment on the tie, is shown in Figure 3-15. This plate uses standard, commercially-available load cells and fits into the AREA 8 x 14-inch 1:40 cant tie plate space envelope. An example of loads from this type of instrumented tie plate is shown in Figure 3-16. The W/R loads can be indirectly derived from the tie plate loads by establishing the percentage of wheel load carried by the single plate. However, this percentage may vary widely from tie to tie, depending on installation and shimming of the instrumented tie plate. This is illustrated in Figure 3-16, where one plate was "slack" (taking less than the nominal percentage of wheel load), while the second plate was "proud". Relating W/R load to tie plate load is also dependent on the somewhat nonlinear track "modulus", which determines the effective influence zone for adjacent wheels. This can change with time and temperature. Measurements in desert territory showed tie plate loads under 32,000 lb locomotive wheel loads to slowly vary from an average 13,000 lb to an average 26,000 lb over a several-day period. This was apparently caused by blowing sand infiltrating between the tie and plate, causing the instrumented tie to stand "proud" and carry a greater percentage of the wheel load.

3.2.2 Load Characterization

3.2.2.1 Vertical Tie Plate Loads

As discussed in the previous section, vertical tie plate load is a direct measurement of rail support and reaction on the tie, but only an indirect measurement of W/R vertical load. During the track response measurements on high-speed tangent track in both Idaho and Southern California [3-7], tie plate loads were recorded at several different locations for

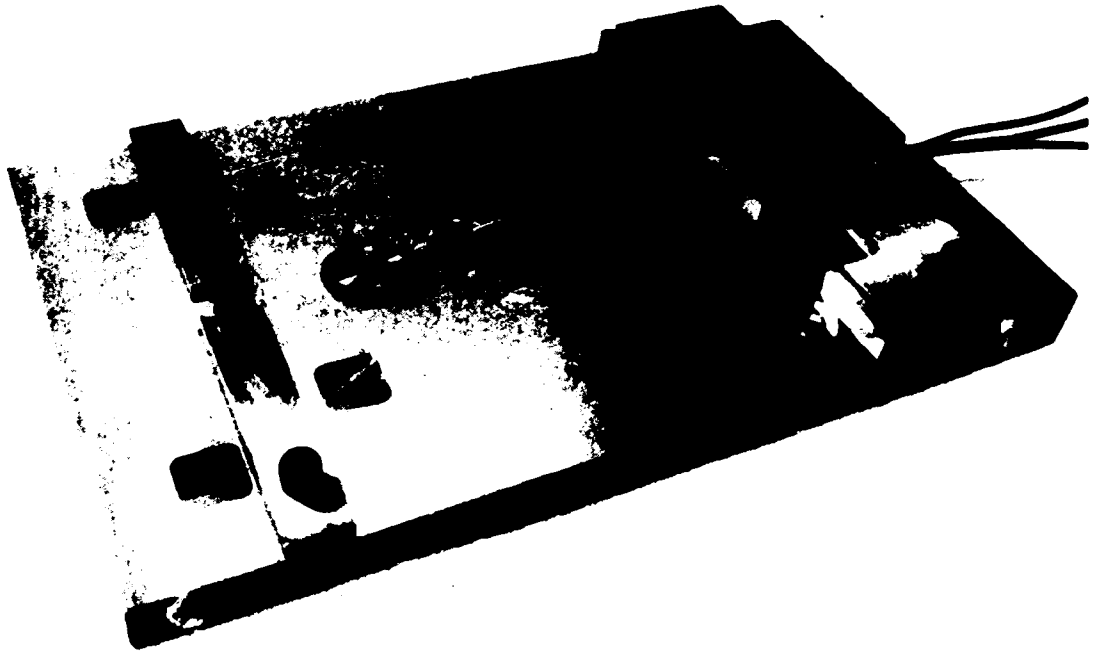

FIGURE 3-15. EXPERIMENTAL TIE PLATE LOAD CELL FOR MEASURING VERTICAL LOAD AND TRANSVERSE TORQUE ON TIE

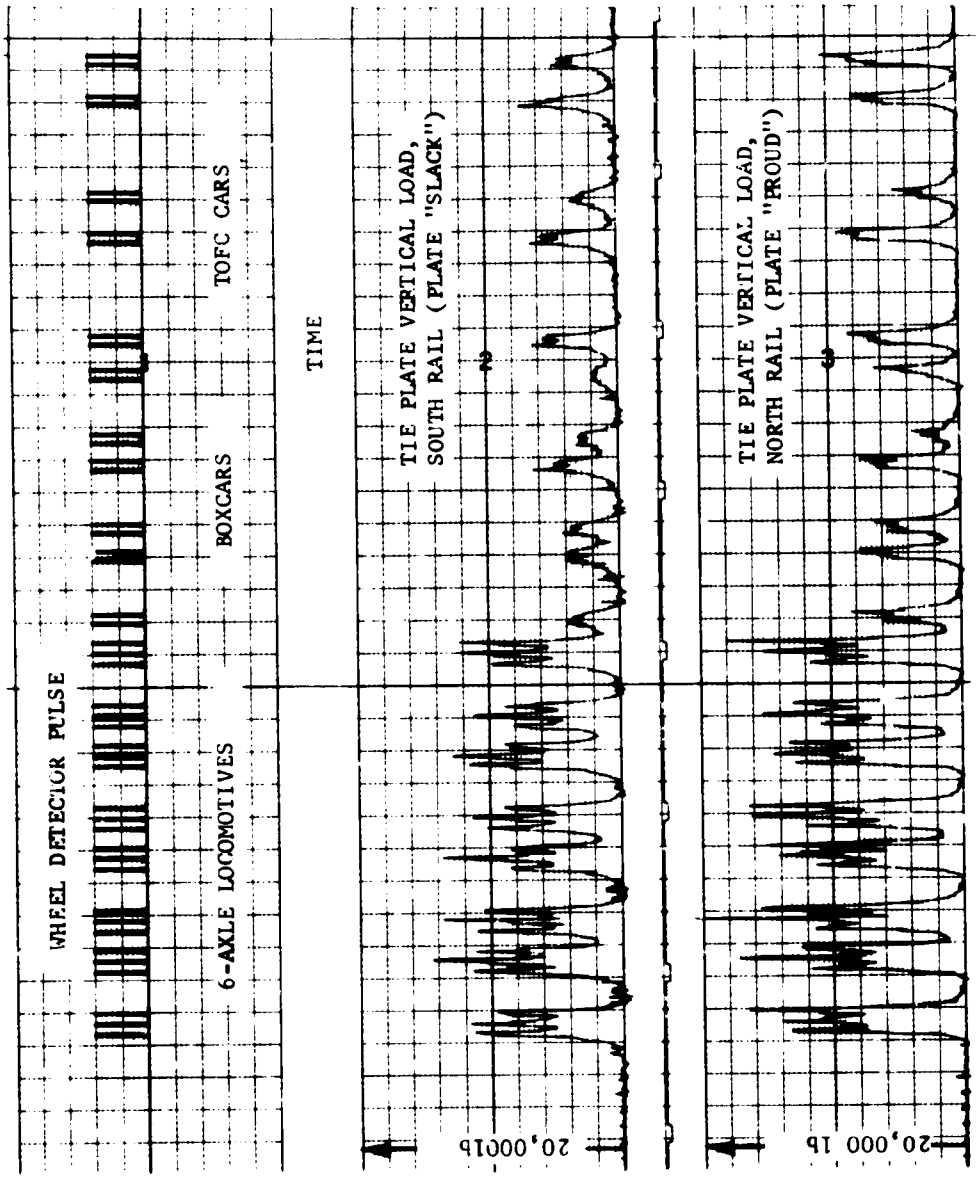

FIGURE 3-16. TIE PLATE LOADS UNDER FREIGHT TRAIN AT 71 MPH, RAIL TEMPERATURE, 106° F

summer and winter (frozen ballast) and blowing-sand conditions. Peak vertical tie plate loads from the different locations have been analyzed to determine both mean and standard deviation values. These values are listed in Table 3-7 for all freight traffic, and in Table 3-8 for just the 6-axle diesel locomotives. A key to the test site conditions is presented in Table 3-9.

Analysis of these data by use of the Student-T and Chi-Square tests [3-32] have established a range of true mean and a range of standard deviation at the 95 percent confidence level (see Appendix A):

Condition	N	$\bar{F}$	S_f	Range of True Mean	Range of Standard Deviation
Summer	10	5320 lb	3470 lb	± 2620 lb	1800-4780 lb
Winter or Sand	10	8695 lb	4650 lb	± 3510 lb	2410-6410 lb

where $\bar{F}$ = mean value of peak tie plate vertical load for all traffic
S_f = standard deviation for all traffic
N = number of test sites .

From this one can see that the variation in tie plate load for nominally identical traffic and traffic conditions is considerable, and that a number of track sites must be examined to achieve accurate estimates. It is apparent that the frozen ballast and sand-infiltrated ballast conditions result in substantially higher loads on the tie plate and tie. This is also borne out in cumulative probability distributions of tie plate peak vertical loads, which are shown for summer and winter conditions in Figure 3-17.

3.2.2.2 Vertical Wheel/Rail Loads

Although the accuracy of W/R loads determined from tie plate loads is not as high as that from rail strain gage circuits, the tie plate loads have been used to establish the statistical characteristics of W/R peak loads under mixed, high-speed freight traffic. A typical probability density histogram of peak vertical W/R load for both summer and winter measurements on the 1:40-cant rail is shown in Figure 3-18. Interestingly, although the

TABLE 3-7. MEAN VALUE AND STANDARD DEVIATION OF PEAK TIE PLATE VERTICAL LOAD PER AXLE, FREIGHT TRAFFIC ON TANGENT TRACK, SPEEDS 30 TO 80 MPH

Test Category (1)	No. Axles	South Rail		North Rail	
		$\bar{F}_N$, lb.	σ, lb.	$\bar{F}_N$, lb.	σ, lb.
UP 0 + 1	26,324	5,080	3,580	5,890	3,860
UP 2	4,544	4,910	3,110	5,210	3,480
UP 3	7,714	4,470	3,070	4,990	3,880
UP 4	8,716	4,560	2,510	7,580	4,260
UP 5	10,786	4,020	2,370	6,480	4,090
UP 10	21,204	10,200	4,840	6,610	4,110
UP 11	17,348	9,610	4,740	7,570	4,870
UP 12	4,105	11,600	5,070	7,660	4,630
SP 1	32,130	10,700	4,410	8,980	5,510
SP 2	13,861	6,830	2,960	7,170	4,910

(1) Refer to Table 3-9.

$$\bar{F}_N = \frac{i}{n} \sum_{i=1}^{n} F_i \text{ , average peak vertical load}$$

$$\sigma = \sqrt{\frac{1}{n-1} \sum_{i=1}^{n} (F_i - \bar{F}_N)^2} \text{ , standard deviation}$$

TABLE 3-8. MEAN VALUE AND STANDARD DEVIATION OF PEAK TIE PLATE VERTICAL LOAD PER AXLE, 6-AXLE DIESEL LOCOMOTIVES* ON TANGENT TRACK, SPEEDS 30 TO 80 MPH

Test Category (1)	No. Axles	South Rail		North Rail	
		$\bar{F}_N$, lb	σ, lb	$\bar{F}_N$, lb	σ, lb
UP 0 + 1	1,218	11,300	2,100	12,800	1,950
UP 2	216	11,200	1,390	12,200	1,770
UP 3	294	10,500	1,340	12,300	1,940
UP 4	372	8,960	1,100	14,200	1,670
UP 5	526	7,690	1,870	12,400	2,990
UP 10	854	17,200	2,650	13,300	1,780
UP 11	735	16,000	2,180	15,200	2,060
UP 12	149	18,900	1,790	14,800	1,780
SP 1	1,494	18,900	2,680	19,900	2,780
SP 2	529	12,400	1,490	17,000	2,310

* SD-40, SD-45, SD-40-2, SD-45-2, SD-45T, U30C, U33C, SD-9, SD-24

(1) Refer to Table 3-9,

$$\bar{F}_N = \frac{1}{n} \sum_{i=1}^{n} F_i \text{ , average peak vertical load}$$

where

F_i = peak vertical load for i^{th} angle

$$\sigma = \sqrt{\frac{1}{n-1} \sum_{i=1}^{n} (F_i - \bar{F}_N)^2} \text{ , standard deviation}$$

TABLE 3-9. KEY TO TEST CATEGORY CONDITIONS *

TEST CATEGORIES:		
UP 0 + 1	-	high quality, uniform (undisturbed) track, 133 lb/yd rail, 14" tie plates with 1:40 cant, 56-1/2" gage, summer conditions
UP 2	-	same track site, gage 1/2" tight, alignment and cross level disturbances
UP 3	-	same track site, gage 3/4" and 1-1/4" wide, alignment and cross level disturbances
UP 4	-	high-quality, uniform (undisturbed) track, 133 lb/yd rail, 18" tie plates with 1:40 cant, 56-1/2" gage, summer conditions
UP 5	-	same track site, gage 3/4" wide, alignment and cross level disturbances
UP 10	-	high-quality, uniform (undisturbed) track, 133 lb/yd rail, 14" tie plates with 1:40 cant, 56-1/2" gage, winter (frozen ballast) conditions
UP 11	-	same track site, two holddown spikes per plate removed
UP 12	-	same track site, gage 3/4" wide, wet rail conditions
SP 1	-	medium-quality, uniform (undisturbed) track, 136 lb/yd rail, 14" tie plates on 1:40 nominal cant, 57" gage, blowing-sand conditions
SP 2	-	same track site, gage 56-1/2", track disturbed

* see Tables 3-7 and 3-8

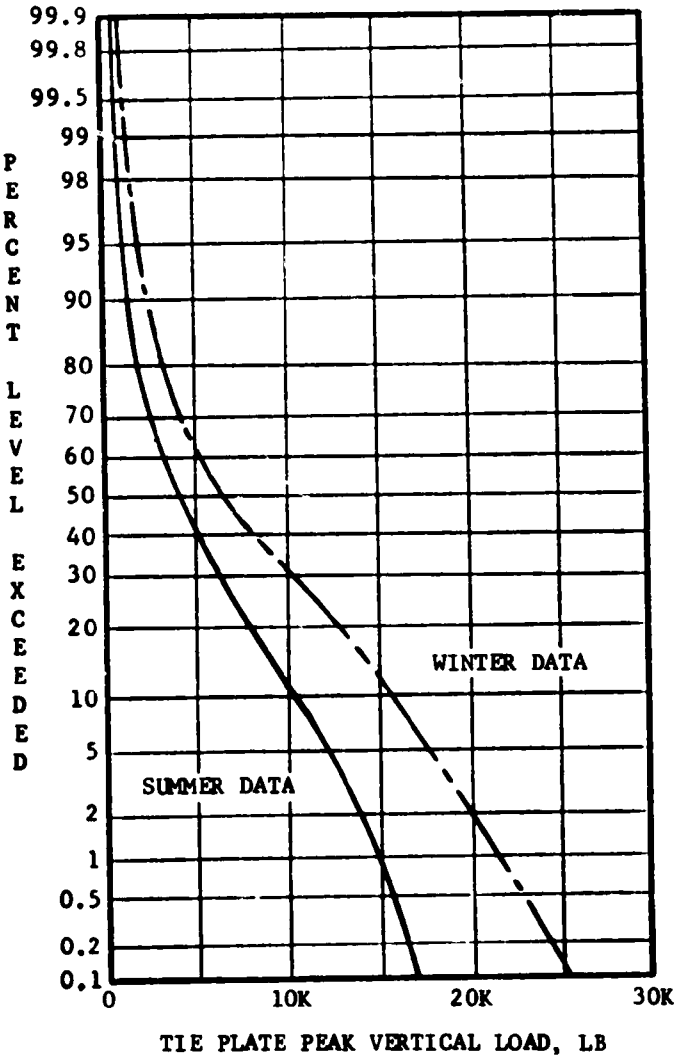

FIGURE 3-17. CUMULATIVE PROBABILITY DISTRIBUTION OF PEAK TIE PLATE VERTICAL LOAD UNDER SUMMER AND WINTER (FROZEN BALLAST) CONDITIONS, MIXED FREIGHT TRAFFIC, 133 LB/YD CWR TRACK

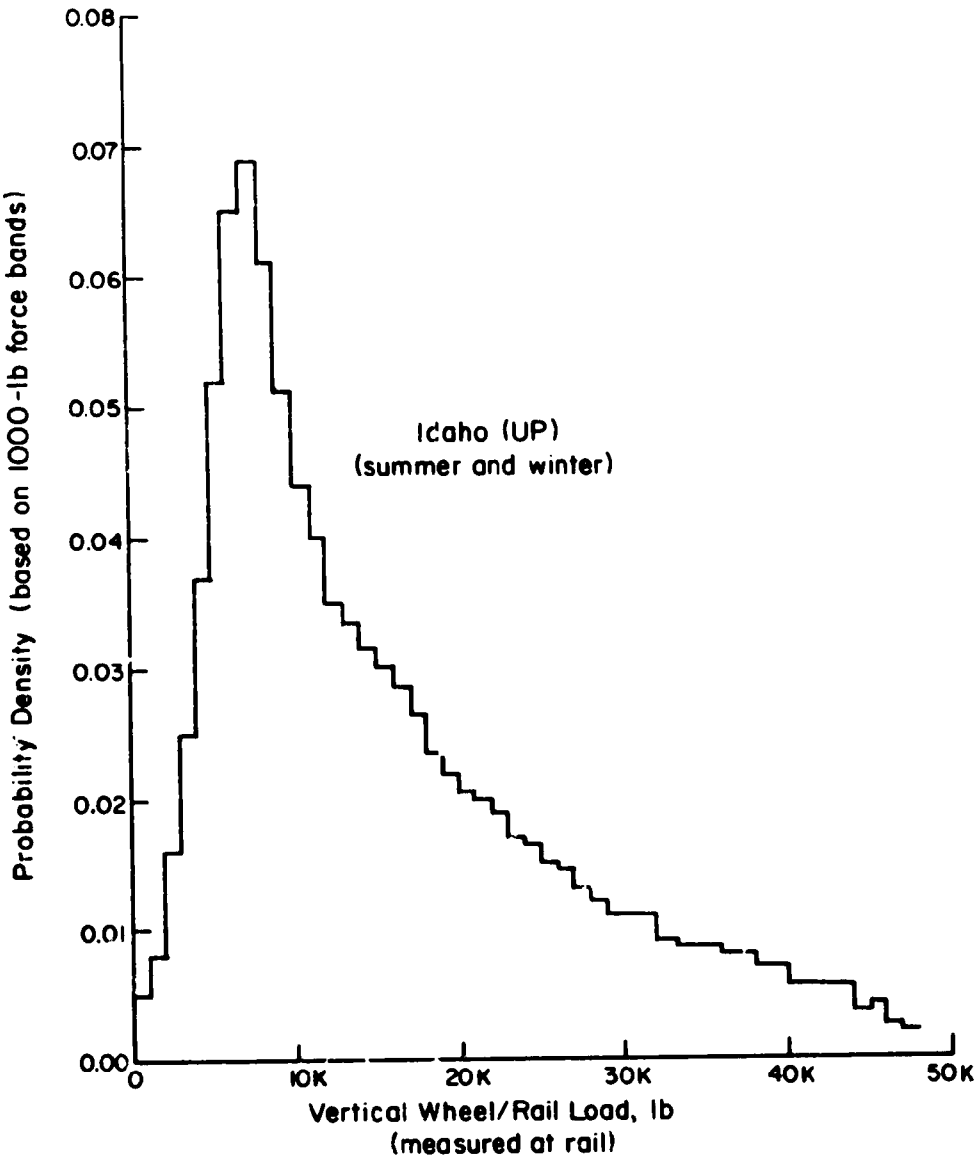

FIGURE 3-18. PROBABILITY DENSITY HISTOGRAM OF PEAK VERTICAL WHEEL/RAIL LOADS UNDER MIXED FREIGHT TRAFFIC, DERIVED FROM TIE PLATE LOAD MEASUREMENTS

peak tie plate loads increased substantially in the winter (Figure 3-17), the derived W/R loads on this excellent CWR track were not statistically different within the range of probability shown. Cumulative probability distribution curves of peak W/R load are shown in Figure 3-19 for both the Idaho and Southern California track. The difference in these curves reflects, more than anything, the differences in traffic characteristics. In Southern California, the slow, heavily-loaded eastbound freights were seldom recorded, so the average axle load was less.

Recent Northeast Corridor track measurements have provided a limited, but valuable data base for characterizing both vertical and lateral W/R loads through the more accurate rail strain gage measuring techniques. Vertical load data from a single location at an interlocking plant (between the switch point and frog on the stock rail of a turnout) are shown in Figures 3-20 through 3-22. Because of an alignment disturbance approaching the turnout, the vertical and lateral loads recorded at this site reflect vehicle dynamic response to a specific geometry excitation. Loads were examined for two conditions: first, for a representative "mix" of freight and passenger traffic through this high-density site; and second, for passenger-only traffic that might reflect future operations. Probability density histograms in Figures 3-20 and 3-21 show characteristic peaks near 12,000 lb (empty and lightly-loaded freight cars), 21,000 lb (Metroliners and conventional coaches*), and 34,000 lb (locomotives and heavy freight cars). Cumulative probability distribution curves in Figure 3-22 similarly reflect the distinction in load environment between passenger and freight operations. The low-probability, high-amplitude loads in passenger service result from the older electric locomotives still in service.

3.2.2.3 Lateral Wheel/Rail Loads

Peak lateral wheel/rail loads were recorded at several discrete points through the same turnout cited in the previous section. Most of the traffic through this site was westbound, a trailing-point movement through the switch, although a few facing-point movements also occurred.

---

* At the time of these measurements, the new AMCOACH cars were not in general service.

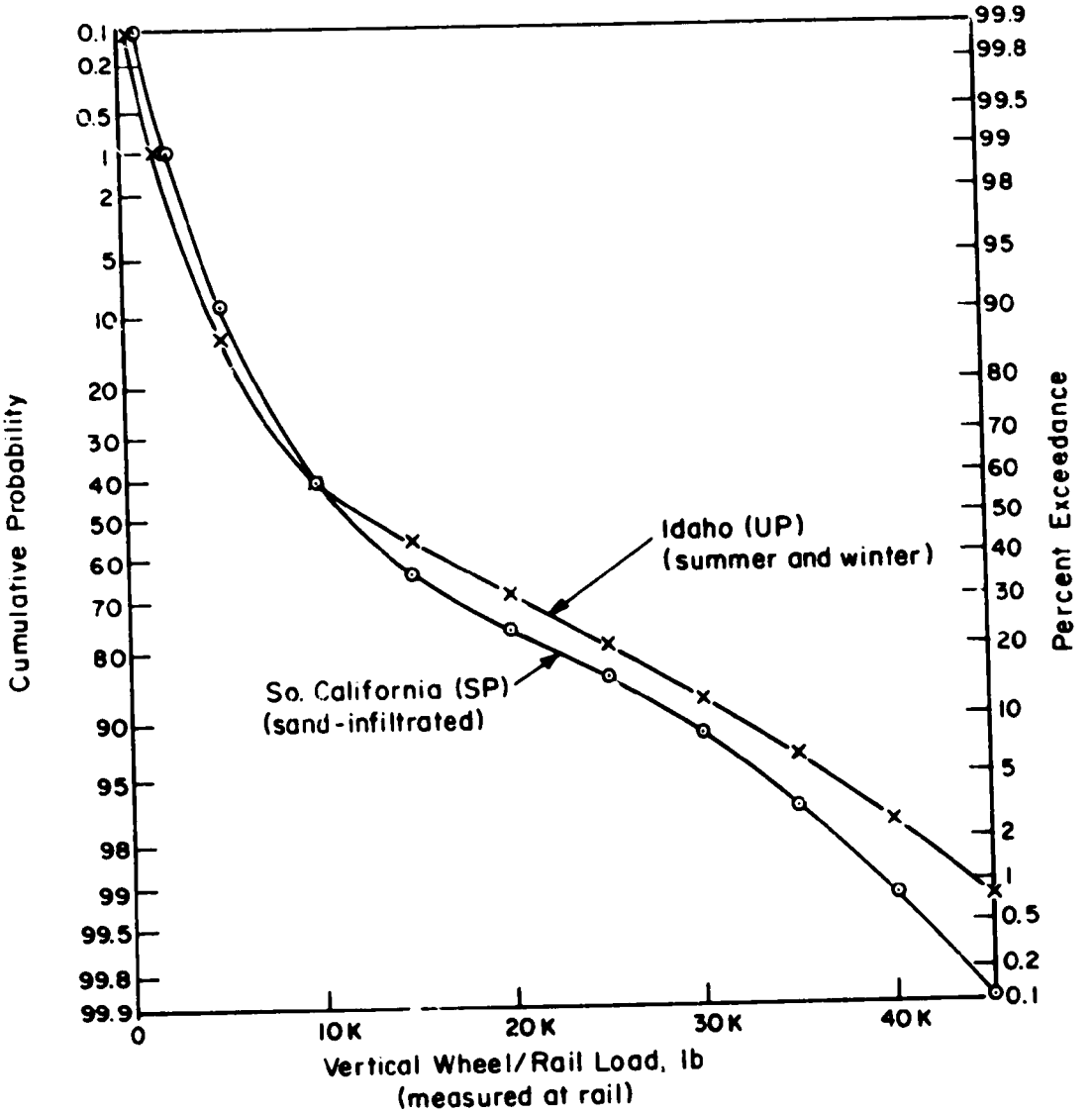

FIGURE 3-19. CUMULATIVE PROBABILITY LEVELS OF PEAK WHEEL/RAIL LOAD UNDER MIXED FREIGHT TRAFFIC AS DERIVED FROM TIE PLATE LOAD MEASUREMENTS

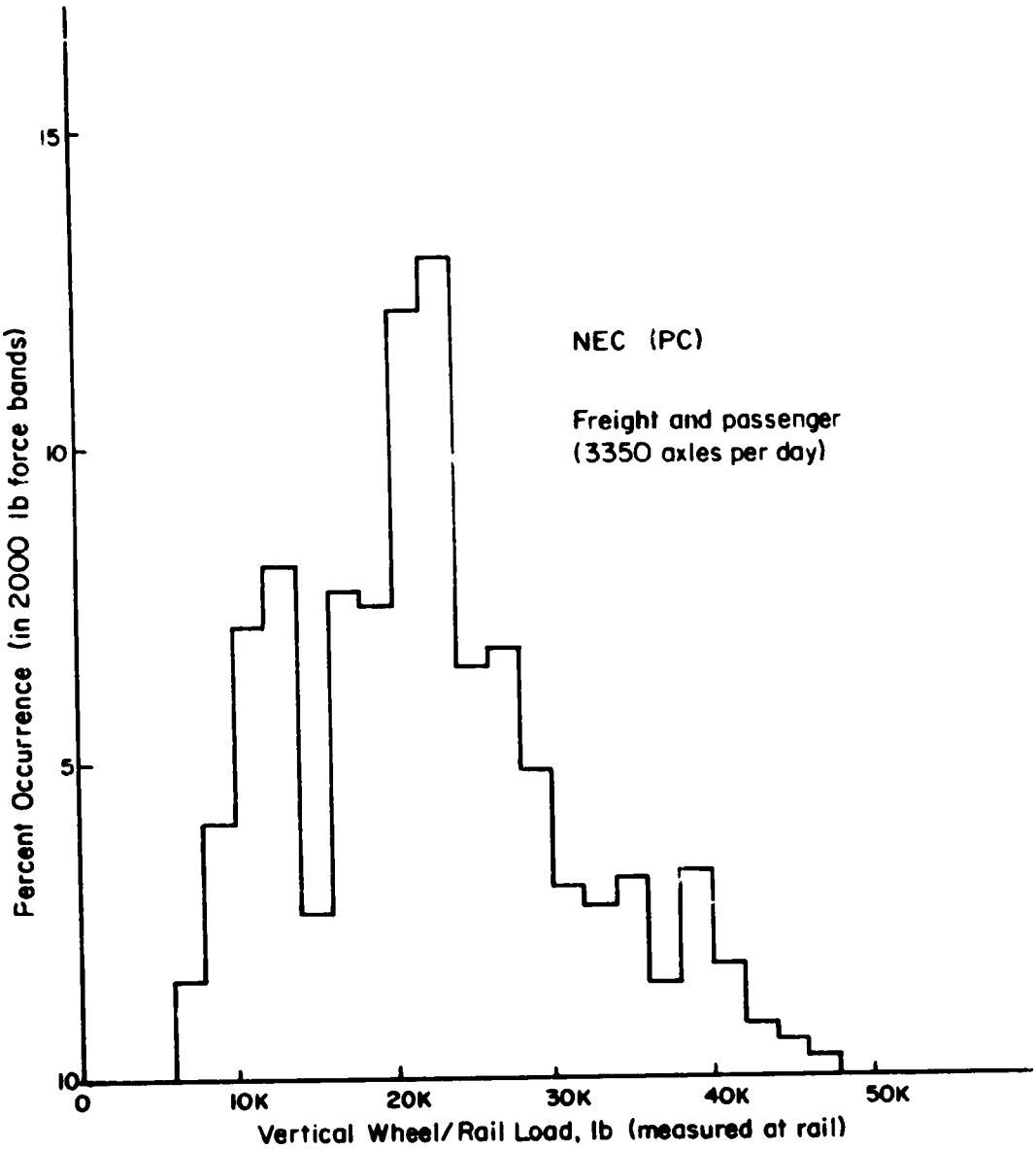

FIGURE 3-20. PROBABILITY HISTOGRAM OF VERTICAL WHEEL/RAIL LOADS UNDER TYPICAL NORTHEAST CORRIDOR TRAFFIC (FREIGHT AND PASSENGER), INTERLOCKING SITE

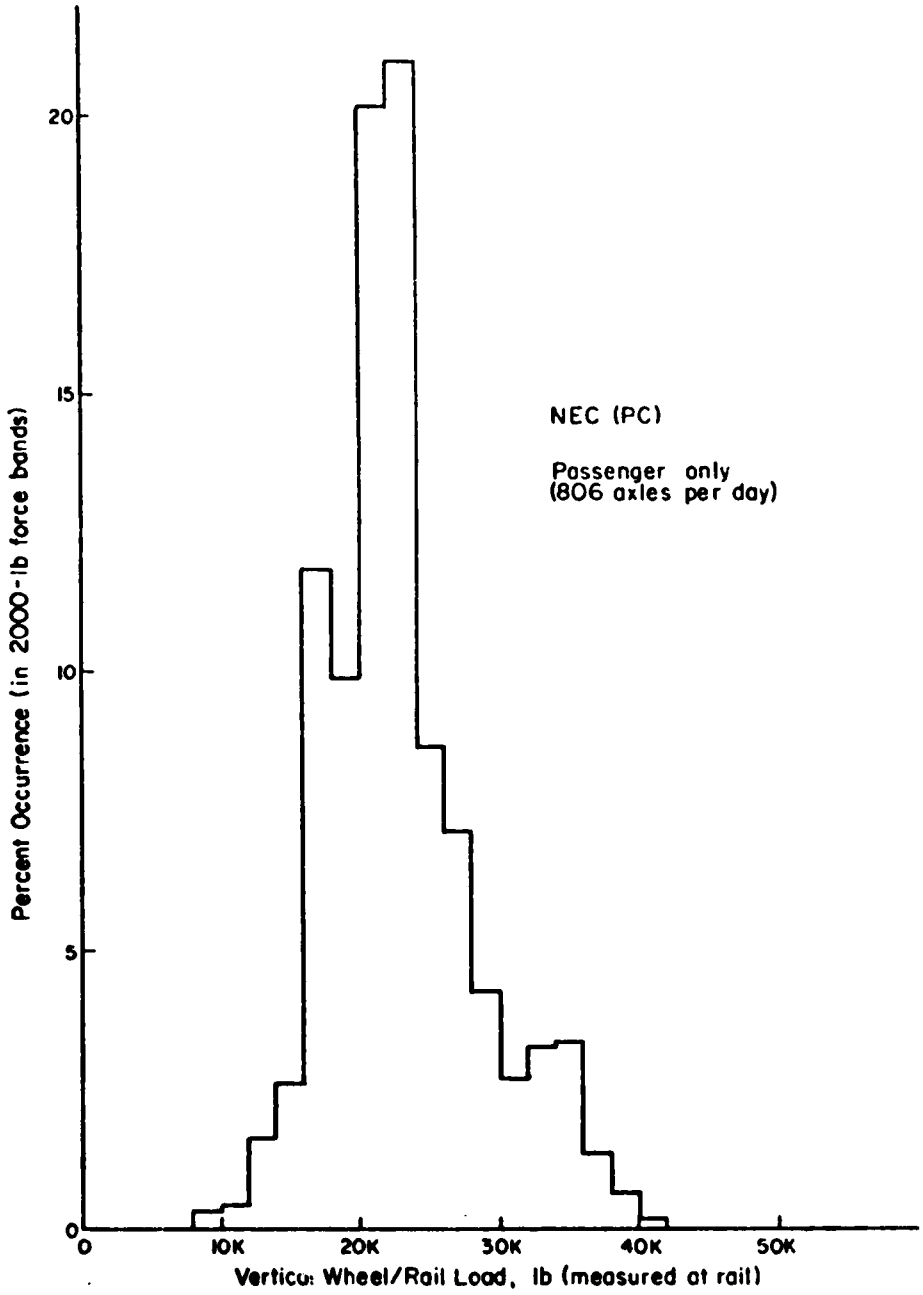

FIGURE 3-21. PROBABILITY HISTOGRAM OF VERTICAL WHEEL/RAIL LOADS UNDER TYPICAL NORTHEAST CORRIDOR PASSENGER TRAFFIC (INTERLOCKING SITE)

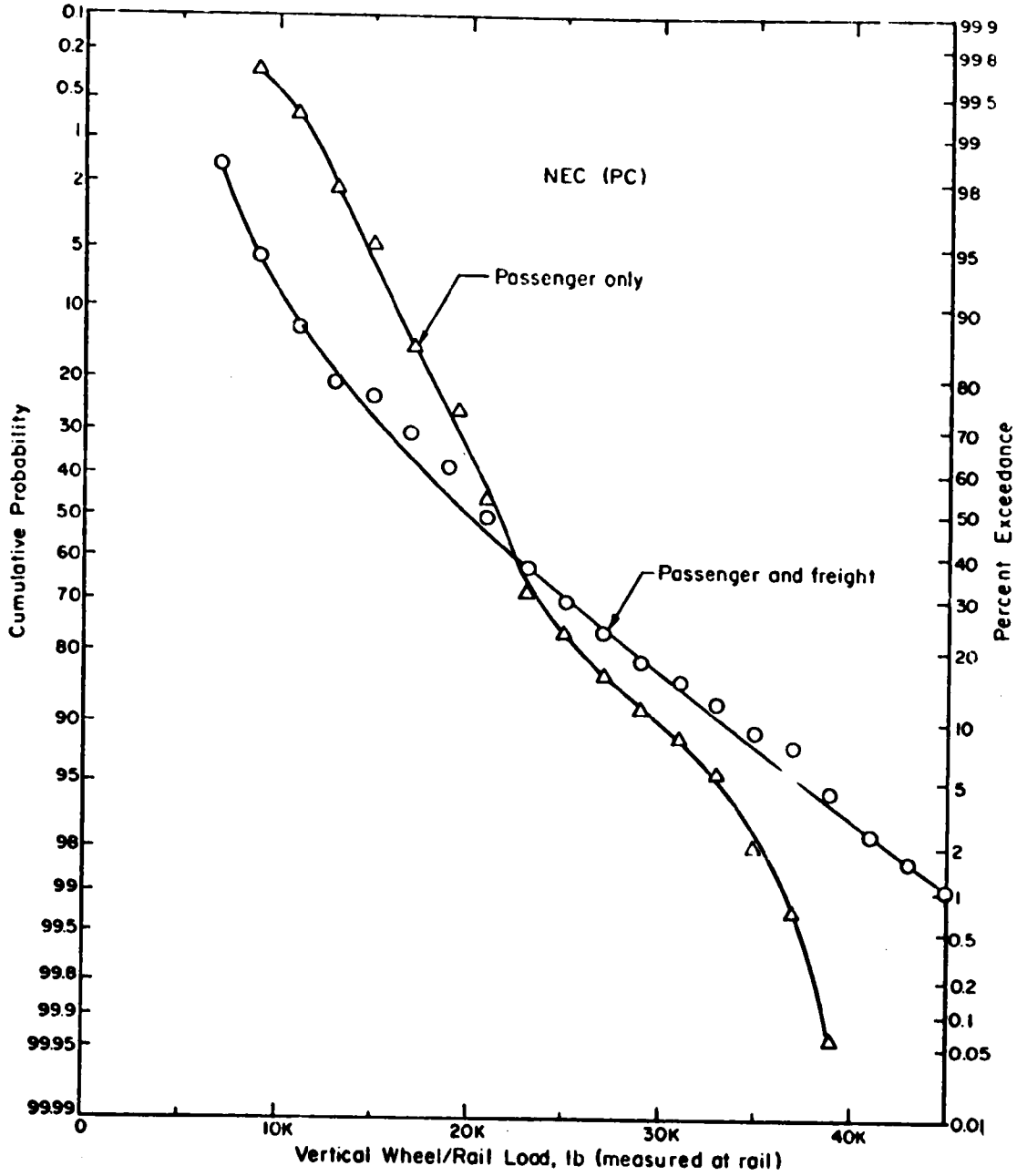

FIGURE 3-22. CUMULATIVE PROBABILITY DISTRIBUTION OF PEAK VERTICAL WHEEL/RAIL LOADS ON NORTHEAST CORRIDOR TRACK (INTERLOCKING SITE)

Typical revenue traffic consisted of Metroliners at 110 miles per hour, electric (GG1) locomotive-pulled conventional passenger trains at 80 mph, and diesel or electric locomotive-pulled freight trains at speeds up to 65 mph.

Typical probability histograms for one of the measurement sites are shown in Figures 3-23 and 3-24, again for mixed or passenger-only traffic. Both the inwardly and outwardly-directed lateral creep forces are apparent in these histograms, as well as flanging forces (greater than about 8000 lb outward). A few high lateral loads with L/V ratios greater than 1.0 were recorded from hunting freight car trucks and (at another of the sites) from the trailing axle of an older electric locomotive, apparently due to excessive lateral clearance in the "pony truck" axlebox. The cumulative probability distribution of lateral loads is shown in Figure 3-25. There appears to be two nearly straight-line (Gaussian) distributions representing lateral creep forces and flanging forces, with the apparent transition being near 8000 lb outward.

Data shown in Figures 3-20 through 3-25 were recorded during October, with temperatures ranging typically from 50 to 70 degrees F. Later recordings during November and December, with temperatures in the 30 to 40 degree range, showed a marked decrease in lateral load levels. Chordal measurements of track alignment showed a decrease in alignment error amplitude, apparently the result of increased tensile forces from low track temperature. This is illustrated in Figure 3-26 by comparing the probability histograms of lateral forces generated by high-speed MU cars during two test periods more than one month apart. No maintenance was performed at this site during the interim period.

3.2.2.4 Lateral Wheel/Rail Loads on Curved Track

Lateral loads on the rail in curved track have been measured during several experimental programs [3-8, 3-33, 3-34], both from wayside and vehicle-borne load measurement systems. Results from these studies are summarized in Figure 3-27, for the lead outer wheel of locomotives under several different operating conditions and track curvature (defined as the angle subtended by a 100-ft chord). Locomotives generate by far the highest

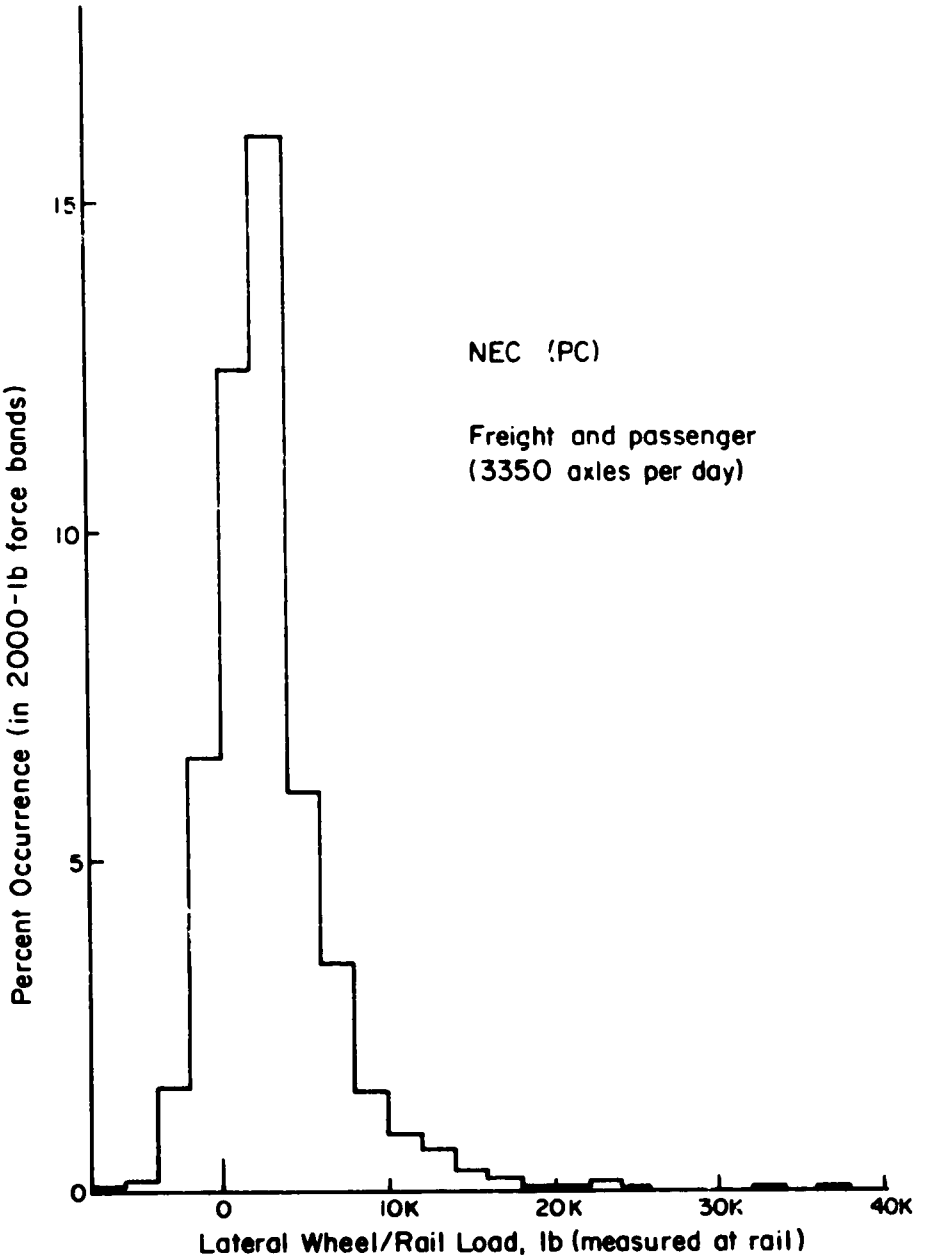

FIGURE 3-23. PROBABILITY HISTOGRAM OF LATERAL WHEEL/RAIL LOADS UNDER TYPICAL NORTHEAST CORRIDOR TRAFFIC (FREIGHT AND PASSENGER), INTERLOCKING SITE

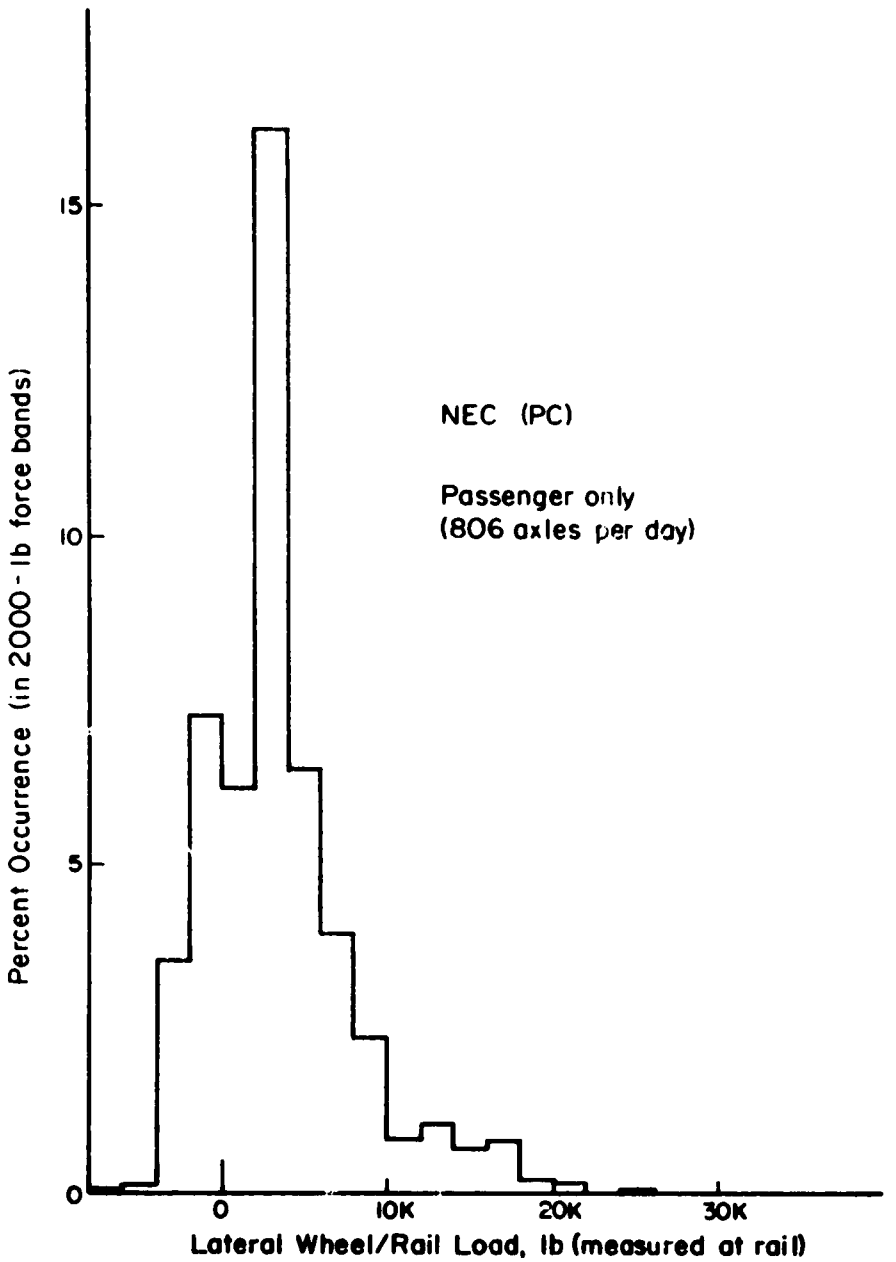

FIGURE 3-24. PROBABILITY HISTOGRAM OF LATERAL WHEEL/RAIL LOADS UNDER TYPICAL NORTHEAST CORRIDOR PASSENGER TRAFFIC (INTERLOCKING SITE)

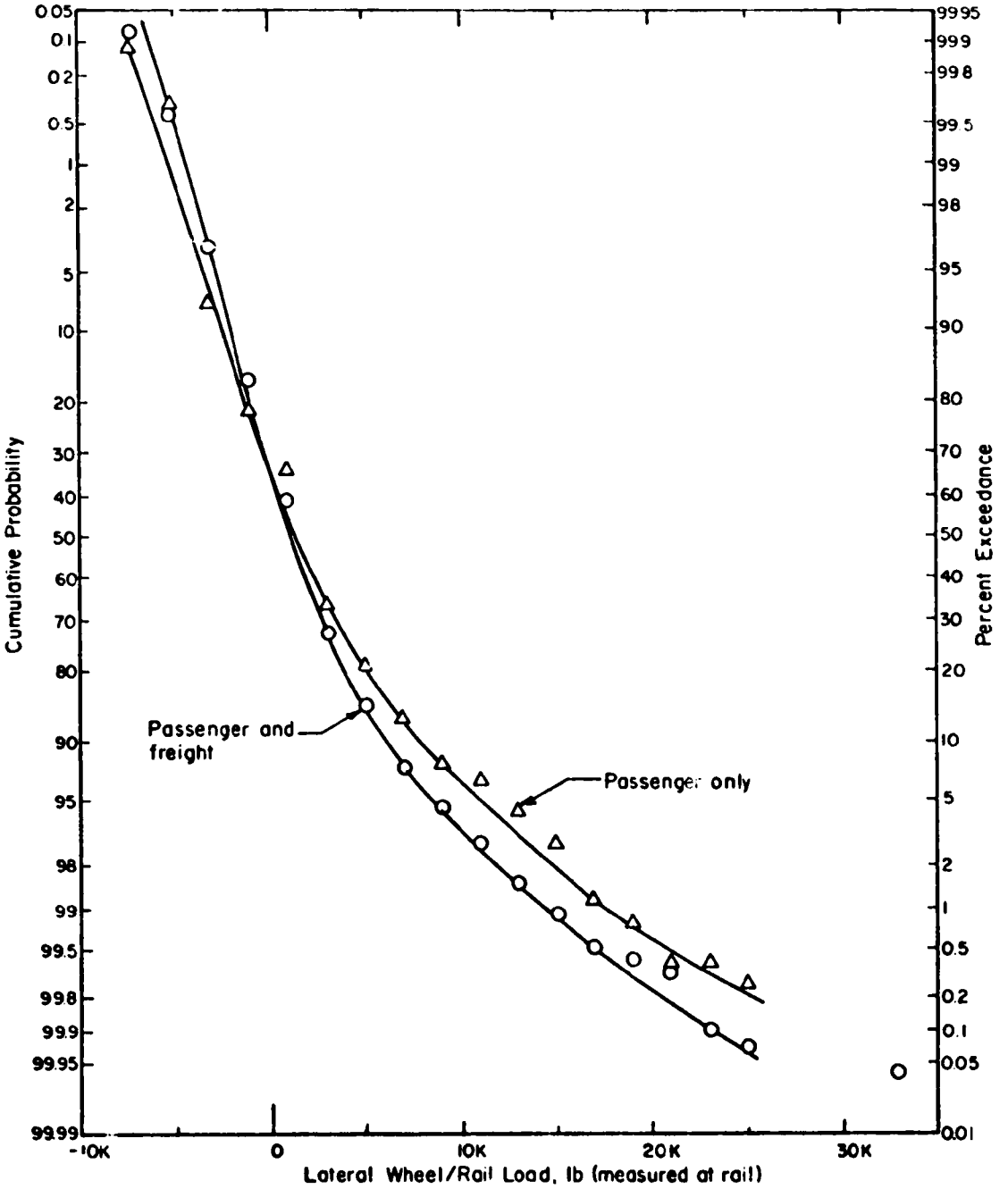

FIGURE 3-25. CUMULATIVE PROBABILITY DISTRIBUTION OF PEAK LATERAL WHEEL/RAIL LOADS ON NORTHEAST CORRIDOR TRACK (INTERLOCKING SITE)

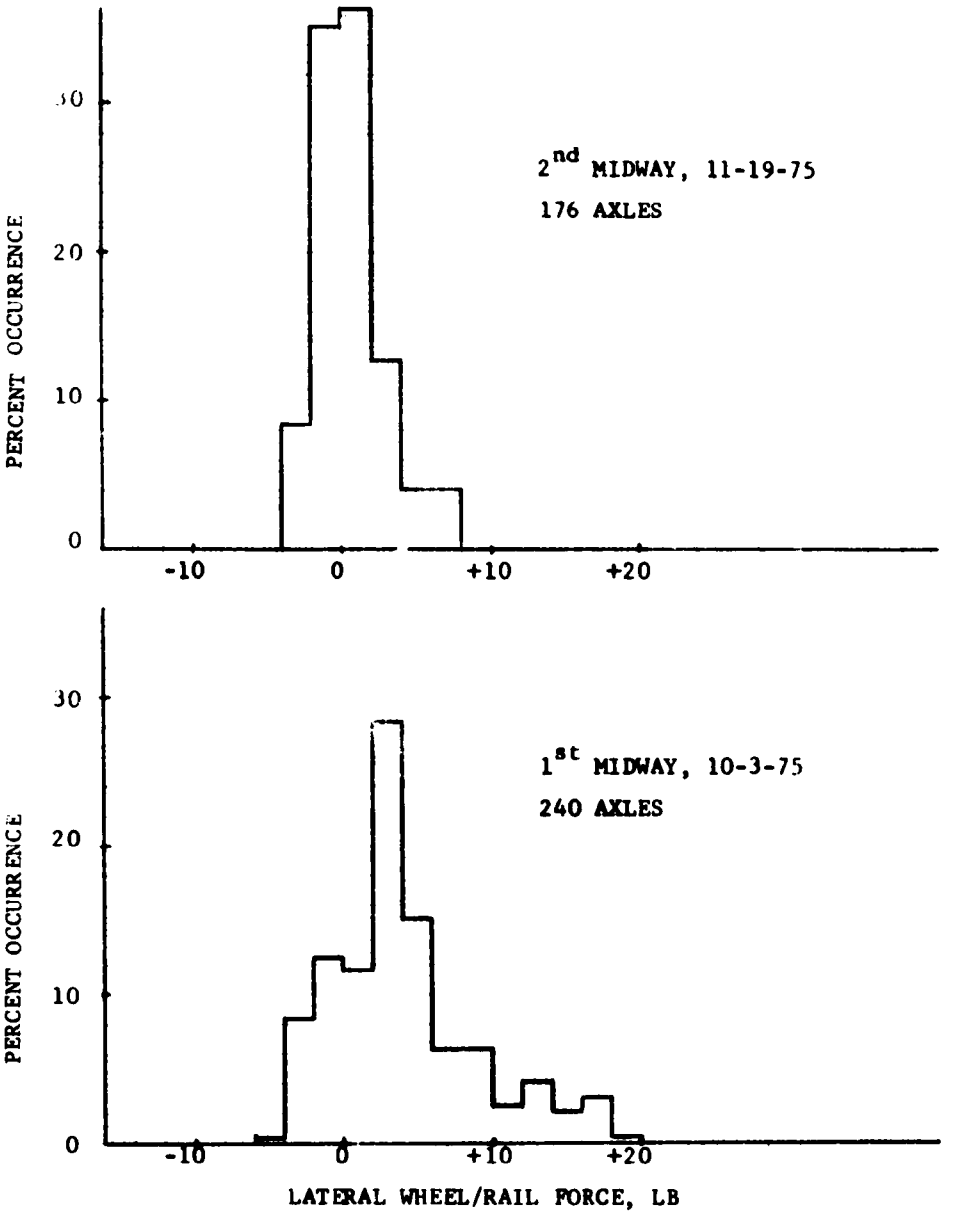

FIGURE 3-26. PROBABILITY DENSITY HISTOGRAMS OF LATERAL WHEEL/RAIL FORCE SHOWING EFFECTS OF TRACK GEOMETRY CHANGE WITH AMBIENT TEMPERATURE; HIGH-SPEED MU CARS AT INTERLOCKING TEST SITE

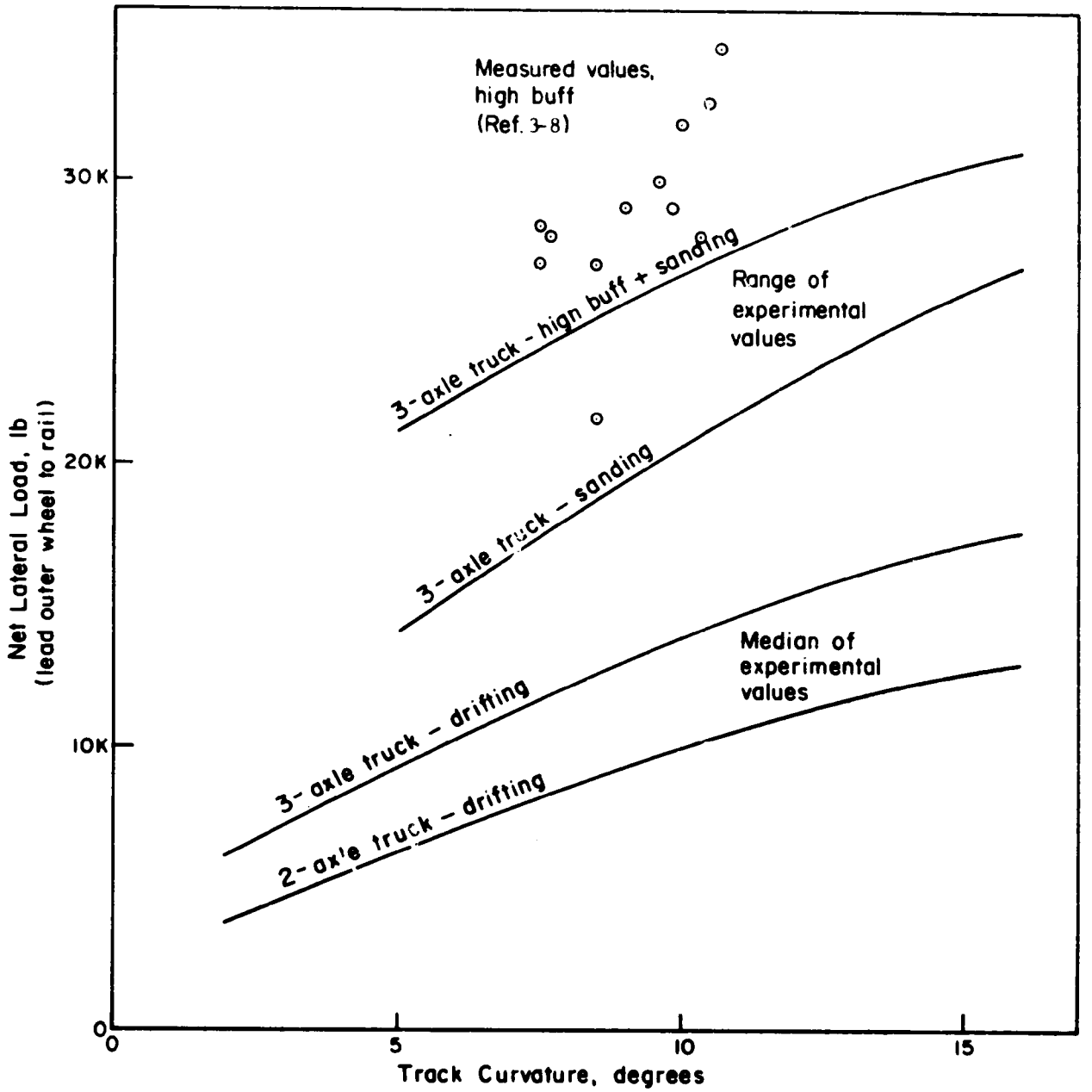

FIGURE 3-27. MEASURED NET WHEEL/RAIL LOADS ON LEAD OUTER WHEEL OF LOCOMOTIVE DURING CURVING UNDER SEVERAL OPERATING CONDITIONS

quasi-static lateral forces on curves, although freight cars may develop lateral wheel forces over 20,000 lb under certain operating conditions on curves.

3.3 WHEEL/RAIL LOADS - VEHICLE-BORNE MEASUREMENTS

This section reviews data analysis techniques for presenting wheel/rail load data which have been measured by vehicle-born instrumentation systems. The objective of this task was to develop data formats which can be used for rail stress calculations and rail failure mode analysis. This review has made use of data which were originally gathered for a study of fatigue damage effects on railroad freight car truck components [3-35]. The data were obtained using an instrumented freight car truck (100-ton capacity, 6-1/2 x 12 in. journals, see Reference 3-36) under a loaded hopper car containing iron-ore (263,000 lbs rail load). The tests were conducted along a 7 mile length of track on the Erie branch of the Bessemer & Lake Erie Railroad between Albion and Girard, Pennsylvania. The track chart for this area is shown in Figure 3-28. This track offers a wide variety of conditions including turnouts, grade crossings and curves up to 10^{o}. The particular data used in this review were obtained from Test Run Nos. 32, 41, and 44 (see page 36, Reference 3-35).

The load summaries presented in the following sections are formats based on vertical wheel load data. Similar data displays may be developed for lateral wheel/rail load data as well as load combinations such as the L/V (lateral to vertical) load ratio. Vertical and lateral loads developed by the test vehicle under several operating conditions are then summarized in Section 3.3.5.

3.3.1 Histograms of Load Intensity

Vertical load at the wheel/rail interface is characterized by a mean load and dynamic fluctuations about this mean load. One method of describing the characteristics of the fluctuating load is to present the data in the form of a histogram showing the percentage of time a given load level is exceeded. This type of data is presented in Figures 3-29 and 3-30 for a vehicle with a mean wheel load of 30,000 lbs. The data was

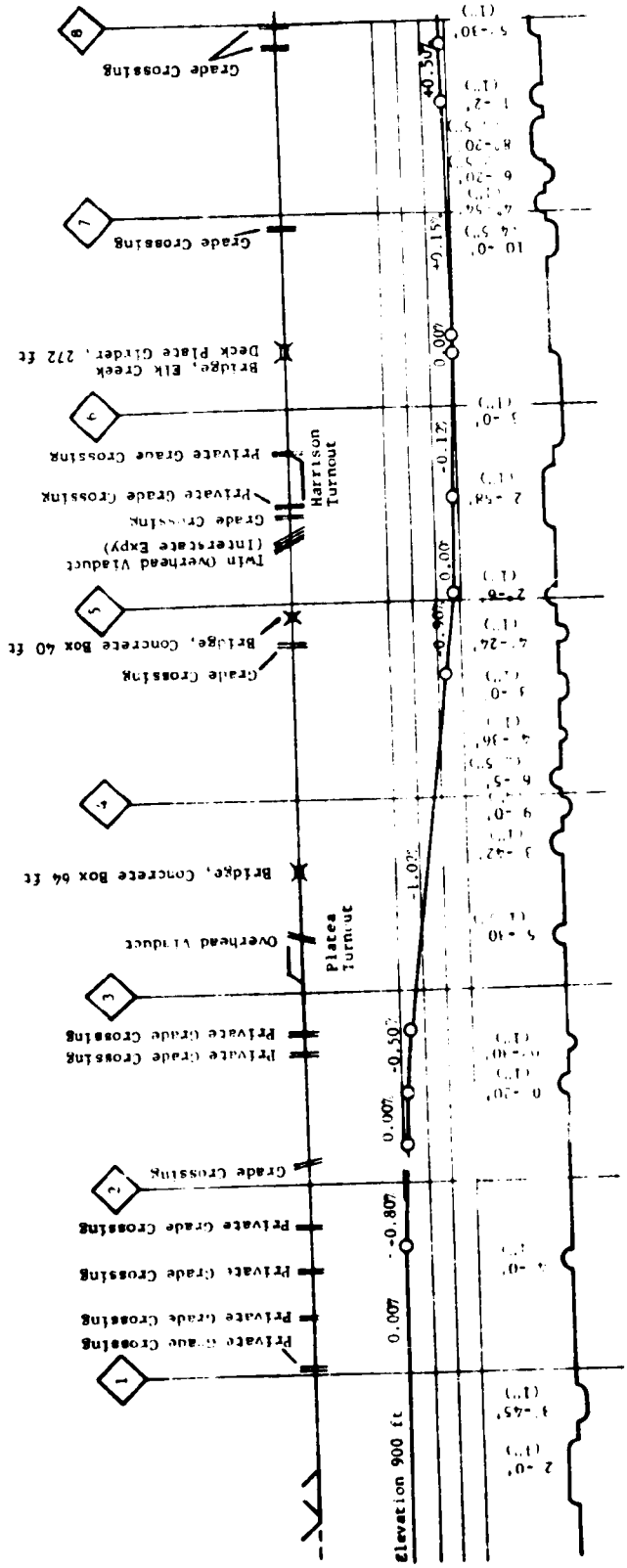

FIGURE 3-28. TRACK DIAGRAM OF THE ERIE BRANCH OF THE B&LE RAILROAD FOR TEST TRACK SECTION

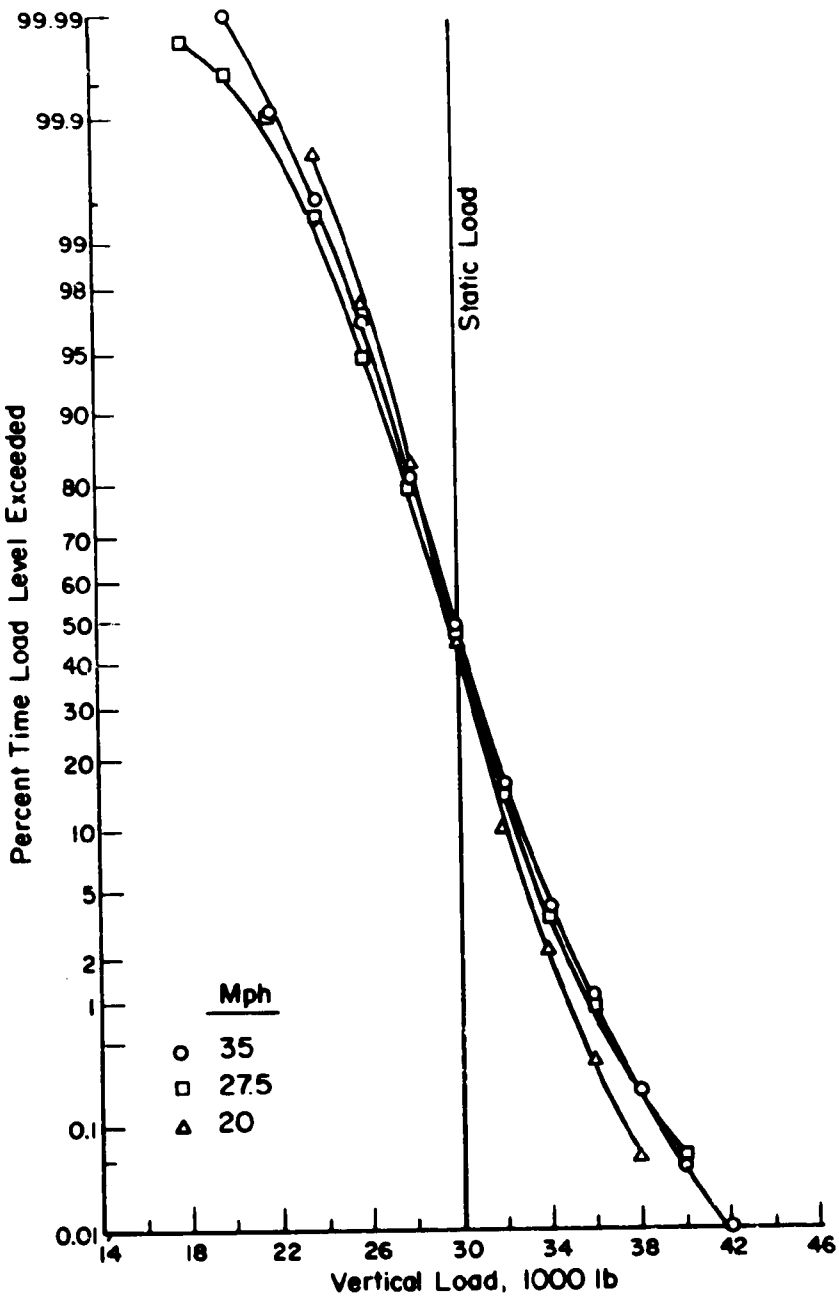

FIGURE 3-29. HISTOGRAMS OF VERTICAL WHEEL/RAIL LOAD AT 20, 27.5 AND 35 MPH, EAST LOAD CELL ON LEAD AXLE, DATA FROM 4 MILES OF TRUCK OPERATION

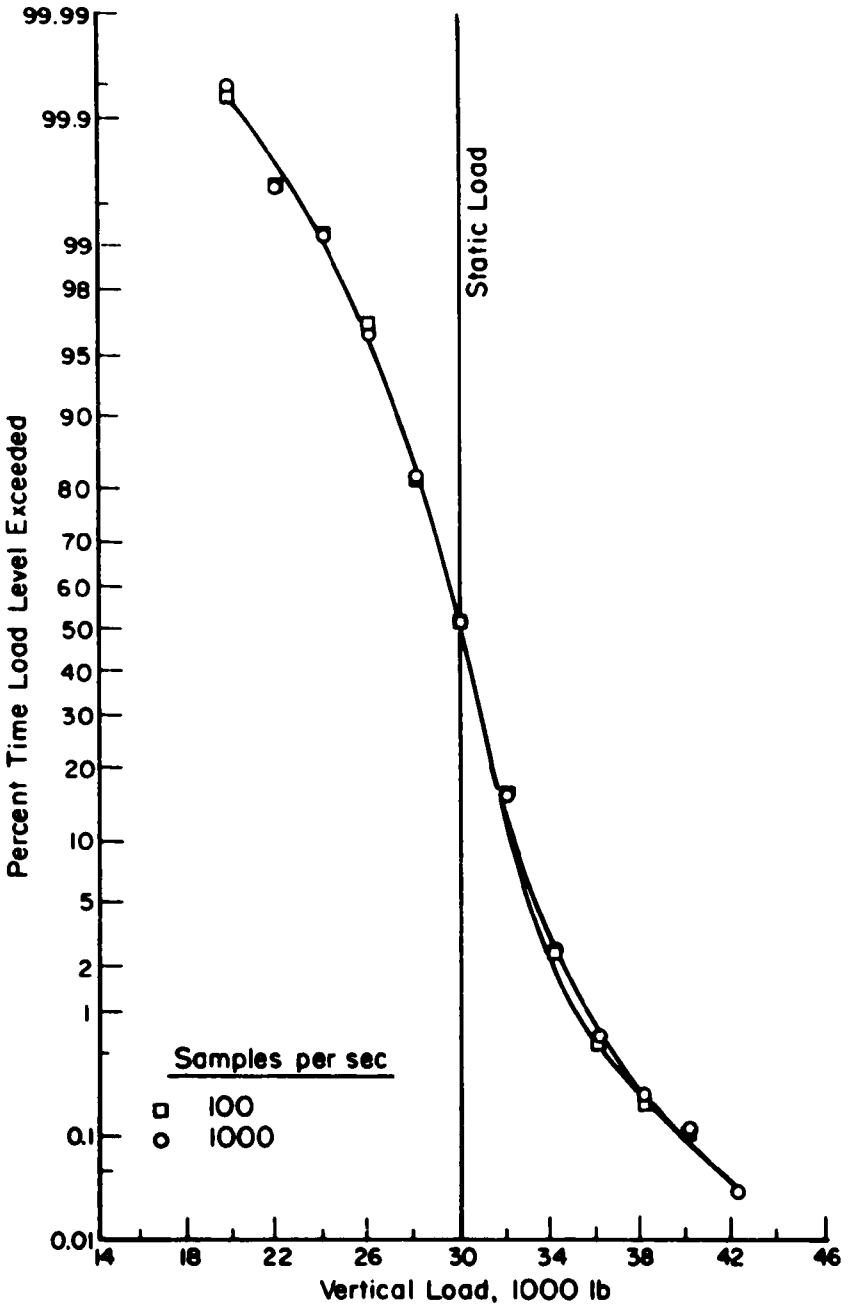

FIGURE 3-30. HISTOGRAMS OF VERTICAL WHEEL/RAIL LOAD FOR 100 AND 1,000 SAMPLES PER SECOND DATA, EAST LOAD CELL ON LEAD AXLE, 35 MPH, DATA FROM 1/2 MILE OF TRUCK OPERATION

recorded by the load cell at the side-frame/roller-bearing-adapter SF/BA interface on the east side of the lead axle.

The data presented in Figure 3-29 were obtained from four miles of operation (miles 3 to 7 of the B&LE test track). This figure compares results for car speeds of 20, 27.5, and 35 mph over this portion of the track. Note that the differences in load distribution are relatively small.

Figure 3-30 demonstrates the effect of the sampling rate on the type of data display. The two sets of data for this comparison are based on a half-mile length of track (miles 3 to 3.5) which includes a turnout and a 5^{o} 30' curve. The data were filtered at 50 Hz when sampling at 100 samples/second and at 500 Hz when sampling at 1000 samples/second. The figure shows a slight difference in data for the two sampling rates. There is a slight improvement in the highest load definition with the higher sampling rate, but these results indicate the load data measured at the SF/BA interface for this CWR track section is predominantly in the 0-50 Hz frequency range.

Individual vertical wheel loads can be measured by load cells at the side-frame/roller-bearing-adapter interface, as is done in the B&LE instrumented truck system. Or, instrumented side frames can be used to measure the total force from two wheels on one side frame, so the wheel load is analyzed. An indication of the differences to be expected when using load cells or when using instrumented side frames is given by the difference between the instantaneous readings of the two load cells on the same side of the truck. Figure 3-31 presents a histogram of the differences between the load cell on the east side of the truck (lead axle east minus trailing axle east), which shows the percent of time this value was less than the indicated value. The data are for four miles (miles 3 to 7) of CWR at 35 mph. Note that for 75 percent of the time the value of this load difference is less than $\pm$ 1000 lbs, which is 3 percent of the static wheel load.

3.3.2 Length of Load Application

The cumulative force data displayed in Figures 3-29 to 3-31 do not define whether load level exceedances occur in one continuous load

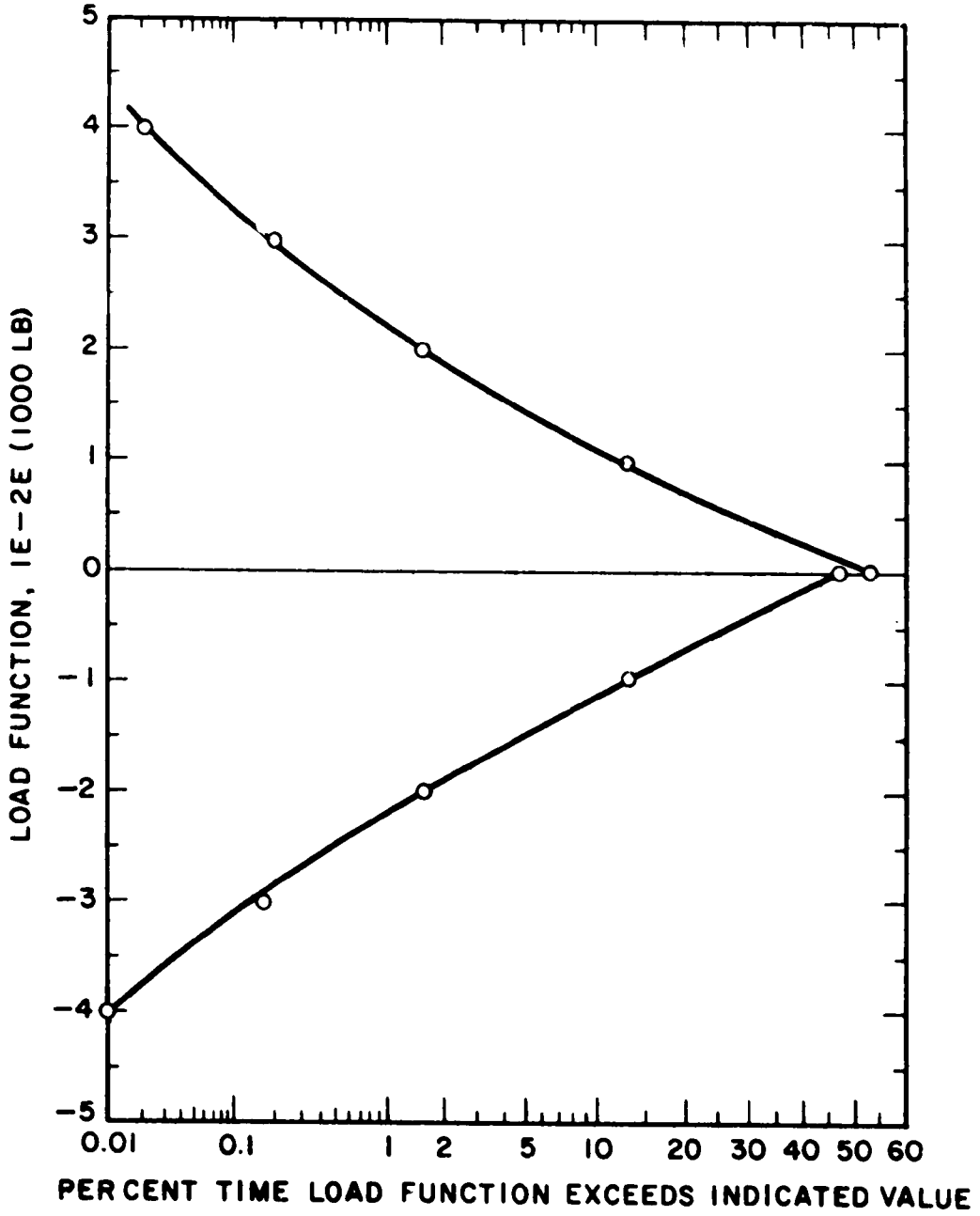

FIGURE 3-31. DIFFERENCE IN VERTICAL WHEEL/RAIL LOAD INDICATED BY LOAD CELLS ON EAST SIDE OF TRUCK, 35 MPH, DATA FROM 4 MILES OF TRUCK OPERATION

application along the rail or in a number of separate, shorter applications. This question has been examined by analyzing the data to determine the length of load application along the rail where a given load level is exceeded. The phenomena is illustrated in Figure 3-32. Note that the application of a 22,000 lb load extends over the entire interval. On the other hand, a load level of 30,000 lbs is exceeded over 6 shorter lengths within the interval. At the 38,000 lb load level there are only 2 relatively short lengths along the rail where this load level is exceeded.

As an example, vertical load data from the 35 mph run has been analyzed for the east load cell of the lead axle to determine the number of occurrences over the four mile run where the load exceeded a given level for a given distance. These data are presented in Figure 3-33. Load lengths along the rail are considered in one foot increments.

3.3.3 Examination of Data at High Load Levels

The highest loads which are measured by a wheel/rail load measurement system will be of particular interest for rail failure mode analysis because they would lead to the highest rail stresses. A technique for reviewing high load data has been utilized to allow detailed study of the nature of these loads. The technique is basically one of noting and displaying load data during time intervals when the high loads occur. This is done while processing the data for other load summaries. Figures 3-34 to 3-36 show the results of such a data display. The numbers shown in these figures are the differences in the running load minus the static load for all four of the side-frame/roller-bearing-adapter load cells on the truck. A load level of $\pm$ 10,000 lbs about the static load has been used to trigger this display. The time interval between load samples is .01 seconds and the data is displayed for approximately $\pm$ .14 seconds about the point where the threshold is exceeded. The track position at which the data is displayed is also noted on each figure with reference to Mile Post 3.

Figure 3-34 shows the high loads associated with the traversal of the turnout. The pattern of load buildup is characteristic of a combined bounce/roll mode of oscillation. Figure 3-35 shows the high load associated with a car body roll motion during traversal of the $5^{\circ}30'$ curve. Note the

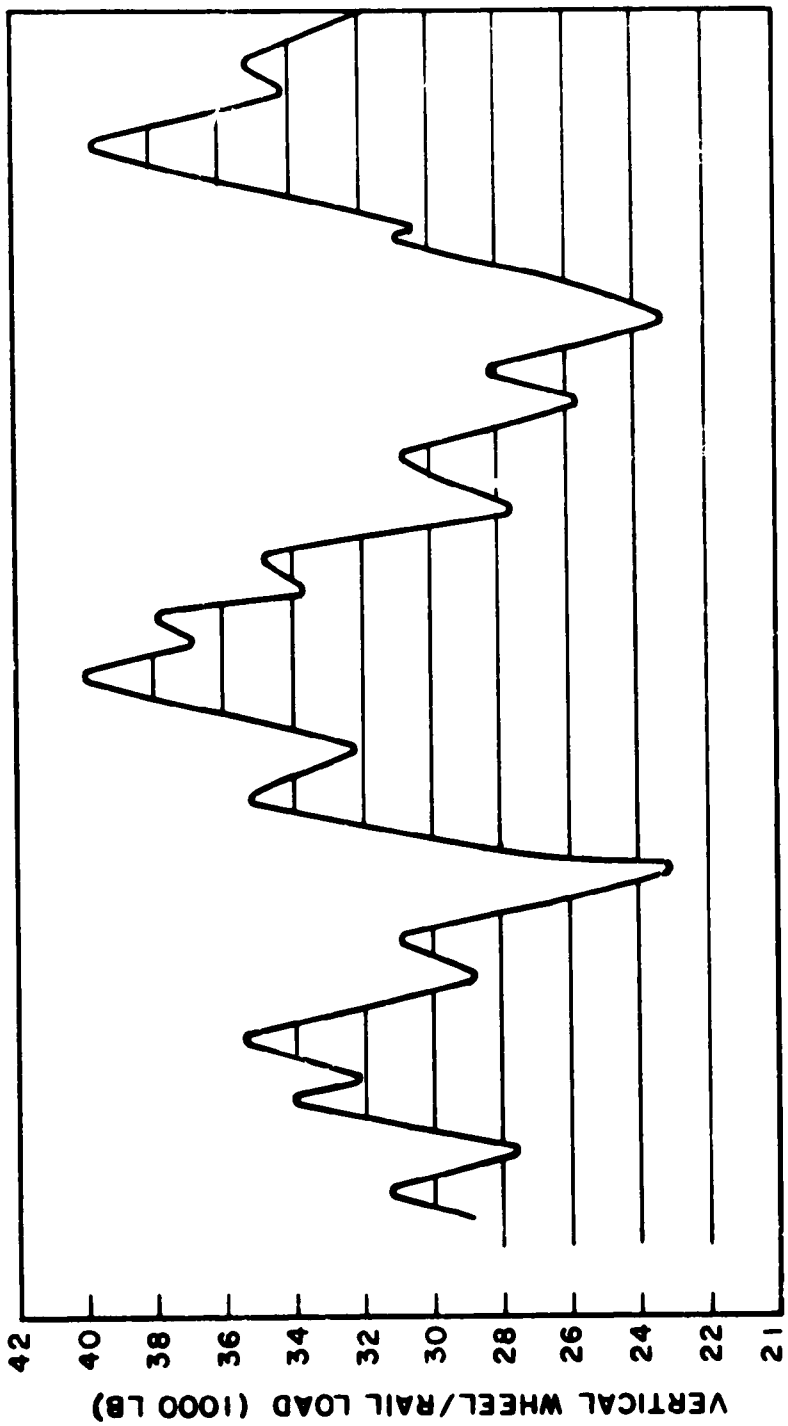

Figure 3-32 FLUCTUATING VERTICAL WHEEL/RAIL LOAD AS A FUNCTION OF DISTANCE ALONG TRACK

Load Level (1000 lb)

Distance (ft)	42	40	38	36	34	32	30	28	26	24	22	20
> 19					1	23	215	335	117	16	3	1
18-19					1	5	20	3				
17-18					2	4	26	4	1			
16-17				1	2	12	31	7				
15-16					1	3	17	9				
14-15				1	1	7	20	11				
13-14			1	1	3	8	29	4	1			
12-13					4	13	37	1	1			
11-12				1	5	12	18	3				
10-11				2	5	19	25	5				
9-10				1	3	26	32	4	1			
8-9			1	1	11	26	39	11	1			
7-8				1	8	28	33	5	1			
6-7				2	8	28	33	7	1			
5-6			2	3	15	31	50	20	3			
4-5		1	1	6	13	41	73	23	3			
3-4			1	5	22	69	83	26	6	1		
2-3	1	2	1	16	32	150	167	65	6	1		
1-2		1	9	21	45	210	195	68	20			1
0-1	1	2	7	15	59	174	202	101	20	3		

FIGURE 3-33. NUMBER OF OCCURRENCES OF VERTICAL WHEEL/RAIL LOAD LEVELS EXCEEDING INDICATED VALUES FOR SPECIFIED DISTANCES OVER 4-MILE LENGTH OF TEST TRACK, 35 MPH

Vertical Load with Reference to Static Load (lb)

Leading Axle		Trailing Axle	
East Side	West Side	East Side	West Side
5,418	-1,022	5,369	-1,014
5,558	-2,142	7,189	-1,794
5,598	-4,242	4,719	-2,964
5,738	-4,242	4,069	-2,574
5,598	-5,642	3,679	-4,264
4,998	-7,042	3,159	-5,044
2,058	-5,922	2,249	-4,004
3,458	-6,482	2,899	-4,524
3,458	-6,342	2,899	-4,784
5,978	-5,782	4,719	-5,614
6,818	-5,922	4,589	-5,614
6,958	-5,922	4,199	-4,654
7,658	-5,922	4,199	-3,484
7,378	-5,362	7,059	-2,184
10,178	-4,892	7,839	-2,704
10,878	-5,922	6,409	-5,434
11,438	-6,342	7,969	-4,524
11,158	-6,762	8,099	-5,564
10,458	-8,022	9,139	-5,954
9,338	-6,902	7,319	-4,524
9,618	-7,182	6,929	-4,264
9,338	-7,322	6,019	-4,734
9,898	-6,622	7,579	-4,654
8,358	-7,462	6,799	-5,694
7,238	-8,032	5,629	-6,344
6,118	-7,742	4,589	-6,344
4,158	-8,022	2,769	-5,824
3,178	-8,302	2,639	-5,954
2,058	-8,302	819	-5,954
2,338	-8,142	1,079	-6,214

Note: Distance from Start of Run 0.041 (mile)

FIGURE 3-34. VERTICAL LOAD CELL MEASUREMENTS OBTAINED 14 SAMPLES BEFORE AND AFTER LOAD PEAK EXCEEDING ± 10,000 LB 35 MPH THROUGH TURNOUT (SAMPLING RATE 100 SAMPLES PER SECOND)

Vertical Load with Reference to Static Load (lbs)

Leading Axle		Trailing Axle	
East Side	West Side	East Side	West Side
-588	1,204	-1,118	1,703
-728	1,764	-1,508	1,183
-1,008	2,324	-1,898	1,183
-1,708	2,744	-2,548	2,223
-2,688	3,304	-2,938	2,743
-2,688	3,164	-2,548	1,833
-3,108	3,864	-2,938	2,093
-3,248	4,844	-4,108	3,263
-3,948	5,544	-3,868	3,523
-3,948	6,104	-3,328	4,173
-3,668	6,804	-4,108	3,653
-3,108	7,224	-4,238	4,563
-3,388	7,924	-4,368	6,123
-4,508	8,764	-3,458	7,423
-5,208	10,024	-4,238	8,593
-4,928	10,864	-5,408	9,113
-5,208	11,984	-5,668	10,153
-5,768	13,664	-5,408	11,193
-6,468	14,364	-5,928	12,233
-6,748	14,644	-6,188	11,973
-7,168	13,304	-6,448	10,283
-8,008	11,904	-7,228	8,463
-8,568	10,444	-7,878	7,033
-8,988	10,444	-8,138	6,903
-8,988	10,584	-8,398	7,163
-9,128	10,164	-8,268	6,773
-9,268	9,744	-8,268	6,253
-9,548	9,884	-8,398	5,733
-9,688	10,164	-8,528	6,123
-9,688	10,724	-8,918	6,383

Note: Distance from Start of Run 0.262 (mile)

FIGURE 3-35. VERTICAL LOAD CELL MEASUREMENTS OBTAINED 14 SAMPLES BEFORE AND AFTER LOAD PEAK EXCEEDING ± 10,000 LB 35 MPH ON CURVED TRACK (SAMPLING RATE 100 SAMPLES PER SECOND)

Vertical Load with Reference to Static Load (lbs)

Leading Axle		Trailing Axle	
East Side	West Side	East Side	West Side
2,058	-742	2,119	13
2,198	-742	2,119	-104
1,638	-882	1,729	273
1,638	-1,302	1,729	-234
1,358	-1,442	1,599	-364
1,078	-1,162	1,599	-234
1,358	-462	1,729	143
1,358	-602	1,599	-234
1,498	-322	1,339	13
798	-742	689	-494
98	-1,722	-208	-1,144
-868	-2,282	-988	-1,794
-1,148	-2,422	-1,378	-1,924
-1,008	-2,142	-1,508	-2,054
-1,008	80,304	-1,508	-1,794
-448	90,804	-1,118	-1,274
-28	18,004	-858	-624
378	784	-468	-494
798	224	-78	-234
658	364	-338	-234
378	364	-728	-104
98	784	-988	143
378	924	-858	13
378	1,344	-728	273
238	1,764	-858	533
378	2,044	-728	793
378	2,464	-858	1,183
98	2,604	-1,118	1,053
-28	2,604	-1,248	1,053
-588	2,604	-1,378	663

Note: Distance from Start of Rim 2.594 (mile)

FIGURE 3-36. VERTICAL LOAD CELL MEASUREMENTS OBTAINED 14 SAMPLES BEFORE AND AFTER LOAD PEAK EXCEEDING ± 10,000 LB 35 MPH (SAMPLING RATE 100 SAMPLES PER SECOND)

high loads on both the west load cells. Figure 3-36 shows the way in which erroneous data can be detected by this type of data display. Note the 90,000 lb load indicated for the west side of the lead axle. The magnitude and time-wise character of this load record and a comparison with data on the other channels demonstrates that this phenomenon is due to electrical noise rather than a physical loading effect.

3.3.4 Frequency Analysis

Vertical load data obtained from the side-frame/roller-bearing-adapter load cell on the east side of the lead axle have been analyzed to determine the frequency content of the fluctuating load data. This information is presented in plots of power-spectral-density (PSD) of the load data shown in Figures 3-37 through 3-40. Figure 3-37 shows results of the PSD analysis for data obtained while traversing a turnout. Figure 3-38 shows similar data for tangent track with welded rail. Figure 3-39 presents PSD data for traversal of the 10° curve where jointed rail is used. Note that the predominant energy level is in the very low frequency band. This is expected, in view of the known suspension characteristics of the freight car truck. The two minor peaks in the 220 and 300 Hz ranges probably represent natural frequencies of the truck side frames or wheels, etc.

The PSD analyses reveal that vehicle dynamics are most severe at the turnout (Figure 3-37) and are least severe while traversing tangent track with welded rail (Figure 3-38). Figure 3-40 presents a PSD analysis of the low-frequency end of the spectrum for a four mile length of the test run. The predominant frequency is 1.2 Hz, which represents roll of the car body. These measurements show very little frequency content above about 6 Hz for this operating mode.

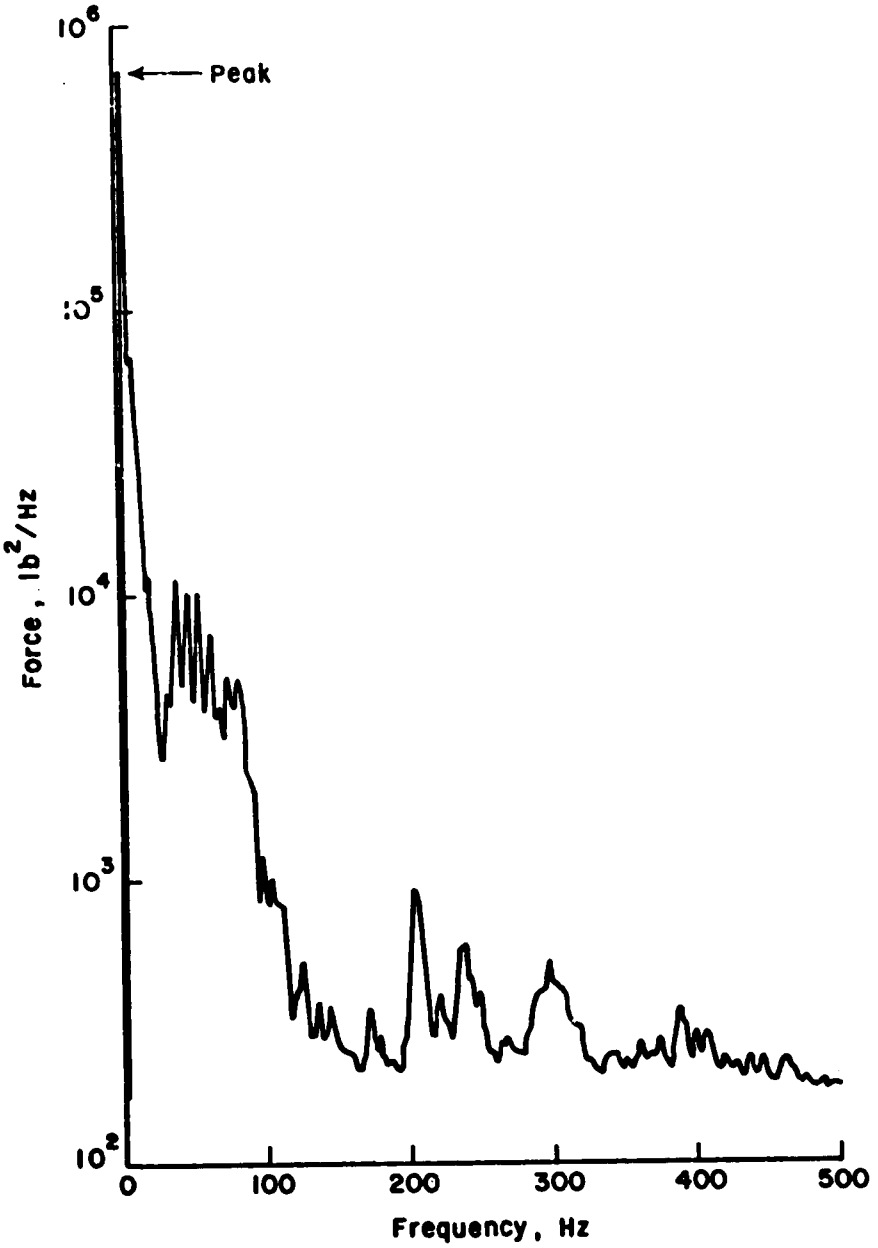

FIGURE 3-37. POWER SPECTRAL DENSITY OF VERTICAL FORCE AT TURNOUT, LEAD AXLE EAST SIDE, 35 MPH, 8 SEC INTEGRATION PERIOD

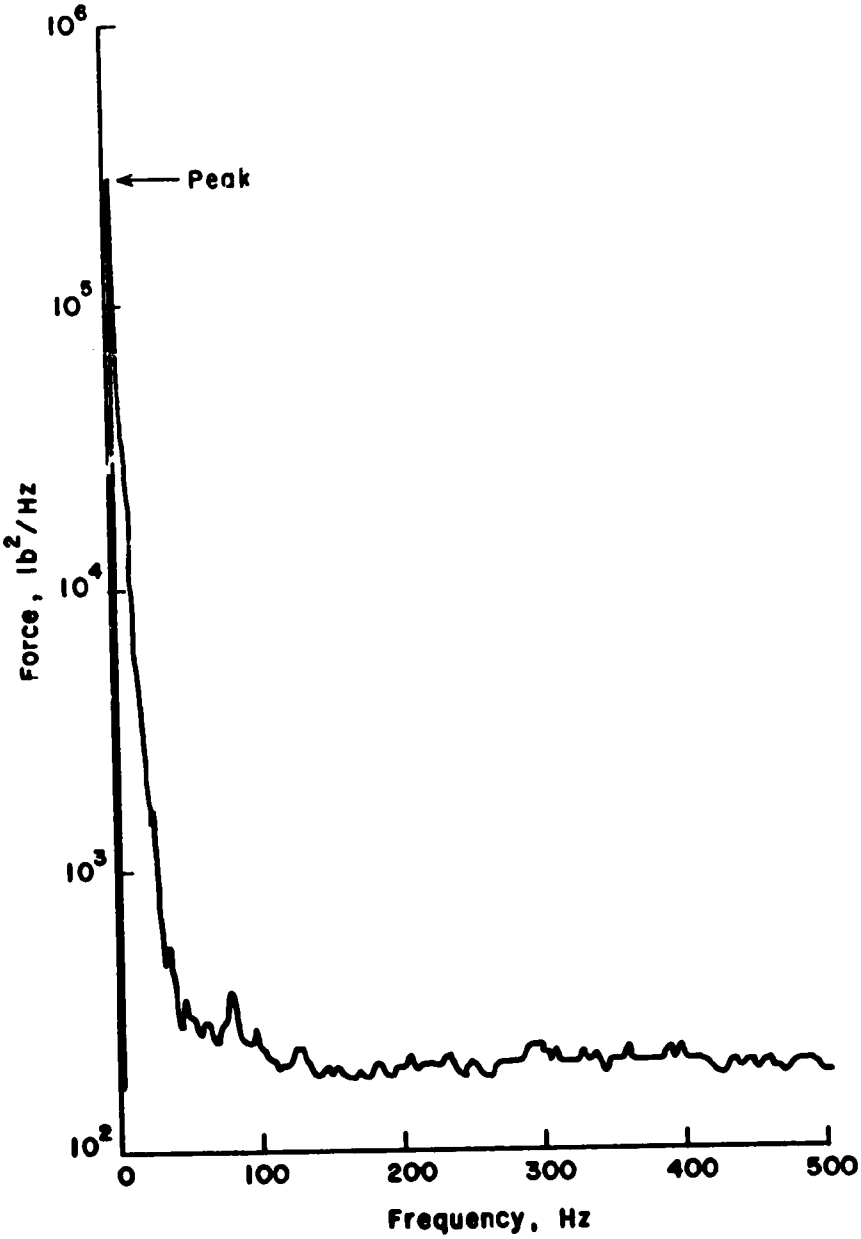

FIGURE 3-38. POWER SPECTRAL DENSITY OF VERTICAL FORCE RECORD ON TANGENT TRACK AND WELDED RAIL, LEAD AXLE EAST SIDE, 35 MPH, 32 SEC INTEGRATION PERIOD

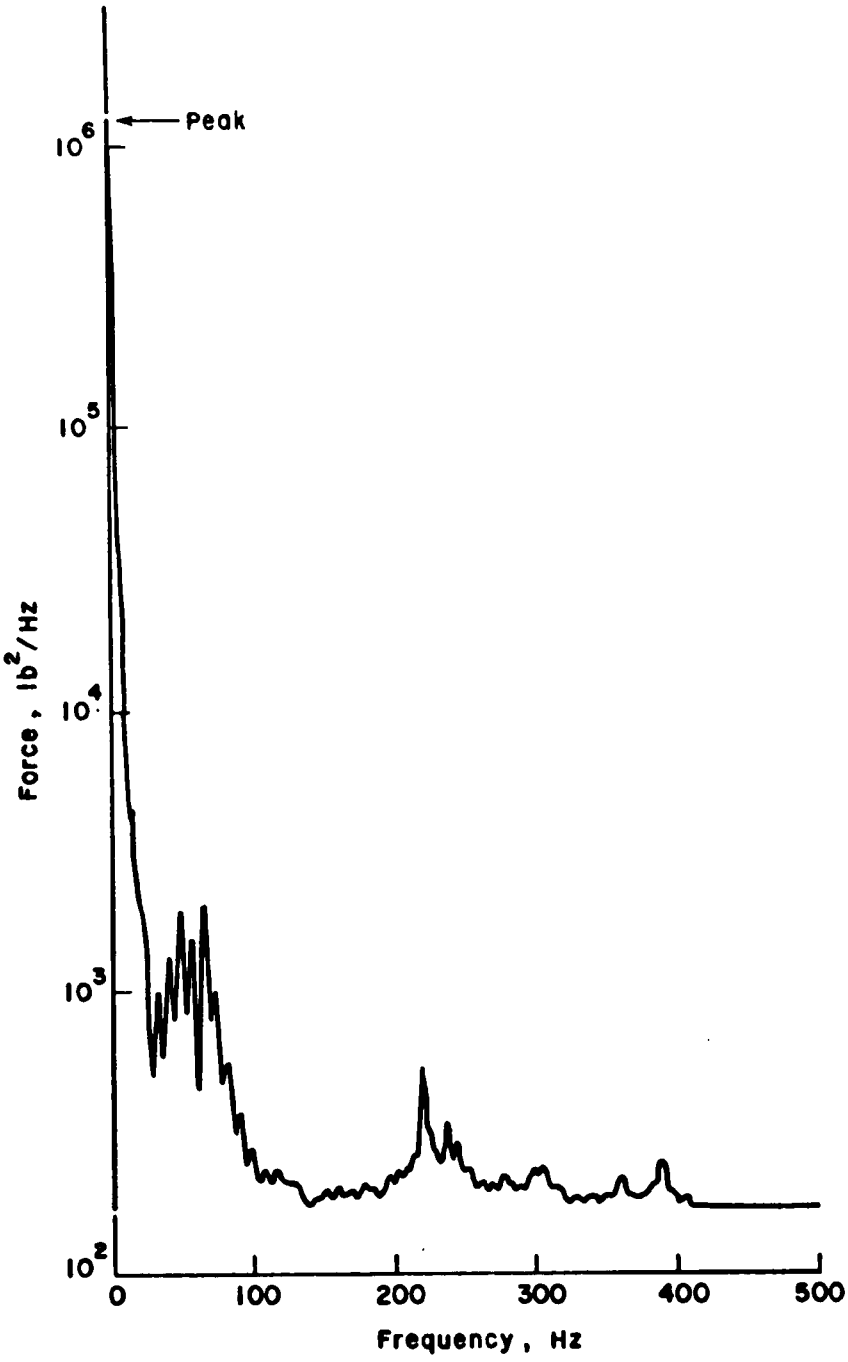

FIGURE 3-39. POWER SPECTRAL DENSITY OF VERTICAL FORCE RECORD AT 10° CURVE, JOINTED RAIL, LEAD AXLE EAST SIDE, 35 MPH, 16 SEC INTEGRATION PERIOD

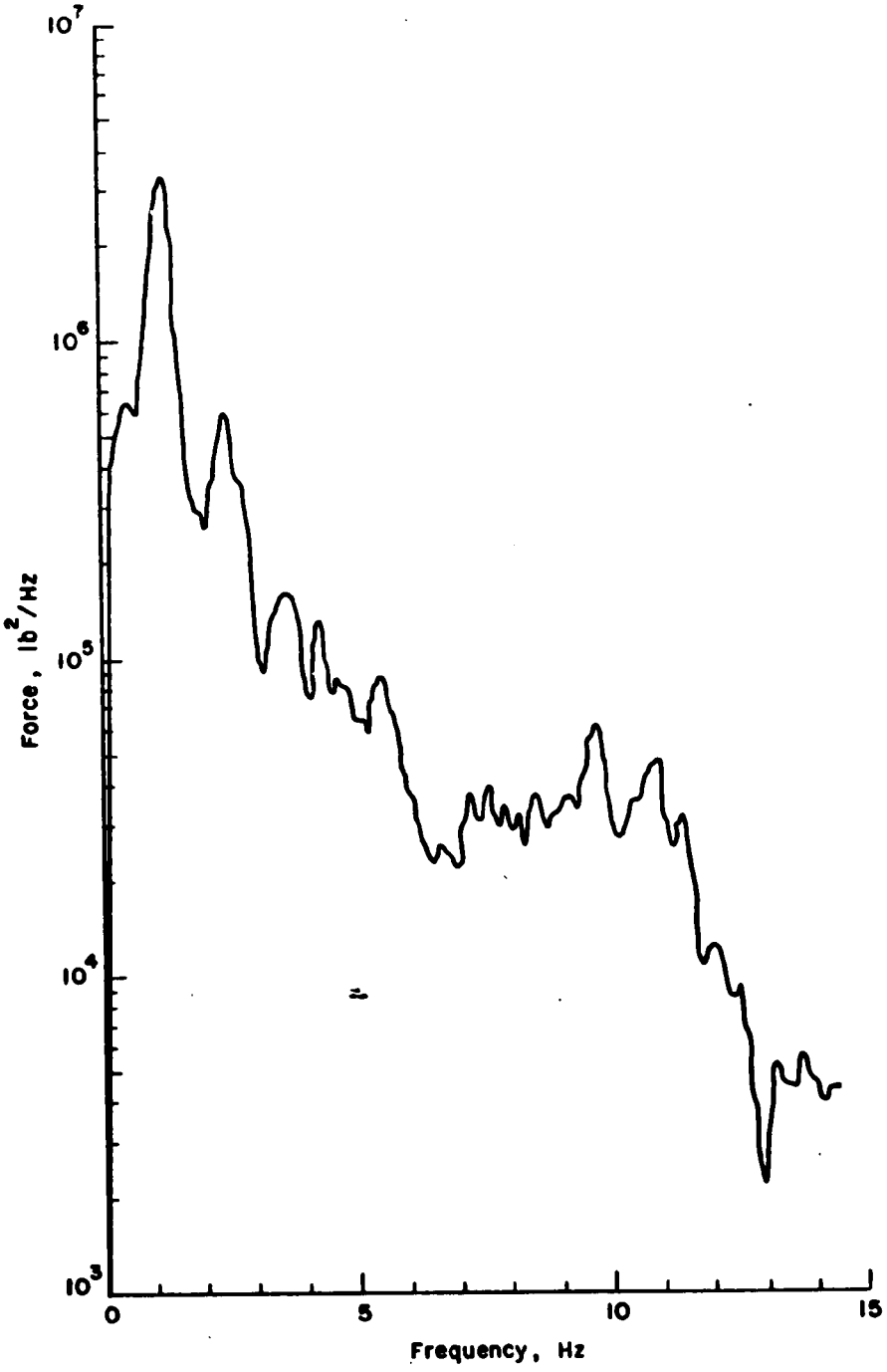

FIGURE 3-40. POWER SPECTRAL DENSITY OF VERTICAL FORCE RECORD OVER 3 MILES OF TEST TRACK, MILEPOSTS 3 to 6, LEAD AXLE EAST SIDE, 35 MPH, 5.3 MIN INTEGRATION PERIOD

3.3.5 Typical Measurements Results

A variety of tests were conducted with the 100-ton hopper car test vehicle over the track shown in Figure 3-28. Results of these tests are described in detail in Reference 3-35, but a few typical statistical plots of vertical and lateral wheel load variations have been included here for reference. Data reduction consisted of a mean level crossing peak count routine (both positive and negative peaks about the static load level), which may be used to summarize the load environment for evaluating fatigue damage. Distributions of positive and negative peaks about the mean load level have been plotted versus the number of times the peak level is exceeded per counting interval. For vertical load, this has been normalized to a number of exceedances per-mile basis; and for lateral load, this has been normalized to a number of wheel revolutions per mile basis.

An average vertical load spectrum is plotted in Figure 3-41 for the loaded 100-ton car on both tangent and curved track at 35 mph, and two different truck designs. One standard deviation values are also plotted in the figure. Note that these loads were measured at the side frame/bearing adapter (SF/BA) load cell, so the actual wheel loads will be higher than shown in the figures due to an additional 1400 to 1500 pounds of unsprung weight located between the adapter and the W/R contact point. Also, the bearing adapter is located outboard from the line of wheel force, so W/R forces due to car roll and cross level inputs are higher than the forces measured at the bearing adapters.

Variations in the vertical load at the SF/BA load cell from tangent to curved track are shown in Figure 3-42. A substantial increase in load is seen on curved track due to excitation of the car body roll mode and operation at an unbalanced speed. Finally, the effect on the vertical load spectrum of the addition of a 2-inch wheel flat is seen in Figure 3-43.

Lateral load spectra were developed in a similar manner for the loaded 100-ton hopper car. Curves analogous to the vertical load spectra of Figure 3-41 are shown in Figure 3-44 for the lead axle of the car, again over both tangent and curved track. The effects of curvature are demonstrated in Figure 3-45: in this curve "average load" refers to the quasi-static curving forces on the axle, while "peak load" refers to the dynamic

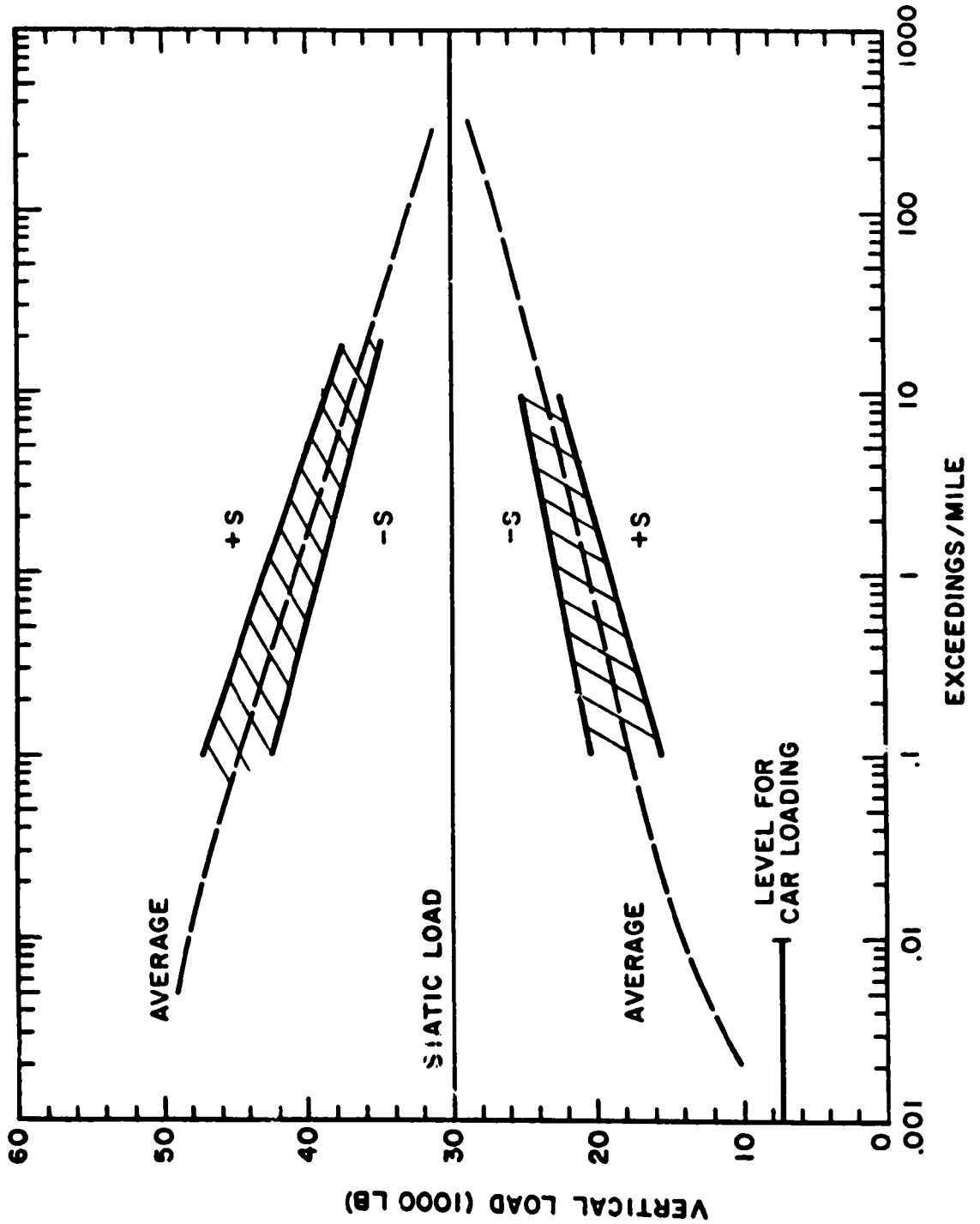

FIGURE 3-41. AVERAGE VERTICAL SF/BA LOAD SPECTRUM AT 35 MPH

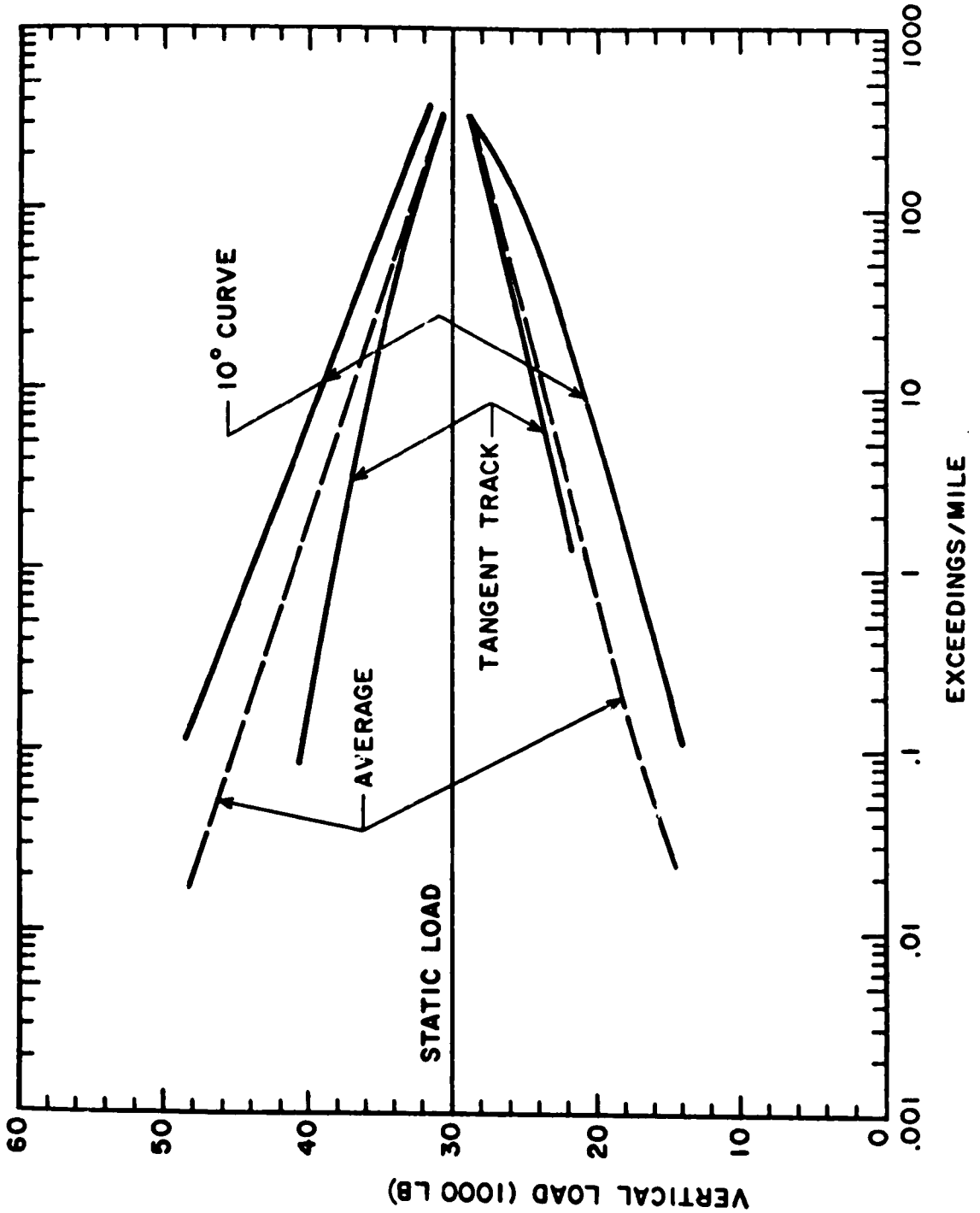

FIGURE 3-42. COMPARISON OF TANGENT TRACK AND 10° CURVE VERTICAL SF/BA LOAD SPECTRA WITH AVERAGE SPECTRUM AT 35 MPH

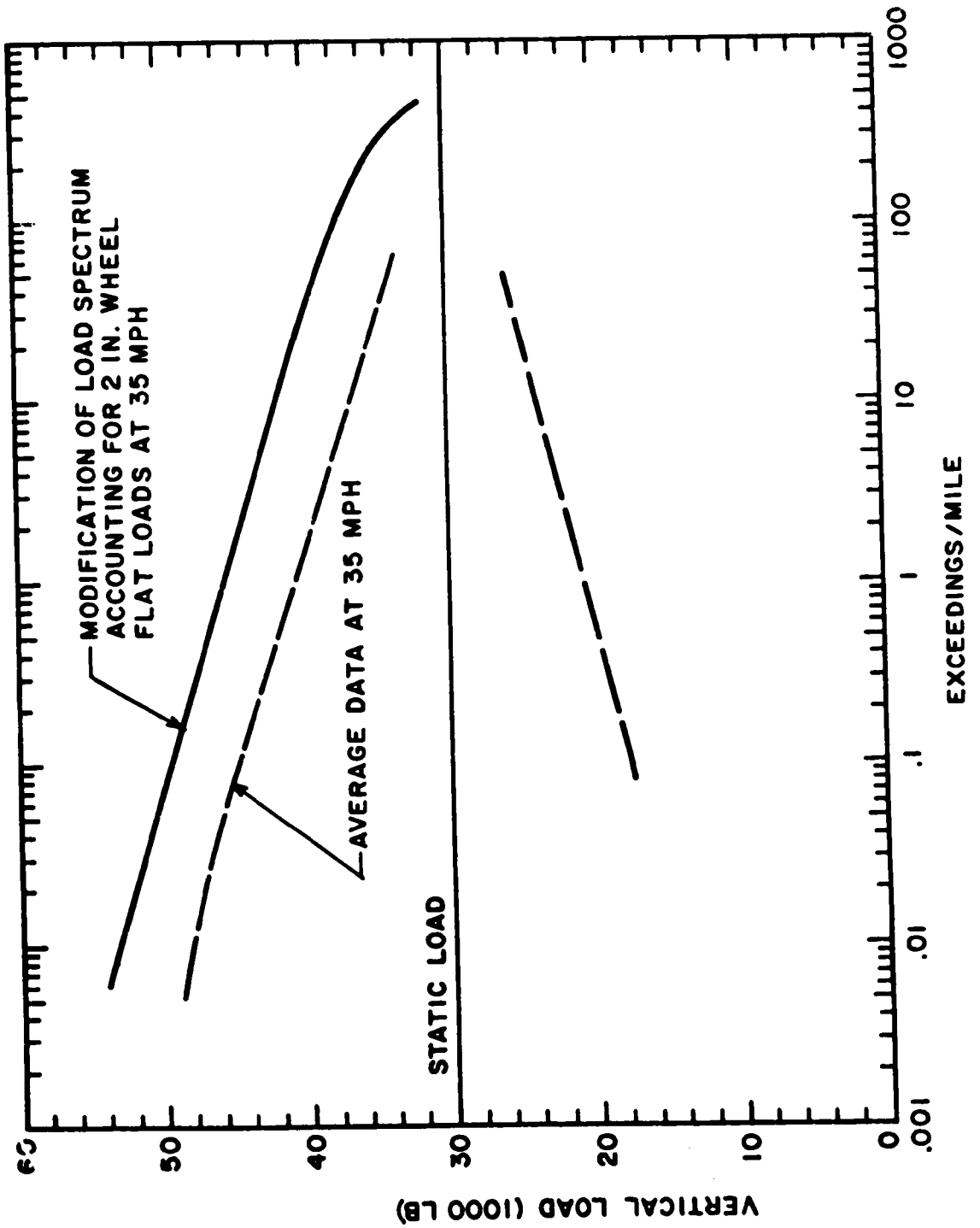

FIGURE 3-43. COMPARISON OF VERTICAL SF/BA LOAD SPECTRA WITH AND WITHOUT WHEEL FLAT LOADS AT 35 MPH

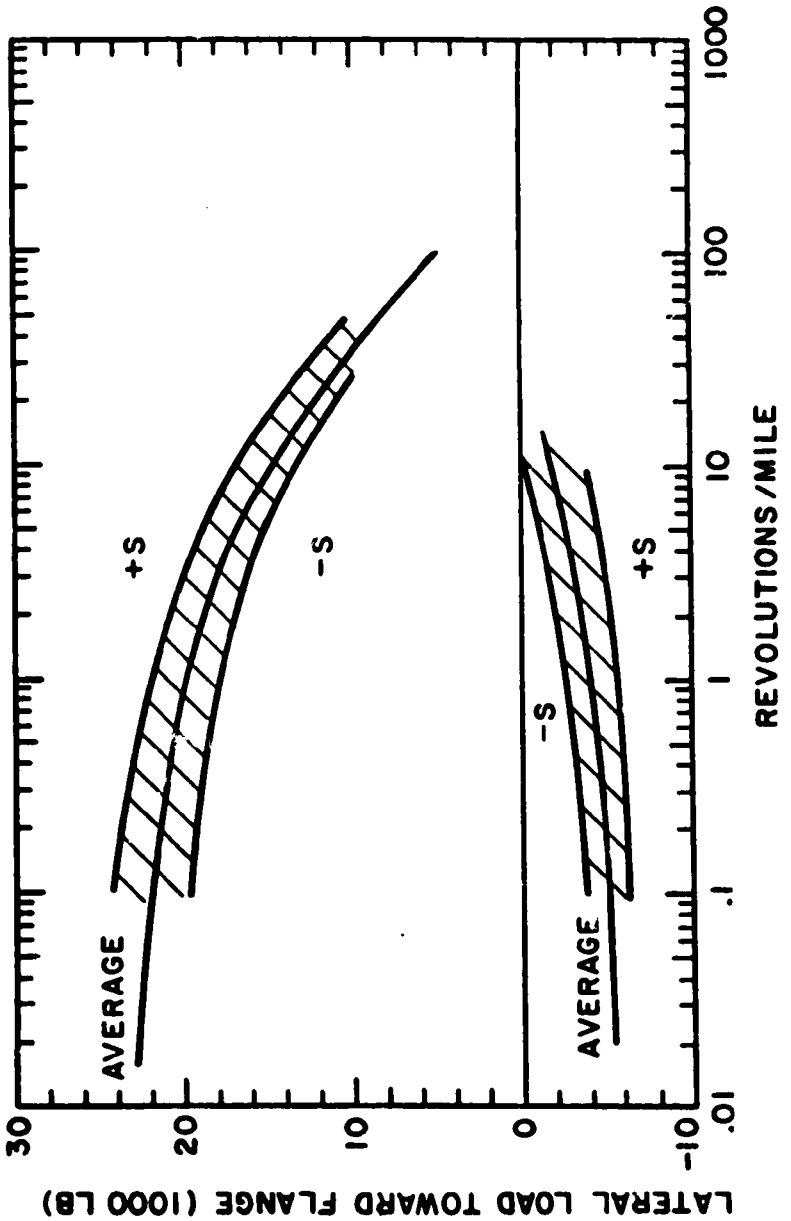

FIGURE 3-44. AVERAGE LEAD AXLE LATERAL WHEEL LOAD SPECTRUM AT 35 MPH

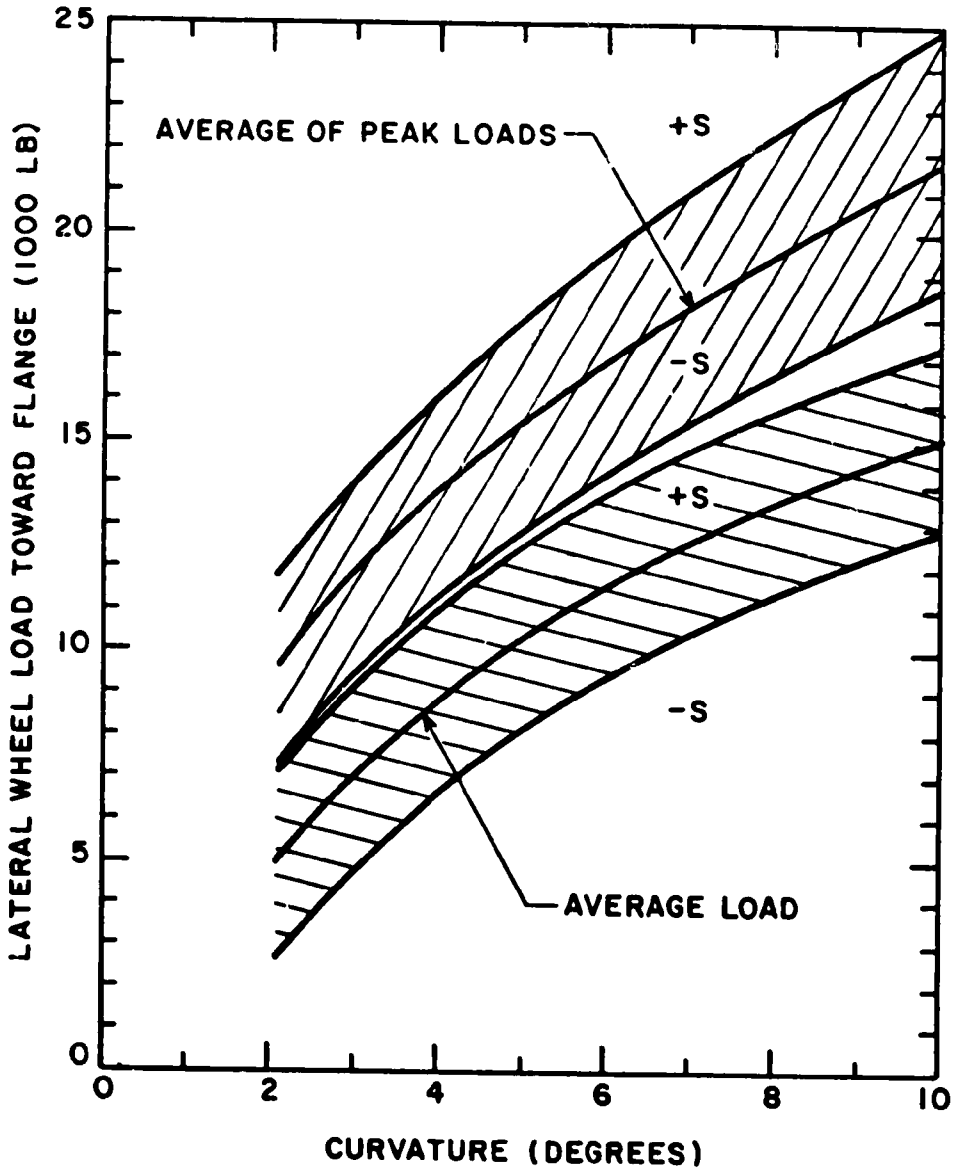

FIGURE 3-45. LATERAL WHEEL LOADS ON LEAD AXLE, HIGH RAIL WITH NORMAL TRUCK CONDITIONS AT 35 MPH

variations due to track geometry and car response. Spectra of loads on a 10-degree curve are shown in Figure 3-46; and a comparison of the "average" spectra (which includes curved-track operation) with tangent track spectra is shown in Figure 3-47.

It must be noted that these load spectra, while representative, are specific to the particular test vehicle, track conditions and operating practices. A range of vehicle parameters (worn snubbers, worn wheel profiles, short-travel spring groups, etc.) or track conditions (particularly low, staggered rail joints on 39-foot rail lengths) would significantly change the results. Longitudinal train action and location of the car in a train would also have a significant effect on the lateral load spectra.

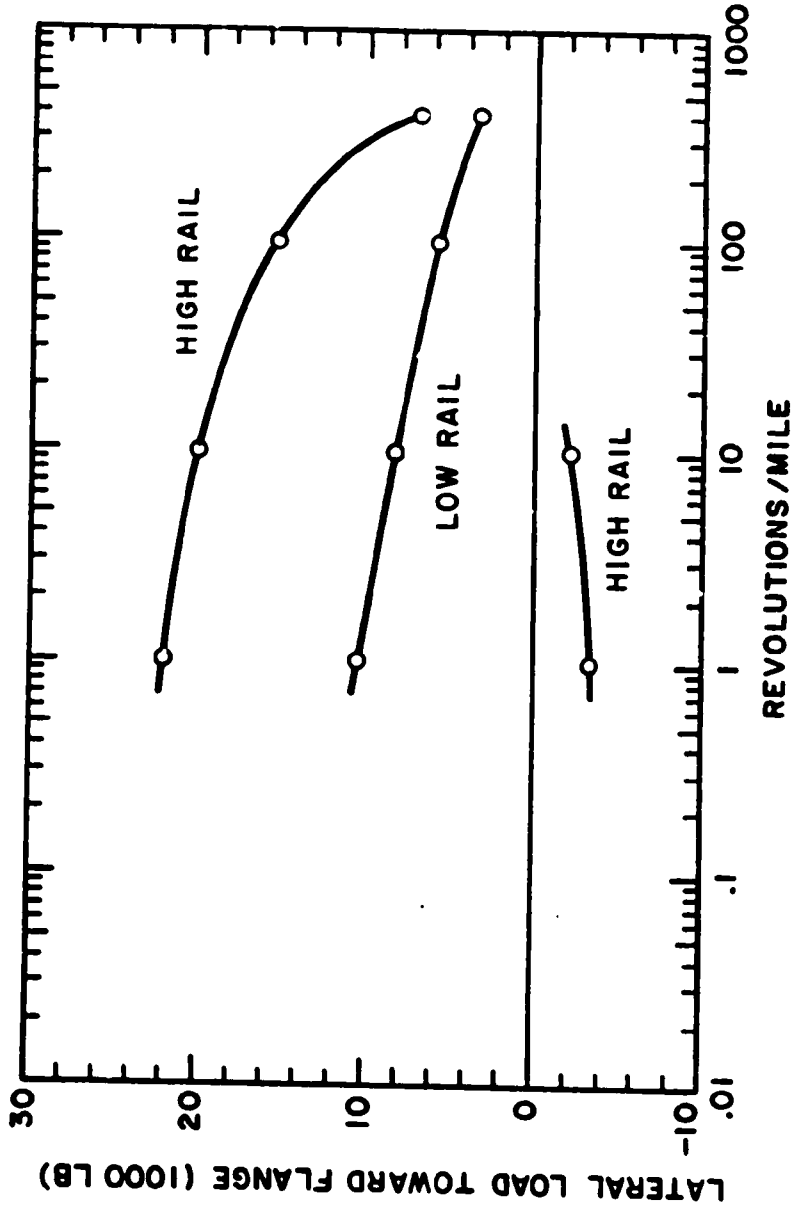

FIGURE 3-46. LEAD AXLE LATERAL WHEEL LOAD SPECTRUM FOR 10° CURVE AT 35 MPH

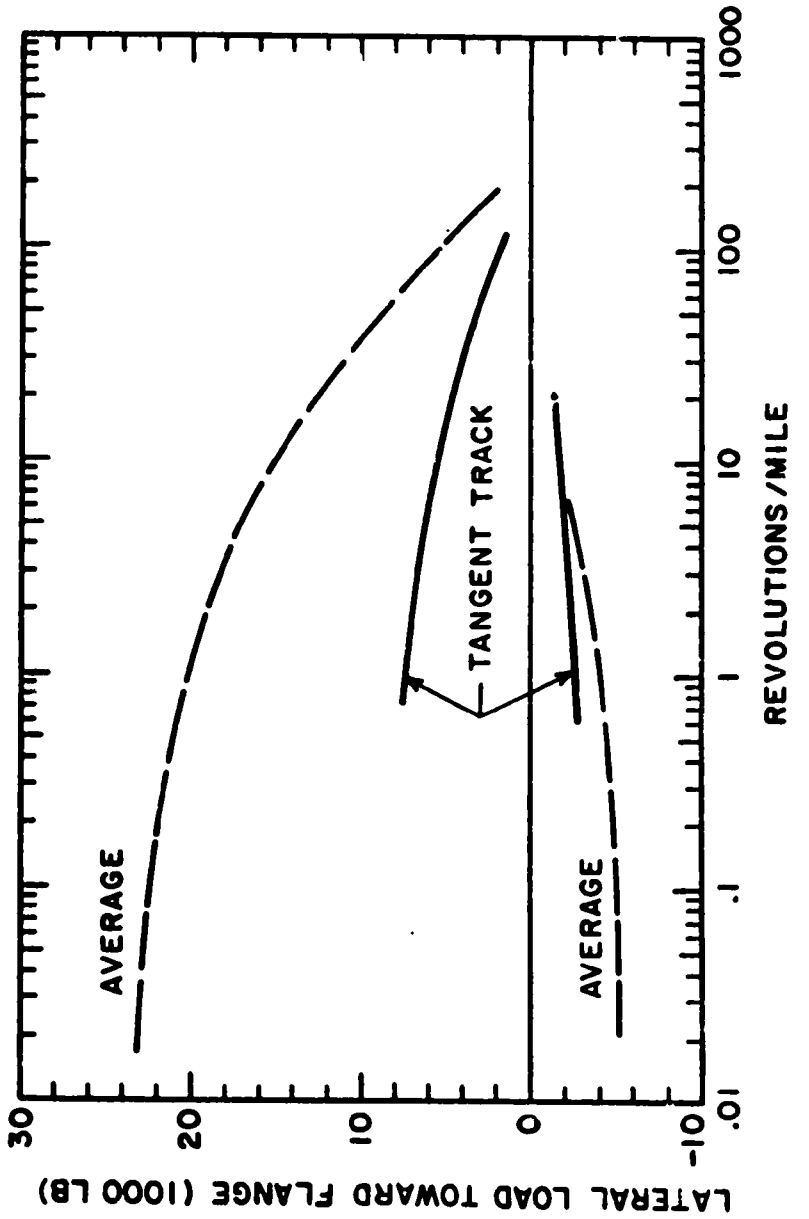

FIGURE 3-47. COMPARISON OF TANGENT TRACK LEAD AXLE LATERAL WHEEL LOAD SPECTRUM WITH AVERAGE SPECTRUM AT 35 MPH

4. LOAD PREDICTIVE METHODOLOGY

4.1 REVIEW OF MODELING TECHNIQUES

In the past the wheel/rail forces developed by rail vehicles and the resulting stresses in rail and track structure have been estimated from empirical relationships. These empirical equations have been derived from measured loads, stresses, etc., where least-square and other curve-fitting techniques were used to establish the coefficients and exponents of the relationships. Prior to about 1955, only a few relatively simple mathematical models of vehicle and track were developed, and solutions were obtained by traditional methods. In the past two decades, advances in computer technology, both analog and digital, have made possible the direct solution of complex sets of differential equations representing a rail vehicle and track structure. This section provides a brief review of rail vehicle/track dynamics modeling techniques and requirements.

4.1.1 Vehicle/Track Mathematical Models

The mathematical model of a rail vehicle and track is a set of equations describing the dynamic and kinematic relationships of this system. Equations may be derived using the generalized Lagrange equation:

$$\frac{d}{dt}\left(\frac{\partial T}{\partial \dot{q}_i}\right) - \left(\frac{\partial T}{\partial q_i}\right) + \left(\frac{\partial V}{\partial q_i}\right) = Q_i \qquad (4\text{-}1)$$

where T = kinetic energy of system

V = potential energy of system

q_i = i^{th} generalized coordinate

Q_i = generalized force acting on the system .

The rail vehicle/track system is defined as an assemblage of track and vehicle components acting as a whole, with each component identified and assigned characteristics based on its specific physical properties. Mathematical models may be conveniently classed as discrete or continuous

systems, where the discrete system (for example. a simple spring-mass-damper) may be described by ordinary differential equations in just one independent variable, usually time. The continuous system, on the other hand, has physical properties which are functions of the spatial coordinates, and its behavior is described by partial differential equations (or integral equations) with two or more independent variables.

Since the partial differential equation presents computational difficulties, other methods for simulating continuous systems must be used. A modal analysis may be implemented by adding the contributions of the normal modes of vibration through superposition:

$$u(x,t) = \sum_{i=1}^{m} q_i(t)\, \phi_i(x) \ , \qquad (4\text{-}2)$$

where u = system displacement, function of t and spatial coordinate x
q_i = system displacement, i^{th} normal mode
ϕ_i = i^{th} normal mode shape .

The normal mode shapes for simple structures (uniform beams, bars, et cetera) may be calculated using classical solutions to differential equations. Mode shapes of complex systems can be determined by the eigenvalue/eigenvector solution of finite element models. As many modes are used to represent the dynamic characteristics of the continuous system as are deemed important within the frequency range of the overall mathematical model. Direct integration procedures using finite-difference (lumped-element) models, or a finite element model itself, can require many more nodal elements to obtain same accuracy as the normal mode model.

Once a satisfactory model of the continuous system is established, it may be combined with other systems (discrete or quasi-continuous) through the use of transfer functions. The overall mathematical model is then used to study system behavior in response to some system excitation, as shown below.

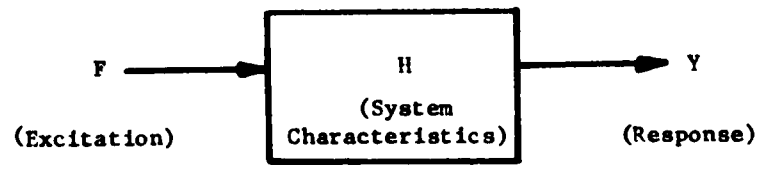

4.1.2 Dynamic Analysis Techniques

Once the mathematical model of a system has been established, a computational technique for obtaining numerical solutions must be selected. The techniques for dynamic analysis by mathematical modeling are conveniently divided into the frequency-domain approach and the time-domain approach. For the frequency domain approach, the differential equations representing the vehicle/track system are transformed to the frequency domain by LaPlace (or Fourier) methods, which require that the model be linear. While the assumption of linearity is often a considerable restriction, this technique is convenient and can provide very useful insight into system behavior. In addition, superposition applies to a linear system, so that the separate responses to several different inputs can be combined.

Differential equations transformed to the frequency domain become algebraic equations with complex frequency (rather than time) as the independent variable. Sets of equations in complex numbers can be set up in matrix form, and the response solution to given inputs versus frequency can be implemented by matrix algebra. Transfer functions describing system output/input relationships can also be developed, and the response calculated by manipulation of complex numbers. Choice of method depends on the particular complexities of the system, but in either case the frequency-domain analysis technique is well-suited to the digital computer.

The effects of many nonlinearities can be included in the frequency domain analysis by approximate methods such as equivalent linear parameters or "describing functions". The steady-state response of a linear element to a sinusoidal excitation is a pure sine wave at the same frequency as the excitation. The ratio of the amplitudes (response to input) and the phase angle between the two are functions of frequency, but invariant with changes in excitation amplitude. On the other hand, the response of a nonlinear element to a sinusoidal excitation is not a pure sine wave, but it is periodic. Therefore, a Fourier analysis of the output can be performed, using the excitation frequency as the fundamental frequency. Fortunately, the higher harmonics can often be neglected because of the low-pass filtering characteristics of the vehicle suspension system. In this way, the

total response can be approximated by using only the fundamental frequency component of the response. The describing function is, therefore, a quasi-linear transfer function based on the first Fourier coefficient, and both the gain and phase are dependent on both the excitation frequency and amplitude.

The time-domain approach is more general then the frequency domain approach because it is equally applicable to systems which are linear o which have significant nonlinearities. With this technique the excitation (or forcing function) is a time-history of forces or displacements that may be artificially generated or taken from actual measurements. System response variables are also time-histories, since time is the independent variable of the solution. Both transient and steady-state response may be calculated by the time-domain approach. Since the resulting response data are in the form of time-varying signals, all the advantages and disadvantages of field-recorded data are present, in terms of data reduction and analysis.

For simulation by the time-domain technique, the differential equations describing the system are used directly in a computer program. Nonlinearities of all types are handled with relative ease. The analog computer is uniquely suited for time domain analysis due to the "parallel" solution that is dynamically analogous to the actual, physical system. The simultaneous display of several system time responses on a strip-chart recorder or oscilloscope can provide a good visualization of system dynamics.

Modern digital computers can perform time-domain analysis using well-developed numerical integration routines and specialized digital programs (such as IBM's CSMP, or the MIMIC program developed at the Wright-Patterson Air Force Base) that simplify the programming of "analog-type" problems. Since problem solution is a "serial" (step-by-step) operation, the digital computer is far less efficient than the analog computer for time-domain analysis. Computational costs can be excessive if many time-domain runs are to be made using a complex rail vehicle model. A good compromise can be found in the hybrid computer, in which the analog computer is combined with the digital computer to take advantage of the unique capabilities of both. The digital computer is used for control, logic, function generation and data processing; while the analog computer is used

for solution of most (if not all) of the differential equations. The digital computer (with generally greater reliability and programming flexibility) is also used for set-up, static check and diagnosis of the analog portion of a program.

4.1.3 Vehicle/Track Model Requirements

The objectives for formulating a mathematical model of a rail vehicle/track system is to evaluate system response for a wide spectrum of environmental excitation or disturbance, to predict (or explain) unusual dynamic behavior in the prototype system, and to evaluate changes to correct this behavior. A well-conceived mathematical model of the vehicle/track system can be used to predict forces, accelerations, stresses, or displacements with a good degree of confidence.

In developing a useful mathematical model, considerable judgment is required to choose between excessive detail (with the attendent computational problems of limited equipment and/or long problem run times) and unrealistic simplicity (with the chance of missing important modes of response). However, available measured data (see Section 3.0) can help define the modes of dynamic behavior that are important in characterizing wheel/rail loads. Vehicle/track interaction can be classified in six broad areas: 1) sprung-mass (car body, truck frame) dynamics, 2) unsprung-mass (wheel/rail impact) dynamics, 3) longitudinal (train action) dynamics, 4) truck hunting phenomena, 5) curve negotiation, 6) traction- or braking-related dynamics, and 7) track structure dynamics.

Based on a practical consideration of the many facets of vehicle dynamics modeling, the following items summarize the requirements of models for wheel/rail load predictions. Models should:

(1) Include all important degrees of freedom for the particular purpose of phenomenon of interest in the frequency range of interest (if in doubt of the importance of a DOF, include it until its effects can be evaluated);

(2) Be limited to the most important degrees of freedom where possible for practical program size and solution time/cost factors (this may require breaking the overall vehicle/track

model down into subsets, such as the wheel/rail unsprung masses, for modeling over limited frequency bandwidths);

(3) Include the important nonlinearities for transient response or large-signal frequency-domain solutions;

(4) Use superposition of steady-state or quasi-static inputs and outputs where possible (care must be exercised that significant nonlinearities, such as suspension motion limits, do not affect the solution).

There are several overriding practical and economic considerations in the choice of model for wheel/rail load prediction. First is, of course, the availability of specific models and programs to meet the W/R load modeling requirements. The time required to implement a specific computer program is important when immediate results are required by other research programs. A second important consideration is the type and size of available computer, which can limit the size and complexity of the mathematical model. Finally, the size and computational speed of the computer facility can have a definite impact on the cost of running the model.

Specifications for several generic computer models for the characterization of W/R loads are listed in Table 4-1, based on the track degradation modes discussed in Section 3.1 (see Tables 1-1 and 3-2). The available models that satisfy the requirements of at least some of these categories are discussed in greater detail in Section 4.2.

4.1.4 Track Geometry Inputs

A railroad track can be characterized by spatial variations in the vertical (surface) and lateral (alignment) position of each rail from the nominal, by the difference in surface of two rails (cross level), and by the variation from nominal gage (distance between two rails). Geometry variations may be randomly distributed in wavelength and amplitude, or they may contain discrete components in spatial frequency due to constructional peculiarities, such as the staggered joints of bolted-rail track. Random variations may be described by a geometry power spectral density (an example of a "raw" PSD

TABLE 4-1. SPECIFICATIONS FOR GENERIC COMPUTER MODELS FOR CHARACTERIZATION OF WHEEL/RAIL LOADS

I. Linear, Frequency-Domain Vehicle Model (Section 4.2.1)
   a. Full car (rigid-body modes, significant bending modes)
   b. Detailed truck model
   c. Vertical (bounce/pitch) and lateral (lateral/roll/yaw) modes
   d. Track geometry PSD/CPSD or spectral component inputs
   e. Track dynamic impedance model (vehicle/track lumped unsprung mass)

II. Quasi-Linear, Frequency-Domain Vehicle Model (Section 4.2.2)
   a. Full car (rigid-body modes, significant bending modes)
   b. Detailed truck model
   c. Vertical (bounce/pitch) and lateral (lateral/roll/yaw) modes
   d. Describing function representation of significant non-linearities
   e. Track geometry PSD/CPSD or spectral component inputs
   f. Track dynamic impedance model (vehicle/track lumped unpsrung mass)

III. Nonlinear, Time-Domain Vehicle Model (Section 4.2.3)
   a. Full car (rigid-body modes, significant bending modes)
   b. Detailed truck model
   c. Vertical (bounce/pitch) and lateral (latera/roll/yaw) modes
   d. Nonlinear springs, clearances, dampers, W/R geometry, mode cross-coupling, etc.
   e. Track geometry spatial profile (transient)
   f. Track dynamic impedance model (vehicle/track lumped unsprung mass)

IV. Quasi-Linear, Frequency-Domain Truck Hunting Model (Section 4.2.4)
   a. Detailed truck model
   b. Lateral (lateral/roll/yaw) modes
   c. Describing function representation of significant non-linearities
   d. Track geometry PSD/CPSD or spectral component inputs
   e. Track dynamic impedance model (vehicle/track lumped unsprung mass)

V. Nonlinear, Time-Domain Truck Hunting Model (Section 4.2.5)
   a. Detailed truck model
   b. Lateral (lateral/roll/yaw) modes
   c. Nonlinear springs, clearances, W/R geometry, dampers, creep coefficients, adhesion limit and slip, etc.
   d. Random or discrete track geometry inputs
   e. Detailed track model (nonlinear spring-damper, rail-tie-ballast masses)

TABLE 4-1. (Continued)

VI. Linear, Frequency-Domain Truck Model (Section 4.2.6)
- a. Detailed truck model
- b. Vertical (bounce/pitch) and lateral (lateral/roll/yaw) modes
- c. Track geometry PSD/CPSD or spectral component inputs
- d. Detailed track model (rail, tie, ballast masses)

VII. Analytical Wheel/Rail Impact Model (Section 4.2.7)
- a. Closed form or iterative solution
- b. Idealized vehicle and track parameters (stiffness, damping, and masses)
- c. Idealized track and wheel geometry/speed factor inputs

VIII. Nonlinear, Time-Domain Wheel/Rail Impact Model (Section 4.2.8)
- a. Simplified wheelset model
- b. Vertical modes
- c. Nonlinear parameters (Hertzian stiffness, wheel lift, nonlinear tie and ballast stiffness, etc.)
- d. Track or wheel geometry inputs (transient)
- e. Detailed track model (rail, tie, ballast masses)

IX. Quasi-Static, Steady-State Curving Model (Section 4.2.9)
- a. Lateral/roll/yaw) modes
- b. Nonlinear of quasi-linear parameters (clearances, wheel/rail geometry, creep coefficient, adhesion limit, and slip, etc.)
- c. Train speed, curvature, superelevation inputs
- d. Central bearing (centerplate) force component inputs
- e. Vertical wheel load inputs

curve is shown in Figure 3-6). The presence of discrete harmonic components at wavelengths of 39 feet (the most common rail length) and sub-multiples of 39 feet are invariably found in the PSD curves from measurements on North American track.

Track geometry variations can be used to excite a model of a rail vehicle as time-histories (implying a time-domain computer model), as singular frequency components, or as stochastic inputs. . .shaped random noise in the time-domain, or geometry power spectra in the frequency-domain. One method of introducing the vertical track geometry forcing function into the truck model is illustrated in Figure 4-1, where variations in track height (surface) about the track datum (the nominal loaded position) are applied at the interface between the wheel and rail. This is represented here as a very stiff contact spring for the Hertzian contact stiffness of the rail head and wheel. The same track geometry input variations are applied to all wheels, except that a time-delay (or phase shift) based on truck wheelbase divided by vehicle speed is used with the input for trailing wheels. The actual position of the rail at any time would be the superposition of the nominal position with the geometry variation and the dynamic deflection due to the wheel load variation. This would also include the interactive deflection of the rail under one wheel due to the load variation at the adjacent wheel. In a similar manner, track geometry variations would be applied at the rear truck of the vehicle after a time delay based on truck spacing divided by vehicle speed.

Random geometry variations of profile and alignment of one rail may be used as an input to a linear, or quasi-linear model by use of the relationship:

$$P_o(\omega) = |H|^2 P_i(\omega) \quad ,$$

where P_i = input power spectrum
P_o = response power spectrum
H = system transfer function
ω = frequency, rad/sec .

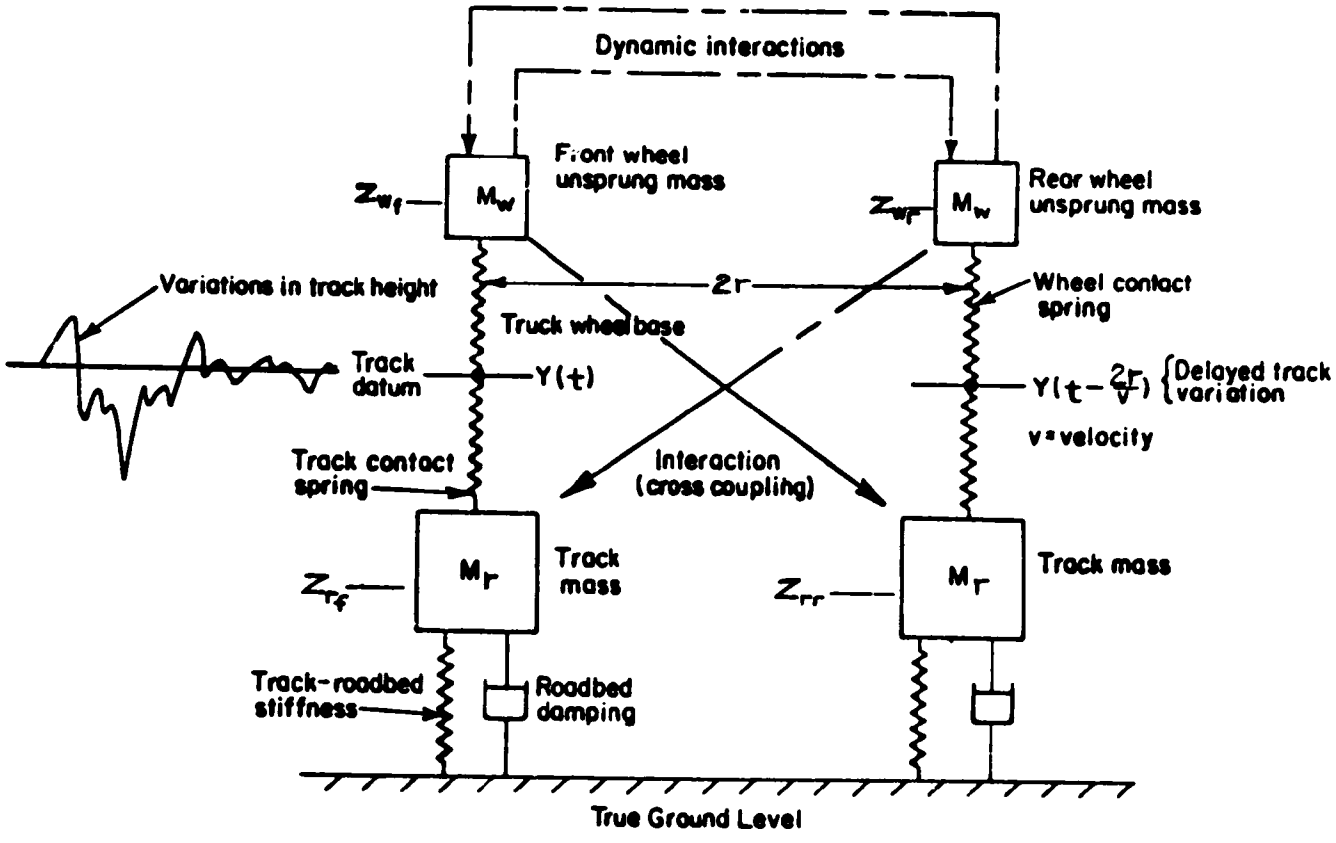

FIGURE 4-1. SIMPLIFIED VEHICLE-TRACK DYNAMIC SYSTEM BOUNDARY WITH VARIABLE TRACK HEIGHT AS INPUT IN THE VERTICAL PLANE

Track geometry inputs at a trailing axle or trailing truck are related to the input PSD by a specific phase relationship (or cross spectral density) defined by the vehicle geometry (axle spacing, truck spacing) and forward speed. For any one track geometry relationship such as surface, alignment or cross level, all phase information is lost; and to provide a relationship between inputs, the cross spectral densities must be obtained. Conservative approximations of response to combined inputs can be obtained from mean-square addition of responses to each input.

Variations in rail lateral alignment and rail head geometry are coupled to the wheel through the lateral creep and flange forces, which are dependent on wheel/rail contact geometry, the vertical W/R force and the vehicle forward speed. A similar coupling exists between the wheel and rail in the longitudinal direction, and the longitudinal forces affect wheelset yaw. Three major nonlinearities are associated with the lateral inputs: flange contact, the wheel/rail adhesion limit, and the dependence of the creep parameters on vertical wheel force. Wheel/rail geometry is also a highly nonlinear function of lateral displacement of the wheelset.

Idealized curves representing the random geometry power spectra can be used as input functions to the vehicle/track model, along with the rail length harmonic spectral lines, suitably broadened [4-1]. A look-up table of values for the spectra could be used, if the measured data were sufficiently accurate to warrant this. Two-slope approximations of surface, alignment and cross level geometry PSD are shown in Figure 4-2 for a "Class 6" track, based on recent measurements [4-2]. For comparison, the approximate curves for "Class 4" bolted-joint track are shown in Figure 4-3. Classification of the track from which these geometry data were taken may be somewhat arbitrary, and the curves may describe track that is in some respects not representative. For example, the "Class 4" alignment seems to be slightly better than "Class 6" in the short wavelengths; and the surface spectral peak is substantially higher at the 39-foot wavelength than the cross level peak. Since this is relay rail, the loss in correlation between existing bolted joints and old joint damage in the ballast may account for the bad surface. On old BJR track, the cross level spectral peak would be expected to dominate at 39 feet.

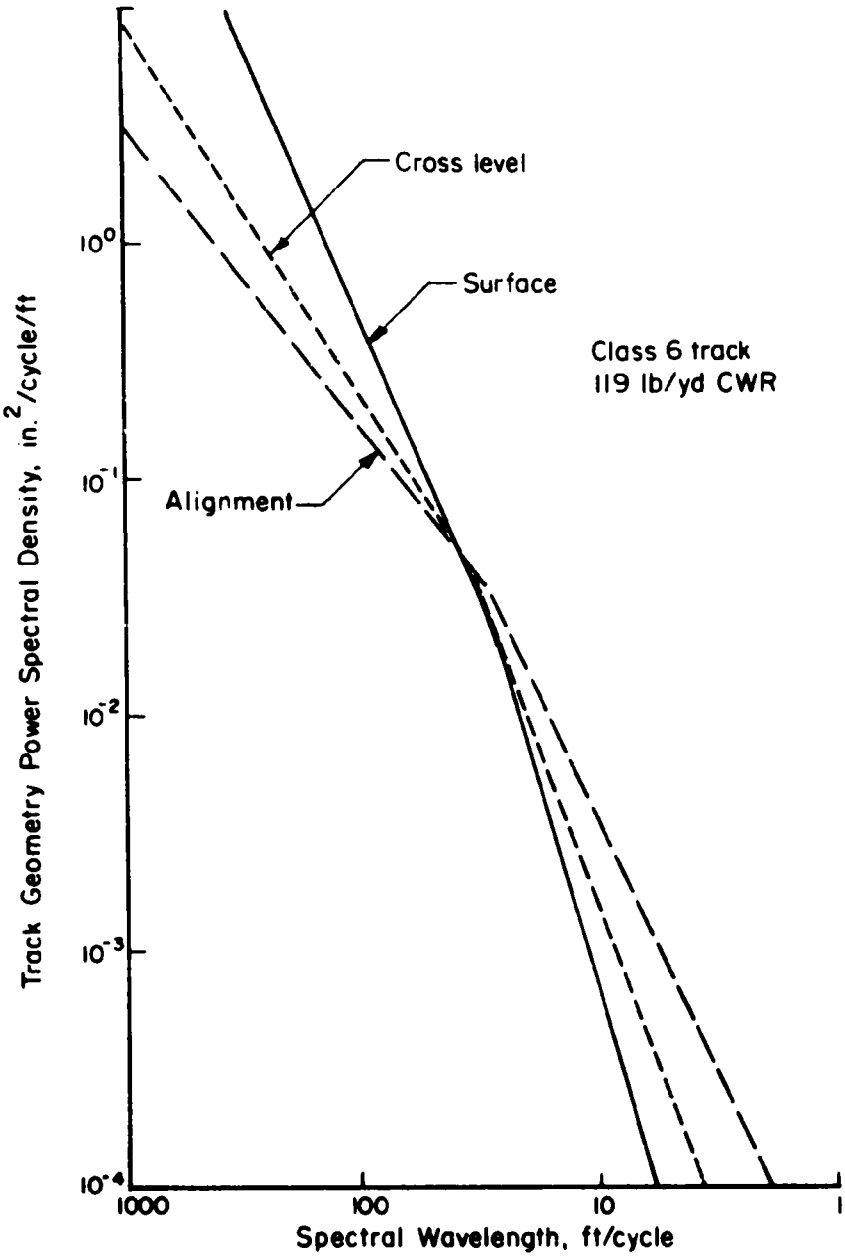

FIGURE 4-2. APPROXIMATE TRACK GEOMETRY PSD CURVES FOR CLASS 6 CWR TRACK

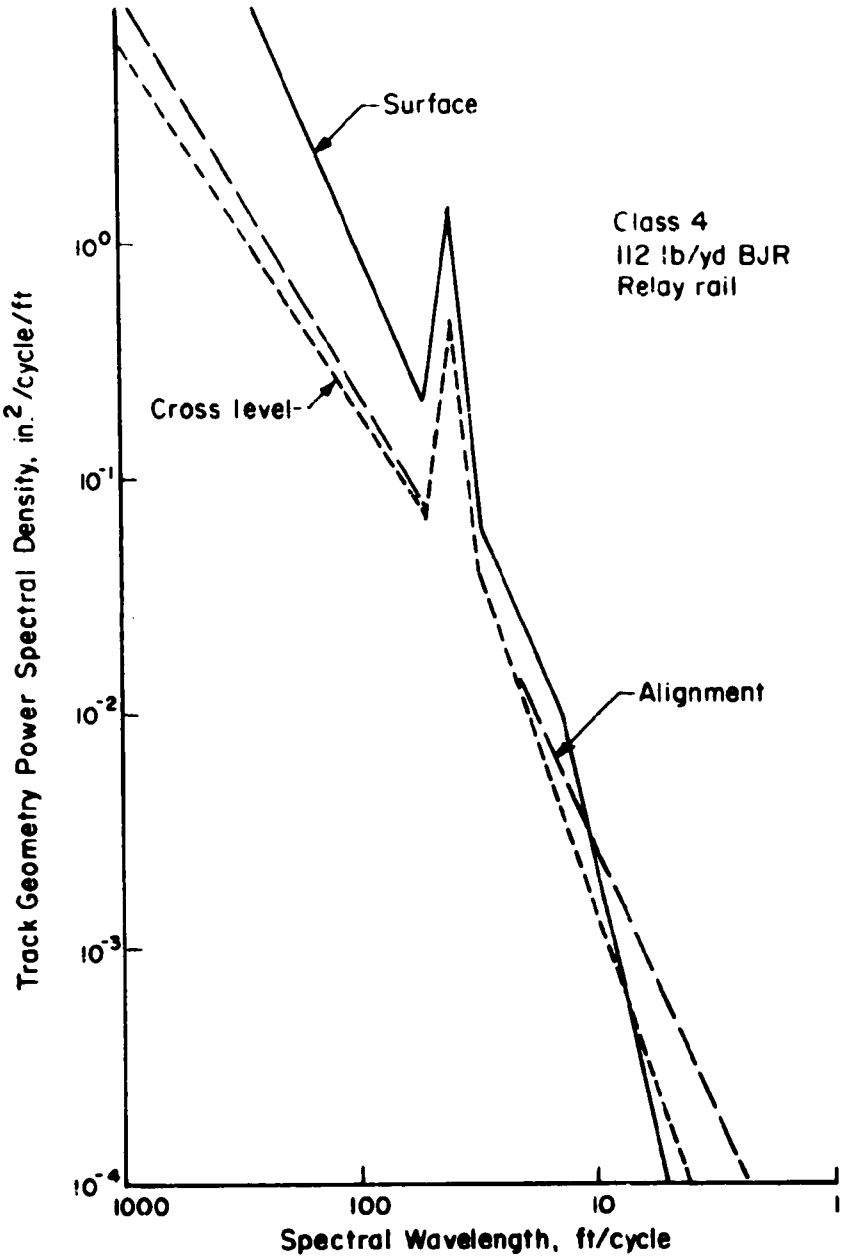

FIGURE 4-3. APPROXIMATE TRACK GEOMETRY PSD CURVES FOR CLASS 4 BJR TRACK

In addition to the track environmental excitation, forces and torques are applied to the rail vehicle from adjacent cars through the couplers. Severe draft and buff loads on the couplers during longitudinal train action (run-out and run-in) can induce lateral and vertical forces on the car body. Lateral W/R forces are developed on curves due to basic steering forces and the centrifugal acceleration. It is expected that in most cases very little direct correlation will be shown between these forces and the track environmental inputs, except for the vertical coupler forces induced by very bad track surface geometry. Other forces may act on the car body and truck. These include braking forces and torques, traction (for powered trucks), aerodynamic effects (induced by passing trains or in tunnels), and wind gusts. These are not included in the scope of the present study.

4.2 REVIEW OF AVAILABLE VEHICLE/TRACK MODELS

An extensive review of existing vehicle and track dynamic models was conducted during the first phase of this research program. The results of this survey are included as Appendix B of this report. Although a number of vehicle dynamics models have been developed, only a few of these models can be used to predict wheel/rail forces without extensive modification. Models that are currently available, or will be available for use in the immediate future, are reviewed in this section in the order shown in Table 4-1.

4.2.1 Linear, Frequency-Domain Vehicle Model

Several linear, frequency-domain vehicle models are currently available for W/R load prediction using geometry power spectral density or discrete geometry spectral component inputs. These programs can be used to predict W/R load power spectral density or root-mean-square values for specific rail vehicles as a function of speed and track geometry wavelength. They are particularly useful for predicting track forces that cause vertical settlement at specific wavelengths.

4.2.1.1 TSC Program HALF

Program HALF is a half-car vertical model consisting of one-half the vehicle body, one truck frame, and two axle masses. The track structural impedance is represented by a beam on a viscoelastic foundation. The truck frame is connected to the car body through a secondary spring/damper suspension, and it is connected through the primary spring and a rigid equalizer bar to the lumped axle masses. The primary application for this model is to calculate vertical W/R forces and track deflections in response to sinusoidal track surface irregularities. Outputs are in transfer function form, or in PSD form for response to a geometry PSD input.

4.2.1.2 BCL Program TRKVPSD

Program TRKVPSD (and the special-purpose variant TRAKVEH) were developed in a recent DOT/FRA study [4-3] for comparing the dynamic response of a number of rail vehicles. In the currently-revised version, the track geometry inputs are introduced between the wheel and track masses to include the inertial effects of the track; and truck pitch has been added to the bounce/pitch model. The program predicts response in the vertical plane for a full car body (bounce, pitch and vertical body bending), one truck in bounce and pitch, and a rear truck represented by an overall, complex impedance. Response in the lateral plane uses a full car body (roll, yaw, and lateral), one truck in roll and lateral, and a rear truck as a complex impedance. Outputs consist of vertical and lateral W/R forces and truck and car body accelerations and displacements in PSD form, and root-mean-square values in octave-bands or in selected wide frequency bands. Input excitation includes geometry PSD inputs, discrete spectral components or a staggered-joint track geometry.

A second revision to the program includes wheelset and truck frame yaw, plus body lateral and torsional bending. This version is currently being debugged.

This program was developed under Contract No. DOT-FR-20077.

4.2.2 Quasi-Linear Frequency-Domain Vehicle Model

Major nonlinearities such as Coulomb friction damping, suspension stops and flange impact can be approximated in some cases by the use of "describing function" techniques. Efforts are currently being directed by several organizations to develop models utilizing these techniques in vehicle/track models.

CU/ASU Vehicle Model (Program 5)

A computer program developed by Dr. Harry Law of Clemson University and Dr. Neil Cooperrider of Arizona State University under Contract No. DOT-OS-40018 is currently operational at Arizona State University. The model represents a nine degree-of-freedom freight car with gravitational stiffness, spin and latera/spin creep, gyroscopic effects and equivalent linear viscous friction for Coulomb friction damping. Lateral rail alignment and cross level irregularities are inputs to each wheelset. By standard frequency-domain analysis, outputs are calculated as transfer functions, power spectral densities, and rms values of displacements, accelerations and contact forces. A quasi-linear "warp" (parallelogramming) degree of freedom is to be added using describing function methods.

4.2.3 Nonlinear, Time-Domain Vehicle Model

A nonlinear, time-domain vehicle model can be used to predict the W/R vertical and lateral impact forces generated by transient response to large-amplitude track geometry irregularities which cause contact with suspension stops and flange impact.

4.2.3.1 AAR/TTD Flexible Body Vehicle Model

A vehicle model was developed as part of the AAR-FRA-RPI-TDA Track Train Dynamics (TTD) Program to predict the dynamic behavior of a freight car operated on jointed track. Nonlinear phenomena such as gib clearances and

wheel lift are included in this model. The degrees of freedom include rigid-body motions for each half-car body which are connected by appropriate stiffness and damping. Lateral, vertical and roll motions are included for the bolster and wheelsets (two wheelsets lumped into one mass) at each truck. The program predicts time histories of accelerations, velocities, displacements, vertical deflections of the rail, and wheel load.

4.2.3.2 Wyle Nonlinear Flexible Rail Vehicle Model

A rail vehicle model has been programmed by Wyle Laboratories for time-domain solution under Contracts DOT-FR-30045 and DOT-FR-64200. Several levels of complexity have been modeled, resulting in from 11 to 17 degrees of freedom. Effects of several types of nonlinearities, such as Coulomb damping, wheel-rail separation, and nonlinear spring force-deflection characteristics, are taken into account. The method of superposition of normal modes is used to analyze the effects of the car body flexibility. Programs are in FORTRAN, and have been run on the CDC CYBERNET system.

The program has been validated by comparison with limited experimental data for the 100-ton hopper car. Although the track is presently simulated by simple springs and dampers, the program may be expanded to include track mass effects and to provide a readout of W/R forces.

4.2.3.3 BCL Program TRAKVEH-Hybrid

A model of a rail vehicle has been programmed by Battelle under Contract No. DOT-FR-20077 for the hybrid computer. This model includes all the degrees of freedom of the basic TRAKVEH program with additional wheelset and track degrees of freedom. Significant nonlinearities such as gib clearances, wheel lift, suspension motion limits, flange clearance and impact, and friction damping were included in the model. Additional degrees of freedom (wheelset and truck frame yaw) need to be programmed, and the model is currently inactive.

4.2.4 Quasi-Linear, Frequency-Domain Truck Hunting Model

One important source of high lateral W/R loads is the truck hunting instability. To predict the impact forces resulting from truck hunting, a quasi-linear or nonlinear lateral truck model must be used. Work is under way at both Clemson University and MIT to develop a quasi-linear wheelset model, but a full truck model has not yet been developed using the quasi-linear (describing function) techniques.

CU/ASU Truck Hunting Model (Program 2)

A two degree-of-freedom model of a wheelset with Coulomb friction and nonlinear conicity, gravitational stiffness and wheelset roll has been programmed for a random input of rail lateral alignment and a describing function analysis. Outputs are power spectral densities and rms values of displacements, accelerations, and W/R contact forces. This program will be documented by Cooperrider, Hedrick and Law under Contract No. DOT-TSC-902.

4.2.5 Nonlinear, Time-Domain Truck Hunting Model

4.2.5.1 CU/ASU Truck Hunting Model (Program 7)

This model consists of a three degree-of-freedom freight car truck (yaw, warp, and lateral degrees), with a two degree-of-freedom car body (lateral and roll). Coulomb friction damping, clearances and nonlinear springs are included, along with actual W/R profiles to model the gravitational stiffness, the difference in wheel rolling radii, and wheelset roll angle. A nonlinear creep function is also used. The program is implemented on either the hybrid computer or on a digital computer by CSMP numerical integration techniques. Outputs consist of displacements, velocities, accelerations and W/R contact forces in response to an arbitrary lateral rail alignment input. This work will be documented by Law and Cooperrider under Contract No. DOT-OS-40018.

4.2.5.2 CU/ASU Truck Hunting Model (Program 8)

A more complete, nine degree-of-freedom freight car model is being programmed to include two trucks each having three degrees of freedom--yaw, warp and lateral--and a car body with roll, lateral and yaw. Nonlinear Coulomb friction, clearances and springs are used, along with actual wheel/rail profiles to model gravitational stiffness, the difference in wheel rolling radii and wheelset roll angle. A nonlinear creep function is used. Outputs include displacements, velocities, accelerations, wheel/rail contact forces, and forces between suspension elements as functions of an arbitrary lateral rail alignment input. Again, the work will be documented under Contract No. DOT-OS-40018.

4.2.6 Linear, Frequency-Domain Truck Model

A more detailed truck and track model is needed to provide better resolution of W/R forces in the important 15 to 150-Hz range of frequencies. For this type of model the car body can be considered "fixed" in space because the secondary suspension isolates the car body from high frequency excitation. The lower frequency range must therefore be predicted using a different model.

BCL Program TRSDEP

This model consists of a single truck with 19 degrees of freedom: a truck frame having yaw, pitch, roll, lateral and vertical motions; two wheelsets with yaw, roll, lateral and vertical motions; and two track masses with roll, lateral and vertical motions. Bounce/pitch and roll/lateral/yaw degrees of freedom are uncoupled by linearity and symmetry. Solution options provide PSD and rms predictions of accelerations and W/R forces in response to random (PSD) geometry inputs, or the eigenvalue/eigenvector solution to check for hunting stability and mode shapes. This program is still under development.

4.2.7 Analytical Wheel/Rail Impact Model

Early work in track design relied on the empirically-derived impact factor to account for speed effects on W/R forces. Analytical work

over the past decade by British Rail [4-4] has resulted in an approximate method for calculating the "P1" and "P2" impact forces at rail joints. This method is used in Section 6.0 to demonstrate the calculation of these impact force levels for track geometries and speed limits of the Track Safety Standards, using typical values for North American rail vehicles and track.

4.2.8 Nonlinear, Time-Domain Wheel/Rail Impact Model

For the calculation of stresses in a rail section, particularly at a bolted rail joint, the time-history of the W/R load and tie reactions on the rail are needed. A detailed, nonlinear model of the unsprung masses (wheelset and track) is best suited for this type of W/R load prediction. No nonlinear, time-domain W/R impact models are readily available at this time. Although British Rail has undoubtedly developed computer models of this type, these are not available for use by others.

4.2.9 Quasi-Static, Steady-State Curving Model

Basic steering forces and flange forces on curved track are important in characterizing the W/R load environment for rail stress and rail wear prediction. Several programs are currently available for use in predicting curving forces.

4.2.9.1 AAR/TTD Curving Program

The curving program developed by the AAR-FRA-TPI-TDA-sponsored Track Train Dynamics Program predicts the steady-state curving forces during negotiation of a constant radius, constant superelevation curve for 2-, 3-, or 4-axle trucks. The program uses an empirical creep relationship of percent of vertical load versus creep angle, with a slip limit. The program will accept longitudinal and lateral centerplate loads to represent centrifugal, buff or draft loads. The model predicts individual wheel loads and includes lateral clearances (axle/frame and flange/rail), a primary lateral stiffness, and a standard truck geometry. The method of solution is to assume a curving configuration or constraint, then allow the computer program to solve iteratively the force and moment balance about the "friction center". Computed and measured results compare well for curves over about 4-1/2 degrees in curvature.

4.2.9.2 CU/ASU Curving Model (Program 10)

A seventeen degree-of-freedom, four-axle rail vehicle has been modeled to provide the quasi-static curving forces. This consists of yaw and lateral motion of each wheelset; yaw, lateral and roll of each truck; and yaw, lateral and roll of a car body. The solution technique is the numerical integration of the equations of motion, with outputs consisting of displacements velocities, W/R contact forces, and forces between suspension elements. The program will be documented by Law, Cooperrider and Hedrick under Contract No. DOT-TSC-902.

4.2.9.3 BCL Program SSCUR2 (SSCUR3)

A steady-state curving program has been developed for 2- or 3-axle trucks, based on linear equations developed by Newland [4-5]. This model includes one truck with lateral and yaw motion of each wheelset, plus lateral, yaw and roll of the truck frame. Creep, gravitational stiffness, centrifugal, flange and friction forces are included at each wheelset, while centrifugal forces are applied from the truck and car body to the c.g. and the centerplate of the truck, respectively. The program uses a step-wise linear procedure to calculate the equilibrium position of the model during curving. An iteration procedure is used to check all possible flanging conditions in the search for equilibrium. Outputs include all forces and moments acting on the wheelsets, and wheelset displacements.

4.3 RECOMMENDED PREDICTIVE METHODOLOGY

The review of track degradation modes and W/R loading mechanisms in Section 3, and the review of modeling techniques and available models in this section provide a basis for the recommended W/R load-predictive methodologies. Five important areas of load characterization can be specified in terms of the required load-predictive models. These are given as follows in the order of increasing "lead time" necessary to mechanize the models or programs:

(1) W/R load PSD - vertical and lateral track geometry degradation at discrete wavelengths due to vehicle response to random or discrete geometry errors. (Models I, II, VI, Table 4-1).

(2) Steady-state curving forces - rail stress and wear, rail stability (with superimposed dynamic loads from vehicle response to geometry errors and train-action forces). (Model IX).

(3) Lateral impact forces from truck hunting - rail and track component stresses and deflections from high lateral loads. (Models IV, V).

(4) Vertical and lateral transient forces - vehicle transient response to large-amplitude, discrete geometry errors. (Model III).

(5) W/R vertical impact forces - impacts due to wheel or rail geometry anomalies. (Models VII, VIII).

The recommended choice for the most immediate results is the W/R load PSD model. An example of the use of this type of predictive methodology is given in Section 6.1.

4.3.1 Computer Model Inputs

The use of track geometry power spectral density inputs has been discussed in some detail in Section 4.1.4. In addition to the random portion of the spectra, discrete components of geometry representing constructional variations or track degradation can be added [4-1]. The BCL TRAKVEH program has in past studies [4-3] used the first several Fourier components of a rectified sinewave to represent deteriorated bolted-rail track with staggered joints.

In addition to variations in surface, alignment, and cross level geometries, some models may use random variations in track gage or rail profile as inputs. Time-domain models use time-history variations in track profile or track stiffness (impedance), in either continuous or transient form. The idealized low joint (see Figure 3-12) has been used in past studies, as well as versine ($1 - \cos 2\pi L/\lambda$) functions to represent typical deviations at grade crossings or turnouts.

A steady-state curving program incorporates speed, curvature, superelevation, and external forces (train-action, draft or buff forces, for example) as inputs to calculate steering and flanging forces. Other programs, particularly the time-domain models, may also incorporate external forces as inputs to the model. Centrifugal accelerations are generally calculated in the programs for steady-state curving as a function of speed and curvature.

The recommended inputs to the first-priority model are geometry PSD descriptions of surface, alignment and cross level, plus discrete spectral components to represent the staggered joints on poorer-quality track.

4.3.2 Computer Model Outputs

Outputs from the frequency-domain models are typically the power spectra of car body, truck or axle accelerations or displacements, and W/R vertical and lateral forces. Tenth-octave, third-octave, or octave-band root-mean-square values of these output variables in response to the given input functions can also be generated. Some frequency-domain models can also provide the eigenvalue/eigenvector solution by which stability and mode shapes can be evaluated. Deflections of the rail or track, and relative motions between suspension elements may also be of value as outputs from the frequency-domain models.

Time-domain model outputs are in the form of time-histories of the model variables -- accelerations, displacements, or forces. While these outputs provide a good evaluation of system response in a real-time sense, the data must subsequently be analyzed if statistical results or root-mean-square values are needed.

The recommended outputs from the first-priority model are the PSD values versus frequency of W/R forces and vehicle component (car body, truck or axle) accelerations, plus octave-band and wide-band root-mean-square values of these forces and accelerations, for each of the individual track geometry inputs and for all inputs combined.

4.3.3 Vehicle and Track Parameters

For the frequency-domain models, linear estimates of vehicle and track system parameters are required. Estimates of nonlinear elements may consist of simple approximations, a tangent spring rate for a hardening spring, for example; or "describing function" approximations, such as the first Fourier coefficient of response to a Coulomb friction damper used as an equivalent viscous damper. Parameters for the vehicle include masses or mass moments of inertias of the major components (degrees of freedom), and the stiffness and damping characteristics of elements between these masses or inertias. The geometry of the vehicle must be defined in terms of mass centers, suspension element centers, axle and truck spacing from some reference, generally the nominal running surface of the track in the vertical and the lead truck center of rotation in the horizontal.

For time-domain, nonlinear models, the more significant nonlinear characteristics (particularly in the suspension elements) must be defined. Hardening springs, clearance and hard stops, friction damping, and suspension motion limits must be added to the parameter requirements, as well as inherent nonlinearities such as wheel lift and geometric cross-coupling between modes.

Track parameters for the W/R load prediction models can be limited to the effective "driving point" impedance parameters in terms of track stiffness, damping, and effective mass. At the wheel/rail interface the model (depending on the level of complexity) may require linear or nonlinear wheel/rail geometry, creep coefficients and adhesion limit.

The example in Section 6.1 illustrates the parameters required for a frequency-domain model.

4.3.4 Validation Data Requirements

Any computer model needs some "baseline" validation, preferably by correlation of several output variables with data from laboratory or field experiments on the prototype system, within an acceptable range of accuracy. Both model and prototype input "forcing function", system parameters, and output data formats must be as closely comparable as possible to provide a validation. Significant difficulties in comparison can be encountered in any of these three areas.

To provide comparable input forcing functions for both the model and the prototype vehicle, a good knowledge of track geometry PSD must be obtained. This is very dependent on the track sample length and the variations that might occur in the sample (for example, whether CWR or BJR track is measured, and whether turnouts or crossings and other anomalies are present). The track dynamic characteristics must also be defined, and the variations in track parameters may have a significant range and frequency of occurrence. Nominal track parameters may of necessity be used until the statistical properties of track impedance are defined at some future time.

Vehicle parameters must also be carefully defined for good validation. Some parameters may vary to some degree as a function of time or ambient conditions. An example of this was the comparison of field test and computer model results from 100-ton hopper car rocking experiments. Over a period of time the load (coal) had settled noticeably, changing the mass moment of inertia and particularly the c.g. height above the rail. This change increased the car rocking critical speed by almost two miles per hour.

Validation data formats must be carefully defined for the field tests. Wheel/rail force PSD curves will be required for direct comparison with computer results; and root-mean-square forces over representative track lengths should also be generated as a function of speed. RMS values should be generated in 1/3-octave and wide-band format. To assist in the validation of the model, several channels of vertical and lateral acceleration

should be monitored on the vehicle body, suitably filtered (at about 50 Hz), to define the rigid-body natural frequencies of the vehicle. Wayside data will be used primarily to define the track dynamic parameters in response to a variety of vehicles, and will not be used directly in the validation of the specific vehicle/track model.

4.3.5 Application of Predictive Methodology

After the validation of the vehicle/track model is complete and confidence has been established in the baseline case, the model can then be used for a variety of purposes. A primary purpose of the model is to explore the effects of parameter variations on W/R forces. The effects of frozen ballast, friction snubber damping levels, load configurations, or a variety of other vehicle and track parameters may be examined, and the trends of these changes defined. By this means the most cost-effective changes in the vehicle/track system may be predicted. Other applications include the examination of the effects of particular vehicles (100-ton ore cars in unit train operation, for example) on track degradation. Loads at specific wavelengths can be predicted from the PSD curves, and rates of differential settlement or alignment change can be predicted from detailed track models, using the load versus wavelength information. Finally, the effects of track geometry and train speed may be predicted by the W/R load amplitudes generated from computer simulation, and appropriate changes in safety specifications can be defined from these data.

5. LOAD MEASUREMENT INSTRUMENTATION

The three general types of wheel/rail load data required for this program are:

- The basic wheel/rail load data taken both from trackside and from the vehicle is the most fundamental information to be attained by field measurements. These measurements will provide the primary data for characterizing the load environment, for validating the load-predictive mathematical models, and for defining inputs to rail and track models and laboratory experiments. These measurements should be taken as close to the wheel/rail interface as possible to insure maximum accuracy over the frequency bandwidth of major interest for specific models or experiments.
- Track and vehicle properties must also be defined in sufficient detail to generate accurate parameter values for models or experiments, corresponding to the wheel/rail loads generated above. Of primary interest here is the "driving point" impedance seen at the wheel/rail interface. Further, the track (including track geometry) and the vehicle should be documented in sufficient detail to provide a basis for comparison with data taken at some future time with other vehicles and at different track locations.
- o A third level of measurement priority is that of the internal track and vehicle reactions occurring simultaneously with the measured wheel/rail loads. These measurements would provide a detailed and statistically significant description of the loads and deflections within the vehicle and the track, and would be useful to other track- and vehicle-related research programs.

Items 1 and 2 above are necessary requirements for the completion of this program and are, therefore, of the highest priority, while Item 3 is,

for the most part, beyond the scope of this program. Serious consideration, however, should be given to Item 3 in support of related research.

5.1 WAYSIDE MEASUREMENTS

The evaluation of wayside instrumentation will generally follow the order of priority outlined in Section 5.0. Due to the nature of measurements made on the track from the passage of vehicles over one instrumented point, frequency domain information consists primarily of the wheel-pass, truck-pass, and vehicle-pass frequencies at the low end of the spectrum. Figure 5-1 illustrates the characteristic influence length of each of several transducer types commonly used for track measurements. None of these measurement techniques provides in itself more than a momentary glimpse of the nature of a particular wheel load as it passes over the instrumented section. In effect, only a point sample is available at the peak sensitivity of the device directly beneath the wheel to be measured. This works exceptionally well for generating statistics of peak loads, but it does not reveal much about the dynamic response of a specific vehicle. It is desirable to have a continuous measurement of wheel/rail load over a finite interval, such as the characteristic influence length of the track structure, to describe a complete load/deflection cycle at a particular point in the track structure. The continuous measurement (longer sampling length) of wheel/rail load across this zone would also produce a wider band of frequencies to describe the dynamic interaction of each wheel passing through that test zone.

Figure 5-2 shows the two regions of the frequency spectrum which are defined by a series of track transducers used for measuring wheel/rail loads. The four break point frequencies f_1, f_2, f_3, and f_4 are defined as follows.

- f_1 is the lower limit of frequency defined by the distance between the end transducers at the two extremes of the test zone and a corresponding velocity of an axle over that test zone.

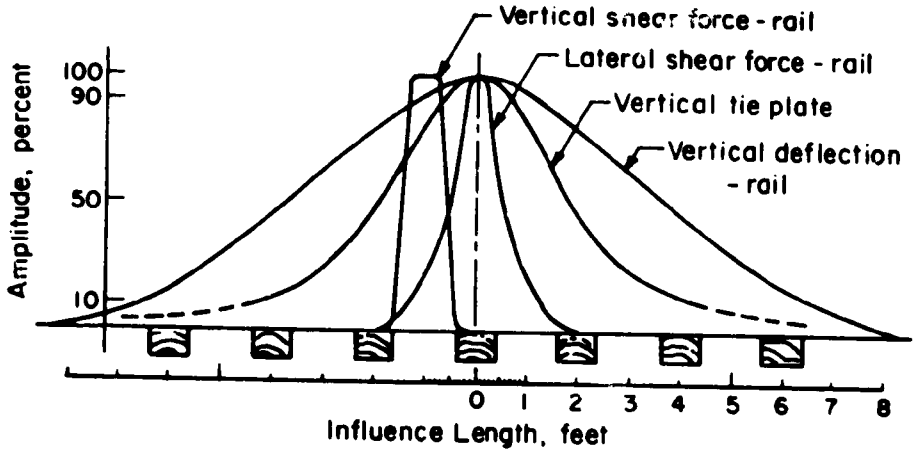

FIGURE 5-1. TYPICAL INFLUENCE LENGTHS OF WAYSIDE TRANSDUCERS

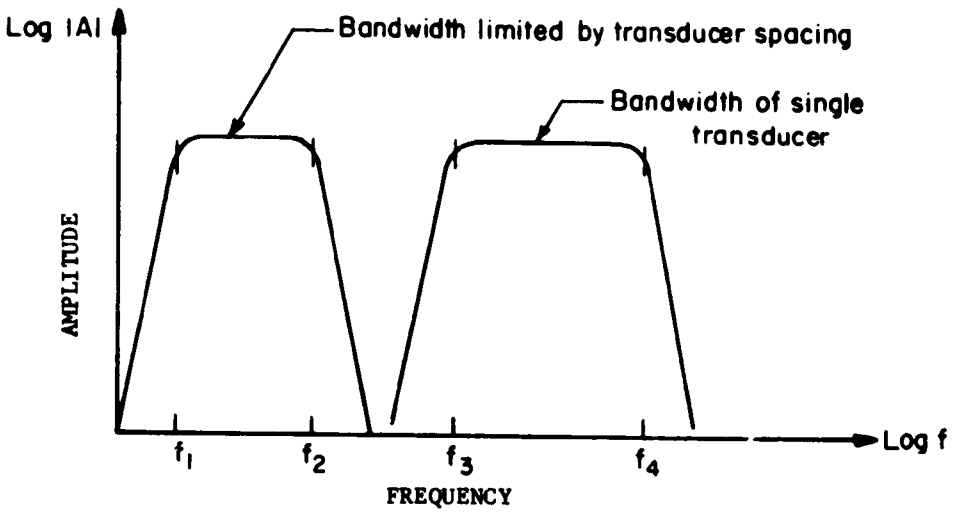

FIGURE 5-2. REGIONS OF FREQUENCY SPECTRUM DEFINED BY A SERIES OF WHEEL/RAIL LOAD MEASUREMENT TRANSDUCERS

- f_2 is the limiting frequency defined by the shortest interval between two transducers where any attempt to measure higher frequencies above this point would produce aliasing similar to those encountered in digital sampling.
- f_3 is controlled by the influence length of the specific transducer being used and is limited by the maximum length of that influence zone of the transducer.
- f_4 may be limited by one of several factors: The bandwidth of the data channel in which this transducer is recorded, the limiting frequency response of the transducer (if there is an inherent internal bandwidth limit), or more likely the bandwidth limit produced by the spring-mass system in which the transducer was placed. If the transducers can be placed at intervals sufficiently close that their influence lengths overlap, then f_2 and f_3 would coincide providing a continuous spectrum between f_1 and f_4.

5.1.1 Evaluation of Instrumentation

5.1.1.1 Strain Gaged Rail Circuits

There are a variety of strain gage circuits that have been applied to rail measurements. Two which have been applied with the greatest success are configured to measure shear force in the rail--one laterally and one vertically.

Lateral Shear Force Circuit. The lateral shear force circuit utilizes the principle that shear force in a cantilever beam is proportional to the change in bending moment. Figure 5-3 illustrates how this is applied to a rail section and schematically describes the idealized cantilever beam concept. Although

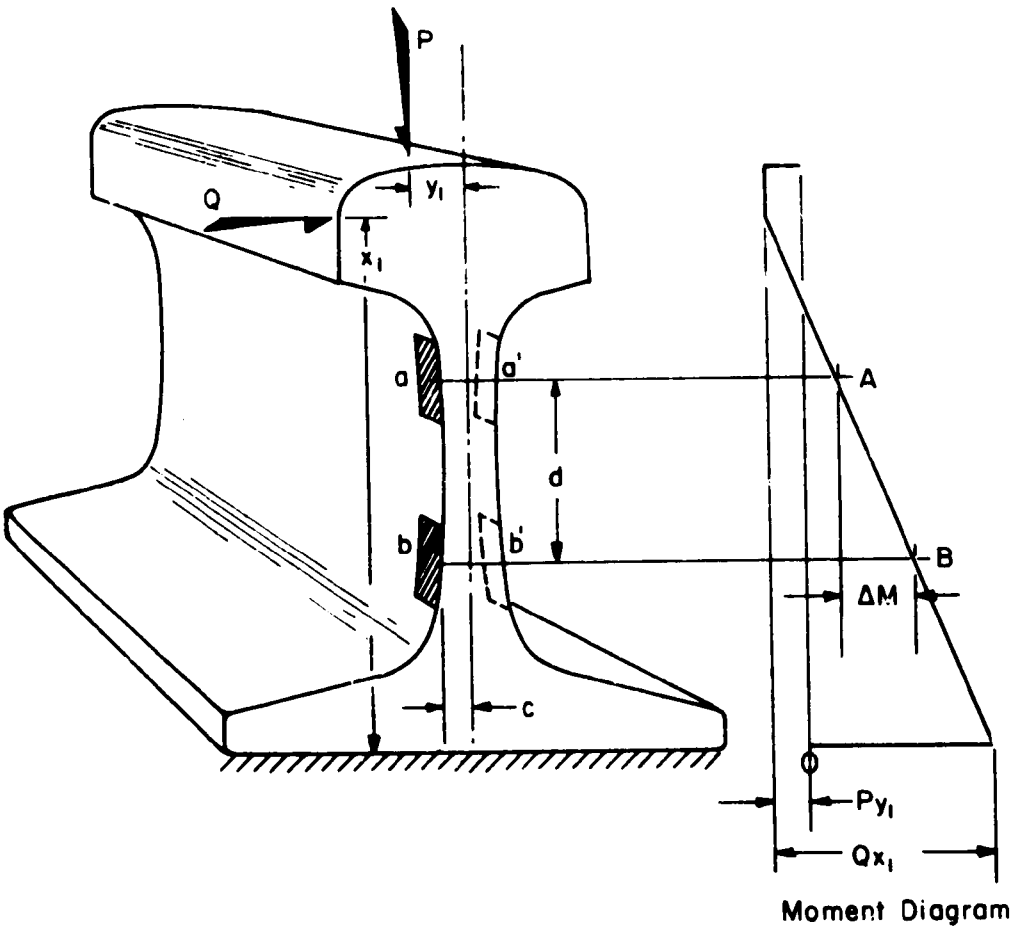

$Q \propto V$ (shear force)

$V = \frac{\partial M}{\partial x}$ (independent of P, x_1, y_1)

$V = \frac{M_B - M_A}{d}$

$M_A = \left(\frac{EI}{c}\right) \epsilon_A$

$V = \frac{EI}{cd} (\epsilon_B - \epsilon_A)$

$Q \propto (\epsilon_B - \epsilon_A)$ where $\begin{cases} \epsilon_A = \epsilon_a - \epsilon_{a'} \\ \epsilon_B = \epsilon_b - \epsilon_{b'} \end{cases}$

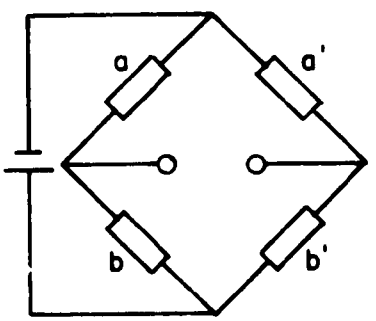

FIGURE 5-3. LATERAL RAIL LOAD MEASUREMENT USING SHEAR FORCE STRAIN GAGE CIRCUIT

there are limitations to the approach in this application, field experience has indicated that this circuit works very effectively, with frequency response limited only by localized structural resonances of the rail. Field static calibrations have shown good circuit linearity when the rail is loaded laterally with a hydraulic ram and vertically with the axle of a test vehicle. Vertical cross talk influences the sensitivity of the circuit because of variations in rail base support with changes in vertical load. (This effect can be reduced with positive hold down fasteners). Field experiments have shown changes in sensitivity (gain). When removing the vertical wheel load, gain may vary from +10 percent with well-supported rail to -30 percent with poorly-supported rail. For best results, this circuit should be installed directly over the center of the tie plate and it should be calibrated for sensitivity under the extreme ranges of axle loads to be measured. This circuit is not affected by variations of the point of application of the lateral load.

As shown in Figure 5-1, the zone of influence of this circuit is quite narrow, being only about 5 inches wide at the 90 percent amplitude and approximately 12 inches wide at the half amplitude. With the restriction that it be placed over the center of each tie, this leaves a gap between f_2 and f_3 as shown in Figure 5-2. The output from this circuit then will best be applied to peak amplitudes used for statistical descriptions of wheel/rail lateral forces.

The Swiss [5-1] have successfully applied this rail measuring technique by using special, 8-inch wide strain gages that are connected in series to increase the total influence zone of the circuit. They measure continuous bending strains along the upper region of the rail web and restrict their measurement of strains at the lower portion of the rail web to the region over each tie. This technique requires the use of these special gages, which are not readily available in this country, and it would require more elaborate installation techniques than are practical in the field.

The single lateral load circuit installations applied in this country have been successfully installed in the field using weldable strain gages, and they require minimum preparation at the test location. This circuit has no effect on track characteristics, and it is not necessary to disturb the track structure to install this device (except where accessability is reduced around special track work such as switch points). Field calibration is necessary after installation, which requires access to the track (track time)

and a test vehicle for applying vertical load. Calibration has been accomplished in past field experiments by applying a lateral load between rail heads directly over the strain gage pattern with a laboratory-calibrated hydraulic jack. The lead axle of a vehicle was placed as close to the jack as practical to provide the vertical loading. A mixture of extreme-pressure grease and molybdenum disulphide powder was placed at the W/R contact patches to minimize the resulting hysteresis from lateral W/R friction, and the average slope of the hysteresis loop was used to establish the strain gage sensitivity factor.

Vertical Shear Force Circuit. The Russians have developed a gaged rail vertical force measurement system [5-2] utilizing web compression strains at the rail neutral axis. Laboratory strain searching techniques indicated that the neutral axis location provided the best compromise between sensitivity, crosstalk, and influence length. The influence length (half amplitude) for one gage at the neutral axis was found to be about 4 in. Bridges were wired with six gage pairs spanning 20 in. Six adjacent circuits provide sufficient length to capture one complete wheel revolution as well as cover the track influence length. Although bandwidth and ripple characteristics of the circuit were not discussed, it was noted that bandwidths to 1 KHz were desirable for characterization of wheel loads. Laboratory experiments were performed within a simple supported section of rail and no reference was made to variations of sensitivity over tie supports.

The vertical shear force circuit used in recent measurements on Northeast Corridor track (shown in Figure 5-4) measures the net shear force difference between two gaged regions. If there is no direct support under the rail within this gaged region, then the output of the circuit is proportional to vertical wheel load. If there is a rail support (tie) within the gaged region, then the output of the circuit is proportional to the net force (P - R). The gaged elements at the one end location are oriented to measure the principle strains due to shear force (which are at 45 degrees from the vertical shear force line of action). The gage configurations at the two zones are identical and they could be wired independently. The outputs would then be subtracted to get the net shear force.

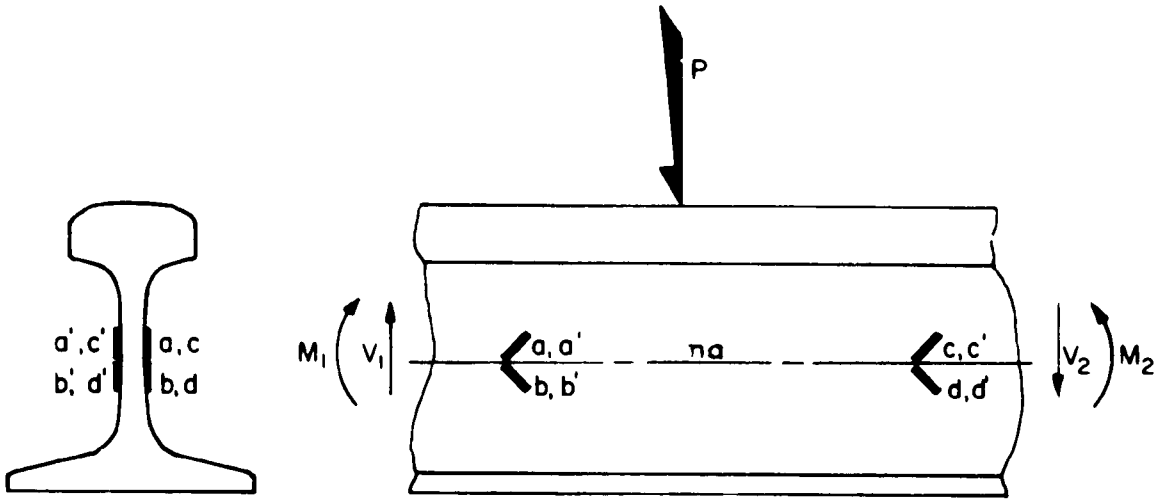

$$P = V_1 - V_2$$

$$V_1 = \frac{EIt}{2(1+\nu)Q}\,\epsilon_1 \qquad V_2 = \frac{EIt}{2(1+\nu)Q}\,\epsilon_2$$

$$\epsilon_1 = \epsilon_a - \epsilon_b + \epsilon_{a'} - \epsilon_{b'}$$

$$\epsilon_2 = \epsilon_c - \epsilon_d + \epsilon_{c'} - \epsilon_{d'}$$

$$P = \frac{EIt}{2(1+\nu)Q}\,(\epsilon_1 - \epsilon_2)$$

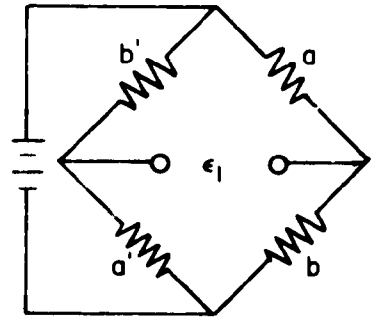

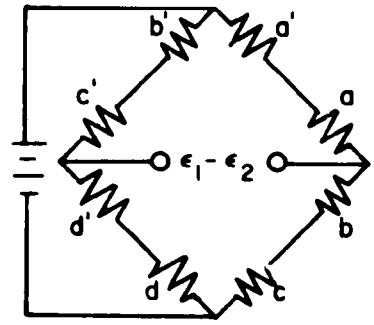

FIGURE 5-4. WHEEL/RAIL VERTICAL LOAD CIRCUITS USING RAIL SHEAR STRESS TO MEASURE LOAD

The zone of influence of this circuit is defined primarily by the distance between the two gaged areas. This allows an influence length of approximately 7 inches at the 90 percent amplitude and 11 inches at the 50 percent amplitude, as shown in Figure 5.1. These values were taken from actual field measurements where the gage circuit was installed between ties at approximately 10 inches between gages.

Although no information is presently available on cross-axis sensitivity tests, field application of this circuit indicates a very low sensitivity to cross-axis inputs. As with the lateral shear force circuit, the output of this device is suitable primarily for the detection of peak amplitudes of instantaneous wheel load, and is not inherently suitable for frequency domain information because of the short sampling length. As with other field-installed circuits, calibration is required after installation. Calibration in the past has been accomplished by observing the output amplitudes underneath several slowly moving locomotives where the total locomotive weight is known within a small percentage error. The average load from several axles can then be used to calibrate the strain circuit.

Similar to the lateral shear force circuit, the installation characteristics of this vertical circuit are quite straightforward and have no effect on track stiffness or load distribution. It does, however, require twice as many individual strain gages which increases total preparation time at a test site and the cost of materials.

An alternative application of this circuit is illustrated in Figure 5-5. By wiring each shear force-measuring circuit separately and providing a circuit at each transition between supported and non-supported sections, a basis for continuous measurement is established. Pairs of gage circuit signals are added sequentially, with the vertical force signal (P, or P-R) from the pair bracketing the wheel. In the zone including a tie plate reaction, the vertical tie plate signal (R) would be summed to obtain the W/R load (P), while the zone between ties this load (P) would be obtained directly. This approach does require vertical tie plate load measurements at each tie within the instrumented zone, but the accuracy of the resulting W/R load measurement will not be affected by changes in the load distribution to any individual tie.

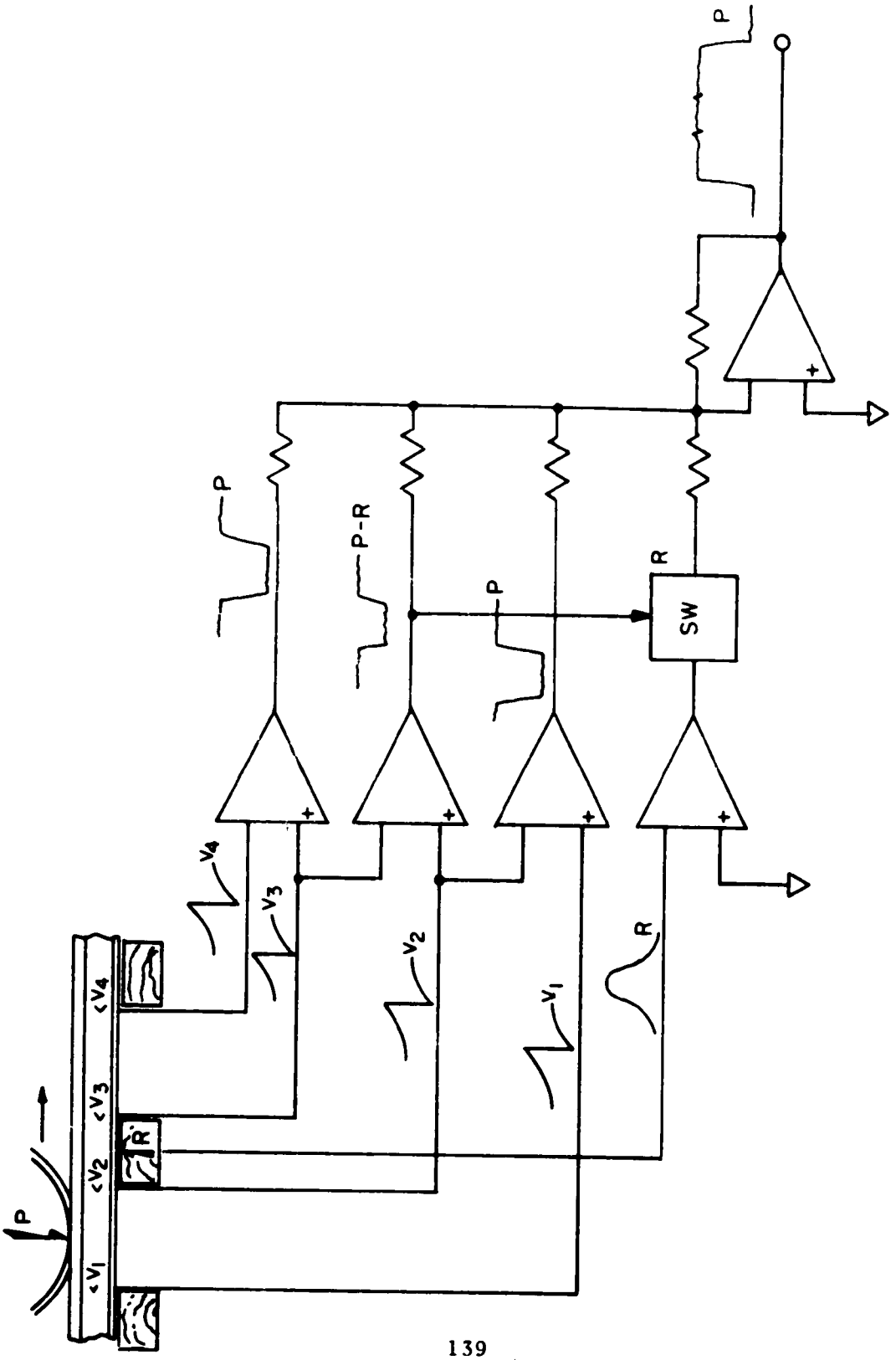

FIGURE 5-5. SWITCHING CIRCUIT FOR GENERATING CONTINUOUS VERTICAL WHEEL/RAIL LOAD SIGNAL OVER MEASUREMENT ZONE

The shear-strain pulse from each strain gage circuit would be used to switch the next gage circuit "downstream" into the sum, plus the tie plate in a supported section, while switching the last "upstream" gage circuit out. Standard analog FET switches would be used in conjunction with logic modules. Switching transients would occur due to the finite width of the gage pattern, and there would be slight variations in circuit gain. These transients would produce high-frequency noise at regular intervals. Although the transients may be filtered, the fundamental repetition rate and its harmonics could be in the range of useful data and could be difficult to remove by subsequent processing. This concept does, however, provide a method for measuring vertical wheel/rail loads over a substantially longer zone, while still providing individual signals for loads at localized points on the rail. Comparison of the frequency content of the measured W/R load P with the tie plate load R can provide a measure of high frequency response through the rail mass. The continuous zone of measurement would be limited in length to less than the minimum axle spacing, unless additional switching logic were added to discriminate between lead and trailing wheel loads.

5.1.1.2 Tie Plate Load Cells

Tie plate load cells are a fundamental technique for the measurement of track forces near the top of the track structure. [5-3, 5-4]. If designed and constructed properly, the tie plate load cell can accurately measure the reaction forces at the rail base as it interacts with the tie. The influence zone is governed by the rail size and track modulus and, as shown in Figure 5-1, is typically 17 inches at the 90 percent amplitude and 43 inches at the 50 percent amplitude.

Tie plate load cells have been used successfully for the measurement of wheel/rail loads, but there are drawbacks to this application. The primary

limiting factor is the variation in sensitivity caused by small dimensional changes in the track structure induced by temperature or moisture changes, and traffic. The output of the load cell must then be calibrated and adjusted relative to wheel load to accommodate these time varying changes in the track structure if W/R load is to be measured with any accuracy. Again it becomes necessary (as with the vertical shear force circuit) to establish sensitivities based on average load readings taken under relatively well-defined vertical wheel loads, such as locomotives. The influence length of an individual tie plate is also insufficient to collect wide-band frequency domain information on the dynamic variation of wheel loads. This can only be accomplished by summations of several circuits.

Summation of the load signals from several tie plate load cells has been successful [5-5], but it requires the installation of tie plates over the entire influence length (deflected length under a point load) of the track. As Figure 5-1 illustrates, five successive ties typically support 90 percent of the total wheel load. Unfortunately, this length is sufficient to interact with adjacent wheel loads for the typical 5-6 foot spacing of freight car axles. A distinct advantage of measuring successive tie reactions over the entire influence length is the ability to establish a local mean and variance of individual tie support for relatively uniform wheel/rail loading. More instrumented ties will be required when using one tie plate, reinstalled at various locations. This is due mostly to the uncertainty generated by the installation of the tie plate at any particular location. This uncertainty is reduced to a minimum when all the tie plates are replaced at the same time in the loaded zone.

The ORE/BR/CN tieplate originally developed by British rail was evaluated in Reference 5-1. Its performance when used for summations is compared to the Dutch, French, and Swedish tieplates in the ORE report 11, Question B10. The British and Dutch designs produced the best results, comparing extremely well with the Swiss instrumented rail. It is significant to note that these two designs were more rigorous in following ideal transducer design principles incorporating flexures. There are no

tie plates available in this country that have the capability of measuring lateral and vertical forces as well as transverse (overturning) torques. A sketch of a vertical and lateral load-measuring tie plate developed by the Canadian National Railways based on the ORE design is shown in Figure 5-6. Experience with this tie plate has shown that vertical and lateral loads measured by the plate depend very much on installation, and that there is a tendency to change the rail/tie load distribution, particularly in the lateral direction. Tie plate load cell designs incorporating sliding or rolling contact to provide isolation between the major axes of sensitivity are not generally reliable and should not be given serious consideration. There are also limitations in the use of a tie plate with "button" load cells where the installation is adjacent to a rail joint. The impact loads, plus edge loading due to excessive rail base motions, can readily destroy the load cell by loading it well beyond its endurance limit.

Tie plate reactions are in themselves important to other research studies in track dynamics, and combined with rail and tie deflections can provide dynamic impedance and track modulus values for characterizing the test track site. The tie plate load cell should, of course, provide a rail support and restraint closely-equivalent to the standard tie plate and fastener arrangement, without disturbing the track during installation.

Spectrum analysis of frequencies recorded by one tie plate load cell will describe primarily the wheel-pass, truck-pass and vehicle-pass frequencies; but the analysis can also reveal characteristic higher frequencies; but the analysis can also reveal characteristic higher frequencies of the track structure. Frequency response of the instrumented tie plate is generally limited only by localized, high-frequency resonances in the plate and rail. However, the W/R loads are attenuated between the rail head and the tie plate by the effective mass of the rail. This may limit the correlation between tie plate load and wheel/rail load to frequencies under 100 Hz, and represents a limitation on using tie plate cells for measuring high frequency W/R load variations.

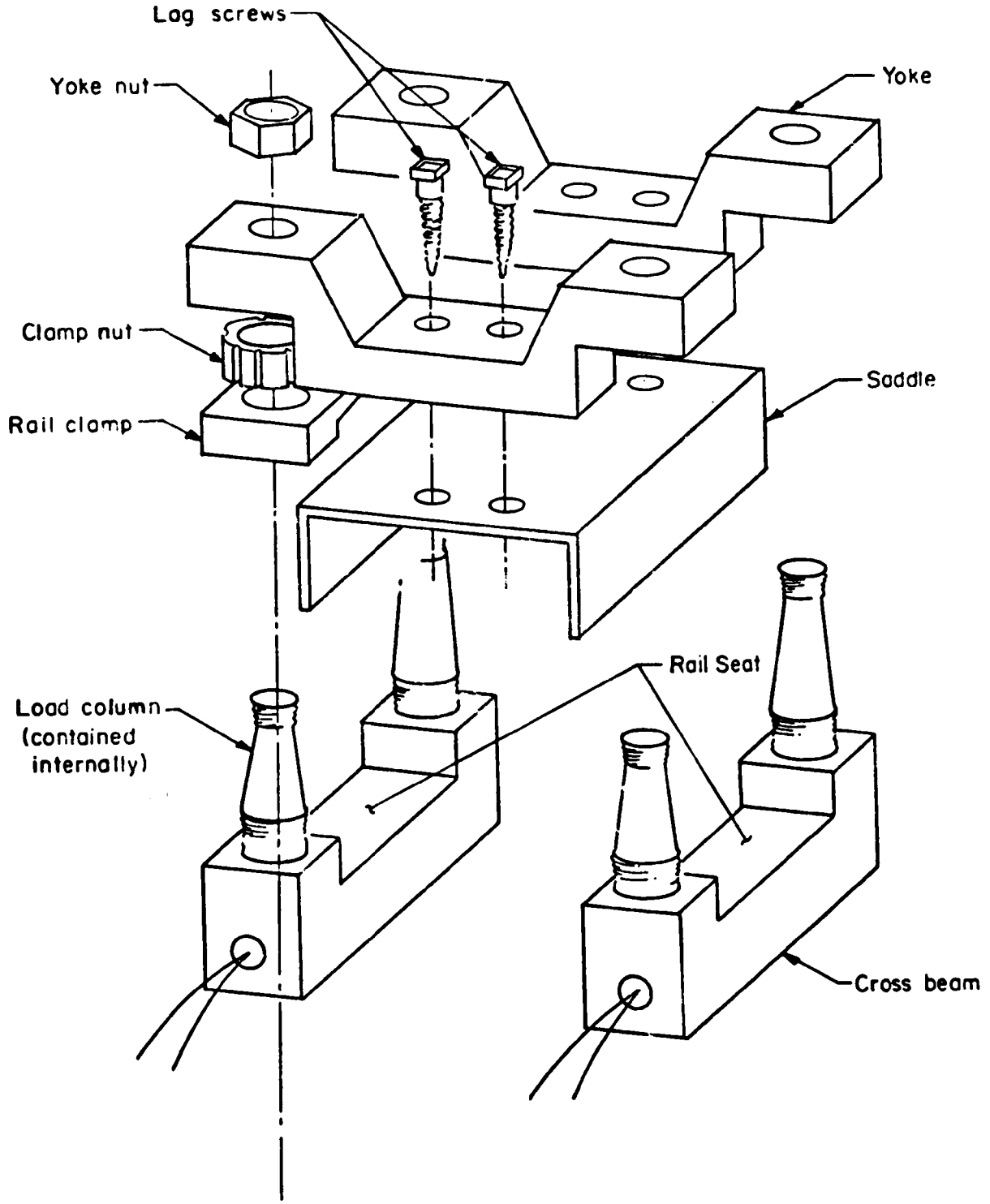

FIGURE 5-6. ASSEMBLY SKETCH OF ORE/CN INSTRUMENTED TIE PLATE

5.1.1.3 Displacement Transducers

A variety of displacement transducers are suitable for maki.g track deflection measurements. The optimum transducer type and range may vary, depending on the specific application. Although the displacement transducer in itself does not affect the track characteristics, it is usually difficult to establish an ideal point of reference from which the deflection measurements can be made. Optical tracking systems have been used in the past, without great success, to measure rail vertical absolute motions from a point well away from the track. Ground vibrations have introduced noise into these measurements. Absolute vertical and lateral displacements of the rail or tie have been referenced in past field experiments [5-4] to a "ground stake", consisting of a 1-inch diameter steel rod driven through a concentric hollow casing through the ballast into the subgrade. The casing ideally isolates the rod from ballast movements, but installation problems make this type of reference somewhat awkward to use.

Relative displacement measurements (rail to tie) may be referenced to a stable fixture which moves as a rigid body only, and is fixed to the tie at appropriate points. This method, used in the recent AAR Track Train Dynamics program [5-4], prevents distortion of rail displacement measurements due to tie bending in the vertical plane. A sketch of the AAR/TTD measurement installation is shown in Figure 5-7.

Displacement transducers have accuracies that are typically better than necessary for this particular application. However, care must be taken to insure that sufficient frequency bandwidth is available to monitor the frequencies of interest. Noncontacting displacement transducers (the magnetic reluctance type) have more than sufficient bandwidth, but generally must be calibrated during installation to correct for target geometry and material properties. Contacting transducers utilize either direct attachment techniques or spring-loaded plungers. It is difficult to provide sufficient spring preload and stiffness to prevent contact separation in the frequency

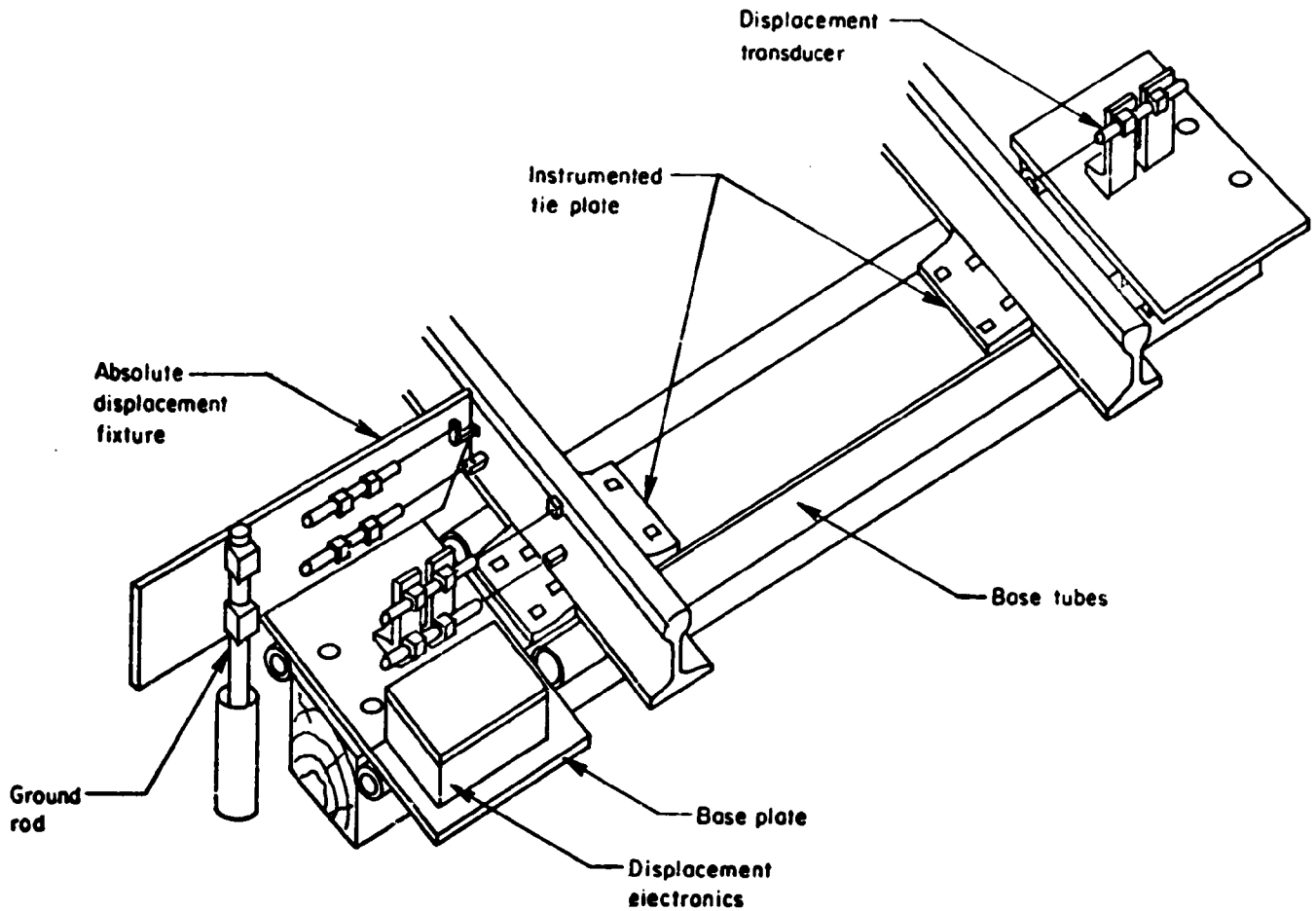

FIGURE 5-7. ARRANGEMENT OF TRANSDUCERS FOR TRACK DYNAMIC RESPONSE MEASUREMENTS IN WIDE GAGE STUDY

range of interest without, at the same time, causing some flexure of the reference fixture. Direct fixation of the core of displacement transducers, through nonmagnetic threaded "ready rod" to a phenolic block cemented to the rail, has proven quite successful in the past, although this arrangement is susceptible to physical damage from ice, ballast or dragging equipment, and distortion from longitudinal movement of the rail under reverse flow of traffic and thermal creep. Contacting displacement transducers are typically LVDT (linear variable differential transformers) or DCDT (direct-current differential transformers), which are self-contained LVDT's. Frequency bandwidth is a trade-off with displacement range: a two-inch total range DCDT has a -3 dB frequency range typically of 100 Hz, while a half-inch total range DCDT has a -3 dB range of 500 Hz.

For short-term tests where frequent attention can be given to the transducers, the contacting type displacement transducer is recommended because of ease in installation without the need for extensive calibration. These transducers are, however, vulnerable to contamination and wear and must be protected from the environment. Noncontacting transducers are impervious to the environment (except, perhaps, a direct hit by dragging equipment), and they are preferable for long-term installations with minimal maintenance. They require extensive calibration during installation to assure proper linearity and sensitivity, and they have been found to be sensitive to noise where the rail provides a ground return in electrified power systems.

The several relative and absolute displacements that are recommended for measurement in the field test program are illustrated in Figure 5-8. These measurements are needed to describe fully the upper track structural deflections for validation of the track model and characteristization of track response to dynamic loads. In order of decreasing priority, these deflection measurements are:

(1) Rail vertical absolute deflection (combining rail/tie and tie/ground deflections) -- used to define the track modulus and dynamic load/deflection characteristics.

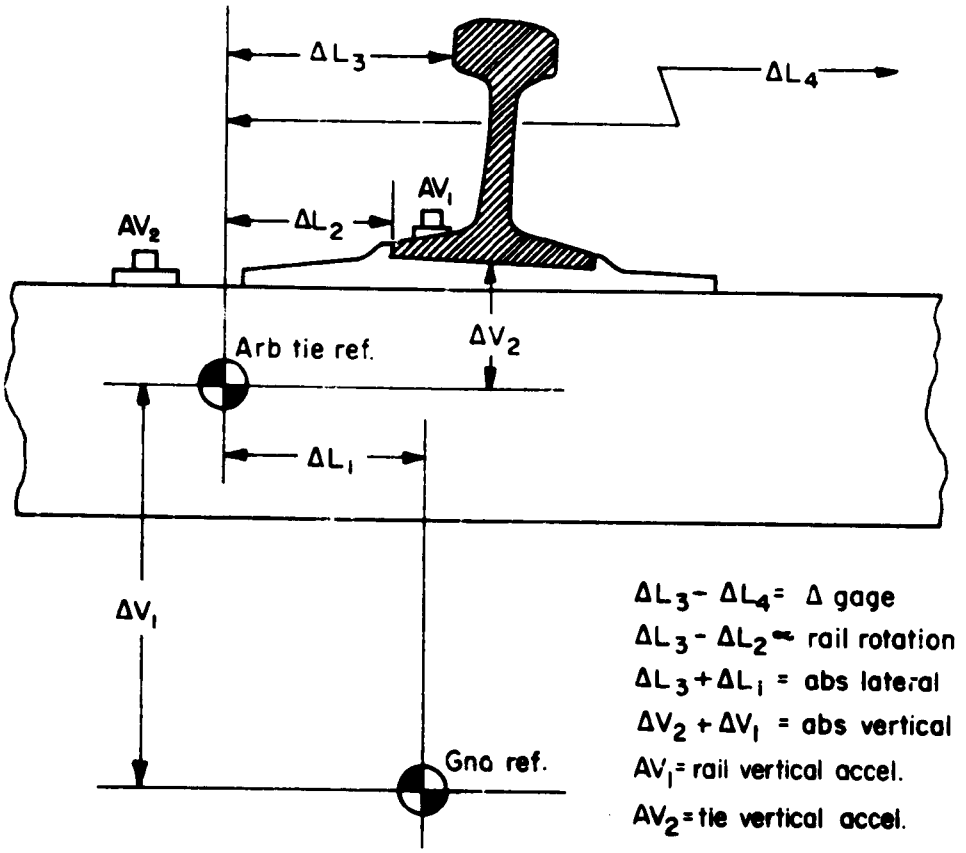

FIGURE 5-8. MEASUREMENTS OF RELATIVE AND ABSOLUTE DISPLACEMENTS NEEDED TO DEFINE UPPER TRACK STRUCTURE DYNAMIC RESPONSE TO W/R LOADS

(2) Rail head/tie lateral deflection -- used to measure rail lateral stiffness characteristics under both lateral and vertical loading. Joint probability densities of lateral deflection, lateral load and vertical load can be developed using this measurement in conjunction with the simultaneous load measurements.

(3) Tie/ground lateral deflection -- data under revenue traffic to document the infrequent occurrence of lateral shift of the tie in the ballast.

(4) Rail rotation (difference of rail head and base lateral deflections) -- used to document the mode of track deflection for more detailed, future track model.

(5) Dynamic gage (difference of left and right rail head displacements) -- used to document track dynamic lateral response and to provide a reference to previous track response studies.

In addition to the displacements, representative measurements of rail and tie accelerations will be recorded to provide an assessment of the frequency content and vibration levels at these points in the track structure. Acceleration measurements will provide an estimate of the force attenuation to the tie through the rail "transfer function", and perhaps allow a calculation of the rail effective mass.

5.1.2 Measurement System Description

Measurement system requirements for acquisition of wayside data are typical of any multichannel data system used to collect dynamic data. The block diagram in Figure 5-9 illustrates the basic system components required. Each system component will be discussed separately.

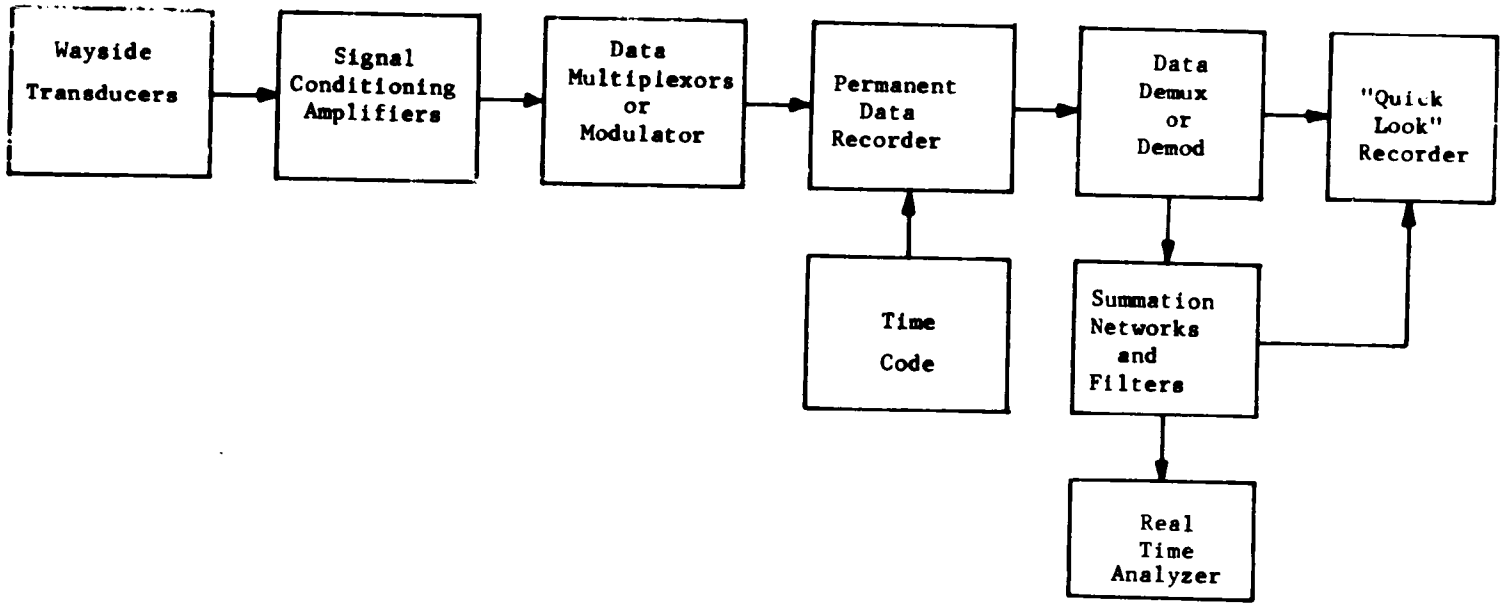

FIGURE 5-9. BASIC MEASUREMENT SYSTEM COMPONENTS

5.1.2.1 Transducers

Table 5.1 outlines the specific applications of the transducers discussed in Section 5.1.1. The priorities placed on each measurement follow the descriptions at the beginning of Section 5.0. Although the priorities imply a "shopping list", Priority I & II measurements must be made and Priority III measurements are sufficiently important to be included in discussions of system channel capacity, etc. Figure 5-10 illustrates the relative location of all transducers at one test installation.

5.1.2.2 Signal Conditioning Amplifiers

The majority of the transducers for the wayside measurements are strain gage devices which require high quality signal conditioning amplifiers. With the low circuit sensitivities and potentially high noise environment, it is important that the amplifiers have high gain, low noise, and excellent common mode rejection. If tests are conducted on electrified rail, common mode voltages may exceed 100 volts. Bridge excitation should be isolated and the balancing circuits (preferably the zero suppression type) should have sufficient range to balance out the field-installed bridges.

Cable length requirements are hard to determine prior to site selection, so laboratory calibrations of tie plate load cells should take this into account. Six or eight-wire circuits are recommended to eliminate this problem unless the signal conditioning is to be placed adjacent to the track. Cable jackets should be able to withstand the abuse of being stepped on while strung across the ballast. It is difficult and time consuming to provide the additional protection of conduit the full length of the cable, but it will be necessary at key locations, such as across access roads.

Displacement transducers typically have their own built-in signal conditioning amplifiers. This equipment, along with the necessary power supplies, calibration and balancing networks, must withstand the environment

TABLE 5-1. RECOMMENDED WAYSIDE MEASUREMENTS FOR CHARACTERIZATION OF W/R LOADS AND TRACK DYNAMIC PROPERTIES

Measurement	Transducer*	Recommended Bandwidth	Max. No. Channels	Priority
Vertical W/R Load (sample)	RV_1 -- RV_{12}	DC-2000 Hz	11	I
Vertical Tie Plate Load	TP_1 -- TP_6	DC-100 Hz	6	I
Lateral W/R Load (sample)	RL_1 -- RL_6	DC-100 Hz	6	I
Vertical W/R Load (continuous)	RV_1 -- RV_{10} TP_1 -- TP_5	DC-2000 Hz	1**	I
Transverse Tie Plate Moment	TP_1 -- TP_6	DC-100 Hz	6	III
Rail Vertical Abs. Deflection	$\Delta V_1 + \Delta V_2$	DC-100 Hz	2	II
Rail Lateral Abs. Deflection	$\Delta L_1 + \Delta L_3$	DC-100 Hz	2	II
Rail Rotation	$\Delta L_3 - \Delta L_2$	DC-100 Hz	1**	III
Dynamic Gage	$\Delta L_3 - \Delta L_4$	DC-100 Hz	1**	III
Rail Vertical Acceleration	AV_1	DC-2000 Hz	1	II
Tie Vertical Acceleration	AV_2	DC-500 Hz	1	II

* Refer to Figures 5-8, 5-10.
** Overlaps with other measurement channels.

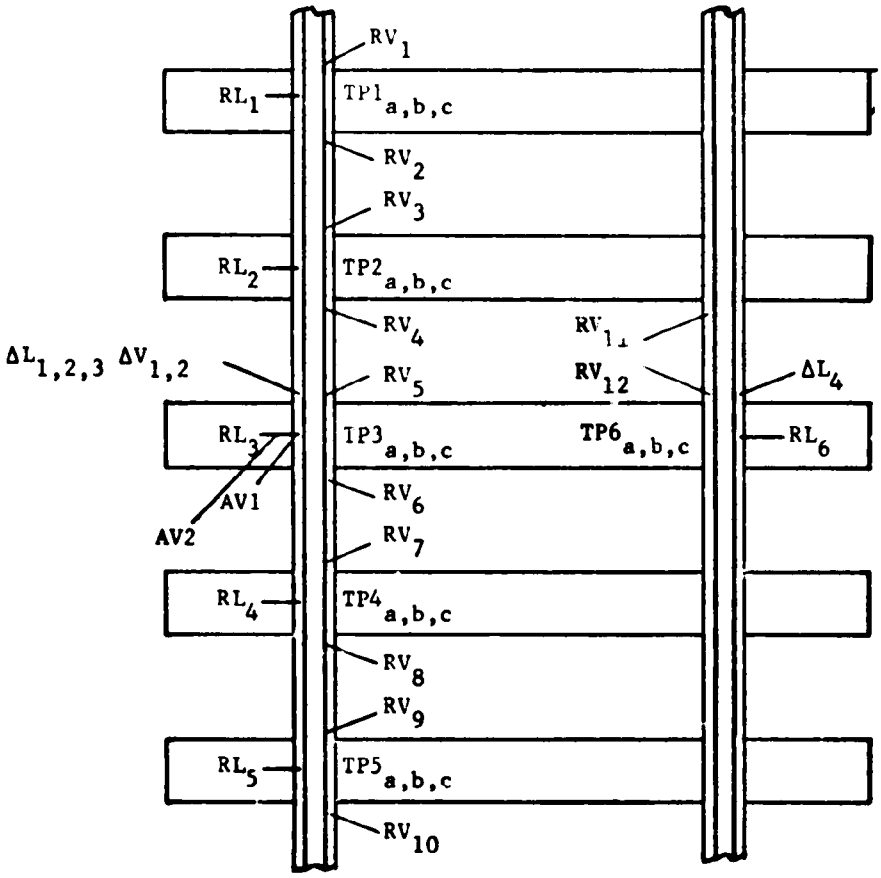

RL = RAIL LATERAL LOAD GAGE CIRCUIT
RV = RAIL VERTICAL LOAD GAGE CIRCUIT
TP = INSTRUMENTED TIE PLATE
ΔL = LATERAL DISPLACEMENT (SEE FIG. 5-8)
ΔV = VERTICAL DISPLACEMENT " " "
AV = VERTICAL ACCELERATION " " "

FIGURE 5-10. RELATIVE LOCATION OF WAYSIDE TRANSDUCERS

normally found adjacent to the track. Shock, vibration and temperature extremes, as well as physical damage from dragging equipment, etc., must all be considered in designing the measurement system installation.

5.1.2.3 Data Multiplexors

Whenever total data channel capacity exceeds 14 channels (IRIG-FM recorder capacity), some form of data multiplexing must be considered. Multiple recorders can be used, but the cost disadvantage plus processing difficulties usually override this approach. Analog or digital multiplexing techniques can be used equally well. Analog techniques such as Frequency Division Multiplexing (FDM) have been used successfully for many years, while digital techniques, such as Pulse Code Modulation (PCM) are newer and have only recently emerged for exotic (costly) aerospace applications. FDM does, however, offer one distinct advantage of simultaneous modulation: that is, no time skew between channels, so that succeeding steps involving summations, or other time-dependent operations, will not have additional errors introduced. On the other hand, data bandwidth and signal-to-noise ratio (S/N) are related in FM processes such that maximum bandwidths have the poorest S/N for any particular subcarrier. We recommend a FDM system to minimize costs and to avoid time skew problems related to later analog summations.

5.1.2.4. Permanent Data Recorder

To maintain a permanent record of data and provide for later computer processing, some form of magnetic recording capability will be required. An IRIG-configured recorder will provide the greatest compatibility, especially the 1.0-inch Intermediate Band or Wide Band Group I configuration. This approach will work equally well for FM or PCM multiplexes (unsaturated recording). Digital (saturation) recording and the associated digital processing system is not economically comparable at the data rates needed for this program. Real time digital data systems are also (currently) less adaptable to the rapid field preparations needed for this type of test program.

5.1.2.5. Time Code

A time code reference is a useful and necessary part of a multi-channel data system. Whenever data processing capacity is smaller than data recording capacity, a time code will provide the synchronization for matching parallel information which is processed in serial fashion. This is also true for multiple recorders where a common, unambiguous signal is needed to match data on adjacent tapes. The IRIG B time code is the most widely used reference and has resolution to 0.001 sec. The time-of-day reading provided by the time code is also a convenient data log identification to help minimize errors caused by mis-labeled test entries.

5.1.2.6. Data Demultiplexor or Demodulator

It will be necessary to transform the permanently recorded data back into a useable form in the field to verify data quality. Monitoring "quick look" data provides insight to the overall system performance as well as the response of key parameters that may influence changes in the test plan. The particular device used for demultiplexing the data will necessarily be matched to the multiplexor. Unfortunately, this equipment is rarely standardized sufficiently to have the raw data deciphered by others. This places the responsibility on the originator to produce final output formats that can be readily incorporated by others.

5.1.2.7 Field Processed Data

Sufficient equipment should be available in the field to assist in cursory analysis of the data. Time histories on oscillographic paper provide sensitivity checks, so they should be at least as accurate as the dynamic accuracy required for the measurements. A real-time analyzer can be used to determine the frequency content of the data and to assist in defining system S/N as well as to help diagnose system problems.

5.1.3 Data Reduction and Format

It will be necessary to present results in a variety of formats to insure a convenient presentation for each individual application. Data reduction techniques will vary, depending upon which format is to be presented. The raw data recorded on magnetic tape is in a time-history format. However, due to the nature of the signals generated by many of the wayside transducers, the basic time history will have little usefulness for characterizing wheel/rail loads. As discussed earlier, summations of several transducers will be necessary to obtain continuous time histories of the W/R load over a track section within the influence zone of one point on the track. As discussed earlier, these summations can be performed during the field data acquisition phase, to reduce the number of data channels required, but the results are more susceptable to irreversible failures if processed in real time. Therefore, the summation techniques should be considered a part of data reduction.

Analog filtering of data should be performed based on analysis of frequency content of the raw data. Data should be processed at a maximum bandwidth commensurate with data frequency contents and acceptable signal-to-noise ratios. Magnetically recorded data typically has signal to noise ratios on the order of 40 dB. Therefore, filter cutoff frequencies can be adjusted to cut off signals above the data frequency which approach 40 dB below maximum data amplitudes. Analysis of tie plate load spectra, for example, indicates a data cutoff frequency (40 dB) of approximately 100 Hz. Other transducers, such as the rail shear force circuits, will require wider bandwidths to accommodate the rapid rise time encountered as the wheel/rail forces enter the influence zone of the circuit. Generally, signal summations such as the one described in Figure 5-6 should be processed at maximum data channel bandwidth and then analog-filtered on the output. In this particular case, the post filtering should reduce the effects of switching transients discussed in Section 5.1.2.

Once filter cutoff frequencies are determined, sampling rates for the A/D converter can be established. If frequency content is to be determined from the digitized data, a sampling rate of 5 times the cutoff frequency should be used to avoid digital "aliasing" problems. However, if the data being digitized is sampled primarily for peak amplitudes, sample rates can be reduced to twice the maximum frequency. Based on the previous criteria of selecting the maximum frequency for amplitudes being about 40 dB down from maximum amplitudes, this would introduce less than 1/2 percent uncertainty on the peak value.

It will be necessary to maintain identity of the data with respect to the axle location within a train so that during later processing, values can be applied to the appropriate vehicle. Individual axles can be identified by either an external wheel detector on an adjacent channel or by monitoring one of the vertical shear force transducers and using that as a gating function to trigger the A/D process and increment a counter. This latter technique is recommended because it does not require additional recording channels. Consecutive axle numbers can be placed on each successive wheel detected, or time of day can be determined by monitoring the time code signal. Other latent information can also be determined at this time. Vehicle speed and truck center spacing can be determined by knowing the time and distance between two transducers. These data, when compared with measured axle loads, can be used to verify train consist sheets so that more detailed identification of specific vehicle types can be obtained.

Further tests can be made at this time to determine whether flat wheels are introducing loads significantly greater than static wheel load, thereby skewing the processed data. Having this kind of flexibility in the initial reduction stages of the data processing is important to insure higher validity of the final data. For example, train consist sheets are typically scrambled because of switching of cars in and out of the train from the time the consist was generated to the time the train passes the test site. Individual blocks of cars can also be out of order in the consist.

Additional data channels can be generated during this stage of data reduction. Simple calculations between processed channels can produce other useful information. For example, calculation of track stiffness taken from concurrent load and deflection measurements can produce impedance values that are not only correlated with vehicle speed, but also vehicle weight. With the large number of axles that will pass over a given test site, these stiffness values can be determined with a high degree of confidence. Although some of these additional parameters are beyond the scope of this program, their importance in related programs will warrant serious consideration. Figure 5-11 illustrates a typical data reduction block diagram and shows the variety of outputs available.

After the raw analog data has passed through any analog processing networks and then filtered, the new signals can be rerecorded on analog tape for any time-domain model inputs or spectrum-analyzed on a real time analyzer to generate PSD's. These PSD's could then be fed directly into the minicomputer for digitizing or plotted on an x-y recorder for later manual curve-smoothing.

The digitized data which by now has gone through the initial stages of reduction is stored on an interim digital magnetic tape and consists primarily of a channel ID number, an axle or vehicle location (which would implicitly include other factors, such as test number, location, etc.), and data amplitude. These data files stored on magnetic tape would then be loaded into a large CPU and stored in a manner convenient for a variety of retrieval sequences. Figure 5-12 is an example of data presented in both the peak amplitude probability distribution and the peak amplitude histogram which were plotted directly from a selection code typed into the computer terminal. This selection code is constructed to pull all data that is stored with the unique combination of variables defined by the code. For example, a plot could be generated from all data points available for cars less than 50 feet in length, less than 70 tons gross load traveling between 50 and 60 MPH through Test Section 3 and monitoring the parameter: dynamic gage. The advantage of having data available at this level of

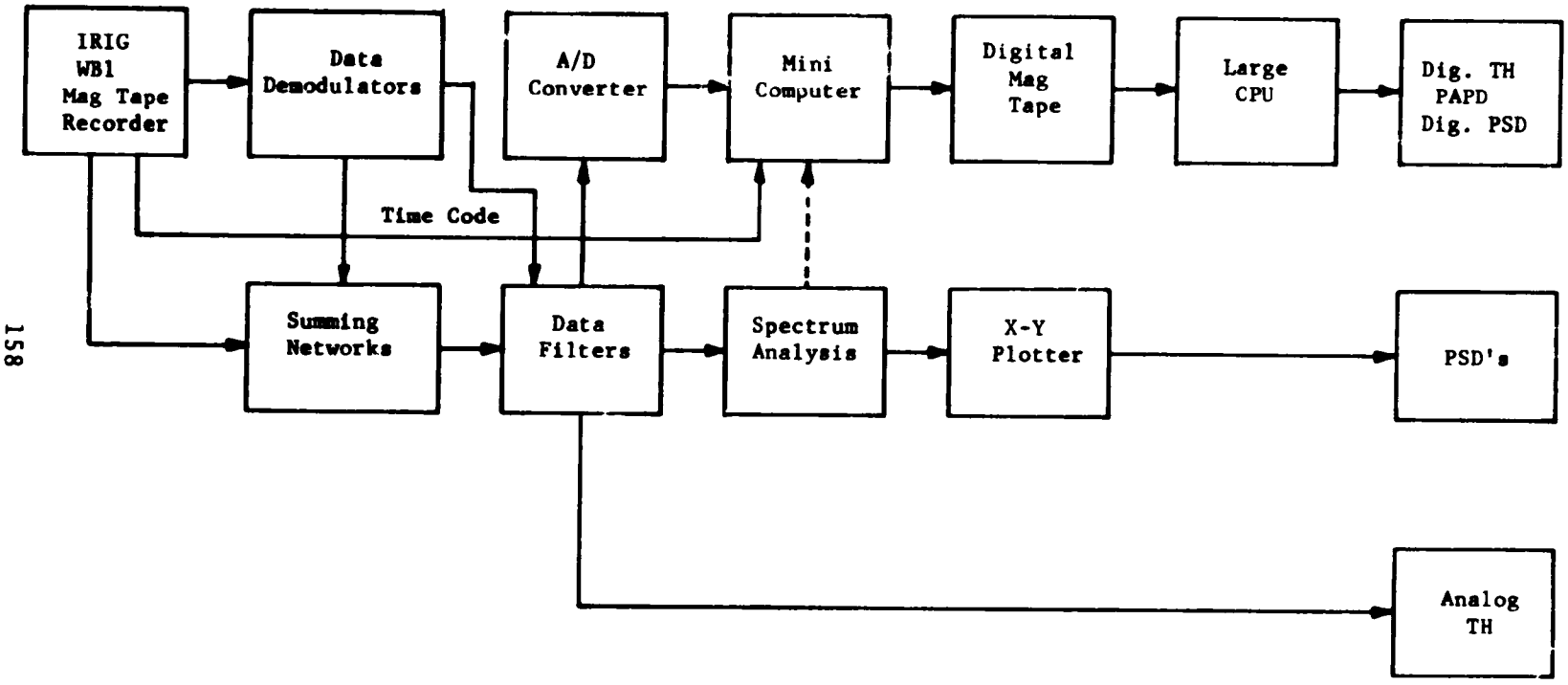

FIGURE 5-11. EXAMPLE BLOCK DIAGRAM OF WAYSIDE DATA REDUCTION AND ANALYSIS

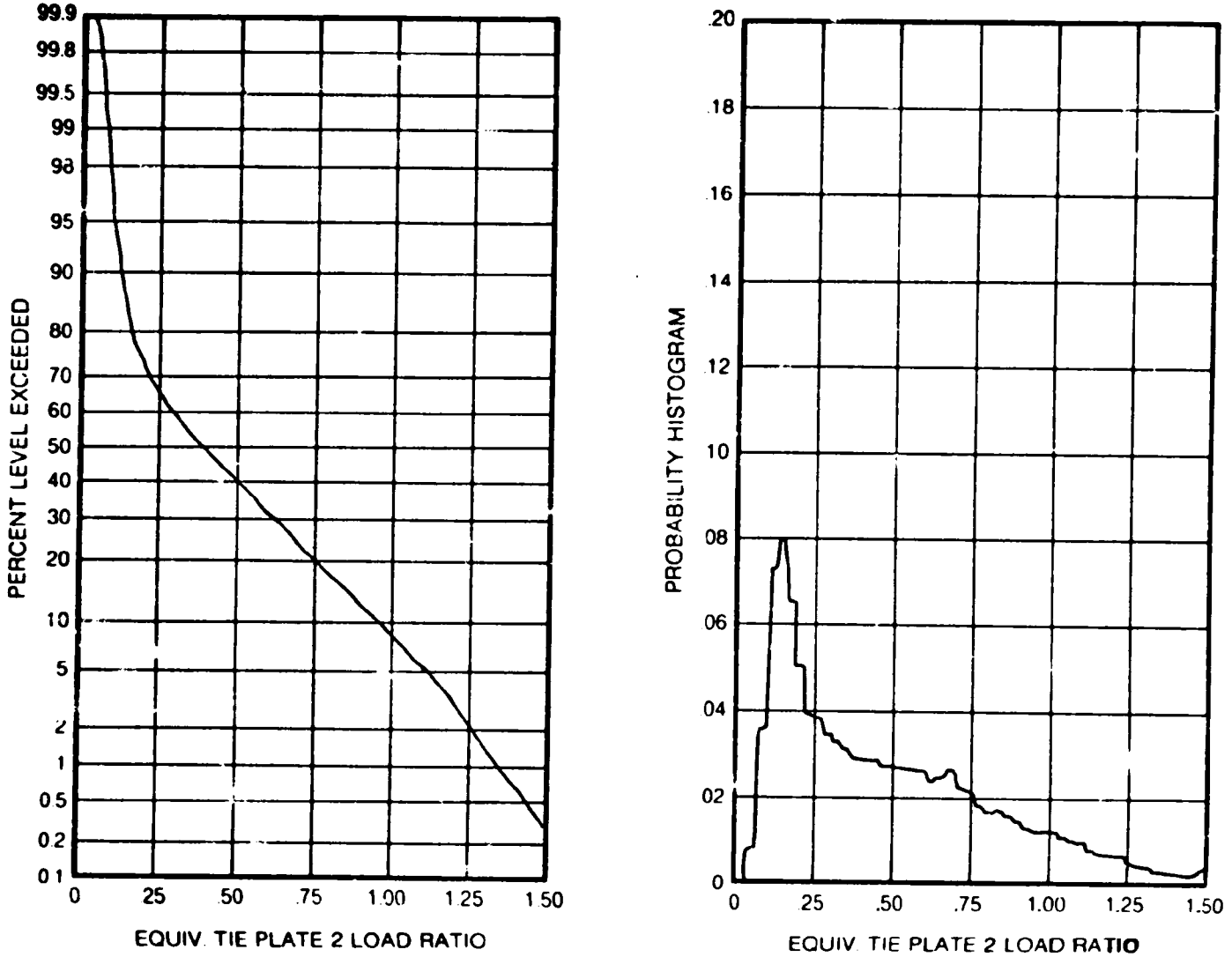

FIGURE 5-12. EXAMPLE OF PROBABILITY DISTRIBUTION AND DENSITY CURVES PRODUCED FROM COMPUTER-SORTED FIELD DATA

manipulation is the ability to spend a relatively short amount of time in front of an interactive terminal and scan a relatively large quantity of data to "zero in" on previously unknown trends in the data. Several different sets of data can be plotted consecutively on the same grid so that variations in the data can be quickly interpreted.

In addition to the probability density and cumulative distribution functions of a single variable, the joint probability density of pairs of variables will be of interest. For example, the definition of track lateral stiffness will depend not only on lateral force and deflection, but also on the simultaneous vertical load. Similarly, a statistical description of lateral to vertical load (L/V) ratio versus the concurrent vertical W/R load is of great interest in defining the load environment. Sets of curves or some method of three-dimensional display will be used to present these statistical functions.

5.1.4 Wayside Test Duration

The data requirements for this field measurement program fall into two distinct categories. One category consists of a complete set of W/R load and track response measurements under the instrumented test vehicle, providing a direct comparison of wayside and vehicle-borne measurements. The test train will also be used in lateral calibration when applying a known load between the rail heads with a simultaneous vertical load from the lead axle of the test train locomotive.

The second category is a compilation of maximum loads and deflections under revenue traffic for statistical analysis. These data will be used to establish the characterization of W/R loads and the track dynamic response to load. Sufficient data will be recorded to analyze trends for different speed ranges, different vehicles (locomotives, light or heavy freight cars, etc.), and different train handling (traction, drifting or braking). The data requirements which arise from this statistical characterization are discussed below.

Amplitude statistics, including mean value, standard deviation, probability density, joint probability density, and cumulative probability distribution functions, have been recommended in Section 3.2 for analyzing many of the track loading and response characteristics required for this program. Statistical criteria can be used to estimate the number of measurement locations and the number of data samples from a single measurement location needed for a desired accuracy and confidence level for a particular "experiment". Several typical experiments in track dynamic response have been reviewed to determine these criteria.

A statistical characterization of a trackside measurement will be influenced by several factors. These include:

- Constructional variations within an otherwise uniform section of track
- Track dynamic impedance variations from one section to another (or from one season to another)
- Track geometry random or deterministic variations
- Ambient variations (rail temperature, wet rail versus dry rail surface, etc.)

Some measurements are more strongly influenced by these factors than others -- tie plate load, for example (see Section 3.2.2), is strongly affected by constructional variations which affect the rail to tie clearances and hence, the tie support condition. To achieve the desired statistical confidence level, measurements from several adjacent locations should be combined to evaluate variations in tie support condition within the deflection-influenced zone. The mean value tolerance (possible variation in the measured mean value from the true mean value) is plotted in Figure 5-13 versus the number of measurement sites for several values of statistical confidence level* and ratio of measured standard deviation to measured mean value. Tie

* Confidence level: if the experiment were repeated 100 times, the measured mean value would fall within the tolerance band 95 of those times for a 95% confidence level.

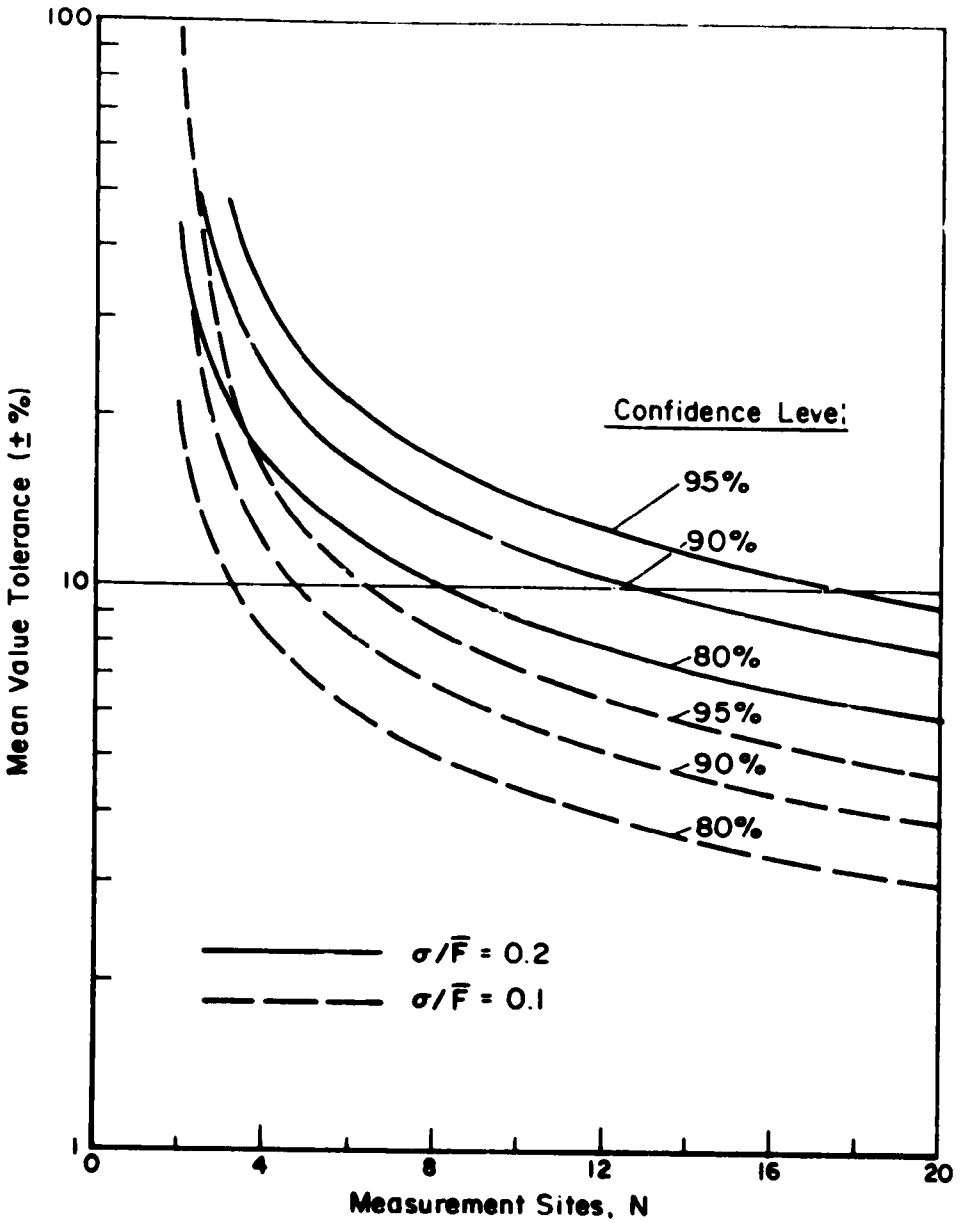

FIGURE 5-13. TOLERANCE BAND ON TRUE MEAN VALUE VERSUS NUMBER OF MEASUREMENT SITES AS A FUNCTION OF CONFIDENCE LEVEL AND RATIO OF MEASURED STANDARD DEVIATION OF MEAN VALUE

plate vertical load data from the TTD experiments in Idaho showed this ratio for a particular vehicle class to range from 10 to 20 percent. These curves show that from 4 to 6 measurement sites are required to establish a mean value tolerance comparable to that anticipated for the predictive model.

Previous work [5-10] on the data requirements for amplitude statistics has shown that the probability density function governs the number of data samples required. The statistical data from wayside measurements will consist of one data point (peak value) for each axle pass, so that the number of data samples is identical with the number of axles passing the site. In order to compute the peak amplitude probability density function for a set of load data, the load range must be established and divided into the minimum number of intervals ("bins") compatible with the desired resolution for the statistical description. Then the number of data values, and percentage of data, in each interval would be calculated to give a probability density histogram.

It is clear that the load intervals must be sufficiently small to provide good resolution of amplitude variations, and the total range must be adequate to cover the desired low-probability events with data collected from a suffcient number of axles so that each interval has several data points to provide a reliable estimate. It is recommended that each interval have at least 5 data points, although two is acceptable for the last interval. It is desirable to be able to determine amplitude statistics over a $\pm$ 3-sigma range for purposes of extrapolating to lower probability, high-amplitude events. Data from 1000 axles are needed to define the $\pm$ 3-sigma with 12 load intervals, and from about 3000 axles to resolve the load into 24 intervals.

Additional recommendations [5-11] are given for the number of intervals (K) required for N data points based on applying a Chi-Square goodness-of-fit equivalence test between a hypothetical and measured probability density function at the 5 percent level of significance. The number of intervals may be approximated by:

$$K = 1.87\ N^{0.4} \qquad \text{number of intervals} \qquad (5\text{-}1)$$

For the same number of data points, this estimate recommends a greater number of load intervals for a hypothesis test than the 3σ criterion.

To estimate the length of a test at a given site, a traffic density of 20 MGT per year can be assumed, or roughly 55,000 gross tons in a day. With an average car weight of 60 gross tons (15 tons per axle), approximately 3700 axles a day will be recorded from revenue traffic. To examine the data for particular trends by means of amplitude statistics, the data must be subdivided into a number of categories, each of which must contain sufficient data points to satisfy the criteria discussed above.

The division of the experimental data may be done in several ways. One variable of interest is, of course, train speed. Speed bands of ten mile-per-hour width over the normal operating speed range are recommended for this program. Different categories of vehicles represent a second division of the data: it is recommended that revenue data be divided into locomotives and four groups of freight cars, lighter or heavier than 50 gross tons weight, and longer or shorter than 50-ft truck center distance. Finally, the data may be subdivided according to the specific experiment: given track sites, train handling conditions, wet rail versus dry rail, et cetera.

On tangent, level track, a test matrix of 5 speed bands and 5 vehicle categories may be anticipated, for a total of 25 subcategories. Four days of revenue traffic would provide an average of 592 data points per subcategory, and a 24-interval resolution (roughly 2000 lb per interval for vertical load range of 0 to 50,000 lb). Because of local traffic patterns and operating conditions, however, some categories would have substantially more or less than this average number, so that the alternatives would be more data (a longer test) or less statistical confidence or resolution for some subcategories.

On curved track, train handling categories -- tractive effort, drifting, dynamic, or train-air braking -- would be important, further expanding the data matrix. Assuming 4 10-mph speed bands, 5 vehicle categories, and 4 train-handling categories, the following alternatives of resolution may be calculated to meet the Chi-Square criteria:

No. of Intervals	Req. No. of Data Points	Req. No. of Test Days
10	66	1.4
16	214	4.6
25	654	14.1

It is recommended that some reduction in resolution, or the use of combinations of subcategories, be accepted to hold the number of test days at the curved-track site to one week maximum.

5.2 VEHICLE-BORNE MEASUREMENTS

This section describes the results of a study to define a vehicle-borne instrumentation system for the measurement of wheel-rail forces. The objective of this task was to review the requirements for a vehicle-borne instrumentation system and recommend the optimum system. The recording system requirements and data processing techniques are also defined.

The recommended instrumentation system consists of a freight car truck on which suitable transducers have been applied for the measurement of vertical and lateral forces at the wheel-rail interface. The discussion in this report assumes that a truck for a nominal 100-ton capacity car will be utilized (5-1/2 x 12 in. journals, 36 in. diameter wheels), although the same procedures could be used to instrument trucks of other capacity. It is intended that the truck be installed on a standard 100-ton capacity car, such as the hopper car, when the wheel-rail load measurements would be made.

Wheel-rail load phenomena occur over a wide range of frequencies Quasi-static lateral wheel loads are developed when traversing curved track. Fluctuating vertical loads due to car body roll motions occur at frequencies of approximately 1 Hz for a loaded car. Car body bounce and pitch motions, again with a loaded car, occur at frequencies in the 2 to 5 Hz range. These motions generally result in a symmetric application of the load to the wheels of the truck. The wheel-rail loads from these motions can be two to three times the static load when the primary suspension springs bottom out under severe vibration. High lateral wheel-rail loads can develop during unstable

truck swiveling or hunting motions. This condition usually occurs during the high speed operation of a light-weight car and results in lateral loads in the 3 to 7 Hz range. Above 8 Hz there are various resonances of the unsprung members of the truck, the track substructure, etc., which may lead to large wheel-rail loads. The highest frequency of interest which has been identified in this study is the transient load which occurs with passage of a wheel over a rail joint. The characteristic loads associated with this phenomena are from 1 to 30 msec. in duration.

We have chosen to describe the characteristics of vehicle-borne load measurement systems for two frequency ranges, which are arbitrarily designated as low and high frequency systems. A frequency of 10 Hz is the approximate division between the two systems. The low frequency system would measure the lateral forces on each of the four wheels of the truck, since the lateral wheel-rail forces are significantly different at each wheel of the truck for such low frequency phenomena as truck curving, car rolling, and truck hunting. The sum of the vertical forces on the two wheels on one side of the truck would be measured by the instrumented side frame in this low frequency range, since the difference between loads on front and rear wheels is minor in this range. The transducers for the measurement of these forces would be mounted on the axle and side frame of the truck as described in the following section. The high frequency system would measure the vertical loads on one wheel of the truck. This would involve the installation of an extensive array of strain gages on one wheel.

The frequency range over which it is possible to measure wheel-rail load phenomena with a vehicle-borne system has been examined in a simplified manner by analyzing a three degree-of-freedom representation of a freight car truck. The results of the analysis are presented in Appendix C to this report.

5.2.1 Low-Frequency System

The system which is recommended for the low frequency load measurements follows the principles utilized by the Bessemer and Lake Erie Railroad

for their test truck [5-6]. This system has provided useful data over a number of years. It makes possible the simultaneous measurement of lateral and vertical forces at the wheel-rail interfaces for each of the four wheels of the truck. This permits the establishment of the lateral-to-vertical load ratio, which is an important parameter in the consideration of rail loads.

The lateral and vertical forces at the wheel/rail interface are determined by the measurement of certain external and internal forces acting on the two wheel-axle sets of the truck. It is assumed that the wheel-axle set can be considered as a rigid free body on which there are acting five unknown components, the lateral and vertical forces at each of the wheel-rail interfaces and the lateral force from the truck frame acting along the centerline of the axle. There are two additional load components, the vertical loads at the two journal bearings, which are assumed to be known from independent measurements.

The system of forces is illustrated in Figure 5-14. The equilibrium equations for the wheel axle set can be solved to determine the unknown forces if the bending moments in the axle can be established at two locations. These locations are designated as M_L and M_R in Figure 5-14. Solving the equilibrium equations yields the following results for the loads acting at the wheel-rail interface:

$$V_L = B_L + \frac{(M_L - M_R)}{(f-e-d)} \tag{5-2}$$

$$L_L = \frac{1}{c}\left[\frac{M_L(f-e) - M_R d}{(f-e-d)} - B_L a\right] \tag{5-3}$$

$$V_R = B_R + \frac{M_R - M_L}{(f-e-d)} \tag{5-4}$$

$$L_R = \frac{1}{c}\left[\frac{M_R(f-d) - M_L e}{(f-e-d)} - B_L b\right] \tag{5-5}$$

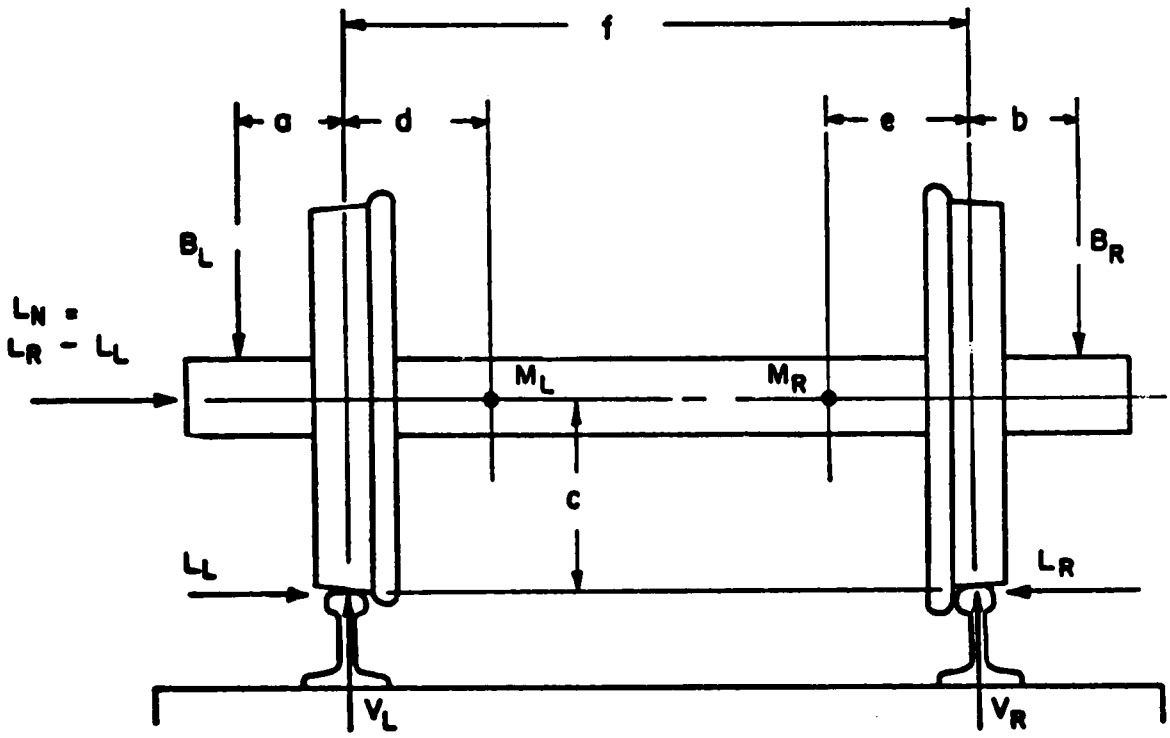

FIGURE 5-14. FREE BODY DIAGRAM OF AXLE

where M_L, M_R, B_L, and B_R are known measured quantities and a, b, c, d, e, and f are physical dimensions.

The bending moments in the axle at locations M_L and M_R would be determined by strain gage measurements at these locations. A strain gage bridge sensitive to the bending moment would consist of two active gages mounted at diametrically opposite positions on the axle and two dummy gages to complete the bridge. Since one is interested in the bending moment acting in the vertical plane, each pair of active gages would provide a measurement of the bending moment twice per revolution when the plane of the gages is oriented in the vertical direction. At other orientations of the axle, the output of the strain gage bridge resulting from a bending moment in the vertical plane would be reduced by a factor equal to the cosine of the angle rotation. Since the loss of sensitivity of the bridge becomes substantial as it rotates to a near horizontal orientation, it is recommended that two additional bridges be installed on the axle where bending moment measurements are desired. These bridges would be oriented at 60 deg intervals around the axle. The output from each bridge would be sampled as it rotates within $\pm$ 30 deg of the vertical plane. The output of the bridge would be adjusted to take into consideration the decrease in sensitivity with increasing angular displacement from the vertical within this angular range. This would require sensing of the angular position of the wheel-axle set by a wheel rotation position transducer.

There are two options for the measurement of the vertical load at the journals (the B_L and B_R loads). One is to use load cells in the roller bearing adapter locations. The other is to use instrumented side frames for sensing of the vertical load on the side frame and then making the assumption that this load is evenly divided between the two journal bearings. Previous measurements (see Figure 3-31) have shown that this is a reasonable assumption to make.

The use of instrumented side frames for sensing the vertical forces is recommended because experience has shown that this is a very reliable method for measuring the vertical load. Four strain gages would be used on each side frame, one on each of the two tension members and one on each of the two compression members, as illustrated in Figure 5-15. These gages would be wired into a four active arm bridge. The output of these bridges as a function of load would be determined by calibration loads applied to the truck up to a total load of approximately 300,000 lbs.

5.2.2 High-Frequency System

For the measurement of high-frequency phenomena, such as the transient vertical load associated with the passage over a rail joint, it is desirable to locate the load transducers as close as possible to the point of load application. This is shown by the analysis presented in Appendix C. The use of strain gages mounted directly on the wheel are recommended for these measurements. It is also recommended that these measurements be made on only one of four wheels of the truck because of the large number of gages that will be required.

The maximum strains in the wheel due to vertical load are located on a radial section between the wheel and rail. Because of the rotation of the wheel, this section is constantly changing with respect to the wheel. Therefore, an array of gages must be placed on a circumferential line at the optimum radial distance for sensing the strains. In addition, some means must be provided for sampling the data from each gage as it passes the zone where maximum strains are developed.

5.2.2.1 Wheel Gaging Techniques

Two basic techniques have been used to determine vertical and lateral loads from wheel mounted gages. Each technique uses a series of equally spaced, radially oriented, strain gages mounted to the wheel on a

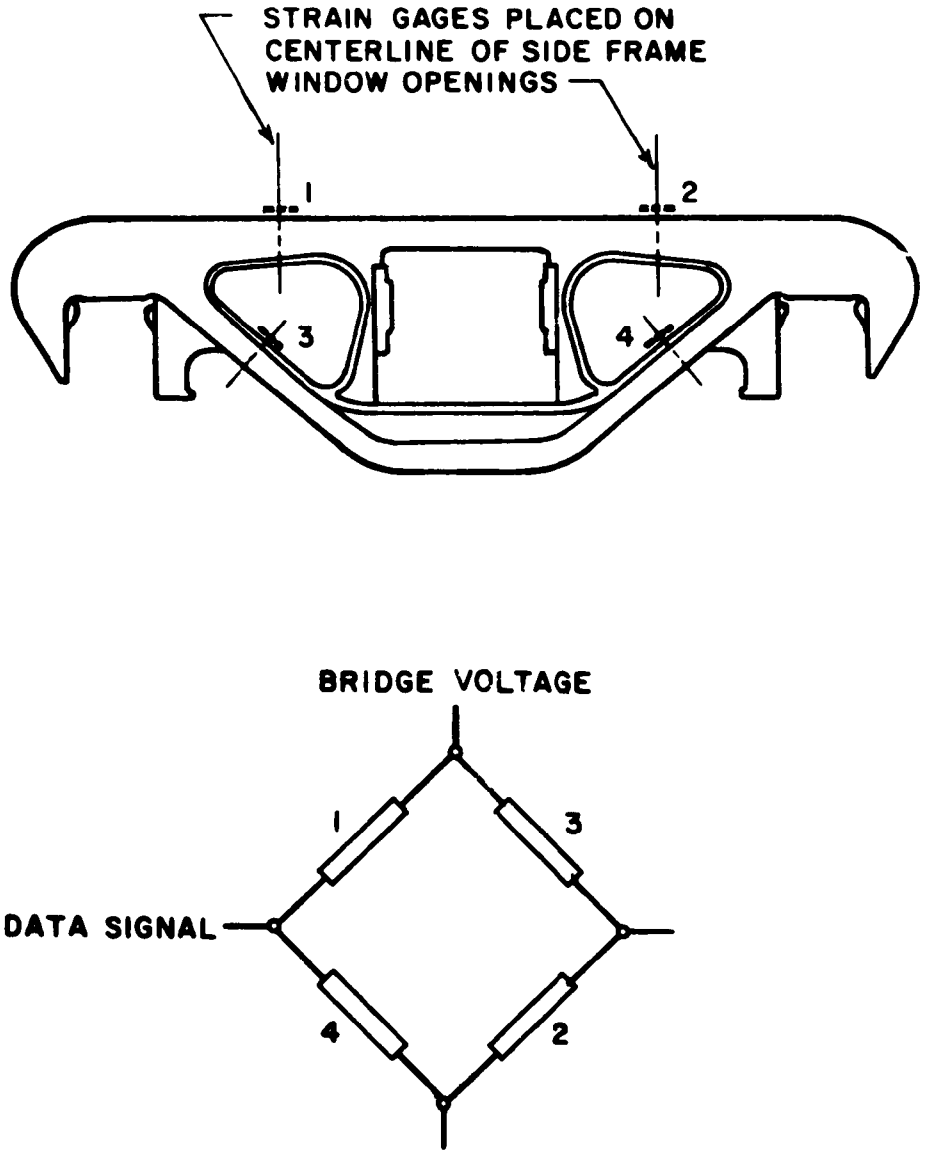

FIGURE 5-15. TRUCK SIDE FRAMES STRAIN GAGED FOR VERTICAL LOAD MEASUREMENT

circular reference line. The radius of the reference line and its location on either the front face or back face of the wheel is selected to give maximum strain output to the desired load being sensed (vertical or lateral). Strains from loads in the opposite direction should be a minimum at this location.

One technique for sensing the output of these gages is to wire all of the gages into a single bridge [5-7]. The gage closest to a vertical reference line produces the maximum signal because the maximum strains are introduced into the wheel at this location. Since all the gages are wired into the bridge, there will be a continuous output as one gage after the other rotates through the zone of maximum strain. The accuracy of this system depends on the number of gages used, because the strains on a radial line drop off rapidly as it rotates away from the vertical orientation. Thus, the output of the bridge from a constant load will not necessarily be a constant, but will reflect the fact that the total output of the bridge fluctuates as the orientation of the gages changes with wheel rotation.

The second technique for sensing the output of wheel mounted gages is to record the signal from the gage only as it passes through the zone of maximum strain [5-8, 5-9]. This is done by using an encoder which is synchronized with a wheel position sensor so that the gage output is sensed only as it passes through an angle equal to $\pm$ 1/2 of the spacing angle between gages, with reference to the vertical orientation. In addition, within the zone where the data is recorded, the gage output is modified by a weighting function to account for the fact that there is a dropoff in sensitivity with an increasing angle from the vertical.

5.2.2.2 Optimum Location for Wheel Gages

A detailed analysis has been conducted of the 36 in. diameter H36 wheels which are available for the tests to be performed under this project. The surface strains on the wheel which are developed from vertical

and lateral loading have been predicted. The results from the analysis can be used to determine the optimum locations for the placement of gages to detect vertical and lateral wheel-rail forces. The results from the analysis can also be used to determine the weighting function for gage output as a function of the gage angle from the vertical.

Figure 5-16 shows the predicted radial surface strains resulting from a 32,000 lb vertical load, the approximate value for a loaded 100-ton capacity car. Figure 5-17 shows the predicted radial surface strains resulting from a 10,000 lb lateral load acting against the base of the flange. A lateral load of this intensity would be a relatively rare event, except in the case of unstable truck hunting. The radial strain in the wheel plate will be a function of the lateral position of the point of load application of the vertical load on the tape line of the wheel. Calculations indicate that at a 14.1 in. radial distance the strain on the inside surface decreases approximately 15 percent (in absolute value) per 1/2 in. lateral movement of the load away from the flange. There is a corresponding increase in the strain (again in the absolute sense) on the other side of the plate at this location. Thus, the sum of the strains tends to remain constant with lateral movement of the vertical load, the change in position of the load by 1/2 in. resulting in less than a 2.5 percent change in this parameter.

The data presented in Figures 5-16 and 5-17 can be used to determine the optimum positions for the placement of gages to detect vertical wheel-rail loads. There appears to be two feasible options. The first is to place the gages, radially oriented, on the inside of the wheel at a radius of approximately 14.1 ins. This position shows a high sensitivity to vertical load (approximately 3.9μ in./ in. per 1,000 lbs) and is at a position where there is low sensitivity to lateral load. The only difficulty is the sensitivity of this output to the lateral position of the load, as previously indicated. The second option is to use the sum of the radial strains from opposite sides of the plate at this position. This results in a signal which is insensitive to fluctuations in the lateral position of the vertical load, but which will be affected by lateral loads acting on the tread. The sensitivity of such a bridge will be approximately

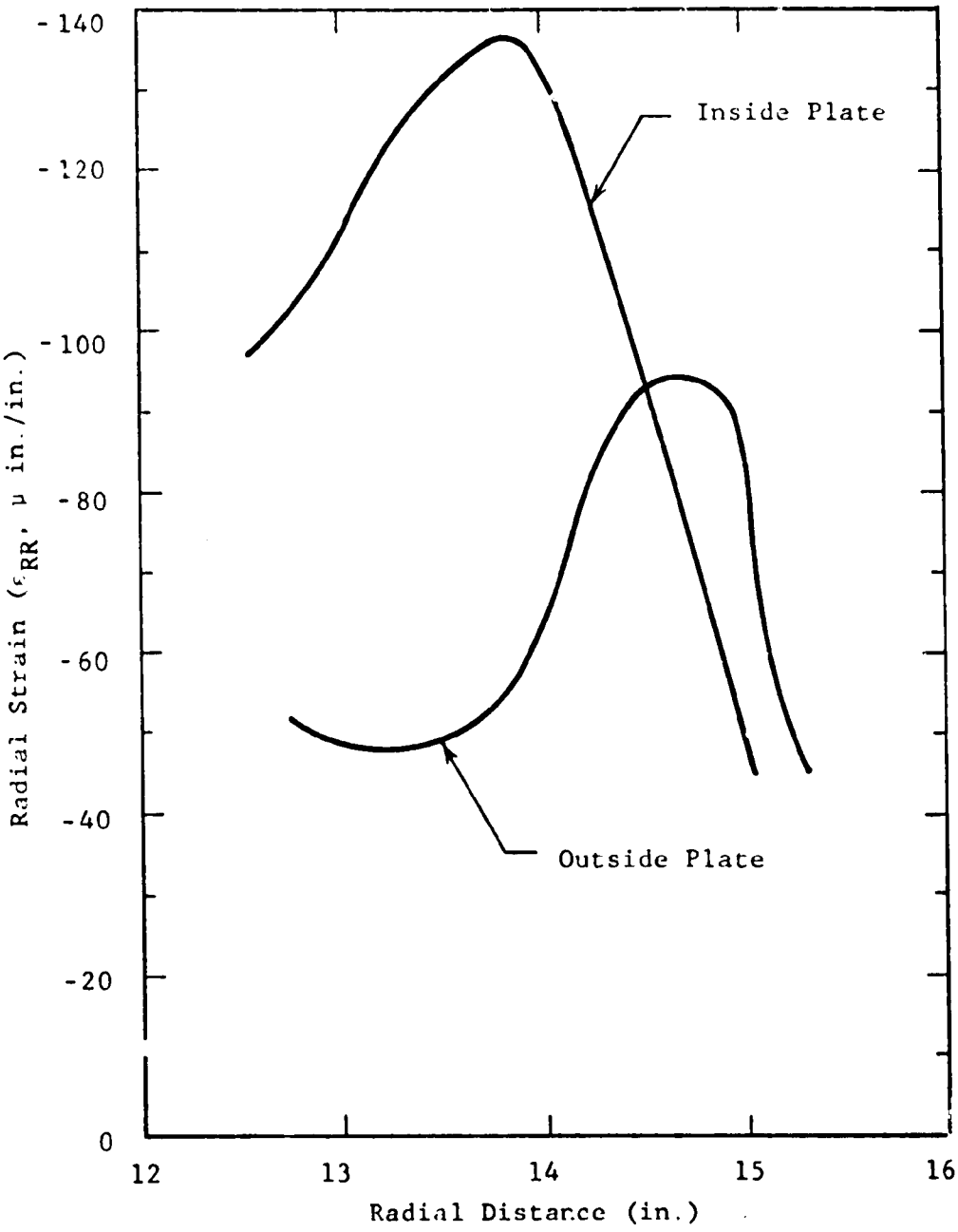

FIGURE 5-16. RADIAL STRAIN ON WHEEL PLATE RESULTING FROM 32,000 LB VERTICAL LOAD AS A FUNCTION OF RADIAL POSITION, ZERO DEGREE WHEEL ORIENTATION WITH RESPECT TO LOAD

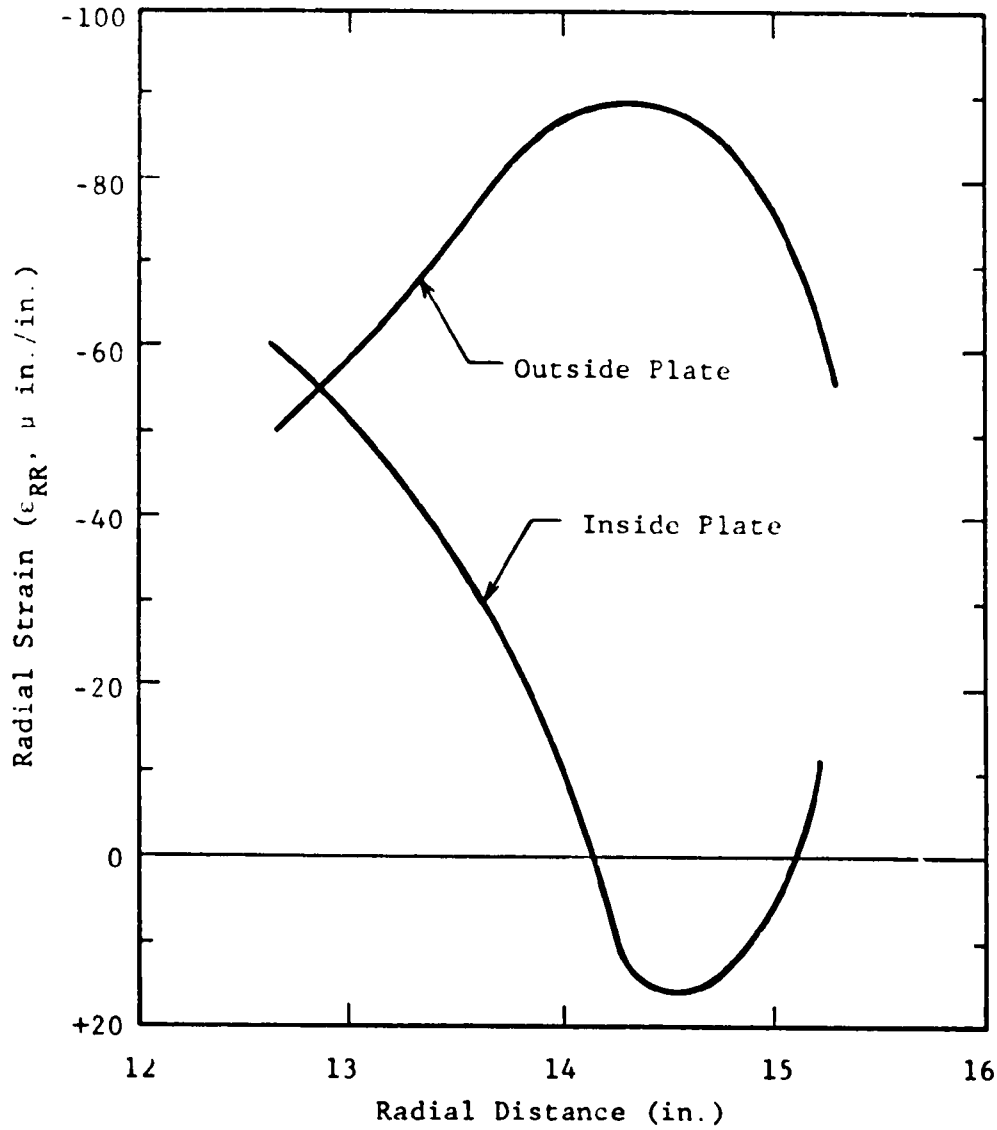

FIGURE 5-17. RADIAL STRAIN ON WHEEL PLATE RESULTING FROM 10,000 LB LATERAL LOAD ACTING TOWARD FLANGE AS A FUNCTION OF RADIAL POSITION, ZERO DEGREE WHEEL ORIENTATION WITH RESPECT TO LOAD

6 μ in./in. per 1,000 lbs vertical load and 8.7 μ in./in. per 1,000 lbs lateral load. For the measurement of various phenomena, one measurement technique will be preferred over the other. For many transient vertical load phenomena, such as the load associated with the passage of the wheel over a rail joint, the vertical load is anticipated to be much higher than the lateral load and the use of gages which are insensitive to the lateral position of the vertical load might be preferable. It also may be feasible to correct for the lateral load effect on the vertical bridges using lateral load data obtained with the low frequency system.

Another factor which must be considered in the placement of the gages is the drop in sensitivity as the gage position rotates away from a vertical orientation. Figure 5-18 shows a plot of the radial strains at the 14.1 in. radial position as a function of the angular position from the vertical. This plot reveals that if a "window" of ± 15 deg is used there is a dropoff in the output of the gage at the 15 deg position of 53 percent. Doubling the number of gages to give a ± 7.5 deg window reduces the dropoff in output to 23 percent.

The results from this analysis indicate that the use of 24 radially oriented strain gages spaced at 15 deg is an acceptable gage array for sensing vertical loads. The change in sensitivity of the signal is not large as a gage passes through its "window" and the change that does occur can be compensated for when processing the signal. The output of the gages is negligible when they are in the top position of the wheel, 180 deg away from the wheel-rail contact. Therefore, it is feasible to incorporate two of these gages, located at diametrically opposite positions, into a single bridge. This will allow a reduction in the number of circuits which have to be brought through the slip rings.

5.2.3 Instrumentation and Data Recording Procedures

5.2.3.1 Strain Measurements

Strain measurements will be taken using conventional compensated foil strain gages since temperatures will be at or near ambient. Slip

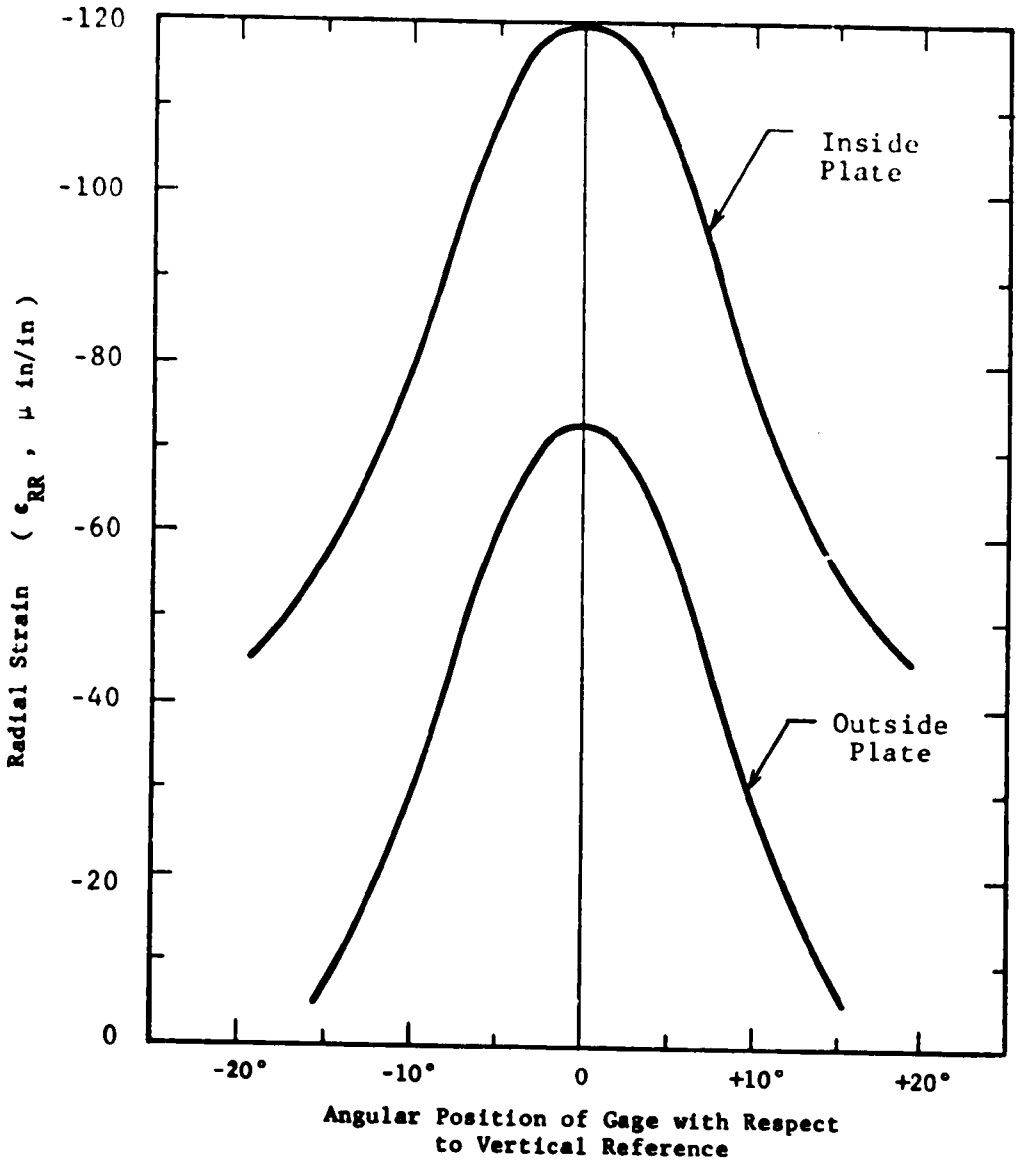

FIGURE 5-18. RADIAL STRAIN AT 14.2 IN. RADIAL DISTANCE RESULTING FROM 32,000 LB VERTICAL LOAD AS A FUNCTION OF ANGULAR POSITION OF THE WHEEL WITH RESPECT TO A VERTICAL REFERENCE

rings will be used to transmit the data signals from the rotating parts. The wheel sets which are available have two 20-circuit slip ring assemblies on each axle. The axles of the wheel sets contain central axial holes and radial ports both inside and outside of each wheel so that power and signal leads can be routed from the sensors to the slip rings. The slip rings are fitted with an electrical connector so that they can be disconnected for shipping and maintenance.

Rotating strain gage circuits will be arranged in groups with a common reference half bridge for 6 or 12 measurements. Each group of strain gages will share a common bridge voltage supply furnished through a separate pair of slip rings. Where single strain gages are used, precision resistors will be mounted on the rotating parts to form half bridges. The strain and reference signal circuits will be brought out individually through the slip rings. A typical arrangement is shown in the schematic diagram of Figure 5-19

Circuit wiring on the rotating parts will be protected from accidental damage and the environment. Sensors will be provided with strain loops and gages will be armored if required. All sensors and cables will be sealed with a protective coating and further protected with a tough outer coating such as RTV.

5.2.3.2 Wheel Position Indicator

The wheel position signal will be obtained from a reed switch mounted on the side frame adjacent to the axle bearing plate. Small bar magnets will be cemented to the bearing plate to actuate the switch and generate a pulse positional reference signal. The angular positions of switch closure will be aligned with selected reference lines. Synchronization of wheel position for switching of wheel devices are available commercially and can also be installed on the axle bearing plate.

5.2.3.3 Recording

There are two options for the format in which to record the data: digital or analog. Digital recording has the advantage that a larger number

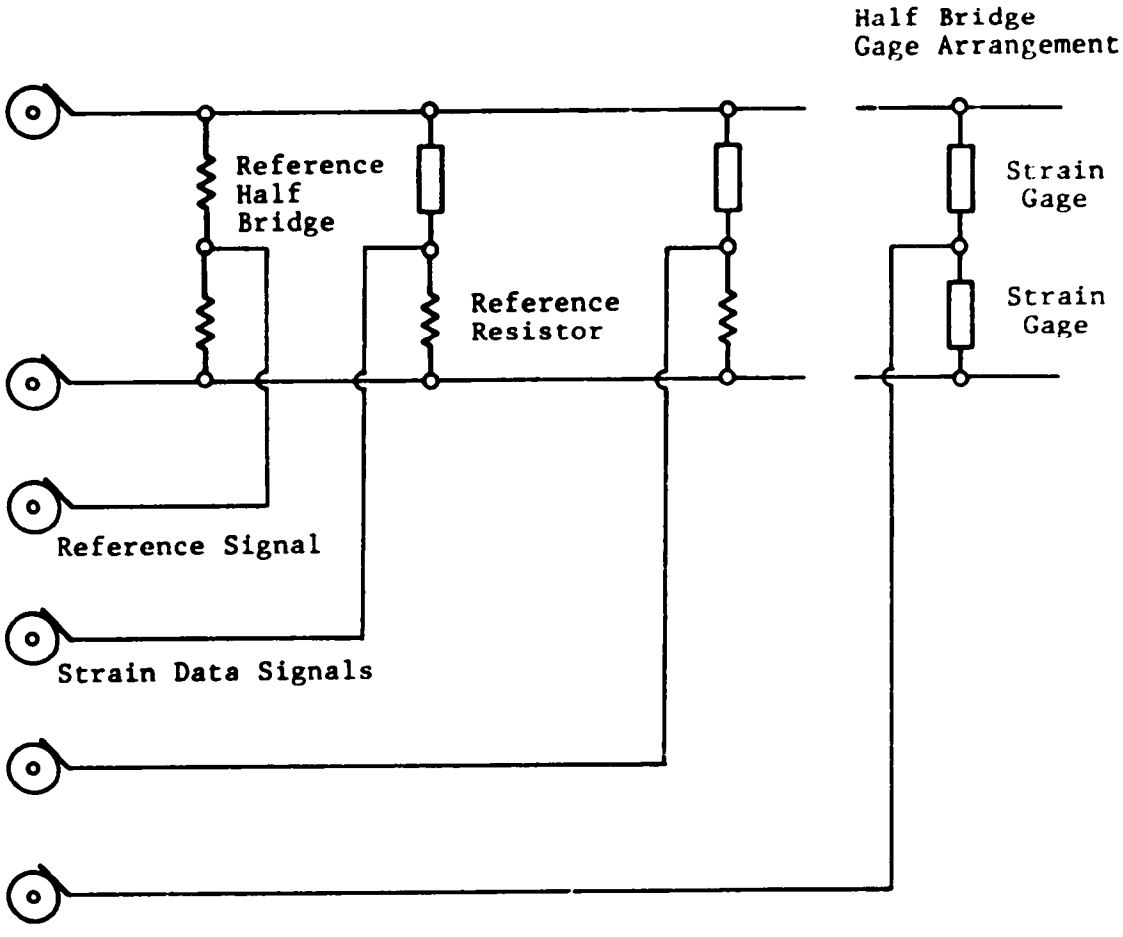

FIGURE 5-19. TYPICAL STRAIN GAGE CIRCUITS USING SLIP RINGS TO TRANSMIT DATA SIGNALS FROM THE ROTATING WHEEL-AXLE

of data channels may be recorded simultaneously on a single data tape. The disadvantage is that the sampling frequency has to be selected before the data is recorded, thus losing flexibility in the processing of the data. FM analog recording has the advantage of permitting a greater number of alternatives when processing the data, but one is generally limited to 14 data channels per tape, as discussed in Section 5.1. A way around this limitation is to multiplex some of the data signals so that several data signals can be recorded per channel.

Tentatively we would plan to utilize three magnetic tape recorders in the FM mode. Two recorders will use the IRIG intermediate band FM system with a tape speed of 1-7/8 ips and a bandwidth of 625 Hz. These recorders will be used to record the low frequency system. Each recorder will take the data channels from one axle along with vertical load and miscellaneous reference signals. The other recorder will be operated at a 7-1/2 ips tape speed and a bandwidth of 2500 Hz for the detailed wheel data associated with the high frequency reference data. Each recorder will have one track dedicated to an IRIG B time code as a precise reference for data processing. Voice commentary will be recorded on an edge track.

Signal conditioning equipment and amplifiers will be furnished for strain and other data channels to provide suitable signal levels for tape recording. Shunt strain gage calibration circuits will be used to record calibration reference signals on the tape, as required, before and during the tests.

A direct-write oscillograph will be included to monitor selected data channels during the conduct of the test. Playback signals will be obtained directly from the reproduce amplifiers of the tape recorder while data is being recorded. All channels will be observed periodically during the tests to insure the data is being properly recorded on the tape.

5.2.3.4 Data Processing

It is recommended that all data processing be performed following the test runs. The analog data would first be filtered and sampled at frequencies consistant with the phenomena being measured. For example, the low frequency system data could be filtered at 20 Hz and sampled at 100 samples per second. Similar sampling rates at 5 times the cut-off frequency would be required for high frequency data. The weighting of strain gage data from the rotating components, such as the axle bending moment data from the low frequency system and the radial strain data from the wheel on the high frequency system, would be accomplished during the processing of the digital data by utilizing suitable algorithms. Also, the utilization of these data channels only within certain angles of rotation would be taken into account in the processing of the digital data.

5.2.4 Vehicle-Borne Test Duration

The length of a vehicle-borne test or "run" under a particular set of conditions (speed, etc.) is dependent on several conflicting requirements. These include, for example, finding a length of track with reasonably uniform characteristics of geometry, modulus and construction over its entire length. This "test track" must be of sufficient length to provide for averaging a statistically significant number of cycles of the lowest frequency of interest for developing power spectral density curves with good resolution. On the other hand, the test section length must also address the logistics of testing in terms of the number of runs at different speeds that can be made within a normal crew shift, without disrupting revenue traffic.

Since integration time is inversely proportional to frequency bandwidth (see Figures 3-39 and 3-40, for example), and the low-frequency range is of particular interest in the validation of the analytical model, integration times up to 5 minutes may be required. For this reason, test track lengths of 3 to 5 miles (or longer) will be needed, and constant-speed runs with the test vehicle at 5 to 10 mph intervals over these test sections will be planned.

6. EXAMPLES OF PREDICTIVE TECHNIQUES

Two examples of existing, well-documented predictive models are examined in this section to provide sample cases of W/R load prediction. These are, first, a simulation of a 100-ton hopper car using a slightly-revised version of the TRKVPSD program described in Section 4.2.1. Second, the effects of track geometry and speed are examined by means of the British Rail analytical equations for W/R impact loads, using typical North American track and vehicle parameters.

6.1 FREQUENCY-DOMAIN MODEL OF 100-TON HOPPER CAR

A detailed description of the frequency-domain model of the rail vehicle used in a recent DOT/FRA vehicle dynamics study is given in [6-1]. For the frequency-domain solution with PSD or spectral component inputs, separate bounce/pitch and roll/lateral/yaw models are combined in the same program. These are illustrated in Figures 6-1 and 6-2, respectively. Equations of motion are transformed to the frequency domain, and the stiffness,mass and damping elements are assembled in a complex matrix. Solution consists of matrix inversion for a given frequency, then multiplication by the input column matrix for a given track input and speed.

Two minor changes were incorporated in the computer model. The first change was to move the spatial "transfer function" accounting for pitch or bounce of the truck upward in the model to modify the side frame motion. Although truck pitch was not included as a separate degree of freedom, the geometric effect of pitch on the W/R forces is included through the bounce and pitch stiffnesses of the spring group. The moment of inertia of the side frame in pitch is not included.

The second change results in the track geometry error being applied between the wheel and the rail (track) masses instead of below the track mass. The equations for this revision are as follows.

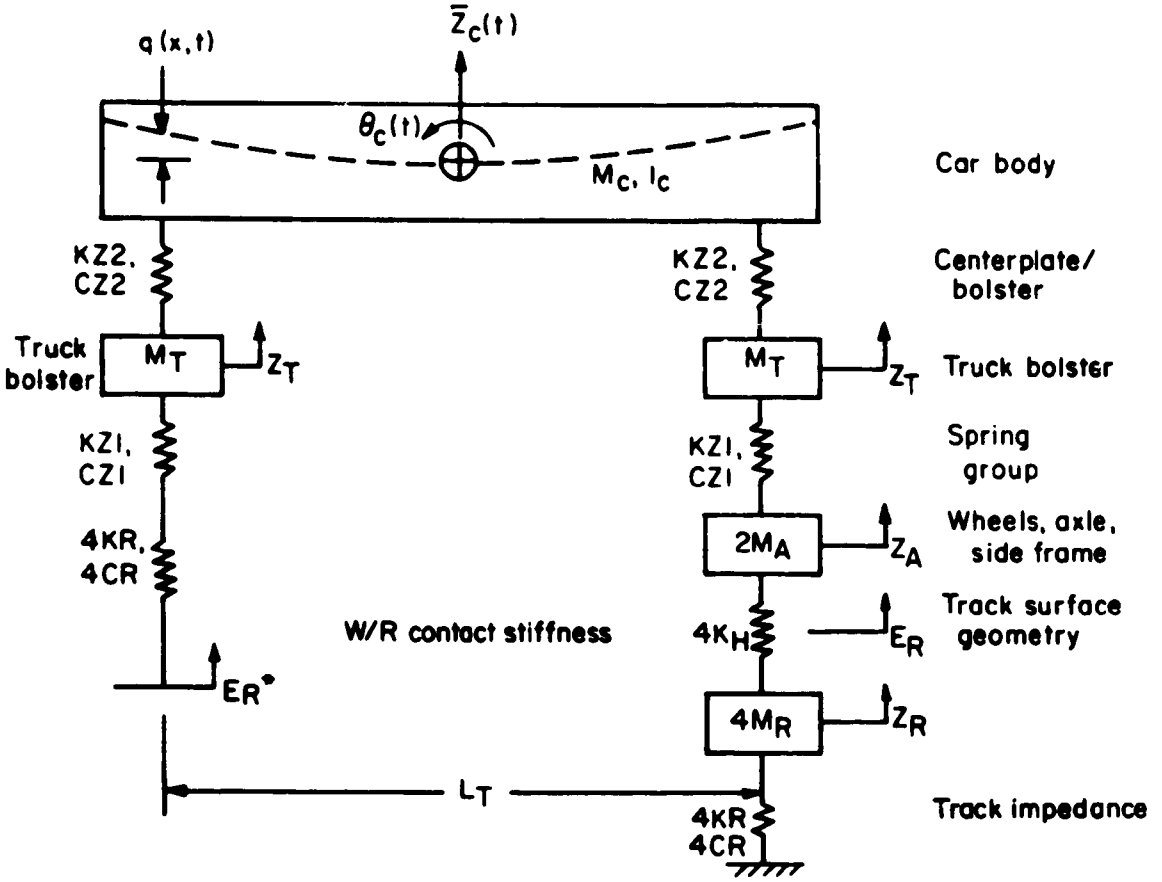

FIGURE 6-1. VERTICAL (PITCH/BOUNCE) MODEL OF FREIGHT CAR AND TRACK STRUCTURE

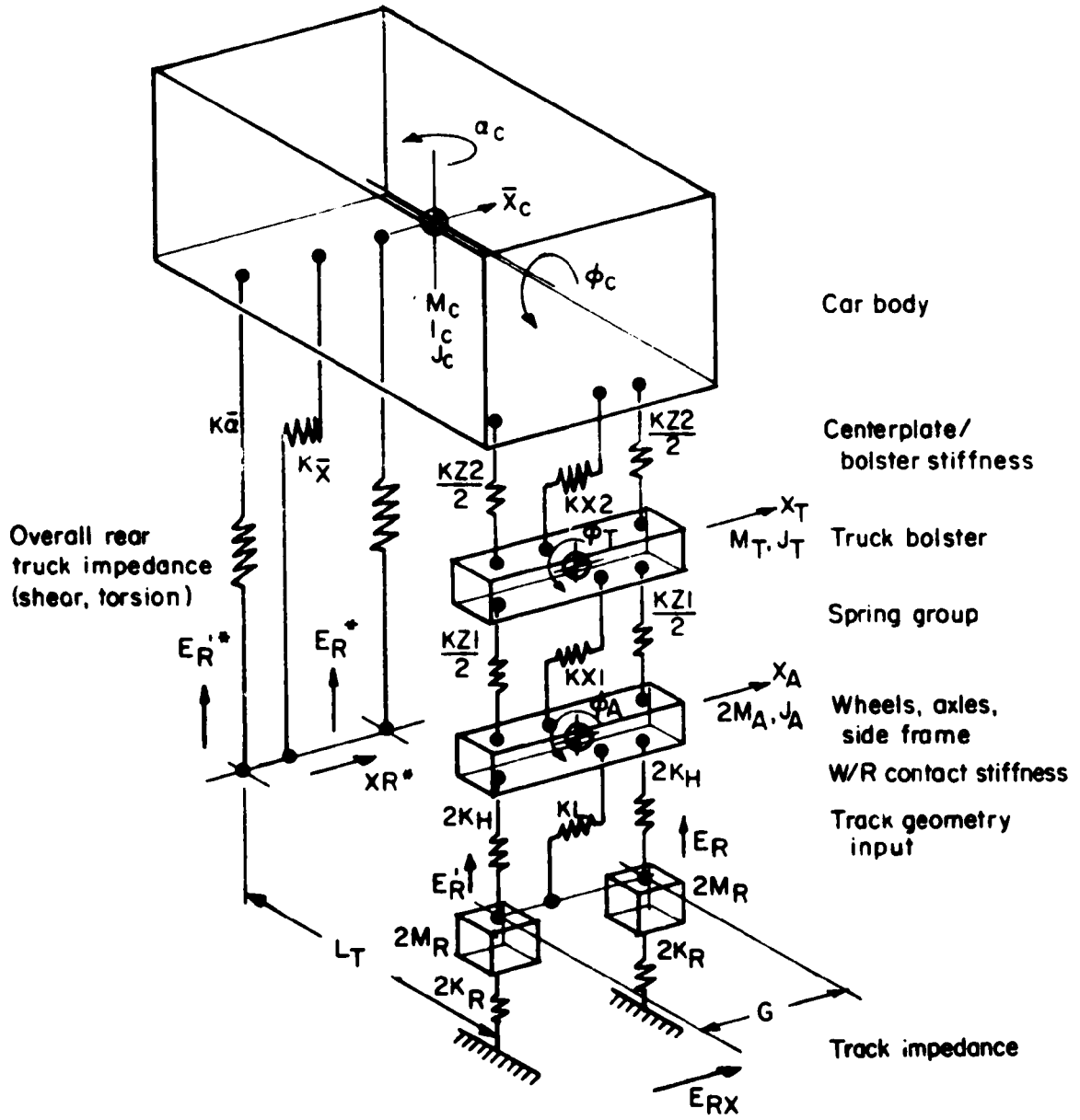

FIGURE 6-2. ROLL/LATERAL/YAW MODEL OF FREIGHT CAR AND TRACK STRUCTURE

$$M_a \ddot{Z}_a + 2F_{BA} - 2F_W = 0 \qquad (6\text{-}1)$$

$$2M_R \ddot{Z}_R + 2K_R Z_R + 2F_W = 0 \qquad (6\text{-}2)$$

$$Z_a = E_Z + Z_R \text{ , for the very stiff W/R contact} \qquad (6\text{-}3)$$

where...

M_a = wheelset (axle) mass

M_R = track effective mass per wheel

K_R = track effective stiffness (complex)

F_{BA} = bearing adapter force

F_W = W/R force

Z_a = wheelset (axle) vertical displacement

Z_R = track mass displacement

E_Z = track geometry error

By combining equations 6-1 through 6-3, the resulting equation for wheelset vertical acceleration becomes:

$$(M_a + 2M_R)\ddot{Z}_a + 2K_R Z_a + 2F_{BA} = 2M_R \ddot{E}_Z + 2K_R E_Z \qquad (6\text{-}4)$$

A complete list of vehicle and track parameters used by the model is given in Table 6-1. Parameters for the 100-ton hopper car were taken from a number of sources, including the AAR/TTD characterization of 70-ton truck parameters [6-2] scaled up by weight or geometry to approximate the slightly heavier truck.

Power spectral density curves of vertical wheel/rail force are shown in Figure 6-3 for the 100-ton hopper car operating at 40 miles per hour on good CWR track. These data were obtained by combining the power contributions from surface, alignment and cross level inputs. In the present version of the TRKVPSD program, either lateral flanging or nonflanging conditions (based on lateral creep forces and gravitational stiffness) may be assumed, and the effects of both are shown. Strong spectral peaks in W/R force are seen at 0.7 Hz due to car body roll, near 1.5 Hz due to bounce, and near 2.5 Hz due to pitch. Under a 32,000-lb wheel static load, lateral rail stiffness per axle is about 400,000 lb/in., which results in a strong 17-Hz lateral resonance. This is coupled through the wheelset into a vertical force peak in the flanging condition. For the nonflanging case, a resonant peak near 24 Hz is noted. Force levels are probably unrealistically high, even though half-Kalker creep values have been employed, because the actual creep forces have a nonlinear, adhesion-limited nature.

Another strong spectral peak occurs at 34 Hz, with the primary contribution being response to cross level excitation. This is the apparent resonance of the track with the vehicle unsprung mass. The contribution from surface excitation was surprisingly small.

Track geometry spectra were approximated by the relationship:

$$P_i(\lambda) = A^N \quad \text{in}^2/\text{cycle/ft} \tag{6-5}$$

where, for a two-slope approximation of good CWR track,

	surface	alignment	cross level
A =	.990E-5	.750E-4	.490E-4
N =	2.35	1.72	1.85
λ_c =	29.0	25.0	23.0
A' =	.186E-6	.116E-4	.363E-5
N' =	3.53	2.30	2.68

The primed values are used for wavelengths less that λ_c.

TABLE 6-1. VEHICLE AND TRACK PARAMETERS FOR SAMPLE CALCULATIONS

	Symbol		Parameter Description	Value	Units
	W_c	WCAR	Car body weight	242,700	lb
	W_t	WTRF	Truck frame (bolster) weight	1,602	"
	W_{sf}	WSF	Side frame weight (one each)	1,362	"
	W_a	WAXL	Wheelset/axle weight (one each)	2,913	"
	$J_{\theta c}$	PJC	Car body pitch inertia	.1810E+08	lb-in-sec^2
	$J_{\theta t}$	PJT	Truck frame pitch inertia	.1170E+03	"
	$J_{\theta sf}$	PJSF	Side frame pitch inertia	.1288E+04	"
	$J_{\phi c}$	RJC	Car body roll inertia	.1640E+07	"
	$J_{\phi t}$	RJT	Truck frame roll inertia	.3077E+04	"
	$J_{\phi a}$	RJA	Wheelset (axle) roll inertia	.6763E+04	"
	$J_{\psi c}$	YJC	Car body yaw inertia	.1810E+08	"
*	$J_{\psi t}$	YJT	Truck frame yaw inertia	.3077E+04	"
*	$J_{\psi a}$	YJA	Wheelset (axle) yaw inertia	.6763E+04	"
	K_{z1}	KZ1	Spring Group (Primary suspension) vertical stiffness (per truck)	49,600	lb/in
	K_{z2}	KZ2	Bolster/centerplate (Secondary suspension) vertical stiffness (per truck)	.2100E+07	"
	K_{x1}	KX1	Spring group (Primary suspension) lateral stiffness (per truck)	38,900	"
	K_{x2}	KX2	Bolster/centerplate (Secondary suspension) lateral stiffness (per truck)	.1000E+07	"
	$K_{\phi 1}$	KPHI1	Spring group (Primary suspension) roll stiffness (per truck)	.7739E+08	lb-in/rad
	$K_{\phi 2}$	KPHI2	Bolster/centerplate (Secondary suspension) roll stiffness (per truck)	.3300E+09	"
*	$K_{\phi c}$	KPHIC	Car body torsional stiffness	.9600E+09	"
	$K_{\theta 1}$	KTHE1	Spring group (Primary suspension) pitch stiffness (per truck)	.3017E+07	"
*	$K_{\theta 2}$	KTHE2	Bolster/centerplate (Secondary suspension) pitch stiffness (per truck)	.1100E+08	"

TABLE 6-1. (Continued)

	Symbol		Parameter Description	Value	Units
*	$K_{\psi ba}$	KSIBA	Bearing adapter yaw stiffness (per bearing)	.9100E+07	lb-in/rad
*	$K_{\psi sf}$	KSISF	Side frame yaw stiffness (per side frame)	.5672E+06	"
	$K_{\psi 1}$	KSI1	Spring group (Primary suspension) yaw stiffness (per truck)	.6069E+08	"
*	$K_{\psi 2}$	KSI2	Bolster/centerplate (Secondary suspension) yaw stiffness (per truck)	.00	"
	ω_b	WB	First vertical bending mode natural frequency	200	rad/sec
	ζ_b	ZETAB	Vertical bending mode damping ratio	0.25	"
	ω_{bx}	WBX	First lateral bending mode natural frequency	100	"
	ζ_{bx}	ZETABX	Lateral bending mode damping ratio	0.25	"
	C_{z1}	CZ1	Spring group (Primary suspension) vertical damping (per truck)	1,824	lb-sec/in
	C_{z2}	CZ2	Secondary suspension vertical damping (per truck)	100	"
	C_{x1}	CX1	Spring group (Primary suspension) lateral damping (per truck)	1,350	"
	C_{x2}	CX2	Secondary suspension lateral damping (per truck)	2,213	"
	$C_{\phi 1}$	CPHI1	Spring group (Primary suspension) roll damping (per truck)	.2846E+07	lb-in-sec/rad
	$C_{\phi 2}$	CPHI2	Secondary suspension roll damping (per truck)	.1000E+06	"
*	$C_{\phi c}$	CPHIC	Car body torsional damping	.1000E+07	"
	$C_{\theta 1}$	CTHE1	Spring group (Primary suspension) pitch damping (per truck)	.8940E+05	"
	$C_{\theta 2}$	CTHE2	Secondary suspension pitch damping (per truck	.1000E+07	"

TABLE 6-1. (Continued)

Symbol		Parameter Description	Value	Units
* $C_{\psi ba}$	CSIBA	Bearing adapter yaw damping (per bearing)	.1645E+04	"
* $C_{\psi sf}$	CSISF	Side frame yaw damping (per side frame)	.6620#+05	"
$C_{\psi 1}$	CSI1	Spring group (Primary suspension) yaw damping (per truck)	.2106E+07	"
* $C_{\psi 2}$	CSI2	Secondary suspension yaw damping	.1010E+05	"
		Vertical heights from rail:		
H_1	H1	Axle c.g.	18.0	inch
H_2	H2	Spring group (Primary suspension)	17.0	"
H_3	H3	Truck frame c.g.	23.0	"
H_4	H4	Center Plate/bolster (Secondary suspension)	25.7	"
H_5	H5	Car body c.g.	88.7	"
g	G	Effective gage	59.5	"
L_a	ELA	Axle spacing	72.0	"
L_T	ELT	Truck spacing	468	"
L_o	ELO	Body overall length	600	"
L_{cg}	ELCG	Longitudinal distance, front truck center to car body c.g.	234	"
L_{ba}	ELBA	Lateral distance to bearing adapter	79.0	"
K_{zr}	KZR	Track vertical stiffness (point load per rail)	.5000E+06	lb/in.
K_{xr}	KXR	Track lateral stiffness (point load, flanging condition)	.4000E+06	"
U	UTRK	Track modulus per rail	.7064E+04	lb/in./in.
C_{zr}	CZR	Track vertical damping (point load)	.1193E+04	lb-sec/in.
C_{xr}	CXR	Track lateral damping (point load)	.2500E+03	"

TABLE 6-1. (Continued)

Symbol		Parameter Description	Value	Units
M_{tr}	MTR	Track effective mass (point load vertical)	.7915E+01	lb-sec^2/in.
M_{trx}	MTRX	Track effective mass (point load lateral)	.00	"
* F_{11}	FCR11	Lateral W/R creep coefficient	.2700E+07	lb
* F_{22}	FCR22	Longitudinal creep coefficient	.2700E+07	"
* ζ	ZET	Rate of change of distance between wheelset centerline and contact points with lateral wheelset displacement	1.0	"
* δ_o	DELTO	Angle between contact plane and horizontal	0.05	radian
* ϵ	EPS	Rate of change of contact plane slope with lateral wheelset displacement	0.05	"
* λ	ELMC	Effective conicity	0.05	"
* R_o	ROWHL	Wheel tread circle radius	18.0	"

* Starred parameters not used in program version for sample case.

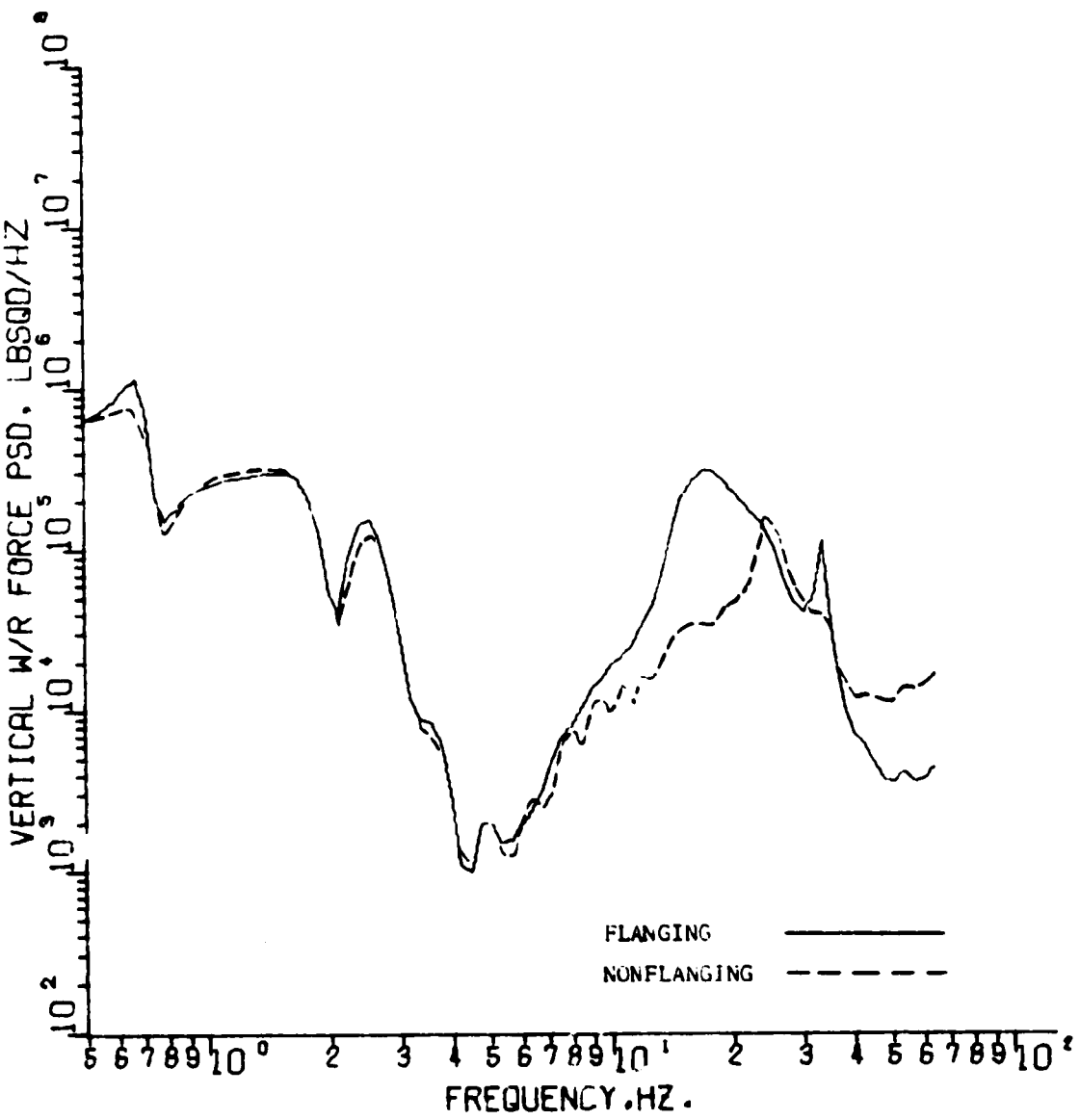

FIGURE 6-3. COMPUTED VERTICAL WHEEL/RAIL FORCE POWER SPECTRAL DENSITY, LOADED 100-TON HOPPER CAR AT 40 MPH, GOOD CWR TRACK (TRKVPSD MOD. 1)

Although the frequency resolution (due to the linear scale) is not good, the spectrum shown in Figure 3 38 shows good correlation in magnitude of the low-frequency peak with the computed value of Figure 6-3. There is a rapid roll-off of the spectrum in Figure 3-38, with little evidence (at least from measurements at the SF/BA load cell) of the higher-frequency track resonance components computed by the model.

Spectral peaks in vertical W/R force due to the freight car rigid body modes of oscillation are shown in Figure 6-4 versus the wavelength of track geometry excitation at which the peak occurs. The numbers on the curves refer to 10-mph increments of speed. It is interesting to note that the 100-ton hopper car roll response, even on CWR track, produces by far the highest W/R vertical force spectral peaks, with the closely-associated lateral response similar in shape, although much lower in amplitude. The bounce spectral peak approaches a maximum near 60 miles per hour, where the geometry wavelength at the resonant frequency (near 1.5 Hz) coincides with the truck spacing. Above this speed, the spectral peak becomes predominantly a body pitch mode excited by wavelengths approaching 1-1/2 times the truck spacing. From the plots in Figure 6-4, one would expect track differential settlement (a degradation in cross level) from consistent operation of the 100-ton hopper car at 20 mph on CWR track. Consistent operation at higher speeds would be expected to cause long wavelength (over 100 ft) differential settlements, again due to roll response.

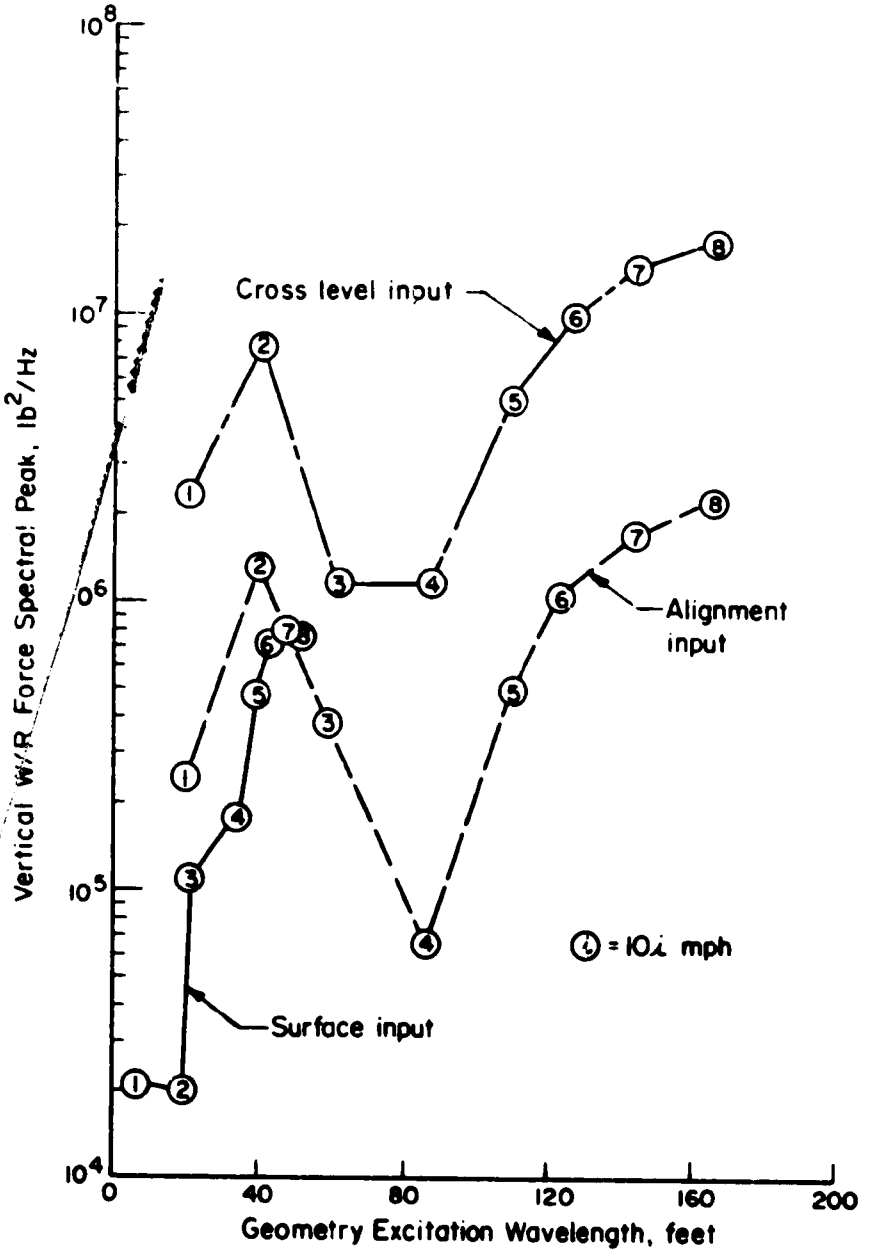

FIGURE 6-4. LOW-FREQUENCY SPECTRAL PEAK VERSUS WAVELENGTH OF TRACK GEOMETRY INPUT AND TRAIN SPEED - 100-TON HOPPER CAR (TRKVPSD MOD. I)

Root-mean-square values of vertical force are shown in Figure 6-5 as a function of train speed. Values are given for the overall (mean square summation) and for the individual track geometry inputs. Note again that the contribution to vertical force from lateral excitation is perhaps unrealistically high due to the assumed flanging condition. Contributions due to car rocking can also be noted at the lower speed range. Vertical loads due to the presence of staggered rail joints are shown in the figure by the dashed line. These are the low-frequency components (rather than joint impact forces) developed primarily by car rocking using the first three Fourier spectral lines in surface and cross level from a rectified sine wave, and an assumed worst-case rms joint depth of 0.21 inch. In the actual case, the nonlinear response of the vehicle produces relatively low-amplitude response up to a joint error of about 5/8 inch, at which point the side bearings contact and a typical nonlinear "jump" resonance results. This cannot be simulated accurately in a linear model, however.

6.2 ANALYTICAL MODEL OF JOINT IMPACT

Analytical equations for estimating the W/R impact forces at dipped joints have been reported by Jenkins [6-3], based on work conducted by British Rail. The equations for the two major force peaks are as follows:

$$P_1 = P_o + 2\alpha V\sqrt{\frac{K_H M_e}{1+M_E/M_U}} \qquad (6\text{-}6)$$

$$P_2 = P_o + 2\alpha V\sqrt{\frac{M_U}{M_U + M_R}}\sqrt{K_R M_U}\left[1 - \xi^2\pi\frac{M_R}{M_U + M_R}\right] \qquad (6\text{-}7)$$

where...

P_1 = high-frequency joint impact force peak

P_2 = lower-frequency geometry-induced force peak

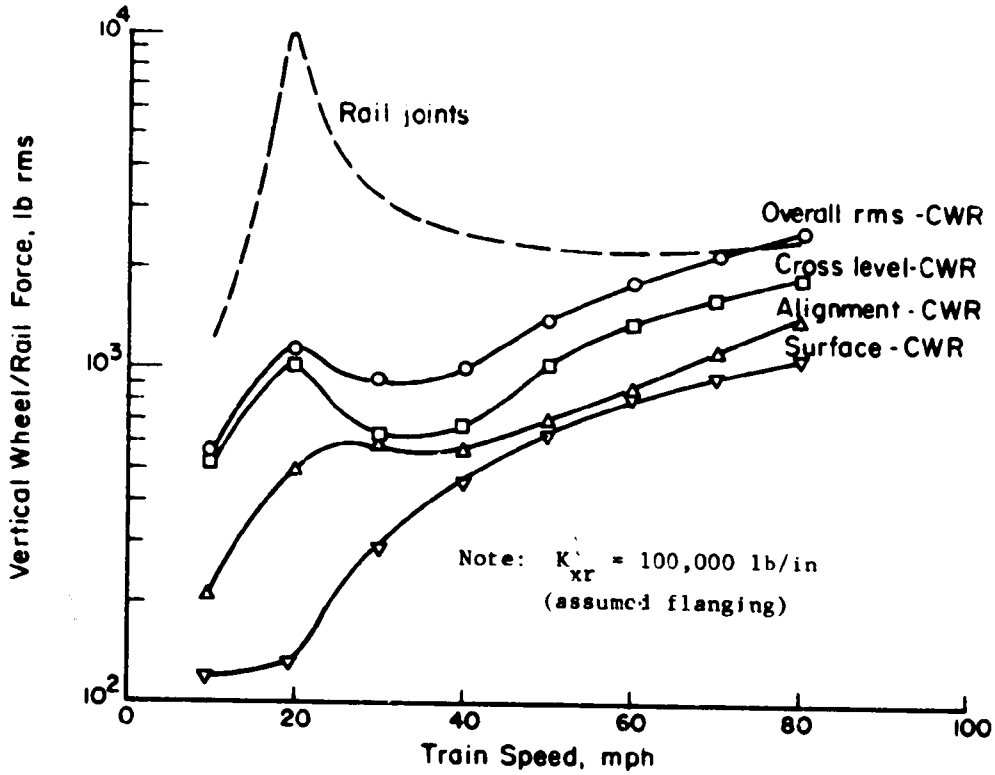

FIGURE 6-5. COMPUTED VERTICAL WHEEL/RAIL RMS FORCES VERSUS TRAIN SPEED, 100-TON HOPPER CAR ON GOOD QUALITY TRACK (TRKVPSD MOD. I)

P_o = vertical static wheel load

α = $2\pi e/d$

e = dipped joint depth

d = dip length (assumed d = 8/)

V = vehicle forward speed

K_H = Hertzian W/R contact stiffness

K_R = track overall stiffness

M_e = rail effective mass

M_R = track effective mass

M_U = vehicle unsprung mass

ζ = track effective damping ratio (assume $0.5(2\sqrt{K_R M_R})$)

Since the Hertzian W/R contact stiffness is a nonlinear function which varies as wheel load, P, to the one-third power, Equations (6-6) and (6-7) require an iterative solution. Fortunately, convergence is rapid, and even hand calculations are rapid. For the Hertzian contact stiffness, the following relationships was used (for a new wheel profile):

$$K_H = 3(10)^5 \, p^{1/3} \text{ lb/in.} \qquad (6\text{-}8)$$

A review of some recent track force/deflection data indicates that the overall stiffness varies approximately by one-half power. The following relationship was, therefore, used:

$$K_{Ro} = 2\sqrt[4]{4EIU_o^3} \text{ lb/in. at } P_o = 20{,}000 \text{ lb} \qquad (6\text{-}9)$$

$$K_R = K_{Ro}(P/20{,}000)^{1/2} \text{ lb/in. at the new value of } P \qquad (6\ 10)$$

where...

EI = track flexural rigidity, lb-in^2

U_o = nominal track modulus, lb/in/in per rail

This assumes the nominal track modulus, U_o, corresponds to a reference wheel load of 20,000 lb. Representative values track parameters were then chosen for the six track classes described in the Track Safety Standards[6-4], and representative track moduli were selected based on the work by Ahlf [6-5], see Table 6-2. Stiffness and mass values for the track were calculated for the representative rail and tie weights, and an effective ballast mass was calculated based on tamped area, ballast/subgrade stiffness, and the seismic shear wave velocity. (Recent field experiments indicate that the actual effective mass may be twice this calculated value.) The rail effective mass was calculated in two ways: first, by the method cited in Jenkins [6-3], and the second, based on the rail beam resting on an elastic foundation. Values by either method of calculation correspond reasonably well.

The dipped joint is described geometrically in Table 6-3 from the track parameters and the Safety Standards, accounting for the allowable low joint (under a 62-foot chord, assumed unloaded) and the deflection under

TABLE 6-2. REPRESENTATIVE TRACK PARAMETERS FOR JOINT IMPACT MODEL

Track Class	Assumed Rail Size lb/yd	EI $\frac{\text{lb-in.}^2}{}$	Nominal Modulus, U lb/in/in (per rail)	Track Stiffness, K_{R_o} lb/in (per rail	Track Stiffness,* K_R lb/in (per rail)	β** in^{-1}
1	90	$11.0(10)^8$	1000	92,000	120,000	.022
2	90	$11.0(10)^8$	2000	150,000	193,000	.026
3	90	$11.0(10)^8$	3000	210,000	270,000	.029
4	132	$25.6(10)^8$	4000	320,000	410,000	.025
5	132	$25.6(10)^8$	5000	389,000	500,000	.026
6	140	$27.7(10)^8$	5000	390,000	501,000	.026

* Under 33,000 lb. wheel static load
** $\beta = 2U/K_{Ro}$

Track Class	ρ_r $\frac{\text{lb-sec}^2}{\text{in-in}}$	Tie Size in.	W_{tie} lb.	ℓ_{tie} in.	ρ_{tie} $\frac{\text{lb-sec}^2}{\text{in-in}}$	ρ_b $\frac{\text{lb-sec}^2}{\text{in-in}}$
1	.0065	6x8x102	125	24	.0067	.014
2	.0065	6x8x102	150	24	.0081	.020
3	.0065	6x8x10	175	24	.0094	.025
4	.0095	7x9x108	200	22	.0118	.030
5	.0095	7x9x108	250	21	.0154	.035
6	.0101	7x9x108	250	21	.0154	.040

Track Class	ρ_t lb-sec^2	M_t lb-sec^2	W_t lb	k_{tie} lb/in.	$M_e^{(a)}$ $\text{lb-sec}^2/\text{in.}$	W_e lb	$M_e'^{(b)}$ $\text{lb-sec}^2/\text{in.}$	W_e' lb
1	.027	1.8	710	$0.5(10)^6$	.18	71	.21	81
2	.035	2.0	780	$0.7(10)^6$	.20	79	.19	74
3	.041	2.1	820	$0.8(10)^6$	.22	86	.19	72
4	.051	3.1	1200	$1.0(10)^6$	.38	150	.31	120
5	.060	3.5	1300	$1.2(10)^6$	.45	170	.29	110
6	.066	3.8	1500	$1.2(10)^6$	.46	180	.32	120

TABLE 6-2. (Cont'd)

ρ_r = rail mass per unit length

W_{tie} = tie weight

ℓ_{tie} = tie spacing

ρ_{tie} = tie mass per unit length

ρ_b = ballast effective mass per unit length

= $0.28 k_b A_t / \pi V_{seis}^2$ (see Leonards, G.A., Foundation Engineering, McGraw-Hill, 1962)

k_b = ballast/subgrade stiffness under half-tie, lb/in/in

A_t = tamped area, half-tie, in^2

V_{seis} = seismic shear wave velocity Assume k_b varies from 50,000 to 200,000, A_t varies from 460 (sunk in fines) to 270 in^2. V_{seis} = 12,000 in/sec.

$\rho_t = \rho_r + \rho_{tie} + \rho_b$, track mass per unit length

$M_t = 3\rho_t / 2\beta$, track effective mass

(a) Method 1 (see Ref. 6-3)

$$M_e = 1.83(4EI/K_H)^{1/3}(\rho_r + \rho_{tie})$$

$= 18(\rho_r + \rho_{tie})$ on heavier track

$14(\rho_r + \rho_{tie})$ on lighter track,

using $K_H = 10^7$ lb/in.

(b) Method 2: Using $U_{tie} = k_{tie}/\ell_{tie}$

$$M_e' = 3\rho_r / 2\beta_r = (3\rho_r/2)(4EI\ell_{tie}/k_{tie})^{1/4}.$$

the nominal wheel load. The speed/geometry factor, aV, is then shown for the maximum speed allowed for passenger and freight trains under the Standards. Representative values of wheel load and unsprung mass were chosen for three North American rail vehicles [6-1]:

Vehicle	P_o, Static Wheel Load	M_U, Unsprung Mass Per Wheel
100-ton Freight Car	32,000 lb	4.2 lb-sec^2/in.
MU Passenger Car	21,000 lb	6.8 lb-sec^2/in.
Diesel Freight Locomotive	33,000 lb	11.4 lb-sec^2/in.

Using these values in Equations (6-6) and (6-7), the P_1 and P_2 impact forces at a dipped joint were calculated versus the speed/geometry factor (V). Plots of the two force peaks are shown in Figure 6-6 for track parameter values representative of Class 5 or Class 6 track. It can be seen that the P_1 forces are little affected by vehicle unsprung mass, while the P_2 force under the high unsprung mass of the locomotive axle can approach the higher-frequency P_1 force in magnitude.

As a check on this method of approximating the P_1 and P_2 force peaks, curves were drawn for the DOT Test Car vehicle parameters and values for the Northeast Corridor (140 lb/yd) track at Bowie, Maryland, at a track joint:

P_o = 12,200 lb

M_U = 4.07 lb-sec^2/in. (1571 lb per wheel)

K_R = 140,000 lb/in.

TABLE 6-3. DESCRIPTION OF DIPPED JOINT BASED ON TRACK PARAMETERS AND SAFETY STANDARDS

Track Class	Dip Length, d, in.	Allowable Low Joint (No Load), in.	Total Low Joint, e (Under P = 20,000), in.
1	364	3.00	3.00 + 0.43 = 3.43
2	308	2.75	2.75 + 0.27 = 3.02
3	276	2.25	2.25 + 0.19 = 2.44
4	320	2.00	2.00 + 0.13 = 2.13
5	308	1.25	1.25 + 0.10 = 1.35
6	308	0.50	0.50 + 0.10 = 0.60

Track Class	* a	Speed Limit Freight	Speed Limit Passenger	αV_{max} Freight	αV_{max} Passenger
	rad	mph	mph	rad-in./sec (rad-m/s)	rad-in./sec (rad-m/s)
1	.059	10	15	10.4 (.26)	15.6 (.40)
2	.062	25	30	27.3 (.69)	32.7 (.83)
3	.056	40	60	39.4 (1.00)	59.1 (1.50)
4	.042	60	80	44.4 (1.13)	59.1 (1.50)
5	.028	80	90	39.4 (1.00)	44.4 (1.13)
6	.012	110	110	23.2 (.59)	23.2 (.59)

* $\alpha = {}^{2\pi e}/_{d} = {}^{\pi e}/_{2(2/\beta)}$ (see Ref. 6-3)

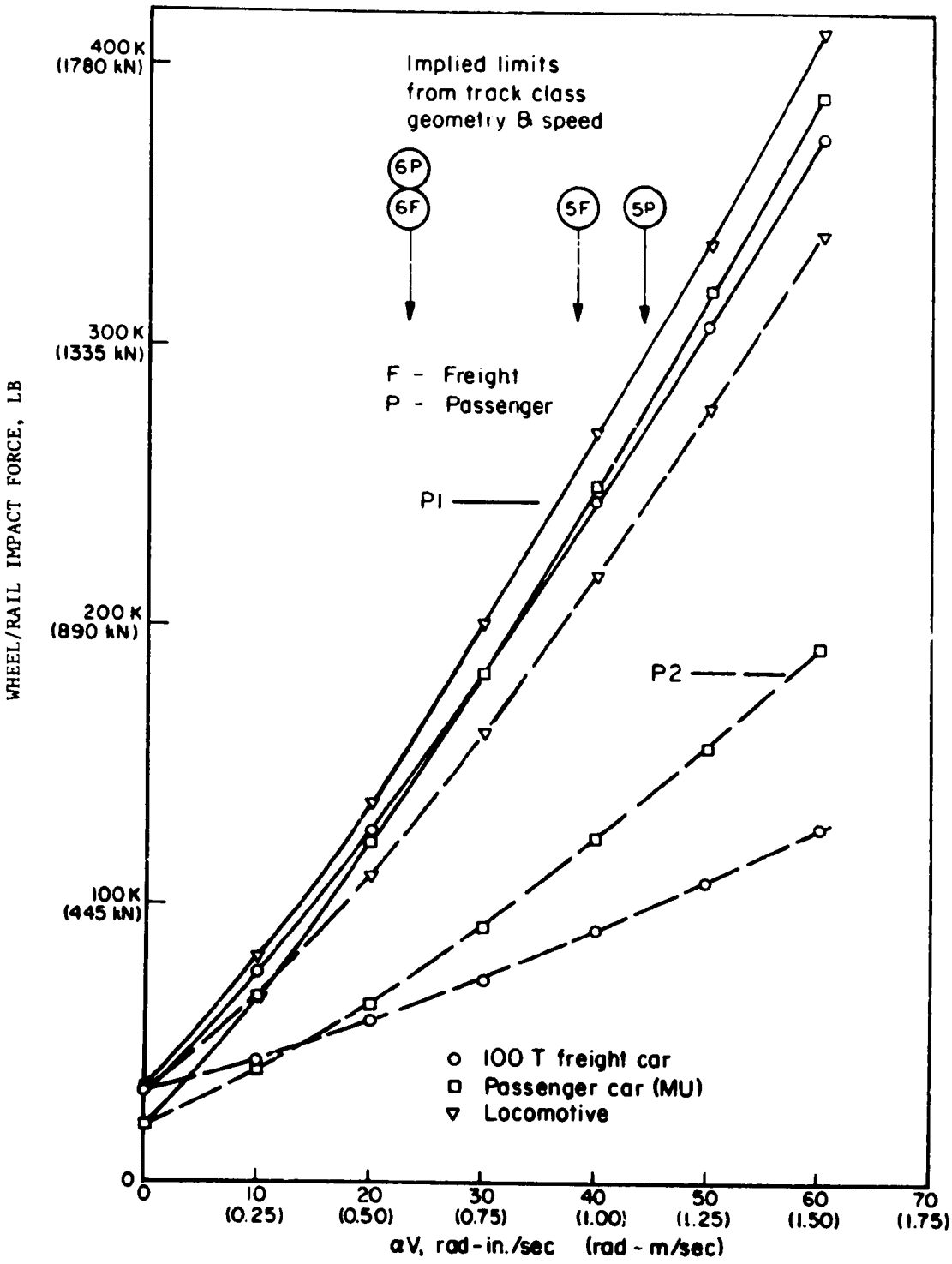

FIGURE 6-6. CALCULATED PEAK JOINT IMPACT FORCES FOR TYPICAL NORTH AMERICAN TRACK AND VEHICLE PARAMETERS

M_R = 4.56 lb-sec^2/in. (1760 lb)

e = 0.3 in total (slack plus deflection under load)

d = 0.0044 radian

M_e = 0.47 lb-sec^2/in. (180 lb, Method 1)

= 0.33 lb-sec^2/in. (130 lb, Method 2)

The results of these calculations are shown in Figure 6-7 compared with some available data from the field measurements [6-6]. Wheel loads were measured using a tie plate load cell on the first running-on tie. These data were recorded on a light-beam oscillograph with flat frequency response to roughly 2500 Hz. Unfortunately, only one P_2 force value was recorded from the traces, but this single value does fall close to the predicted curve. On the other hand, P_1 force peaks from tie plate loads show a substantial attenuation through the rail effective mass as train speed increased.

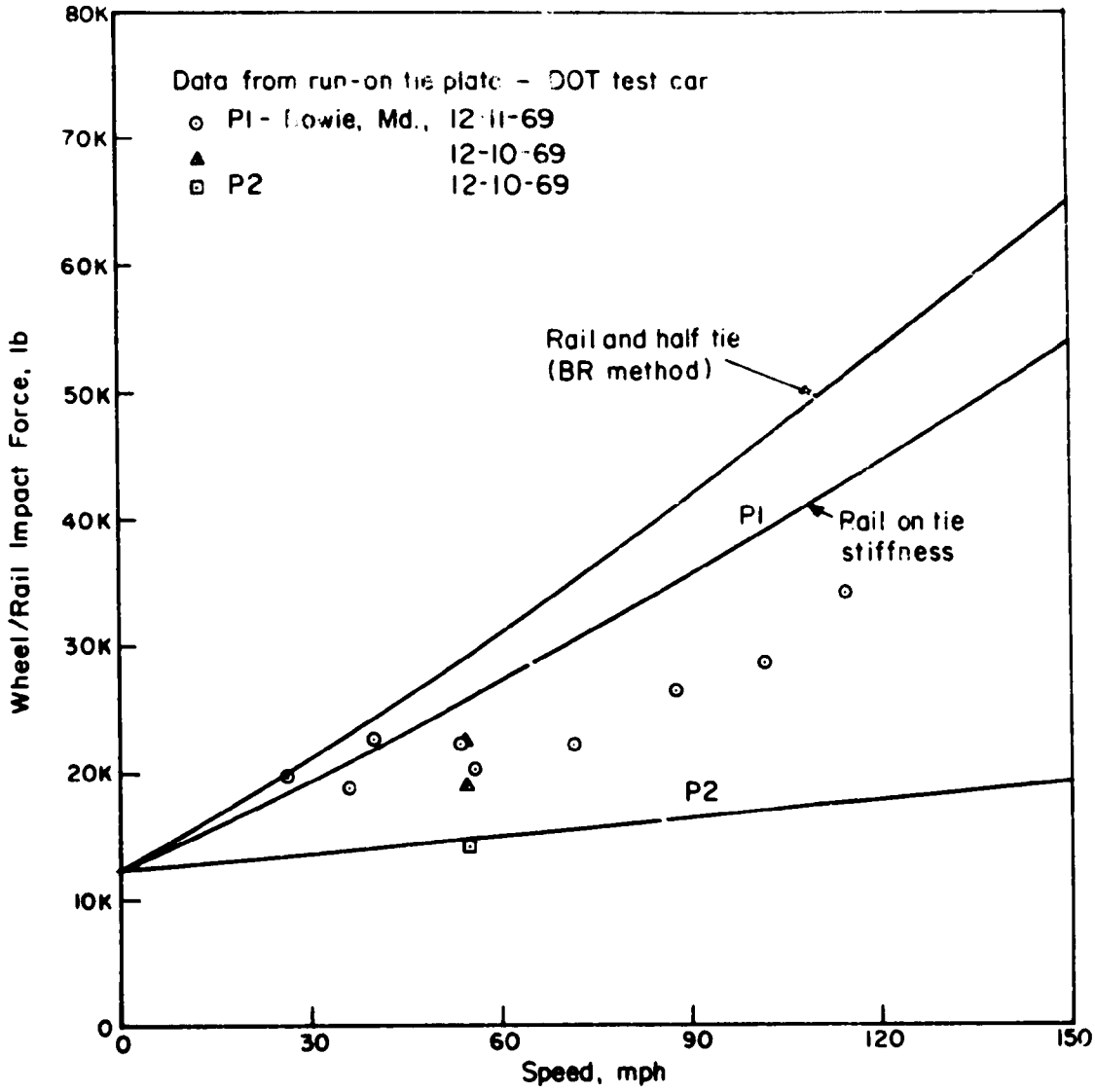

FIGURE 6-7. COMPARISON OF PREDICTED JOINT IMPACT LOADS WITH IMPACT LOADS WITH WHEEL/RAIL LOADS MEASURED FROM INSTRUMENTED TIE PLATE

APPENDIX A

STATISTICAL ANALYSIS OF TIE PLATE LOADS

Tie plate peak vertical loads have been analyzed statistically from a number of test sites in terms of mean and standard deviation. It is desirable to know the range of true mean and the range of standard deviation of tie plate loads based on the statistics of several sites.

In order to develop these statistical characteristics for a 95 percent confidence level, the Chi-square and Student-t tests of the data have been performed, as described in Bendat and Piersol, Measurement and Analysis of Random Data (Wiley, 1966), in Chapter 4, pages 133-141. From this source, the following equations were used:

$$\bar{F} - \frac{S_F\, t_{n;\alpha/2}}{\sqrt{N}} \leq \bar{F}_t < \bar{F} + \frac{S_F t_{n;\alpha/2}}{\sqrt{N}}$$

$$\frac{n\, S_F^2}{\chi^2_{n;\alpha/2}} \leq \sigma_F^2 < \frac{n\, S_F^2}{\chi^2_{n;\,1-\alpha/2}}$$

where... $\bar{F}$ = mean value of peak tie plate force at given test site

S_F = standard deviation of peak tie plate force at given site

N = number of test sites

n = N-1

σ_F = true standard deviation of peak tie plate force (all sites)

$\bar{F}_t$ = true mean value of peak tie plate force (all sites)

The values of $t_{n;\alpha/2}$, $\chi^2_{n;\alpha/2}$, and $\chi^2_{n;1-\alpha/2}$ can be found in the tables on pages 162-163 of Bendat and Piersol.

APPENDIX B

CHARACTERIZATION OF WHEEL/RAIL LOADS - REVIEW OF EXISTING ANALYTICAL MODELS FOR PREDICTING W/R LOADS

Introduction

Wheel/rail loads are determined not only from the speed and characteristics of the vehicle, but also from the features of the track structure. Therefore, it is essential to incorporate analytical techniques with which both vehicle and track structure components can be varied. While this scope does seem all encompassing, certain mathematical models are not applicable. Vehicle models used to predict hunting, ride comfort, or vehicle safety are not of interest as such, although they may be modified to include wheel/rail interaction. In addition, detailed ballast pressure distribution, cross tie behavior, and fastener strength are not prime considerations. Yet the flexibility and dynamic response of the track structure will strongly influence the W/R loads and must be included to obtain the proper rail response.

In this review, the analytical models have been separated into six distinct categories: algebraic expressions, exact solutions of a continuous system, lumped parameter steady state, lumped parameter frequency domain, lumped parameter time domain, and finite element models. All of the following models will provide a wheel/rail force which depdnds on one or more vehicle or track parameters.

Algebraic Expressions

Wheel/rail forces developed by vehicle and track interaction have in the past been estimated from empirical relationships, from which stresses in rail and track components could be calculated. These empirical equations have been derived from measured loads, strains, etc., where least-square and other curve fitting techniques were used to establish the coefficients and exponents of the relationships.

Speed Factors

Speed factors are simple expressions which have been used by different railroads to account for speed related dynamic effects in calculating maximum stresses in rail. For example, the Indian Railways [B-1] uses a speed factor K given by

$$K = 1 + \frac{V}{3\sqrt{u}} , \qquad \text{(B-1)}$$

where

V = train speed, mph

u = track modulus, lb/in./in. (per rail).

An expression used for the Washington MATA [B-2] is

$$K = [1 + .0001\ V^2]^{2/3} . \qquad \text{(B-2)}$$

A third speed factor recommended by AAR [B-3] is

$$K = 1 + \frac{33V}{100D} , \qquad \text{(B-3)}$$

where

D = wheel diameter, in.

These speed factors are then used to define the peak dynamic load on the rail,

$$P = K\ P_o \qquad \text{(B-4)}$$

where

P_o = static wheel load.

The use of speed factors to define peak dynamic loads on the rail is obviously a rough approximation that is limited in accuracy and frequency range.

Dynamic Loading at Rail Joints - BR

British Railways has suggested that the unsprung weight has a large effect on joint impact. From a simple analysis assuming (a) perfect impact of the wheel with the run-on rail, (b) symmetric profile of the running surface at the joints, i.e., no gap or end batter, and (c) that the joint and the wheel can be characterized by a simple spring-mass system, the dynamic force, P, developed can be expressed [B-4] as

$$P = P_o + 2\alpha\ V\sqrt{\frac{K_R W}{g}} , \qquad \text{(B-5)}$$

where

P_o = the static wheel load

α = slope of the rail at the joint, radian

V = velocity of the vehicle

K_R = effective track stiffness at joint

g = gravitational constant

W = unsprung weight.

The values of K_R are obtained by using the different joint deflections obtained under known static loads. Typical values for K_R are 100,000 lb/in. to 500,000 lb/in. Values of W are usually derived by adding the total weight of wheelset and axle boxes to a portion of the weight of springs, linkages, and traction motor (if axle-hung), anddividing by two. This assumes that the vehicle secondary suspension is very much softer than the wheel disk and the track, and that the suspension characteristics will exert only a minor influence on the effective unsprung weight.

A somewhat more complicated expression is used by Jenkins [B-5] to predict the peak W/R forces at a rail joint. Chronologically, the first force, P1, is a high-frequency peak due to the vehicle unsprung mass and track mass connected by the Hertzian contact stiffness. This force, occurring near the rail end, is absorbed by the rail and ties. A second force peak occurs near the first tie following the joint and is transmitted to the ballast. The P1 and P2 forces are given by

$$P1 = P_o + 2\alpha V \sqrt{\frac{K_H M_e}{1 + M_e/M_u}} \quad . \tag{B-6}$$

$$P2 = P_o + 2\alpha V \left(\frac{M_u}{M_u + M_t} \right)^{1/2} \left(1 - \frac{C_t \pi}{4K_t (M_u + M_t)} \right) \sqrt{K_t M_u} \quad , \tag{B-7}$$

where

P_o = static wheel load

α = slope of rail at joint

V = vehicle velocity

M_u = vehicle unsprung mass.

The other variables in Equations (B-6) and (B-7) are not as easily obtained. K_H is the linearized Hertzian contact stiffness and depends on both the static load, P_o, and the total load, P1.

$$K_H = \frac{P1 - P_o}{G\,(P1^{2/3} - \Gamma_o^{2/3})} \quad . \tag{B-8}$$

G is the Hertzian flesibility constant which depends on the wheel radius and tread profile. For a worn profile

$$G = 3.86\ R^{-.115} \times 10^{-8}\ m/N^{2/3} . \tag{B-9}$$

For a 1/20 coned wheel

$$G = 4.57\ R^{-.149} \times 10^{-8}\ m/N^{2/3} . \tag{B-10}$$

The other variable in Equation (B-6) is M_e, which is the effective track mass given by

$$M_e = \left[M_r + M_s/\ell\right] \left[\Gamma(3/4)\ \Gamma(5/4)\ \sqrt{2}\right]^{4/3} \left[\frac{4\,EI}{K_H}\right]^{1/3} , \tag{B-11}$$

where

M_r = rail mass per unit length

M_s = half tie mass

ℓ = tie spacing

EI = rail bending stiffness

$\Gamma(3/4) = 1.2254$

$\Gamma(5/4) = .9064.$

The nature of the definition of the variables in Equation (B-6) requires an iterative solution involving Equations (B-6), (B-8), and (B-11).

The remaining terms to be defined in Equation (B-7) are

$$M_t = \frac{3}{2\lambda}\ \left[M_r + M_s/\ell\right] . \tag{B-12}$$

$$K_t = \frac{2}{\lambda}\ \left[K_s/\ell\right] . \tag{B-13}$$

$$C_t = \frac{3}{2\lambda}\ \left[C_s/\ell\right] , \tag{B-14}$$

where

K_s is the ballast sfiffness per half tie

C_s is the ballast damping per half tie

$$\lambda = \left[\frac{K}{4EI}\right]$$

K = track stiffness modulus for a beam on an elastic foundation.

Exact Solutions of Continuous Systems

The second approach to modeling track structure is by using the solution of a differential equation describing a loaded continuous system. The method is applicable to both the rail and to the tie as individual units.

Rail on an Elastic Foundation (Vertical) - BCL

The basic equation for a beam on an elastic foundation is

$$EI\ Y^{IV} + KY = 0\ . \qquad \text{(B-15)}$$

Assuming a point load, P, acting on the rail, an exact solution to Equation (B-15) is

$$Y = \frac{P}{2}\ \frac{\beta}{K}\ e^{-\beta X}\ [\cos\beta X + \sin\beta X] \qquad x \geq 0, \qquad \text{(B-16)}$$

where

$$\beta = \left[\frac{K}{4EI}\right]^{1/4}$$

K = effective spring constant per unit length of elastic support.

In this model, the spring constant includes a pad stiffness, a ballast stiffness, and a soil stiffness. The ballast is represented by the pyramid stress model. Because of the continuous system assumption, all individual stiffnesses are constant. The effective spring constant, K, is determined by tie spacing. The program will accept four wheel loads to simulate the track structure in the vicinity of two trucks.

Output includes the rail deflection and moment at several points, the pressure at the base of the tie and ballast, and the rail bending stress.

This model does have several unrealistic assumptions: equal tie spacing, homogeneous, isotropic ballast, equal pad stiffness, no joints in the rail, a foundation modulus which acts in tension, and a uniform deflection and pressure distribution in the ballast.

Rail on an Elastic Foundation under Axial Compression (Vertical) - BCL

For this problem, Equation (B-15) is modified

$$EI\ Y^{IV} - N\ Y^{II} + KY = 0\ , \qquad \text{(B-17)}$$

where

N is the axial load.

The solution to Equation (B-16) for N less than the buckling load, $N < 2\ KEI$, is

$$Y = e^{-ax}\ \frac{p\ (a^2 + b^2)}{4K}\ \left[\frac{1}{a}\ \cos\ bx + \frac{1}{b}\ \sin\ bx\right], \qquad \text{(B-18)}$$

where

$$a = \left[\sqrt{\frac{K}{4EI}} + \frac{N}{4EI}\right]^{1/2}$$

$$b = \left[\sqrt{\frac{K}{4EI}} - \frac{N}{4EI}\right]^{1/2}$$

Remarks pertaining to the rail on an elastic foundation can be made for this model. The only restriction is that the compressive load must be kept below the buckling load.

Lumped Parameter Steady-State Models

Steady-state vehicle/track models have been formulated primarily to investigate curving effects. Several mathematical models are available which generate steady-state W/R forces on curves.

Steady-State Curving of Two Car Bodies - Nishio

Equilibrium equations for two connected car bodies on a constant curvature are written [B-6]. The given equations assume that only the outside front wheel of each of the four trucks is flanging. The primary suspensions are rigid on the second and third trucks; the first and fourth trucks have loose wheels. In both cases, the wheelsets are arranged in parallel. A secondary lateral suspension between each truck and car body is included. All six bodies

have a lateral and yaw degree of freedom for a total of 12 degrees of freedom. A constant friction coefficient is used between the cylindrical wheels and rail. Lateral rail forces are generated from this formulation.

Flexible Truck on Curved Track - Newland

This analysis is based on a 6 degree of freedom, 2-axle, flexible truck negotiating a constant radius curve [B-7]. The degrees of freedom are radial and yaw displacements of each wheelset and radial displacement of the front and rear ends of the truck. Equal lateral and longitudinal creep coefficients are assumed. Slipping and flange contact are ignored. The wheel profiles are assumed to be conical and a lateral load (centrifugal force) is applied at the truck frame c.g. Secondary yaw stiffness is not included in the equations.

Although the main point of interest in this paper is the radial displacements of the wheelsets from the track centerline, gravitational and creep forces can also be easily calculated once the equilibrium conditions are established. An expression for negotiating a minimum radius curve without slipping is also given, as a function of the primary suspension parameters.

Curving of Rail Vehicles - Boocock

Steady-state linear theory is used to predict the behavior of a 2-axle truck [B-8]. Wheel slip, gravitational stiffness, spin creepage, and flanging are neglected. The wheel profiles are assumed to be conical. Both primary and secondary lateral and yaw stiffnesses are included. The equations of motion for 7 degrees of freedom are solved simultaneously to give algebraic expressions for the lateral and yaw displacements of two wheelsets and the truck frame plus the lateral displacement of the car body. Centrifugal force is applied to the wheelsets, truck and car body. A rear truck with six additional similar equations of motion is also included. Creep forces can be calculated from the equilibrium conditions.

Steady-State Curving Analysis - EMD

EMD's curving analysis predicts the steady-state lateral W/R forces during negotiation of a constant radius, constant superelevation curve for a 2-, 3-, or 4-axle truck. The program uses an empirical creep relationship of percent of vertical load versus creep angle with a limit at the maximum of 0.28 times the vertical wheel load. If this limit is exceeded, no solution is given. The program will accept longitudinal and lateral forces at the centerplate for tractive, and centrifugal braking loads, individual vertical wheel loads, lateral clearance (axle/frame and flange/rail), primary lateral stiffness, and standard geometry. There is no rail lateral stiffness included in the model, but lateral flange forces are developed. Also, no center bearing torque or yaw stiffness is included.

The method of solution used in this analysis is to assume a configuration and allow the computer program to iterate until a force and moment balance based on a "friction center" is achieved without wheel slipping. This may be a somewhat unrealistic approach, since the user may not make a judicious choice of configuration, and thereby comes to the conclusion that no solution exists. Computed and measured data are found to correspond well for curves over $4\text{-}1/2^{\circ}$.

Side Thrust of Curving Wheels - Kunieda

This paper [B-9] presents several algebraic equations from which flange forces on the outer front and rear wheels and the rear inner wheel can be calculated. The model is a half car 4-wheeled truck running under steady-state curving conditions. Gravitational restoring forces are neglected, the wheel treads are assumed to be conical, and longitudinal and lateral creep coefficients are equal. An unbalanced centrifugal acceleration based on radius of curvature, velocity, cant, and gage is applied to the truck.

Three different possibilities are considered. The first condition assumes that the front outer wheel is flanging and the rear outer wheel is not. If the rear outer wheel is also flanging, a second set of flange forces is given. For the third condition of outer front and inner rear wheels flanging, two flange force equations are also presented.

The actual derivation of the equations is not given.

Steady-State Curving Analysis - BCL

This model consists of one 2-axle truck with a total of 7 degrees of freedom: lateral and yaw on each wheelset, lateral, yaw and roll on the truck. Creep, gravitation, centrifugal, flange, and friction forces are included on each wheelset. Centrifugal force from the truck and car body are applied to the c.g. and centerplate of the truck, respectively, Centrifugal forces due to the wheelsets are applied at the c.g. of each wheelset. The program calculates the equilibrium position of the 7 degrees of freedom during steady-state curving. Flange forces are included by a linear lateral rail stiffness, which is a function of rail, fastener, tie, and ballast stiffness. Lateral deflection of the rail is an output. All possible flanging conditions are checked as a possible equilibrium position. Outputs include equilibrium condition of the 7 degrees of freedom, plus all the forces and moments acting on the wheelsets.

The 3-axle steady-state curving model is directly comparable to the 2-axle program except two more degrees of freedom are added for the third axle. A major difference is the increased number of possible flanging conditions that must be checked for equilibrium to exist.

Both of Battelle's steady-state curving models will be updated in the near future to include nonlinear suspension stiffnesses, axle-truck frame clearance, nonlinear creep coefficient, and W/R slippage.

Quasi-Static Rail Vehicle Curving Models - Law and Cooperrider

Several curving models are (or will be) available through Clemson/ASU (Law and Cooperrider). One model is a quasi-static solution of a 7 degree of freedom, 2-axle rail vehicle (yaw and lateral at each axle; yaw, roll and lateral of the body) by numerical integration of the equations of motion. In this model, quasi-static means that the motion is slow enough to ignore inertia terms. Actual wheel/rail profiles are used to model gravitational stiffness, the difference in wheel rolling radii, and wheelset roll angle. Nonlinear creep is modeled, and the adhesion limit and rail lateral flexibility are being added. Arbitrary rail lateral irregularities are superimposed on variations in curve

radius and superelevation. The model also included suspension nonlinearities and misalignments. Outputs include displacements, velocities, wheel/rail contact forces, and forces between suspension elements. A linearized version of this model is in current operation.

A second quasi-static model includes four axles, with 17 degrees of freedom, adding the yaw, roll, and lateral of the truck frame for two trucks, plus the additional two axles. This model is planned to be operational by late 1975 and will be documented under Contract DOT-TSC-902.

Steady-State Curving of 2-Axle Rail Vehicle - Law and Cooperrider

A linear steady-state 7 degree of freedom curving program has been developed to investigate L/V ratios up to slip. The 2-axle vehicle includes yaw and lateral motions of each wheelset, and yaw, roll, and lateral of the body. Suspension misalignment capabilities are available with this program. In addition to displacements and L/V ratios, slip and flange contact boundaries are generated.

The program is currently operational at Clemson University and will be documented in a M. S. E. thesis by December, 1976.

Lumped-Parameter, Frequency Domain Models

Frequency domain analyses of lumped-parameter models of rail vehicles have been often used in recent years to predict dynamic response of proposed vehicles, including stability, ride comfort, and wheel/rail forces. The approach has in general been to develop the differential equations of motion for lumped masses, dampers and springs; to linearize and transform these equations to the frequency domain (the LaPlace or Fourier transformations); and to generate matrices or transfer functions between an input and a specified output. Distributed systems (body bending modes of vibration, for example) have been handled by assumed mode or finite lumped-element methods to account for a few low-frequency resonances.

For rail vehicle analyses, track geometry variations (rail surface, alignment, or track cross level or gage) have been used as inputs. Methods have ranged from discrete sinusoidal amplitude spectra (JNR) to random geometry "power" spectra, (BR, BCL) representing geometry variations as a function of wavelength

along the track. Constructional variations of a discrete nature (bolted rail, for example) have been handled by harmonic (sinusoidal) inputs in the form of Fourier coefficients of the apparent geometry waveform.

To obtain a harmonic analysis for a frequency domain model, the transfer function is simply multiplied by the magnitude of the input at a given frequency, and the output is the magnitude and phase of the response at that frequency. If inputs represent random signals, the power spectral density (PSD) or cross spectral density input is multiplied by the transfer function squared, to give an output PSD for which phase information is lost. For response to several discrete components (bolted rail), a vector or root-mean-square (RMS) summation of output components must be taken. Frequency domain solutions are particularly well suited to digital computation. While linearization of the model is a disadvantage, recent work has evolved quasi-linear "describing function" techniques for handling the amplitude-dependent characteristics of some common nonlinearities such as flange clearance, friction, and wheel profiles.

Rail Vehicle - Roadbed Study - TRW

Two models give vertical and lateral frequency response as a function of rail input, either harmonic of PSD [B-10]. The vertical model is treated as three vertical degrees of freedom: one half the car body, the truck frame, and the unsprung mass (which includes two wheelsets and the effective mass of the rails). A secondary, primary, and roadbed suspension system are included. The effective rail mass is found by considering the forced oscillation of a mass resting on a beam on an elastic foundation. Roadbed stiffness is obtained from the classical beam on an elastic foundation. The lateral dynamics utilize a three mass, seven degree of freedom model which can determine lateral response to both hunting and rail irregularities. Two trucks with their wheelsets have yaw and lateral freedom, while the car body has yaw, roll, and sway capabilities. Coning and creepage effects are included so that a body hunting mode is possible, but truck hunting is not a well defined mode. In the lateral model, the roadbed is rigid.

The main purpose of this program is to design a vehicle for ride comfort. The reactive force between the wheel and the roadbed is also determined from the vehicle dynamic response. In the lateral model, the contact force arises from the wheel conicity and creep, whereas the roadbed stiffness provides a rail load in the vertical model. Also, critical speeds are determined by solving for the eigenvalues of the lateral model.

Theoretical Analysis of Variation of Wheel Load - Hirano

A three degree of freedom model is used to calculate the frequency response function of the wheel load by application of a harmonic displacement at the base of the ballast [B-11]. The mass of the carbody, bogie, and unsprung mass are included in the model. The unsprung mass is made up of the wheelset plus an effective rail. The rail supporting spring (ballast) provides the wheel load. A plot of wheel load versus frequency shows the effect of vehicle components.

The variation of wheel load due to passing through a low spot of track is analyzed by a single mass model suspended between the primary suspension and an effective rail spring. The low spot is modeled by a cosine function. Documentation of this program is not currently available.

Railway Truck Response to Random Rail Irregularities - Cooperrider

A linear 7 degree of freedom truck model (lateral and yaw of 2 wheelsets; lateral, yaw, and roll of one truck frame) is subjected to random alignment and crosslevel inputs [B-12]. To maintain a linear model, flange contact and slipping are neglected. Additional assumptions are conical wheels, and longitudinal and lateral creep terms only. The rail irregularities are represented by a 2-piece approximation to PDS's obtained from British Railways.

The output of this model includes an eigenproblem solution which provides insight into the overall lateral dynamic behavior of the vehicle. More importantly, frequency responses for the degrees of freedom and the lateral

and longitudinal creep forces are given. In addition, PSD's and RMS values of the displacements and creep forces can be obtained. RMS values of creep forces versus vehicle velocity are displayed for varying vehicle parameters.

Two additional frequency domain models are currently in use by ACORN (Cooperrider and Law). One consists of a 15 degree of freedom passenger car model with gravitational stiffness, spin and lateral/spin creep, and gyroscopic effects. The equations are solved by a state space analysis using the Lyapunov equation and produces RMS values of displacement, acceleration, and creep forces. The second model is a 9 degree of freedom freight car for standard frequency domain analysis, generating PSD's and RMS values of displacements, accelerations, and W/R contact forces. Both models are "lateral" models, with no vertical modes included.

Dynamic Response of Rail Vehicle due to Random Input - DCL

This program is a frequency domain solution of a set of 14 linear differential equations representing the track and vehicle [B-13]. The track is modeled as a spring-damper vertically under each rail and laterally for both rails. The effective mass of the rail, ties, ballast, and unsprung mass of the truck is lumped. Track geometry inputs are PSD representations of surface, cross level, and alignment.

Due to the linearization procedure, the equations of motion decouple into two 7 degree of freedom models. In the vertical model, the following degrees of freedom are included: rigid car body vertical and pitch, first car body bending mode, vertical motion of a transformer mass suspended from the car body, vertical motion of both sprung (truck) masses, and vertical motion of the front unsprung mass. The roll/yaw/lateral model contains: rigid body roll, yaw, and lateral translation, sprung and unsprung masses of the front truck both in roll and lateral translation. The rear truck is simulated as a complex impedance representing the "massless" truck.

Outputs of the computer simulation are in three forms: PDS's, RMS values, and ride quality index. In particular, PDS's of W/R force in both the vertical and lateral direction between frequencies of .2 Hz and 51 Hz are given. RMS values are also calculated by integrating the PSD.

There are recognized limitations associated with this simulation. The total model contains only 14 degrees of freedom, neglecting the important truck hunting mode, among others. Creep coefficients are included only as a lateral effective stiffness and damping, with the more conservative, flange-contacting condition an alternative condition. Cross spectral densities were not used, and an RMS combination of response to surface, alignment, and cross level PDS's was generated.

An offshoot of the random analysis simulation is a separate computer program (containing the same equations of motion) which considers the effect of staggered joints on bolted rail track. The first three even coefficients of the Fourier series of a rectified sine wave are combined to give surface, and the first three odd coefficients to give cross level inputs. The alignment input contains the first harmonic component only. Steady-state solutions are found by vectorially combining the effects of the frequency components. W/R forces are one of the outputs of this program.

Linear Rail-Vehicle Model - BCL

This linear model contains 46 degrees of freedom as listed below.

Body	Degree of Freedom	Total
Car body (rigid)	Yaw, pitch, roll, lateral, vertical	5
Car body (flexible)	Torsional, lateral, vertical (first modes)	3
Truck frames (2)	Yaw, pitch, roll, lateral, vertical	10
Wheelsets (4)	Yaw, roll, lateral, vertical	16
Track (4)[a]	Roll (crosslevel), lateral, vertical	12
Total		46

(a) One section of rail associated with each wheelset.

As usual, linearization decouples the problem into a vertical model and a roll/yaw/ lateral model. The primary incentive for linearization is to be able to solve the eigenproblem and find transfer functions between the input track geometry and the output degrees of freedom. Both of the above solutions involved transferring the equations into the frequency domain. The procedure

is similar to that conducted for the 14 degree of freedom program developed by BCL and now operational. Added features, in addition to the greater number of degrees of freedom, is the ability to include a cross spectral density between alignment and cross level and to find the natural frequencies and mode shapes of a particular track vehicle model. Although the equations are available and the implementation would be relatively straightforward, a digital computer program does not exist for this frequency domain problem. Plans are now being made to implement these equations in a computer program.

Linear Rail-Truck Model - BCL

Reducing the rail-vehicle model to a single truck model results in 19 degrees of freedom, six equations in the pitch plane and 13 in the yaw/roll/lateral modes.

Body	Degrees of Freedom	Total
Truck frame	Yaw, pitch, roll, lateral, vertical	5
Wheelsets (2)	Yaw, roll, lateral, vertical	8
Track (2)	Roll (cross level), lateral, vertical	6
Total		19

Transforming the equations into the frequency domain, the user can elect to use either or both sets of equations for a particular problem. Furthermore, there is the option to solve eithe the eigenproblem or the random input problem, for either the pitch plane or the yaw/roll/lateral degree of freedom.

The eigenproblem will give natural frequencies and mode shapes for a rail-truck configuration, including the truck hunting solution. The random input option is similar to BCL's 14 degree of freedom simulation. It does not have the added capability of using a cross spectral density input between alignment and cross level. Although a computer program does exist, the output format has not been fully established yet, but it will include frequency responses and mean square values of important variables in addition to results at an output location which can be specified by input data. In this way, a PSD output, at some arbitrary location, can easily be monitored experimentally and compared to the theoretical model.

The computer program is completely functional for solving the eigenproblem, and 75 percent complete in solving the random problem.

Quasi-Linear Wheelsets - Law and Cooperrider

Two separate computer programs, which will be available during the fall of 1975, have been developed to analyze a 2 degree of freedom (yaw and lateral) wheelset. Coulomb friction, and nonlinear conicity, gravitational stiffness, and roll are included in the model. Two solution techniques are employed using a describing function analysis: (1) harmonic input, and (2) random input. Both inputs are lateral rail alignments.

Outputs are displacements, accelerations, and W/R contact forces as a function of frequency.

Lumped-Parameter, Time Domain Models

Time domain analyses of lumped-parameter models of rail vehicles have been used by a number of researchers in recent years to investigate the transient response of the vehicle to discrete track geometry errors, such as low rail joints. Similar to the lumped-parameter frequency domain model, the differential equations of motion have been developed from the Lagrangian equations for the dynamic system. These equations have then been used directly in the simulation. One distinct advantage of the time-domain solution is that the nonlinearities may in almost all cases be handled directly in the model.

Because of the integration techniques used by the two classes of computer, digital (a serial integration) versus analog (a parallel integration), time domain modeling is most efficiently mechanized on the analog computer. Limitations on analog components, particularly integrators, at a specific facility can inhibit the size of a model. On the other hand, while a digital computer can in theory handle any size of model, practical limitation on running time (cost) also limit both model size and frequency bandwidth. A most practical combination of computers is found in the hybrid facility, where the analog computer can perform high-speed integration in a parallel manner, while the digital computer can perform control, function generation, and low-speed integration tasks.

Track Forces Due to Dipped Rail Joints, Wheel-Flats and Rail Welds - Lyon

A rather detailed analytical approach is used to establish vertical W/R forces and contact stresses, and rail displacements and bending moments due to displacement irregularities between the wheel and rail [B-14]. The track model is a beam of uniformly distributed mass resting on an elastic foundation of continuously distributed linear springs and dashpots. Beam flexural rigidity and mass, and foundation stiffness modulus and damping are input data. An alternative approach to a beam on an elastic foundation is to model the rail as a beam resting on a number of supports. A maximum of 23 supports, representing the rail pad, tie, and ballast, consist of a system of springs, masses and dashpots.

The vehicle is modeled by a system of springs, masses, and dashpots. The equations of motion are written in matrix form and solved by using Hamming's predictor-corrector numerical integration technique. These matrix equations can incorporate the car body, the trucks, axle-hung motors, resilient wheels, and bending vibrations of the axle.

Hertzian theory for contacting elastic bodies is used to describe local deformations at the W/R contact area. The contact deformation is a function of Young's modulus, Poisson's ratio, wheel load, and the contact geometry of the wheel and rail. Unit impulse responses are developed to represent wheel and rail displacements.

Idealized forms of dipped rail joints and wheel flats are represented by cosine functions. W/R force time histories show two distinct peaks for dipped rail joints, while a wheel flat shows a sharp rise in dynamic rail displacement in the speed range of 5 to 15 meters/second.

The computer program or a listing is not currently available.

Dynamic Rail Joint Loading with Resilient Wheels - Bjork

A simple dynamic model has been constructed to investigate the dynamic W/R load when running over a dipped joint with a resilient wheel [B-15]. Four vertical degrees of freedom are used to represent the vehicle: truck frame, axle, wheel rim, and rail. Stiffnesses and dampers between the four masses are: the primary suspension, the resiliency of the wheel, and the rail-track compliance. The track geometry is idealized by two quarter cosine waves (the

dipped joint), and its displacement is used as the input disturbance. Since the displacement of the rail is known, the dynamic force can be solved as the fourth unknown.

The above system of differential equations is solved numerically. If during the simulation, the wheel rim leaves the rail, a different set of equations is used until the rim impacts again. The impact and subsequent motions are not included in the simulations.

Dynamic W/R loads and displacements of the truck frame, axle, and wheel rim as a function of vehicle speed, unspring, weight, etc. can be determined for wheels of variables resiliency. This somewhat sophisticated analysis is compared to a simple analysis presented by Nield and Goodwin for solid wheels [4]. The difference in peak wheel load is about 4 percent. It is also shown that the use of resilient wheels results in a decrease in dynamic force by as much as 40 percent.

Vertical Vibration of a Vehicle on a Bridge - Matsuura

This model is used to calculate the response of a beam (bridge) being traversed by a constant velocity two axle load model [B-16]. The degrees of freedom include the vertical displacements of the half car body, a truck, and two wheelsets which remain in contact with the beam at all times. A fifth degree of freedom is the pitch rotation of the truck. The resulting differential equations are integrated, providing dynamic bending moments, and deflections of the beam in addition to vertical vibration of the car and wheel load decrements.

Documentation is very limited.

Derailment of Two-Axle Freight Car - Matsui

The system in this study is a two-axle freight car [B-17]. The suspension system is treated as a pendulum with restoring forces represented by polygonal curves with frictional hysteresis. A change in the equations of motion is effected if one wheel leaves the rail. Inputs into the model are suddenly applied sinusoidal excitation to the wheelsets in both the lateral and vertical directions. The criteria for judging the system is the ratio L/V at each W/R contact.

Only three lateral equations of motion of the car body are mentioned, lateral, roll, and yaw. From the nomenclature, other degrees of freedom apparently are: wheelset lateral, wheel vertical. The equations of motion are numerically integrated for a time domain solution.

Wheel Loads at Rail End - Kuroda

The actual model is poorly described in this paper [B-18]. From a sketch, it appears to be an unsprung mass between two springs, a primary suspension and a rail supporting spring. An effective rail mass is included in the wheel mass. Five shapes of unevenness of running surface of rail are given including: sine wave concave, sine wave convex, sine wave drop, sine wave rise, and V-shaped concave. The dynamic variation of wheel load as the wheel rolls over the unevenness is the output.

It is not clear how the equations are solved. Possibly, a numerical solution in the time domain with a change in rail displacement simulating the unevenness may provide the solution.

Nonlinear Wheelset Dynamic Response to Random Lateral Rail Irregularities - Law

The mathematical model used in this analysis is a 2 degree of freedom wheelset assumed to be moving at a constant forward velocity on nominally tangent track [B-19]. The wheelset is constrained in both the yaw and lateral directions by a primary suspension system. Lateral, longitudinal, spin, and lateral/spin creep coefficients along with a linear spring, which resists lateral wheelset displacements once flange clearance is taken up, are included in the W/R interaction forces. In addition to a slip regime of the wheel on the rail and the possibility of a flanging force, profiled wheels introduce a third nonlinearity. As a result the two equations of motion are integrated numerical using a 4th order Runge-Kutta routine.

Since it is desired to obtain a time domain solution, it is necessary to determine a random alignment history of the left and right rails. To do this a series of impulses with zero mean and Gaussian amplitude distribution were generated by the computer. The RMS level was then adjusted to approximate known PSD's of lateral alignment.

Outputs of this program include not only the time histories of the degrees of freedom, but also L/V ratios. Law shows that L/V ratios increase as the RMS value of lateral misalignment increases from 0 to 0.5 in. Such variables as creep, speed, wheel profile, flange clearance and lateral rail stiffness can be varied to show its effect on L/V.

Two additional time domain models are currently under development by ACORN (Law and Cooperrider) and should be available by late 1975. The first of these is a freight car truck with dummy car body, with three degrees of freedom (yaw, warp and lateral) in the truck, plus lateral and roll of the car body. Coulomb friction damping, clearances and nonlinear springs are included, along with actual wheel/rail profiles to model gravitational stiffness, difference in wheel rolling radii, and wheelset roll angle. Nonlinear creep is also simulated. Inputs are arbitrary lateral rail alignments, and outputs include displacements, velocities, accelerations and W/R contact forces.

The second model a nine degree of freedom freight car model, three degrees of freedom (yaw, warp and lateral) for each truck, and three for the car body (lateral, yaw and roll). Both of these models are essentially lateral models, with no vertical modes of oscillation. Programs are implemented on a hybrid computer or on IBM-CSMP numerical integration routines.

Dynamic Railcar Simulation Program - Melpar

A generalized digital simulation calculates forces and motions of a multiunit rail vehicle [B-20]. A minimum of three bodies (one truck and two wheelsets) to a maximum of 15 bodies (one carbody, two bolsters, four side frames, four motors, and four wheelsets) is possible. Each body has 6 degrees of freedom. Linear interaction is characterized by a spring and damping coefficient; nonlinear interaction may be programmed by the user. Nonlinear forces such as friction, air springs, rubber bushings, and bumpers, and hard stops are contained in the program. Forces or moments may be generated by acceleration, braking or turning.

The rail has linear vertical and lateral flexibility. The user specifies the vertical and lateral displacements of the left and right rails as actual measured data or any desired mathematical form. Statistical contours may also be defined.

The simulation includes lateral and longitudinal creep forces, coned-flanged wheels, gyroscopic forces due to rotating wheels, gravitational wheelset stiffness (lateral and yaw), and aerodynamic drag. It is possible for any wheel to physically leave the track.

The equations of motion are integrated twice to give velocities and displacements at any interaction point. Besides using the program as a vehicle design tool, it can be utilized to study W/R interaction and track deterioration.

A listing of the program is available.

Flexible Body Vehicle Model - Martin

The main purpose of the model [B-21] is to predict the dynamic behavior of a freight car during roll and bounce modes over low joints. The car body is composed of a front and rear car body with torsional stiffness between. Nonlinear phenomenon such as gib clearances and wheel lift are included in the model. The degrees of freedom are lateral, vertical, roll, pitch, and yaw for each half of car body; lateral, vertical, and roll for the bolsters and lateral, vertical, and roll for the wheelsets. Apparently there are some rail degrees of freedom.

The program provides a time-history (numerical integration) solution of all accelerations, velocities, and displacements in addition to vertical deflections of the rail, and wheel load. Maximum wheel load as a function of speed is a possible output showing the car rocking effect. It is not possible to tell how wheel load is obtained from the model description, but track stiffness is a parameter input.

The analysis was done as a Master's Thesis by Terry Tse.

Vehicle/Track Interaction Model - BCL

A 10 degree-of-freedom model representing one-half a rail vehicle model and supporting track structure was developed [B-22,B-23] primarily to study track dynamic response. The model includes the car body and truck frame (bolster) in vertical motion, the "spider" or side frames in vertical and pitch, and the axles and track structure in vertical motion. "Unsprung" masses include the wheelset, rail, and tie/ballast masses separated by the W/R contact stiffness,

rail/tie pad stiffness, and tie/ballast stiffness, respectively. Track dynamic parameters are calculated based on a beam on elastic foundation. Track geometry variations are introduced at the W/R contact (for example, low joint geometry), along with spatially-varying stiffness or damping parameters.

Two versions of this model were programmed for analog computer (time domain) solution, one representing the DOT Test Car, the other representing a 100-ton freight car. Nonlinearities such as hardening spring rates, wheel lift, and Coulomb friction were used in the simulation. Outputs from the model included vehicle and track mass accelerations, velocities and displacements, W/R forces, and subgrade pressures.

Nonlinear Freight Car Model - BCL

A fourteen degree-of-freedom model of a 100-ton freight car was developed in 1966 for an industrial sponsor [B-24] to study the car rocking phenomenon. Because of the in-phase excitation of 39-foot rail lengths with half-staggered joints, one half the car body was modeled in bounce, lateral and roll. The front truck was modeled in detail to include the bolster in vertical, lateral and roll; each wheelset in vertical and roll; and an effective track mass beneath each wheel in vertical motion. Nonlinearities such as vertical and lateral friction snubbing, side bearing clearance and contact, centerplate clearance, sliding and lift-off, gib clearances, flange clearance and hard contact, and wheel lift were included.

Validation of the model was provided by comparison with test data from the prototype car recorded during test runs over a specially-shimmed track at Hollidaysburg, Pennsylvania. The computer model was then used to investigate a number of devices for control of car rocking, including various dampers and constant-contact side bearing devices. Outputs from the model included vehicle and track accelerations, velocities and displacements, and both vertical and lateral W/R forces. A staggered-joint track geometry in the form of a rectified sinewave was primarily used as an input.

This nonlinear model was later expanded to include both front and rear trucks (simplifying and reducing the truck degrees of freedom), adding the rigid-body yaw and pitch modes, as well as a first-order torsional dynamic mode of car body oscillation. In this form, the model was used to investigate

short, high 100-ton freight cars on truck centers less than 39 feet. In final form [B-25] the model was used to simulate both freight and passenger rail vehicles with a detailed front truck (14 degrees of freedom), a detailed car body (7 degrees of freedom, including vertical, pitch, yaw, roll, lateral; first mode of vertical body bending; and a mid-car suspended transformer in vertical motion), and a simplified rear truck as a complex impedance. Track geometry transients based on the FRA Track Safety Standards, and the staggered-joint track geometry were used as inputs. This final version of the model was run on a hybrid computer (Beckman 2133 analog, PDP 7 digital computers).

Generalized Nonlinear Rail Vehicle Model - BCL

A model has recently been developed [B-26] which will simulate many of the important degrees of freedom of a general vehicle and track. The resulting forty-six equations of motion are

Body	Degree of Freedom	Total
Car body (rigid)	Yaw, pitch, roll, lateral, vertical	5
Car body (flexible)	Torsional, lateral, vertical (first modes)	3
Truck frames (2)	Yaw, pitch, roll, lateral, vertical	10
Wheelsets (4)	Yaw, roll, lateral, vertical	16
Track (4)*	Roll (crosslevel), lateral, vertical	12
Total		46

These equations are strongly coupled and nonlinear. Creep and gravitational forces at the wheel/rail interface in addition to rail geometric error in both the lateral, vertical, and crosslevel are included. Hardening springs such as W/R lateral stiffness (simulating a flange condition) can be implemented. A digital time domain computer program can provide a transient simulation of a four axle, 2 truck, rail vehicle.

As in all models, there are limitations. Pad, tie, ballast, and subgrade are modeled as one dynamic element in the vertical direction and one in the lateral direction. Therefore, the rail mass must include the effective

* One section of rail associated with each wheelset.

mass of all parts of the track structure. Another limitation of this model is the deletion of all longitudinal degrees of freedom.

Outputs may include a time history of the displacement, velocity, and acceleration of the 46 degrees of freedom. From these variables, primary, secondary, W/R, and rail/roadbed forces in both the vertical and lateral directions can be obtained.

This model is expected to be programmed in the near future. When it is, the first task will be to investigate the effect of nonlinear inertia terms in the equations of motion. A second task will be to determine the sensitivity of certain output variables to the simulated degrees of freedom. It is hoped that the model can then be simplified by eliminating some nonlinear terms and degrees of freedom in order to reduce computer solution time.

Generalized Nonlinear Rail Truck Model - BCL

Several rail vehicle models of reduced size are the direct result of the generalized nonlinear rail vehicle model. One program based on this 46 DOF model considers only one truck. The degrees of freedom resulting include:

Body	Degrees of Freedom	Total
Truck frame	Yaw, pitch, roll, lateral, vertical	5
Wheelsets (2)	Yaw, roll, lateral, vertical	8
Track (2)	Roll (crosslead), lateral, vertical	6
Total		19

The resulting nonlinear, time domain model will be programmed in the near future.

Finite Element Models

Finite element models are another common attempt to represent the track structure. In general, these models not only analyze the ballast and subgrade, but also give information pertaining to the tie, pad, fastener, and rail. Another distinct advantage in using finite element is the ability to vary the properties of each element, so that the analysis is no longer that of an ideal system. The biggest disadvantage is the cost of making a computer run to obtain results. This includes setting up the input data in addition to actual execution time.

3-D Finite Element Model - by Svec

This three dimensional model of a railway track structure [B-27] includes the rails, ties, and ballast. The rail-tie system is based on a simple beam having vertical and rotational displacement at each end, while the ballast is made up of hexahedron and triangular prisms. Young's modulus of the ballast is computed by using a bicubic spline function. Since the rail properties are nonlinear and stress dependent, an incremental step-by-step analysis together with an iterative no-tension assumption is used. That is, a vertical incremental static load is placed on a rail. If tensile stresses develop, they are eliminated and the structure is reanalyzed for remaining tensile stresses. This interation removes all tensile loads, whereupon another load increment is added. At each addition of a load increment, a new Young's modulus is calculated.

Outputs of this model are the stress and deformation distribution in the ballast. There is little mention of the other parts of the track structure - no pad, fastener, or subgrade. In fact, only vertical force is transmitted between the rail and tie to the ballast.

Finite Element Model by Robnett

A two-stage finite element approach is used to model the track structure, since a three dimensional solution would be cost prohibited [B-28]. In the two-stage analysis, a longitudinal analysis is first performed, followed by a transverse analysis.

In the longitudinal case, a single rail-tie subsystem is considered as a continuous beam supported on springs representing the ties. The ballast, subballast, and subgrade are represented as rectangular planar elements whose thickness varies with depth to account for the spread of the loading (three dimensional load spread). Multiple wheel loads are used as point forces on the rail.

After the vertical displacements and reactions have been calculated, they are used as inputs into the transverse analysis. Rectangular elements represent the tie, ballast, subballast, and subgrade materials. As in the longitudinal case, all displacement components are assumed to vary bilinearly

over each element. Utilizing summetry, only half of the track structure is modeled with one point wheel load.

A pseudo plane strain state is used to obtain a realistic stress distribution with depth. The angle of distribution, which accounts for an increase in element size with depth, is constant. An incremental load technique is used in developing the final stress distribution. This allows the use of stress dependent material properties. After the last load increment is applied, a single iteration is performed to obtain the stress state which is compatible with the total load. During the incremental loading, failure criteria for the ballast and subgrade are incorporated.

For the longitudinal analysis, a symmetrical loading is assumed and only half of the system is modeled. Grid points along a vertical boundary representing the centerline of the system are restrained from horizontal movement as are grid points along the other vertical boundary at a distance of 260 inches. Grid points along the bottom boundary (300 in.) are fixed.

In the transverse direction, grid points on the vertical centerline and on the vertical boundary at a distance of 120 in. are restrained from horizontal motion. Grid points along the bottom boundary (300 in.) are fixed as in the longitudinal model.

The outputs from this analysis are rail deflection and moment, tie reaction, and stress and deformation in the ballast and subgrade.

Finite Element - Lundgren

A computer solution by methods of matrix structural analysis is given [B-29] for a track structure under static vertical loads. A two-dimensional finite element method gives deflection, strain, stresses, moments, and track modulus. The soil is assumed to be small square plate elements; the ties are represented by a spring or springs; the rail is a continuous beam resting on the tie springs. Separate springs for fastener pads are not mentioned.

The model is capable of accepting randomly assigned soil properties. The solution is modified to take into account the inability of the soil to take high tensile loading and high shear stresses. A new stiffness matrix is formulated when shear or tensile failure occurs. This provides an iterative solution for nonlinear soil behavior under high loadings.

The boundary conditions are chosen such that the surface boundary is free to move while the lower boundary is fixed. The model will accept any boundary condition on the sides. The rail end may be fixed or free in the vertical direction with a zero or full moment restraint.

In this model, the weight of the ballast/subgrade material is taken into account. Rail, fastener, and a portion of the tie weight is applied at grid points to reduce positive deflection of the rail. During the iteration procedure, negative stiffnesses are removed from the rail.

Finite Element - Kilmartin

This finite element program [B-30] attempts to model the rail-tie structure accurately, but does not include detailed modeling of the ballast. Rail segments between ties are assumed to be primatic beams, and the cross ties are finite sections of a beam on a continuous elastic foundation. A variable number of static vertical and lateral loads can be placed on the rail at any point. In general, grid points exist at the intersection of the cross tie and each rail. If a load is placed between cross ties, an imaginary tie is used.

The program will accept variable tie, right rail, and left rail properties, and a variable number of points. Joint stiffness is scaled from 0 to 1 compared to CWR. At each grid point vertical and lateral deflections along with 3 rotations are calculated. The analysis does not consider pad stiffnesses, fasteners, or variable ballast modulus.

An iteration procedure is used to eliminate upward tie deflections. This is accomplished by selecting a second foundation modulus for ties with an upward deflection and recomputing a solution. An iteration procedure is continued until the solution does not change.

Comparison to theoretical results of a rail on an elastic foundation is favorable.

Finite Element - BCL

A single rail is divided into n grid points with a variable distance between each grid point. Associated with each grid point is a vertical spring (tie) a torsional spring (fastener), a beam flexual stiffness (EI), and a vertical

static load. Any of the above quantities can vary from grid point to grid point. An investigation of ineffective ties or fasteners, rail joints, and multiple wheel loads can be handled in the vertical plane only.

The solution is obtained by writing equilibrium equations at each grid point in the form of a matrix equation. By assuming free-free boundary conditions, the unknown deflections, slopes, moments and shears of the rail at each grid point are calculated. Outputs also include tie vertical support load, and fastener torsional support load.

Lateral Rail-Tie-Foundation Model - AAR

A static finite element model [B-31] of the rail-tie-foundation lateral reaction due to multiple wheel loads has been formulated and somewhat validated with experiments. This 2-dimensional model (lateral translation and rotation about the vertical axes) is represented by 1-dimensional finite elements. A beam is used to represent a single rail supported by springs at the tie locations. These springs, which may be nonlinear, simulate the total lateral stiffness of the tie, fastener, and ballast. A rotational stiffness about the vertical axis at the tie is provided by the fastener.

This analysis is capable of handling rail irregularities such as rail joints, nonlinear foundation support, missing ties and off-loading. A rail joint is simulated by inputting joint bar properties at the desired location. The nonlinear characteristics of the fastener and ballast -subgrade are incorporated into the program by a multi-linear stiffness. Missing ties can be represented by negligible tie and fastener stiffness. Forces or displacements in the lateral, longitudinal, and rotational direction can be applied at all node points. The other forces or displacement are the unknowns.

Outputs of the finite element program include lateral and longitudinal rail-tie-reactions, and rotational rail-fastener reactions about the vertical axis. In addition, member axial and shear forces, bending moment, and deflection of the rail are given.

The model has been partially verified with test data of lateral rail deflections obtained in the mid 30's. The effect of rail joints, missing ties, and nonlinear ballast characteristics have not been determined experimentally. Consequently, the usefulness of this model cannot be adequately validated.

Parameter studies with the model have shown small changes in rail lateral deflection and bending moment due to fastener and rail stiffness. But a significant reduction in deflection and bending moment is obtained for increased lateral tie-foundation stiffness.

The documentation of this model includes an input/output explanation but no listing of the program.

Three-Dimensional Track Model by Member Representation - AAR

The model [B-31] suggested here is a 3-dimensional track model representing the rails, fasteners, ties, and ballast-subgrade by structural members and springs (1-dimensional finite elements). Rails and ties are represented by beams; the ballast-subgrade by springs. Each fastener group can be separated into fastener components, each component being represented by a structural element or spring. Nonlinear ballast-subgrade, and fastener characteristics can be incorporated. Multiple loads, off-loading, staggered joints, ineffective ties, and fasteners can also be modeled. Rail joints are simulated by a beam equivalent to a joint bar.

Predictions of this model include rail and tie bending moments and deflections, fastener deflections, and the loading environment for the ties, fasteners, and ballast-subgrade.

A comparison of predicted vertical rail deflection with test data obtained some 60 years ago shows good agreement for a large vertical track load (25,000 lb) but poor correlation for a light load (5,000 lb). Lateral deflections are also verified by test data developed in the 1930's. The many other possible cases which need to be validated have not been because of a lack of experimental data.

A parameter study with this model indicates that the vertical deflection of each rail is independent of the loading on the adjacent rail.

A general purpose 3-dimensional structural analysis program (SAP-IV) [B-32] is used to solve this problem. Although SAP-IV does contain dynamic analysis capability, it is ignored. Input/output documentation is included in the AAR report, along with a sample problem. It should be noted that SAP-IV is a linear structural analysis program in its original form. Apparently it has been updated to simulate nonlinear behavior.

Additional Rail Vehicle Models

Several past and current rail vehicle models have not been included in this review because the wheel/rail forces have not been addressed per se in the existing documentation. For example, a digital computer version of the nonlinear freight car simulation was generated by Liepins [B-33] and reported in late 1968. Other versions of car rocking programs have been, or are currently used by railroad suppliers and the railroads [B-34,B-35].

A number of models have been generated by universities, ranging from simple suspension dynamics studies [B-36] to complex models of a six-axle locomotive [B-37,B-38]. Additional vehicle models have been developed under sponsorship of the Department of Transportation for studies of active ride stabilizers [B-39], auto and passenger rail transport studies [B-40], the Metroliner ride improvement program [B-41,B-42], and the LIM Research Vehicle program [B-43]. There are any number of vehicle mathematical models extant with the various subcontractors on these diverse programs that may or may not be applicable to the generation of wheel/rail forces. Perhaps the most detailed, best known model of this nature is DYNALIST II [B-44], which was developed to compute the response of rail vehicle systems to sinusoidal or stationary random rail irregularities. Both lateral and vertical motions can be utilized with a maximum of fifty degrees of freedom. Since the user can do his own modeling, a track structure could be incorporated into the program. W/R forces would then be obtained indirectly from a frequency response of wheel and rail displacements.

APPENDIX C

LOAD CELL RESPONSE TO RAIL INPUT FORCES

In order to gain some insight into the problem of obtaining forces at the rail using a load cell mounted between the axle and side frame of a railroad car (or alternately by mounting transducers on the wheel or the side frame), we have investigated the simplified model of a railroad car truck shown in Figure C1. This model represents a quarter of the railroad car truck in simple vertical bounce motion.

The equations of motion for the three masses comprising this model are

$$M_1\ddot{Y}_1 + C_1(\dot{Y}_1-\dot{Y}_2) + K_1(Y_1-Y_2) = 0 \qquad \text{(C-1)}$$

$$M_2\ddot{Y}_2 - C_1(\dot{Y}_1-\dot{Y}_2) + C_2(\dot{Y}_2-\dot{Y}_3) - K_1(Y_1-Y_2) + K_2(Y_2-Y_3) = 0 \qquad \text{(C-2)}$$

$$M_3\ddot{Y}_3 - C_2(\dot{Y}_2-\dot{Y}_3) - K_2(Y_2-Y_3) = F_R. \qquad \text{(C-3)}$$

A harmonic wheel/rail interaction force, F_R, can be expressed in the complex plane rotating vector notation

$$F_R = \bar{F}_R\, e^{i\omega t}, \qquad \text{(C-4)}$$

where $\bar{F}_R$ is the amplitude of the applied force. The solutions for the motions of the masses will be of the form

$$Y_1 = A_1 e^{i\omega t} \qquad \text{(C-5)}$$

$$Y_2 = A_2 e^{i\omega t} \qquad \text{(C-6)}$$

$$Y_3 = A_3 e^{i\omega t}, \qquad \text{(C-7)}$$

where A_1, A_2 and A_3 are, in general, complex constants.

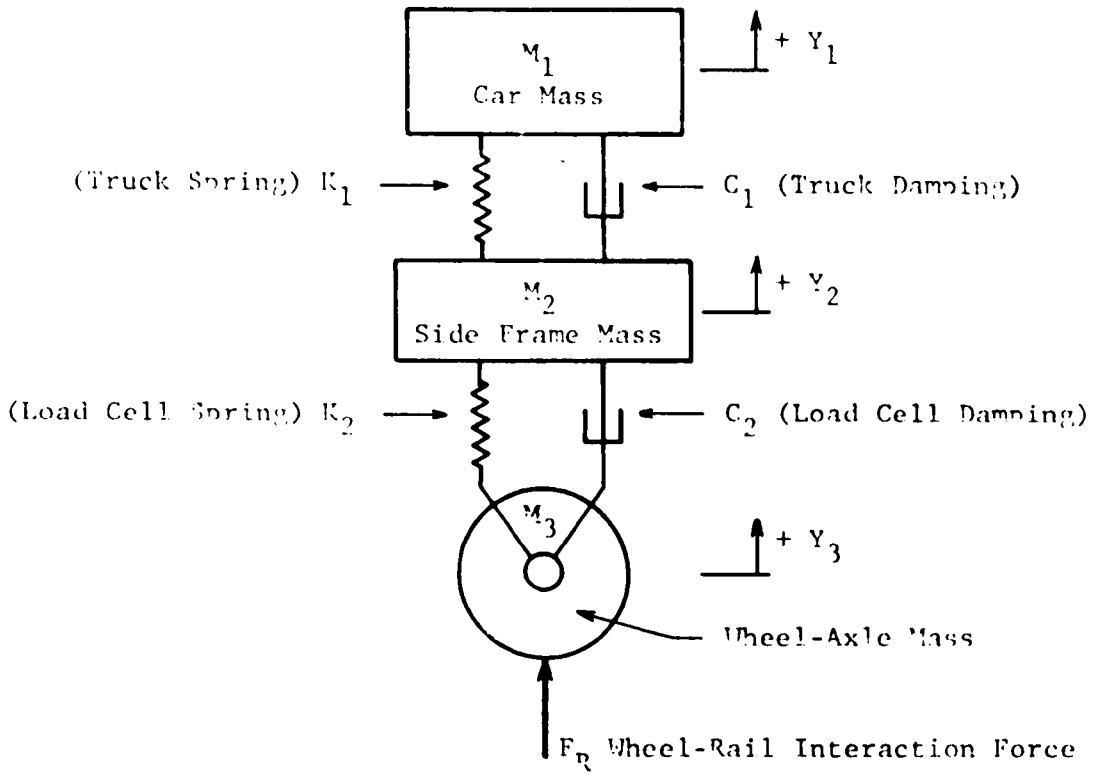

Figure C-1. RAILROAD CAR TRUCK MODEL

Substituting Equations 4, 5, 6 and 7 (and the derivatives of 5, 6, and 7) into 1, 2 and 3 we obtain in matrix form

$$\begin{bmatrix} K_1+i\omega C_1-M_1\omega^2 & -(K_1+i\omega C_1) & \\ -(K_1+i\omega C_1) & K_1+i\omega C_1+K_2+i\omega c_2-M_2\omega^2 & -(K_2+i\omega C_2) \\ 0 & -(K_2+i\omega C_2) & K_2+i\omega C_2-M_3\omega^2 \end{bmatrix} \begin{bmatrix} A_1 \\ A_2 \\ A_3 \end{bmatrix} e^{i\omega t} = \begin{bmatrix} 0 \\ 0 \\ F_R \end{bmatrix} e^{i\omega t}. \tag{C-8}$$

Solving for A_1, A_2 and A,

$$A_1 = (K_1+i\omega C_1)(K_2+i\omega C_2)\ F_R/\Delta \tag{C-9}$$

$$A_2 = (K_1+i\omega C_1-M_1\omega^2)(K_2+i\omega C_2)F_R/\Delta \tag{C-10}$$

$$A_3 = [(K_1+i\omega C_1-M_1\omega^2)(K_1+i\omega C_1+K_2+i\omega C_2-M_2\omega^2)-(K_1+i\omega C_1)^2]\ F_R/\Delta \tag{C-11}$$

where the determinant of the coefficient matrix, Δ, is given by

$$\Delta = (K_1+i\omega C_1-M_1\omega^2)(K_1+i\omega C_1+K_2+i\omega C_2-M_2\omega^2)(K_2+i\omega C_2-M_3\omega^2)$$
$$-(K_1+i\omega C_1-M_1\omega^2)(K_2+i\omega C_2)^2-(K_2+i\omega C_2-M_3\omega^2)(K_1+i\omega C_1)^2. \tag{C-12}$$

The undamped natural frequencies of this system can be obtained by determining those values of ω which cause Δ to vanish with the damping, C_1 and C_2 set to zero.

The force measured by the load cell is

$$F_L = F_L\ e^{i\omega t} = K_2(Y_3-Y_2). \tag{C-13}$$

Substituting Eqs. 6, 7, 10 and 11 into this equation and simplifying

$$F_L = K_2[M_1M_2\omega^4-(K_1+i\omega C_1)(M_1+M_2)\omega^2]\ F_R/\Delta\ . \tag{C-14}$$

The complex frequency response (or transfer function) relating the load cell force to the wheel/rail interaction force is (from Eq. 14)

$$H(i\omega) = \bar{F}_L/\bar{F}_R = K_2[M_1M_2(i\omega)^4+(K_1+i\omega C_1)(M_1+M_2)(i\omega)^2]/\Delta. \quad \text{(C-15)}$$

Let $\bar{F}_L'$ be the real part of $\bar{F}_L$ and $\bar{F}_L''$ be its imaginary part. Then the phase angle between the load cell force and the wheel/rail interaction force is given by

$$\phi = \tan^{-1}\,[-\bar{F}_L''/\bar{F}_L']. \quad \text{(C-16)}$$

The power spectral density of the load cell force, $S_L(\omega)$, related to the power spectral density of the wheel/rail interaction force, $S_R(\omega)$, by

$$S_L(\omega) = |H(i\omega)|^2\, S_R(\omega) \quad \text{(C-17)}$$

or

$$S_L(\omega) = |\bar{F}_L/\bar{F}_R|^2\, S_R(\omega) \quad \text{(C-18)}$$

or

$$S_L(\omega) = (|\bar{F}_L|/|\bar{F}_R|)^2\, S_R(\omega). \quad \text{(C-19)}$$

For a typical railroad car and load cell the following properties are assumed.

$W_1 = M_1g = 60{,}000$ lbs

$W_2 = M_2g = 400$ lbs

$W_3 = M_3g = 1{,}200$ lbs

$K_1 = 12{,}000$ lb/in.

$K_2 = 1{,}200{,}000$ lb/in.

The damping factor C_1 is approximately 10 percent of critical for M_1 vibrating on spring K_1.

$$C_1 = (.10)(2\sqrt{K_1 M_1}) = (.10)(2)\sqrt{(12{,}000)(60{,}000/386)} = 273 \text{ lb sec/in.}$$

The damping factor C_2 will be of the order of 1 percent of critical for M_2 vibrating on spring K_2.

$$C_2 = (.01)(2\sqrt{K_2 M_2}) = (.01)(2)\sqrt{(1{,}200{,}000)(400/386)} = 22 \text{ lb sec/in.}$$

Solving numerically for the natural frequencies of this system we obtain

$$W_1 = 8.65 \text{ Hz}$$
$$W_2 = 198.3 \text{ Hz.}$$

Figure C2 is a plot of the modulus of the complex frequency response ($|H(i\omega)|$ or $|\bar{F}_L|/|\bar{F}_R|$) versus the frequency of excitation for the systems described above. Figure C3 is a plot of the phase angle versus frequency. The next seven figures, Figures C4 thru C10, show the sensitivity of the modulus of the complex frequency response and of the phase angle to changes in the 7 parameters which describe the system. This is done for two discrete frequencies; 5 and 50 hertz. Note that the modulus is relatively insensitive to changes in the assumed weights, spring constants and damping constants. Also the phase angle modification occurs only over a limited range. Note also that the modulus tends toward unity with increasing M_2 (Figure C5) and decreasing M_3 (Figure C6) which shows that if its load cell is located closer to the wheel/rail interface the fidelity of load measurement will be improved.

A computer program was also written to numerically integrate Eqs. 1, 2 and 3 to determine the response of the system to rectangular pulse inputs. This analysis was performed to evaluate the ability of the system to respond to transient loads such as rail joint loads.

The results of this analysis are given in Figures C2 thru C18 for a series of pulse durations. Note that for pulse durations in the 1/500 to 1/100 record range the response of the load cell would be about 1/2 the peak rail load. For pulse durations greater than 1/50 seconds the load cell responds accurately to the peak rail load. The response to the shorter duration pulses would be improved by placing the load cell closer to the rail. This could be accomplished by mounting the "load cell" gages on the plate of the wheel near the rim.

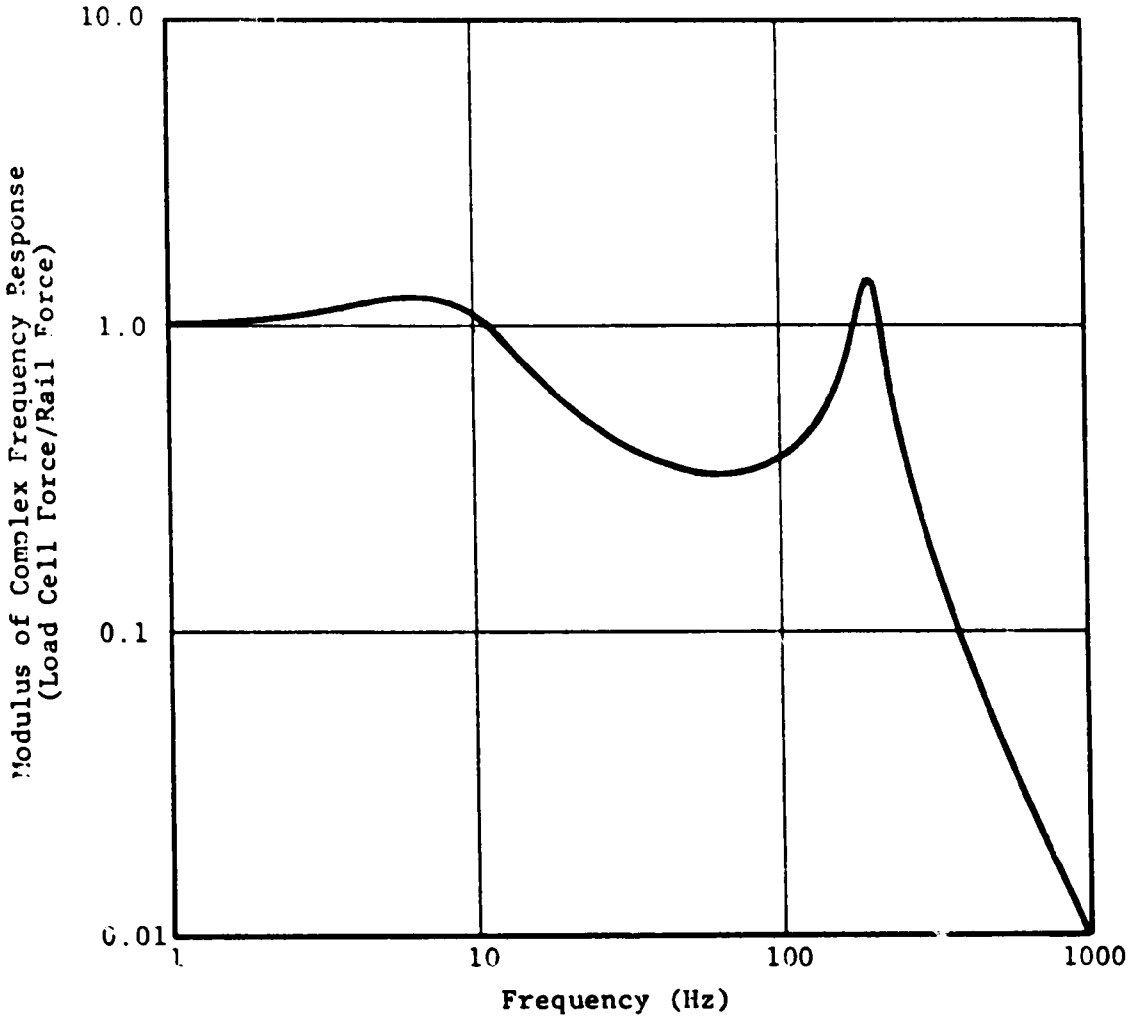

Figure C2. LOAD CELL RESPONSE

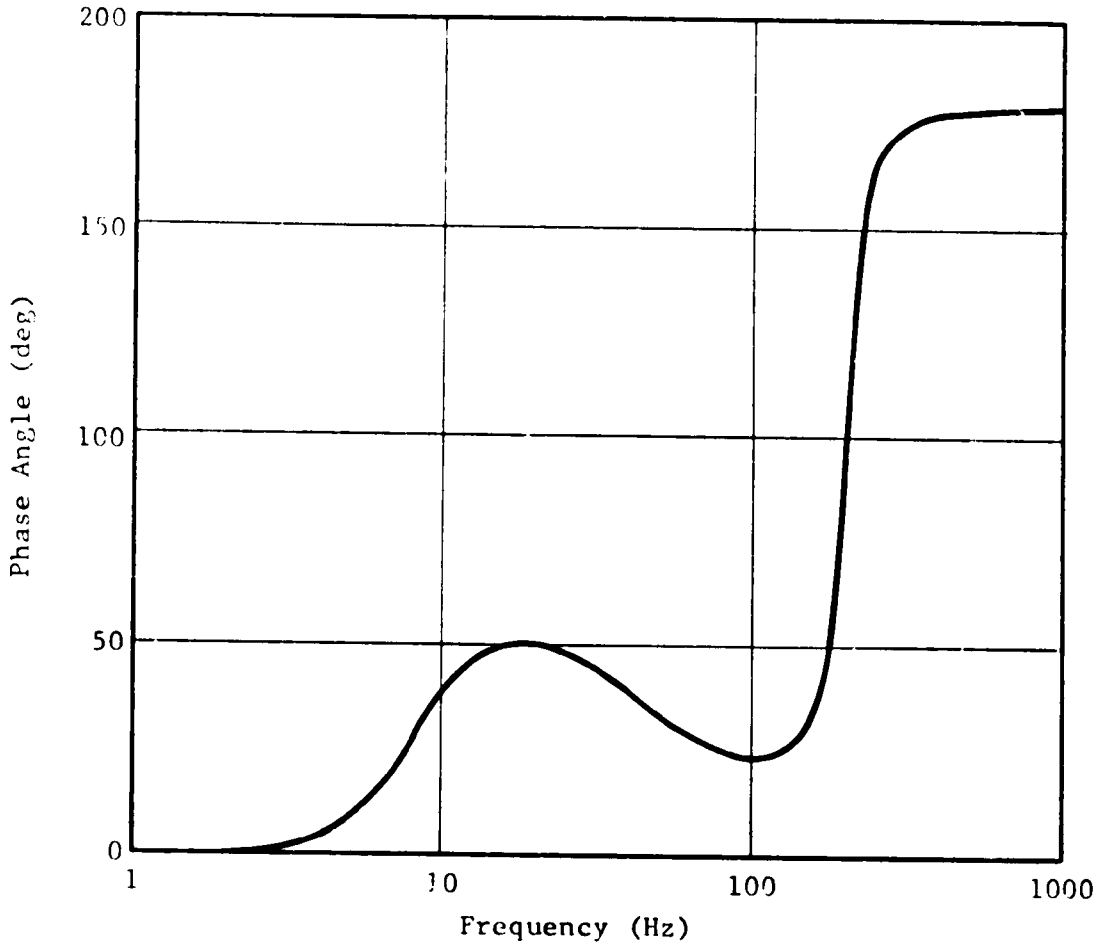

Figure C3. LOAD CELL PHASE ANGLE

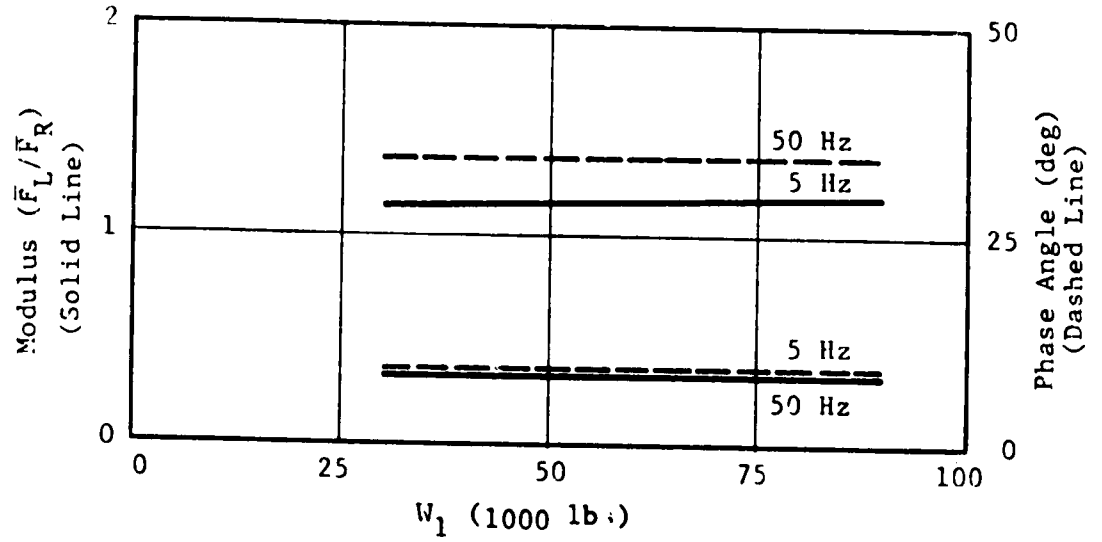

Figure C-4. VARIATION OF MODULUS AND PHASE ANGLE WITH W_1

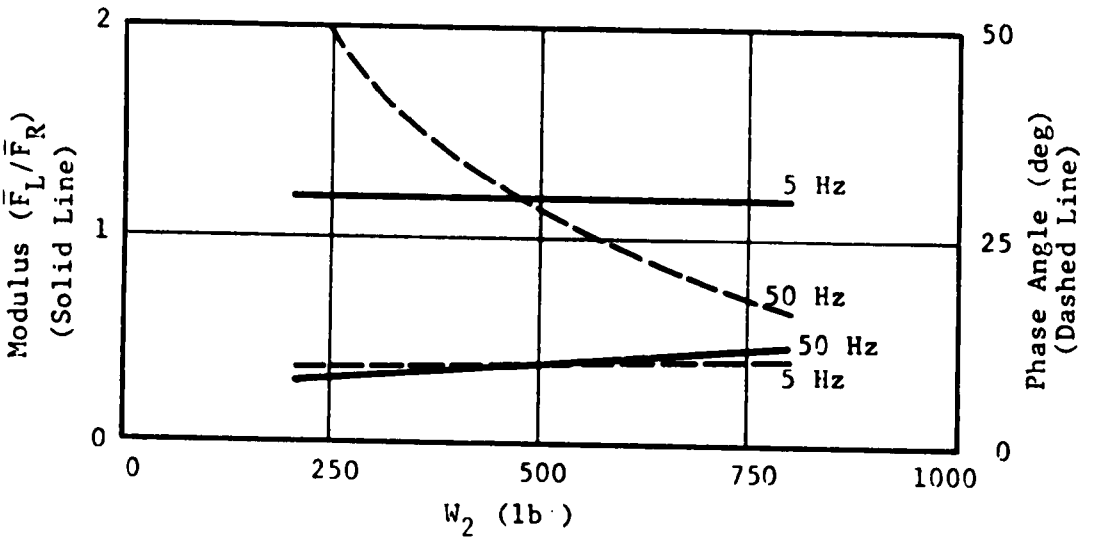

Figure C5. VARIATION OF MODULUS AND PHASE ANGLE WITH W_2

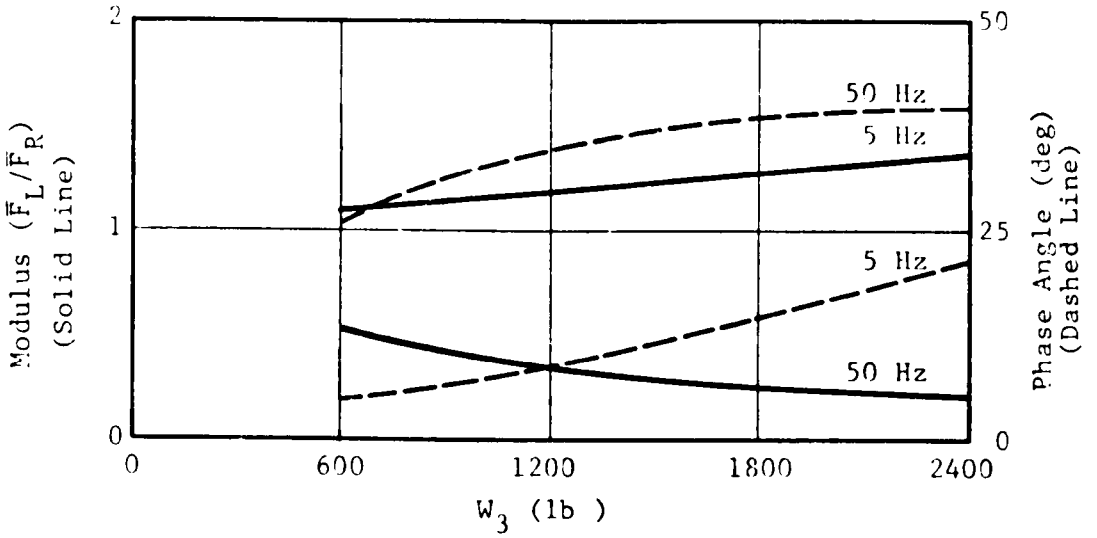

Figure C6. VARIATION OF MODULUS AND PHASE ANGLE WITH W_3

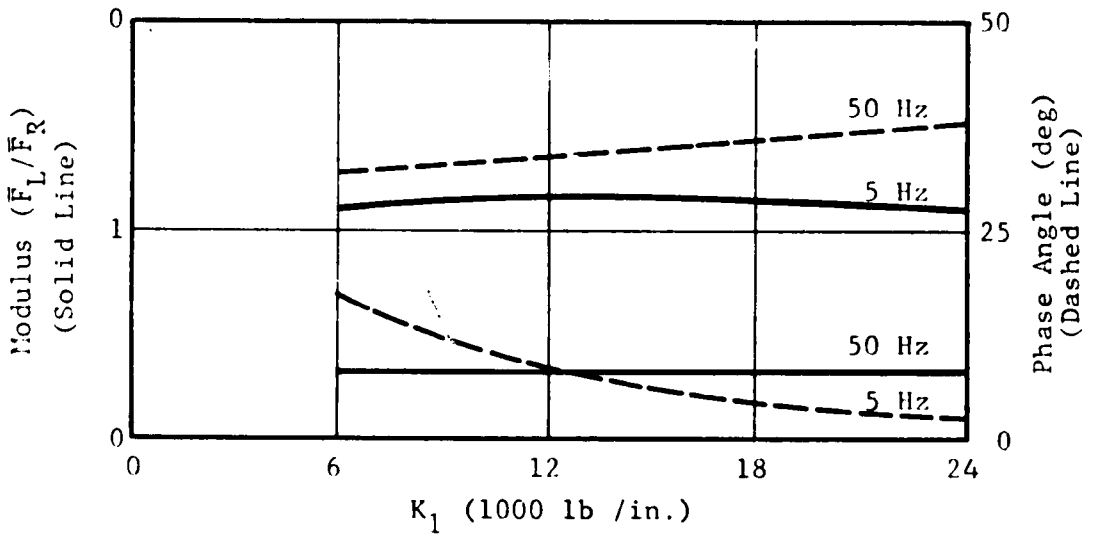

Figure C7. VARIATION OF MODULUS AND PHASE ANGLE WITH K_1

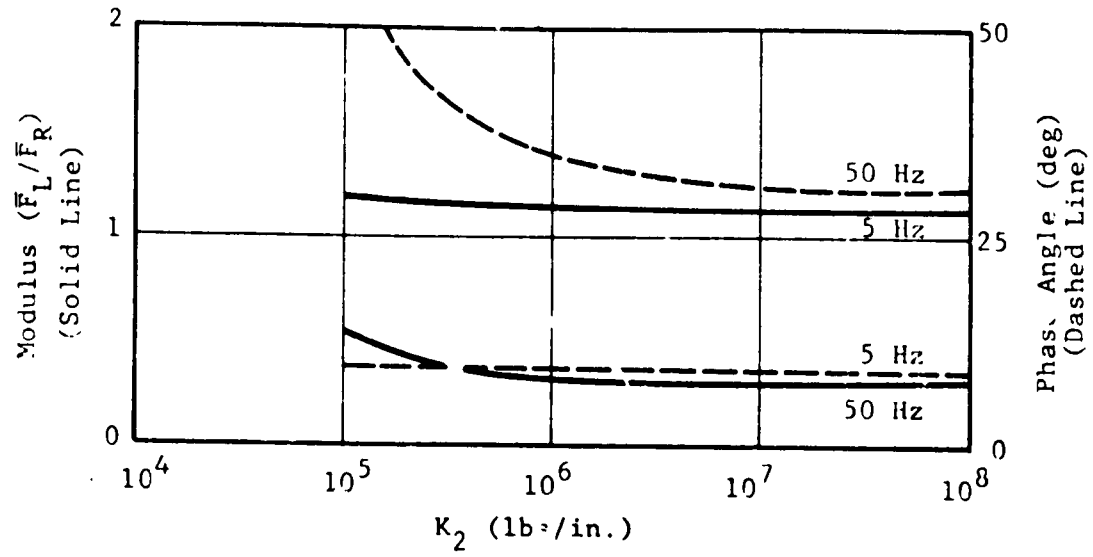

Figure C8. VARIATION OF MODULUS AND PHASE ANGLE WITH K_2

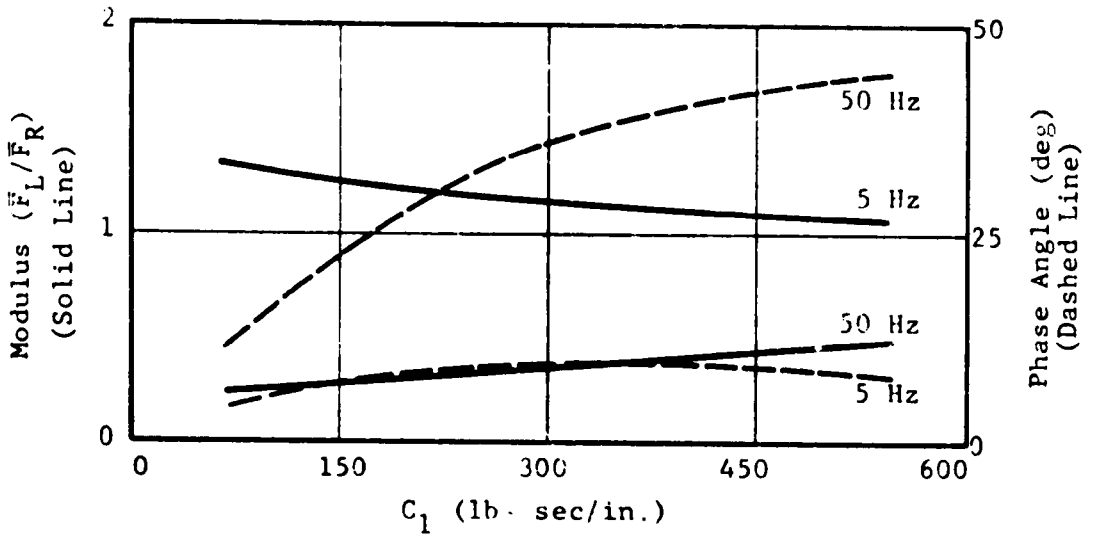

Figure C9. VARIATION OF MODULUS AND PHASE ANGLE WITH C_1

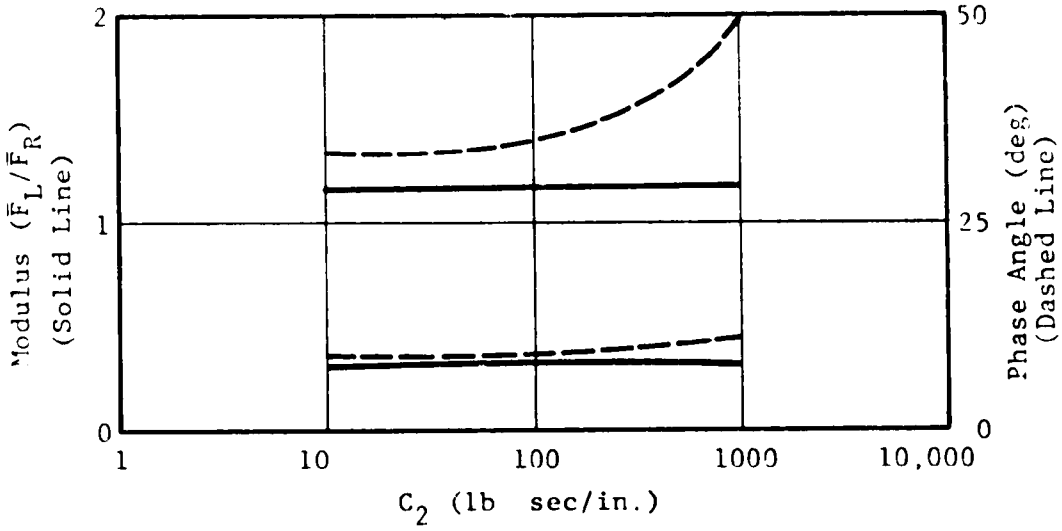

Figure C10. VARIATION OF MODULUS AND PHASE ANGLE WITH C_2

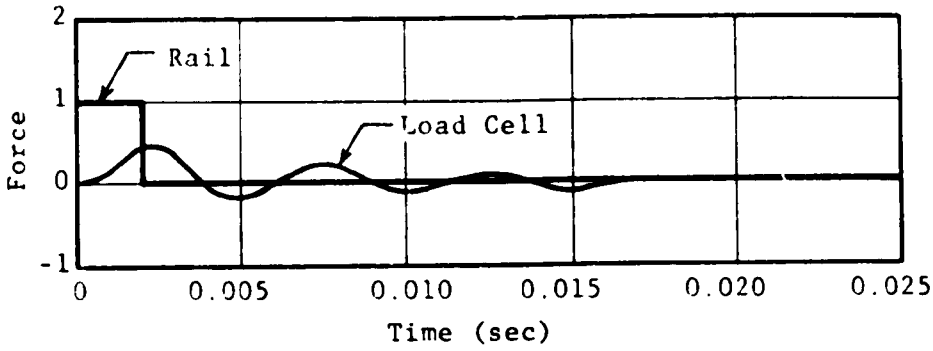

Figure C11. LOAD CELL RESPONSE -- 0.002 SEC PULSE

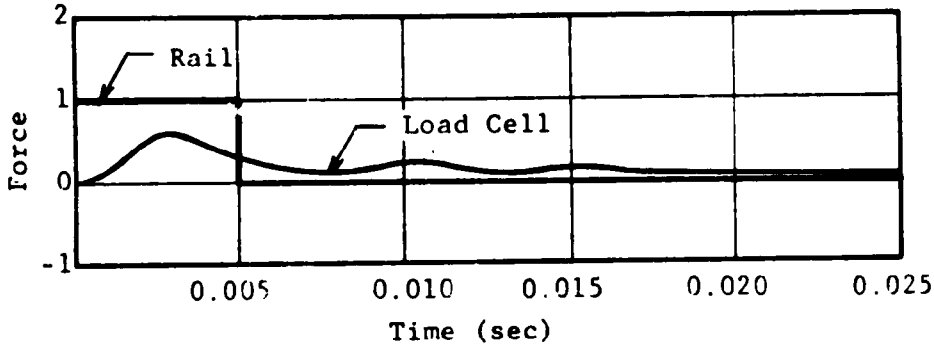

Figure C12. LOAD CELL RESPONSE -- 0.005 SEC PULSE

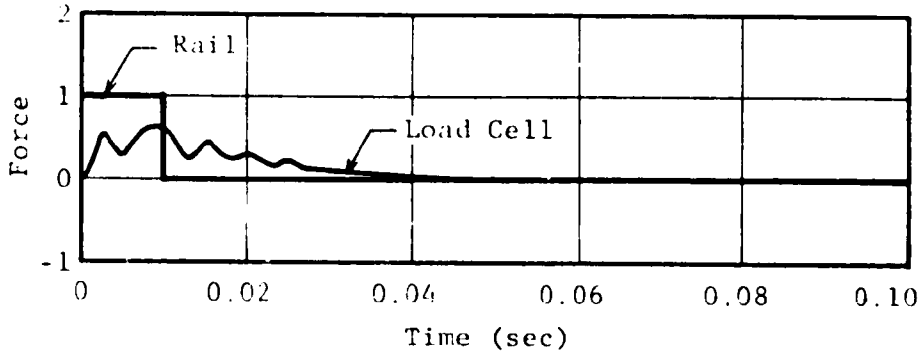

Figure C13. LOAD CELL RESPONSE -- 0.010 SEC PULSE

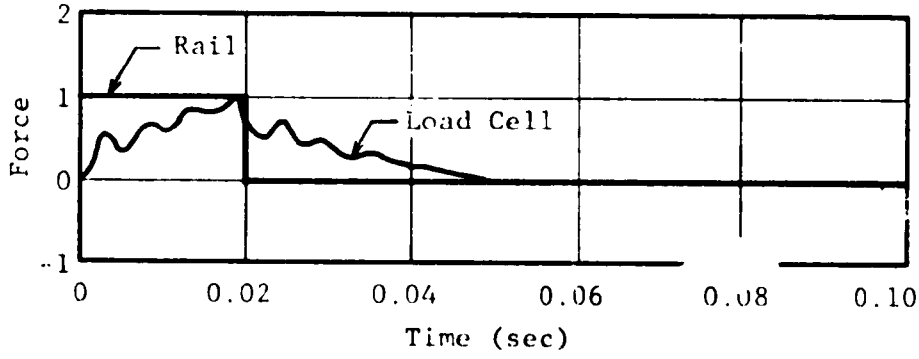

Figure C14. LOAD CELL RESPONSE -- 0.020 SEC PULSE

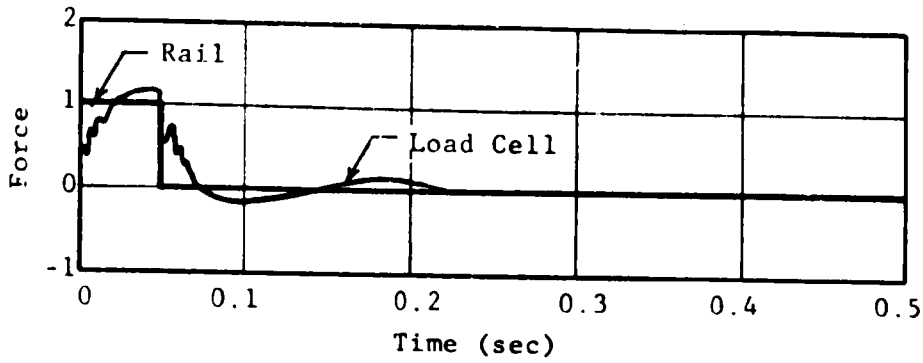

Figure C15. LOAD CELL RESPONSE -- 0.050 SEC PULSE

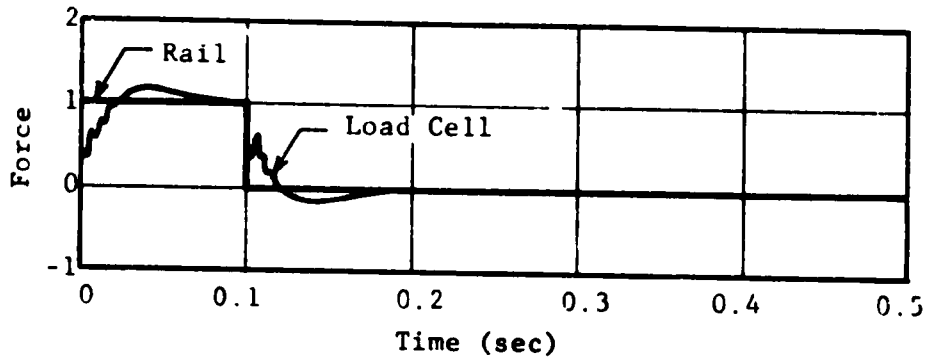

Figure C16. LOAD CELL RESPONSE -- 0.100 SEC PULSE

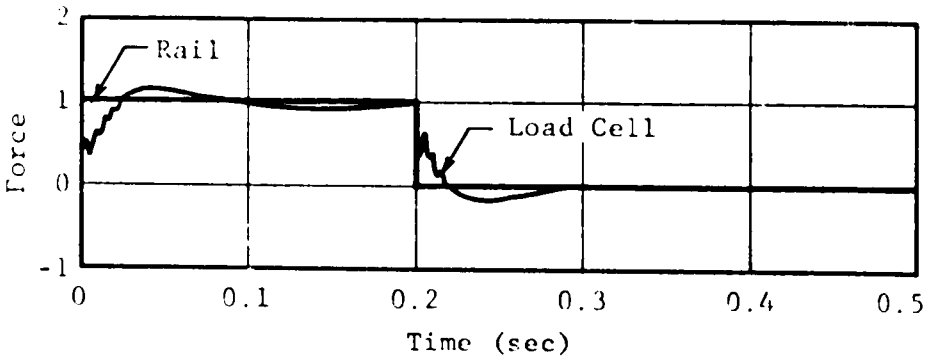

Figure C17. LOAD CELL RESPONSE -- 0.200 SEC PULSE

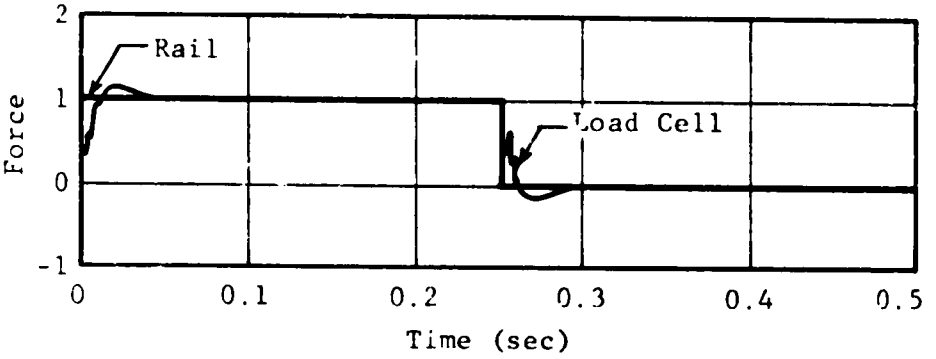

Figure C18. LOAD CELL RESPONSE -- 0.500 SEC PULSE

APPENDIX D

REPORT OF INVENTIONS

This report contains a comprehensive review of reported work on track measurements to establish requirements for wheel/rail load characterization. We believe the concepts for summing rail web strain gage and instrumented tie plate load signals to achieve a continuous vertical wheel/rail load signal (see Section 5.1.1) represents an improvement over current techniques which may lead to an invention.

REFERENCES

3-1. Orr, David G., "Track Train Dynamics Harmonic Roll Series, Volume I", AAR-TTD Task 13 report, 1975.

3-2. Wiebe, D., "The Effects of the Lateral Instability of High Center of Gravity Freight Cars", ASME Journal of Engineering for Industry, Vol. 90, Series B, No. 4, Nov. 1965, pp 727-736.

3-3. Meacham, H. C., and Ahlbeck, D. R., "A Computer STudy of Dynamic Loads Caused by Vehicle-Track Interaction", ASME Journal of Engineering for Industry, Vol. 91, Series B, No. 3, Aug. 1969, pp 806-816.

3-4. Jenkins, H. H., et al, "The Effect of Track and Vehicle Parameters on Wheel/Rail Vertical Dynamic Forces", The Railway Engineering Journal, Vol. 3, No. 1, Jan. 1974, pp 2-26.

3-5. Satoh, Y., "Dynamic Effect of a Flat Wheel on Track Deformation", Bulletin of Permanent Way Society of Japan, Vol. 12, No. 7, July 1964, pp 14-22.

3-6. "Effect of Flat Wheels on Track and Equipment", Proc. AREA, Vol. 53, 1952, pp 423-448.

3-7. "Wide Gage Investigation", Vol. I, Vol. II, AAR Track Train Dynamics Program, 1975.

3-8. Lynch, J. F., et al, "Track Train Dynamic Study -- Project TR-14, Rail Vehicle Interaction Study", Report #1, Southern Pacific Transportation Co., June 1970.

3-9. Marta, H. A., and Mels, K. D., "Wheel-Rail Adhesion", ASME Journal of Engineering for Industry, August 1969, pp 839-859.

3-10. Ferguson, R., and Leitze, L. W., "Special Report on Field Tests on Continuous Welded Rail on the Great Northern Railway", AREA Proceedings, Vol. 60, 1959, pp 642-653.

3-11. Track Data; ENSCO, Inc., Report TG-69, 1974.

3-12. Prud'homme, A., "Stresses and Behavior of Rail Tracks During the Passing of Trains Travelling at Very High Speeds", Symposium on Railroad Track Mechanics, The Princeton University Conference, Meeting No. 126, April 1975.

3-13. Ahlbeck, D. R., Harrison, H. D., and Noble, S. L., "An Investigation of Factors Contributing to Wide Gage on Tangent Railroad Track", ASME Paper No. 75-WA/RT-1, December, 1975.

3-14. Koffman, J. L., and Fairweather, D. M. S., "Some Problems of Railway Operation at High Axle Loads", Railway Engineering International, June/July 1975, pp 156-159.

REFERENCES (Continued)

3-15. King, F. E., "Rail Wear and Corrugation Problems Related to Unit Train Operations--Causes and Remedial Action", The 1975 Pueblo Conferences, Pueblo, Colorado.

3-16. Srinivasam, M., Modern Permanent Way, Somaiya Publications Pvt. Ltd., Bombay, India, 1969.

3-17. Myers, E. T., "Maintenance of Way--The Gap Widens", Modern Railroads, December 1975, Vol. 30, No. 12, pp 88-90.

3-18. Railway Age, March 10, 1975, pp 52-53, 70.

3-19. Northeast Corridor High-Speed Rail Passenger Service Improvement Project, Task 3 - Track and Structures Standards Development, Final Report, DOT-FR-40026, Sept. 1975.

3-20. Cassidy, R. J., "Cooperative Research Programme to Develop Improved Track Maintenance Equipment and Procedures", Cornell Aeronautical Laboratory, CAL No., VJ-3008-K-1, Nov. 11, 1970.

3-21. "Natural Frequencies of Vibration--Heavy Freight Cars", Canadian Pacific Railway, Dept. of Research, Report No. S-456-73, June 1973.

3-22. Luebke, R. W., "Investigation of Boxcar Vibrations", U.S. DOT Report No. FRA-RT-70-26, Aug. 1970.

3-23. Meacham, H. C., et al, "Studies for Rail Vehicle Track Structures", Report No. FRA-RT-71-45, U.S. DOT, April 30, 1970, pp 57-59.

3-24. Ahlbeck, D. R., Rodman, C. W., and Meacham, H. C., "Collection and Analysis of Data on Penn-Central High Speed Track Response at Bowie, Maryland", Battelle report to DOT/FRA, Contract No. DOT-FR-10018, Oct. 27, 1971.

3-25. Nessler, G. L., Prause, R. H., and Kaiser, W. D., "An Experimental Evaluation of Techniques for Measuring the Dynamic Compliance of Railroad Track", Battelle Interim Report to DOT/FRA, Contract No. DOT-FR-30051, June 1975, (to be published).

3-26. Nelson, J. T., "Vibration and Strain Measurements on Aluminum Wheels Used in Rapid Transit System Cars", presented at 90th Meeting of Acoustical Society of America, San Francisco, California, 1975.

3-27. Sonneville, R., "Experience of the New Tokaido Railroad of the Future." Le Genie Civil, February 1970.

3-28. Way, G. H., Jr., "Progress Report--Concrete Tie Track at Noble, Illinois", C&O/B&O Railroad, Research Services Report No. 73-102, March 15, 1973.

3-29. Kurzweil, L., "Dynamic Track Compliance", DOT/TSC Report No. GSP-067, May 22, 1972.

3-30. Cass, R., et al, "Dynamic Measurement of Absolute Track Properties", ASME Paper No. 69-RR-6, 1969.

3-31. Bradley, K., et al, "Acquisition and Use of Track Geometry Data in Maintenance-of-way Planning", U.S. DOT Report No. DOT/FRA ORD&D 75-27, March 1975.

3-32. Bendat, J. S., and Piersol, A.G., Measurement and Analysis of Random Data, Wiley, 1966, Chapter 4, pp 133-141.

3-33. Koci, L. F., and Marta, H. A., "Wheel and Rail Loadings from Diesel Locomotives", Electro-Motive Division, GM, paper to AREA Annual Convention, Chicago, Illinois, 1971.

3-34. Scott, J. F., Blevins, W. G., and Wilson, J. T., "Technical Studies to Evaluate the Influence of Operational Factors on Track Loading", ASME Paper 72-WA/RT-11.

3-35. Johnson, M. R., "Analysis of Railroad Car Truck and Wheel Fatigue: Part I - Service Load Data and Procedures for the Development of Fatigue Performance Criteria", Federal Railroad Administration, Report No. FRA-OR&D-75-68, May 1975.

3-36. Peterson, L. A., Freeman, W. H., Wandrisco, J. N., "Measurement and Analysis of Wheel-Rail Forces", ASME Technical Paper 71-WA/RT-4, November 1971.

4-1. Corbin, J. C., and Kaufman, W. M., "Classifying Track by Power Spectral Density", Mechanics of Transportation Suspension Systems, ASME AMD-Vol. 15, 1975, pp 1-20.

4-2. ENSCO, Inc., Track Data Report, TG-69, 1974.

4-3. Ahlbeck, D. R., et al, "Comparative Analysis of Dynamics of Freight and Passenger Rail Vehicles", U.S. DOT Report No. FRA-ORD&D-74-39, March 1974.

4-4. Jenkins, H. H., et al, "The Effect of Track and Vehicle Parameters on Wheel/Rail Vertical Dynamic Forces", The Railway Engineering Journal, Vol. 3, No. 1, January 1974, pp 2-26.

4-5. Newland, D. E., "Steering a Flexible Railway Truck on Curved Track", Trans. ASME, Journal of Engineering for Industry, Aug. 1969.

REFERENCES (Continued)

5-1. Question B10, "A Comparison of the Methods of Measuring on the Track and on Wheels the Lateral Forces (y) and Vertical Loads (Q) Caused by Rolling Stock..." Interim Report No. 11 Office of Research and Experiments of the International Union of Railwasy (ORE), Utrecht, Netherlands, October, 1964.

5-2. Kudryavtsev, N.N., Melentyev, L.P., and Granovskiy, A.N. "Measurement of Vertical Forces Acting From the Wheels of a Moving Train on the Rails," (Institute of Railroad Engineering, Moscow, U.S.S.R), Herald of the All-Union Scientific-Research Institute of Railroad Transport, No. 6, 1973, pp 31-33, 4 figs., 3 refs.

ACKNOWLEDGMENT: Battelle's Columbus Laboratories.

5-3. Scott, J.F., Blevins, W.G., and Wilson, J.T., "Technical Studies to Evaluate the Influence of Operational Factors on Track Loading", ASME Paper 72-WA/RT-11.

5-4. Ahlbeck, D.R., Harrison, H.D., and Noble, S.L., "An Investigation of Factors Contributing to Wide Gage on Tangent Railroad Track", ASME Paper 75-WA/RT-1.

5-5. Loach, J.C., "Research into Some Factors Which Influence the Vertical Loading of Railway Track", Proc. Instn. Civil Engrs., Vol. 30, April, 1965.

5-6. Peterson, L.A., Freeman, W.H., Wandrisco, J.N., "Measurement and Analysis of Wheel-Rail Forces, "ASME Technical Paper 71-WA/RT-4.

5-7. Shafranovskiy, A.K., "Continuous Recording of Vertical and Lateral Forces of Interaction Between a Wheel and a Rail", TsNII MPS (Central Scientific Research Institute, Ministry of Rolling Stock), English translation of Russian report, available through FRA.

5-8. "Instrumentation for Measuring Forces on Wheels of Rail Vehicles," Federal Railroad Administration Report FRA-ORD&D-75-11, May 1974.

5-9. Dolecki, E.A., Hartzell, C.E., "Operating and Ride Qualities, Three Axle Floating Bolster Truck," G.E. Technical Information Series DF74LC2690, Feb. 8, 1974.

5-10. Prause, R.H., and Harrison, H.D., "Data Analysis and Instrumentation Requirements for Evaluating Rail Joints and Rail Fasteners in Urban Track", U.S. Dept. of Trans., Report No. UMTA-MA-06-0025-75-8, Contract DOT-TSC-563, Feb. 1975.

5-11. Bendat, J.S., and Piersol, A.G., Measurement and Analysis of Random Data, John Wiley and Sons, New York, N.Y., 1966.

REFERENCES (Continued)

6-1. Ahlbeck, et al, "Comparative Analysis of Dynamics of Freight and Passenger Rail Vehicles", U.S. DOT Report No. FRA-CR-D4D-74-39, March 1974.

6-2. "70-Ton Truck Component Data", AAR-FRA-RFI-TDA Track Train Dynamics Program Report, 1974.

6-3. Jenkins, H.H., et al, "The Effect of Track and Vehicle Parameters on Wheel/Rail Vertical Dynamic Forces", Railway Engineering Journal Vol 3 No. 1, January 1974.

6-4. U.S. Dept. of Trans., Federal Railroad Administration, Track Safety Standards Section 213, Federal Register, October 20, 1971; amended Sept. 8, 1972. (See Railway Track & Structures, Nov. 1972, pp 24-32.)

6-5. Ahlf, R.E., "M/W Costs: How They are Affected by Car Weights and Track Structure", Railway Track and Strcutures, March 1975, pp 35.

6-6. Meacham, H.C., et al, "Studies for Rail Vehicle Track Structures", U.S. DOT Report No. FRA-RT 71-45, April 1970, pp 50-55.

[B-1] Srinivasan, M., "Modern Permanent Way", Somaiya Publications, Bombay, India, 1969, p 134-136.

[B-2] "Trackwork Study - Volume II - Recommended Trackwork Standards", prepared by DeLeuw, Cather and Co. for the Washington Metropolitan Area Transit Authority, August, 1968.

[B-3] Magee, G.M., "Calculations of Rail Bending Stress for 125-Ton Tank Cars", AAR Research Center, Chicago, Illinois, April, 1965

[B-4] Nield, B.J., Goodwin, W.H., "Dynamic Loading at Rail Joints", Railway Gazette, August 15, 1969.

[B-5] Jenkins, H.H., et al., "The Effect of Track and Vehicle Parameters on Wheel/Rail Vertical Dynamic Forces", Railway Engineering Journal, V 3. No. 1, January, 1974.

[B-6] Nishio, A., et al., "Study of High Speed Running on a Curved Track", Sumitomo Search, No. 4, 1970.

REFERENCES (Continued)

[B-7] Newland, D.E., "Steering a Flexible Railway Truck on Curved Track", Journal of Engineering for Industry, Trans. ASME, Vol. 91, Series B, No. 3, August 1969, pp. 908-918.

[B-8] Boocock, D., "Steady State Motion of Railway Vehicles on Curved Track", Journal of Mechanical Engineering Service, Vol. IX, No. 6, 1969.

[B-9] Kunieda, M., "Theoretical Study on the Side Thrust of Truck Wheels Running on Curves", Quarterly Reports, Tokyo Railway Technical Research Institute. Vol. 11, No. 2, 1970.

[B-10] "High-Speed Ground Transportation Systems Engineering Study--High Speed Rail Systems", Report No. FRA-RT-70-36 prepared for the U.S. Department of Transportation by TRW Systems Group, Redondo Beach, California, Februa.y, 1970.

[B-11] Hirano, M., "Theoretical Analysis of Variation of Wheel Load", Quarterly Reports, Tokyo Railway Technical Research Institute, Vol. 13, No. 1, 1973.

[B-12] Cooperrider, N.K., "Railway, Truck Response to Random Rail Irregularities", ASME Paper No. 74-WA/RT-2.

[B-13] Ahlbeck, D.R., et al., "Comparative Analysis of Dynamics of Freight and Passenger Rail Vehicles", Report No. FRA-ORD&D-74-39, March, 1974.

[B-14] Lyon, D., "The Calculation of Track Forces due to Dipped Rail Joints, Wheel-Flats, and Rail Welds", British Rail Research Department, Track Group, Technical Note TS.2, February, 1972.

[B-15] Bjork, J., "Dynamic Loading at Rail Joints - Effect on Resilient Wheels", Railway Gazette, June 5, 1970.

[B-16] Natsuura, A., "Vertical Vibration of a Beam and its Effect Under the Passage of Bogie Car", Quarterly Report, Tokyo Railway Technical Research Institute, Vol. 9, No. 2, 1968.

[B-17] Matsui, S., "A Study of the Derailment of 2-Axle Freight Car Due to Interaction Between Track and Vehicle", Quarterly Report, Tokyo Railway Technical Research Institute, Vol. 14, No. 4, 1973.

[B-18] Kuroda, S., "Dynamic Variation of Wheel Load Attributed to Vertical Deformation of Rail End", Quarterly Report, Tokyo Railway Technical Research Institute, Vol. 14, No. 3, 1973.

REFERENCES (Continued)

[B-19] Law, E.H., "Nonlinear Wheelset Dynamic Response to Random Rail Irregularities", ASME Paper No. 73 WA/RT-3.

[B-20] Dynamic Railcar Simulation Program, Melpar, An American-Standard Company, Report No. FRA-RT-20-24, February, 1970.

[B-21] Martin, G., "Flexible Body Vehicle Model", preceedings of Second Conference on Track Train Dynamics Interaction, Vol. 2, p 517, Chicago, Illinois, December, 1974.

[B-22] Meacham, H.C., et al., "Studies for Rail Vehicle Track Structures", Report No. FRA-RT-71-45, April 30, 1970.

[B-23] Ahlbeck, D.R., Meacham, H.C., Prause, R.H., "The Development of Analytical Models for Railroad Track Dynamics", Symposium on Railroad Track Mechanics, The Princeton University Conference, Meeting No. 126, April 21-23, 1975.

[B-24] Meacham, H.C. and Ahlbeck, D.R., "A Computer Study of Dynamic Loads Caused by Vehicle-Track Interaction", Trans. ASME, Journal of Eng. for Industry, August, 1969, pp 808-816.

[B-25] Ahlbeck, D.R., et al., "A Comparative Analysis of Dynamics of Freight and Passenger Rail Vehicles", Report No. FRA-ORD&D-74-39, March, 1974.

[B-26] Ahlbeck, D.R., et al., "Analytical Studies in Support of High-Speed Passenger Train Ride Comfort and Safety", unpublished, Office of Passenger Systems, June, 1975.

[B-27] Svec, O.J., et al., "Analytical and Experimental Investigation of a Rail Track Structure", Department of Civil Engineering, Queens University, Kingston, Canada, presented at the Second Symposium: Applications of Solid Mechanics, June 17, 1974.

[B-28] Robnett, Q.L., et al., "Ballast and Foundation Materials Research Program - Development of a Structural Model and Materials Evaluation Procedure", Department of Civil Engineering, University of Illinois, May, 1975.

[B-29] Lundgren, J.R., et al., "A Simulation Model of Ballast Support and the Modulus of Track Elasticity", Department of Civil Engineering, University of Illinois, September, 1970.

REFERENCES (Continued)

[B-30] Kilmartin, M.D. "A Numerical Discrete Element Analysis of Railroad Track", Masters Thesis, Tufts University, November, 1972.

[B-31] So, W., et al., "Description of Track Structures, Models and Computer Users Guide," Contract DOT-FRA-30038, Assoc. of American Railroads Technical Center, Sept. 1975 [unpublished].

[B-32] Bathe, K.J., et al., "SAP-IV" A Structural Analysis Program for Static and Dynamic Response of Linear Systems", University of California, Berkeley, 1973.

[B-33] Liepins, A.A., "Digital Computer Simulation of Railroad Freight Car Rocking", Trans. ASME, Journal of Engineering for Industry, November, 1968, pp 701-707.

[B-34] Manos, W.P., "The Dynamics of Rail Car Suspension Systems", and Carman, R.W., "Railway Freight Car Suspension - The Effect Upon the Car Body Structure", Proceedings of the 1970 Dresser Conference, pp. 28-31, pp. 58-63.

[B-35] Wiebe, D., "The Effects of the Lateral Instability of High Center of Gravity Freight Cars", Trans. ASME, Journal of Engineering for Industry, November, 1968, pp 727-736.

[B-36] Diboll, W.B., Jr., Brenieckl, H.S., "Suspension Dynamics by Computer Simulation", Trans. ASME, Journal of Enginnering for Industry, November, 1968, pp 708-716.

[B-37] Siddall J.N., Dokainish, M.A., and Elmaraghy, W., "On the Effect of Track Irregularities on the Dynamic Response of Railway Vehicles", ASME Paper No. 73-WA/RT-1.

[B-38] Elmaraghy, W.H., Dokainish, M.A., and Siddall, J.N., "Minimax Optimization of Railway Vehicle Suspensions", ASME Paper No. 74-WA/RT-3.

[B-39] Osbon, W.O. and Putnam, T.H., "Engineering Design Study of Active Ride Stabilizer for the Department of Transportation's High-Speed Test Cars", Contract No. 3-0267, Westinghouse Research Labs, June, 1969, PB-185008.

[B-40] Robinson, R.R., "Dynamic Simulation of Auto and Passenger Rail Transports (Dart Code)", Contract No. 7-35086, ITTRI Project M6167 Final Report, January, 1968.

[B-41] Sewall, J.L., Parrish, R.V., and Durling, B.J., "Dynamic Responses of Railroad Car Models to Vertical and Lateral Rail Inputs", NASA TN D-6375, November, 1971.

REFERENCES (Continued)

[B-42] Herring, J.M., "Metroliner-Ride Improvement Program", Report No. FRA-RT-73-30, February, 1969.

[B-43] Pearce, T.G., and May, B.J., "A Study of the Stability and Dynamic Response of the Linear Induction Motor Test Vehicle", Report No. FRA-RT-70-25, September, 1969.

[B-44] Hasselman, T.K., et al., "DYNALIST II, A Computer Program for Stability and Dynamic Response Analysis of Rail Vehicle Systems", Vols. I, II, Report No. FRA-ORD-75-22,I and -22,II, Feb., 1975.